Stony Brook University

OFFICIAL COPY

The official electronic file of this thesis or dissertation is maintained by the University Libraries on behalf of The Graduate School at Stony Brook University.

© All Rights Reserved by Author.

Role and Regulation of Sphingolipids in Neuropathy

A Dissertation Presented

by

Nicholas Urban Schwartz

to

The Graduate School

in Partial Fulfillment of the

Requirements

for the Degree of

Doctor of Philosophy

in

Neuroscience

Stony Brook University

December 2017

Copyright by
Nicholas Urban Schwartz
2017

Stony Brook University

The Graduate School

Nicholas Urban Schwartz

We, the dissertation committee for the above candidate for the

Doctor of Philosophy degree, hereby recommend

acceptance of this dissertation.

Dr. Lina M. Obeid, MD – Dissertation Advisor
SUNY Distinguished Professor of Medicine
Dean of Research, School of Medicine

Dr. Maya Shelly, PhD – Chairperson of Defense
Assistant Professor of Neurobiology and Behavior

Dr. Michael A. Frohman, MD/PhD
SUNY Distinguished Professor and Chair of Pharmacology

Dr. Shaoyu Ge, PhD
Associate Professor of Neurobiology and Behavior

Dr. Chiara Luberto, PhD
Research Associate Professor of Physiology and Biophysics

This dissertation is accepted by the Graduate School

Charles Taber

Dean of the Graduate School

Abstract of the Dissertation

Role and Regulation of Sphingolipids in Neuropathy

by

Nicholas Urban Schwartz

Doctor of Philosophy

in

Neuroscience

Stony Brook University

2017

Charcot-Marie-Tooth (CMT) disease is the most commonly inherited neurological disorder, but its molecular mechanisms remain unclear. One variant of CMT, Charcot-Marie-Tooth 2F (CMT2F), is characterized by mutations in heat shock protein 27 (Hsp27). Bioactive sphingolipids have been implicated in many neurodegenerative diseases, but it was unknown if they were dysregulated in CMT. Liquid chromatography/mass spectrometry was used to profile sphingolipids in CMT models. Hsp27 KO mice demonstrated decreases in ceramide in peripheral nerve tissue at an increased age, suggesting that sphingolipid metabolism may be involved in CMT2F. Indeed, the disease-associated Hsp27 S135F mutant demonstrated decreases in mitochondrial ceramides. Given that Hsp27 is a chaperone protein, its role was examined in regulating Ceramide Synthases (CerSs), an enzyme family responsible for catalyzing generation of ceramide. Using confocal microscopy, CerSs co-localized with Hsp27, and upon the presence of S135F mutants, CerS1 lost its co-localization with mitochondria, suggesting that decreased mitochondrial ceramides result from reduced mitochondrial CerS localization rather than decreased CerS activity. Mitochondria in mutant cells appeared larger and demonstrated increased interconnectivity. Furthermore, mutant cell lines displayed decreased mitochondrial respiratory function and increased autophagic flux. Mitochondrial structural and functional changes were recapitulated by blocking ceramide generation pharmacologically. These results suggest that mutant Hsp27 decreases mitochondrial ceramide levels, producing structural and functional changes in mitochondria leading to neuronal degeneration.

Dedication Page

I dedicate this work to my parents, who have always supported me in every endeavor. My mother may be gone, but her love and belief has made this journey possible.

"The most perfect philosophy of the natural kind only staves off our ignorance a little longer"

~David Hume

Table of Contents

List of Figures

List of Tables

List of Illustrations

List of Abbreviations

2-DG, 2-deoxyglucose

ALS, amyotrophic lateral sclerosis

ASAH1, N-acylsphingosine amidohydrolase 1 or acid ceramidase

Cer, ceramide

CerS, ceramide synthase

CMT, Charcot-Marie-Tooth

CMT2F, Charcot-Marie-Tooth 2F

co-IP, co-immunoprecipitation

CoA, coenzyme A

deoxyCer, deoxyceramide

deoxydhCer, deoxydihydroceramide

deoxySA, deoxysphinganine or deoxydihydrosphingosine

deoxySL, deoxysphingolipid

deoxySO, deoxysphingosine

dhCer, dihydroceramide

dhSph, dihydrosphingosine

DRG, dorsal root ganglia

ER, endoplasmic reticulum

FA2H, fatty acid 2-hydroxylase

FB1, fumonisin B1

GBA2, beta-glucosylceramidase 2

HA, hemagglutinin

HSAN1, Hereditary Sensory Neuropathy type 1

HSP, Hereditary Spastic Paraplegia

Hsp27, heat shock protein 27

iPSC, induced pluripotent stem cell

LC/MS, liquid chromatography/mass spectrometry

MAG, myelin-associated glycoprotein

MAM, mitochondrial associated membrane

MNCV, motor nerve conduction velocity

MOC, Manders' Overlap Coefficient

MT, microtubule

MTT, 3-(4,5-dimethylthiazol-2-yl)-2,5-diphenyltetrazolium bromide

NF, neurofilament

NF-L, neurofilament light chain

OCR, oxygen consumption rate

PCC, Pearson's Correlation Coefficient (PCC)

S1P, sphingosine-1-phosphate

SA, sphinganine

SIM, Structured Illumination Microscopy

SK, sphingosine kinase

SM, sphingomyelin

sHsp, small heat shock protein

SMA-PME, spinal muscular atrophy with progressive myoclonic epilepsy

SO, sphingosine

SOD, superoxide dismutase

Sph, sphingosine

SPL, sphingosine-1-phosphate lyase

SPT, serine palmitoyltransferase

TLC, thin-layer chromatography

V, vector

WT, wild-type

Acknowledgments

I would first like to acknowledge my father and the rest of my family. They have always demonstrated great interest in the work that I have undertaken in the lab and have never wavered in encouraging me to attain my goals of translating discoveries to treat neural disease.

I would like to especially thank my dissertation advisor, Dr. Lina Obeid. Dr. Obeid is a world-renowned expert in sphingolipid signaling, and it has been a tremendous privilege to work under her direction for my dissertation. It is incredibly rare to encounter someone of her stature who is so invested in student training and mentoring, and I am grateful for the opportunity to learn and develop as a researcher in her lab. Despite a continuously busy schedule, she has never declined an opportunity to meet with me and has been especially patient and understanding even when I often insist on opposing hypotheses and experimental strategies.

I would like to express gratitude to Dr. Yusuf Hannun for always pushing me to produce the most rigorous results and to draw the most logically accurate conclusions. My interactions with him have greatly helped develop my scientific reasoning.

I would like to thank Dr. Can Senkal for generously sharing his preliminary data that allowed me to form the foundation of this project. Furthermore, Dr. Senkal initially trained me in many of the techniques fundamental to this work and has offered suggestions and technical advice throughout the duration of my thesis research.

I would like to thank Ryan Linzer for his non-wavering commitment and dedication to research. Ryan is atypically mature for an undergraduate and has never hesitated to attempt both highly repetitive and challenging experiments with great success. I'm confident he will be a terrific physician and researcher in his career.

I thank all members of the TLC Lab. It has been incredible to work in such a large, dynamic environment with so much diversity in academic background and culture. I cannot mention every lab member by name, but there are a few people I must specifically thank.

I would like to especially thank Janet Allopenna and Maria Hernandez for their support. Both have been instrumental in teaching me techniques in the lab and helping support my research. This work would not be possible without either of them.

Dr. Ashley Snider has been very helpful in managing mouse lines used for this project. Leiqing Zhang has also been very generous in helping me transport the mice.

Dr. Jean-Philip Truman has been very helpful in training me in experiments examining mitochondrial function as well as assisting with analysis of metabolomics data.

Dr. Chiara Luberto has been very helpful in discussing lipidomics data. She always gives more thorough and nuanced answers to my questions than I can even anticipate.

Dr. Mel Pilar Espaillat was very kind in offering advice and allowing me to utilize lab reagents and supplies that belonged to her.

Many other members and former members of the lab have trained me in techniques, including Dr. Justin Snider, Dr. Sitapriya Moorthi, Dr. Christopher Clarke, and Dr. Michael Pulkoski-Gross. Dr. Mohammad Salama, Dr. Daniel Canals, Dr. Kai Wang, and Dr. Masayuki Wada have also been very helpful in discussing data. Dr. Ben Newcomb has been very helpful in offering advice pertaining to lab work as well as the preparation of this Dissertation. Joe Bonica always provides insightful sports commentary during incubations.

The Stony Brook Lipidomics Core has been especially crucial to the competition of this project. I would like to specifically thank Izolda Mileva for working closely with me throughout my research as we developed new strategies for the Core to measure lipids from organelles and tissue types not common in our lab as well as developing strategies for measuring novel types of lipids.

I would like to further thank the Stony Brook Central Microscopy Imaging Center, especially Director Dr. Guowei Tian. Dr. Tian was very helpful in instructing me on utilizing Super-resolution Microscopy, live-cell imaging, and other tools in image analysis. I would further like to thank the Proteomics Core, including Irina Zaitseva, for assistance in metabolomics experiments.

I would like to thank the Stony Brook Program in Neuroscience for its continual support. Dr. Mary Kritzer has always been supportive and understanding of my concerns, and Odalis Hernandez is always timely and helpful in assisting with administrative manners.

I would like to thank the Medical Scientist Training Program for their continual support during my training at Stony Brook. Dr. Michael Frohman, Dr. Markus Seeliger, and Carron Allen have constantly supported me and helped keep me on track.

I would like to thank all the students from other labs with whom I have collaborated: Alex Jares, Michael Gurevich, Gregory Kirschen, and many others.

I would like to thank Dr. Tanvir Khan and Peter Dong for technical draining in DRG culture. Dr. Khan was extremely generous in offering his time and expertise in initially assisting me in learning DRG culture. Mr. Dong hosted me for DRG training at the University of Pennsylvania, and led the Dorsal Root Ganglia Culture Training session at Stony Brook. Day 1 had to be canceled due to an impending blizzard that caused my car to be stuck repeatedly in attempt to reach Nicolls Rd. Mr. Dong led a 12+ hour session on Day 2, altering his travel plans the following day. He also helped dig other cars that were stuck on the road out of the snow.

On a personal note, I would like to thank my girlfriend Mary for her constant support and interest in ceramide, so far as it is a common ingredient in many lotions. She was absolutely critical in formatting this document.

The text of this dissertation in part is a reprint of the materials as it appears in "Decreased ceramide underlies mitochondrial dysfunction in Charcot-Marie-Tooth 2F" in *The FASEB Journal*. The co-authors listed in the publication (Dr. Obeid and Dr. Senkal) directed and supervised the research that forms part of the basis for this dissertation.

Curriculum Vitae

Nicholas Urban Schwartz
75 Mud Rd, Setauket, NY 11733
734-355-8230
Nicholas.Schwartz@stonybrookmedicine.edu

EDUCATION

Stony Brook University, Stony Brook, NY

Medical Scientist Training Program (MD/PhD), exp. May 2020
Graduate GPA: 3.97/4.0

Duke University, Trinity College of Arts and Sciences, Durham, NC

BS in Neuroscience with Distinction & Philosophy, Minor in Biology, May 2012
Magna Cum Laude
GPA: 3.84/4.00

Stanford University, Stanford, CA

Summer College Program, 9 credits, Aug 2007
GPA: 4.10/4.00

PUBLICATIONS

Schwartz, NU, Linzer, R. W., Truman, J.-P., Gurevich, M., Hannun, Y. A., Senkal, C. E., & Obeid, L. M. (2018). Decreased ceramide underlies mitochondrial dysfunction in Charcot-Marie-Tooth 2F. *The FASEB Journal*, *32*(3), fj.201701067R. doi.org/10.1096/fj.201701067R

Leung, W, … **Schwartz, NU**, … Elgin, SCR (2017). "Retrotransposons Are the Major Contributors to the Expansion of the *Drosophila ananassae* Muller F Element.", *G3: GENES, GENOMEs, GENETICS*, 7(8), doi.org/10.1534/g3.117.040907

Leung, W, … **Schwartz, NU**, … Elgin, SCR (2015). "The Drosophila Muller F elements maintain a distinct set of genomic properties over 40 million years of evolution." *G3: GENES, GENOMEs, GENETICS,* 5(5), doi.org/10.1534/g3.114.015966

Corrado, T, Jacob, Z, Firor, A, Carrero, D, Rios-Dorio, E, Oladeru, O, Zhou, G, **Schwartz, N,** Riccio, G, Cavanaugh, S, Rowe, C, Gallagher, C (2013) Simulation in Medical School.

Nikam, V., Ng, C.L., Xu, T., **Schwartz, N**., Norton, D., Spana, E. (2011.5.2). Microarray analysis of Df(2L)ast2. (http://flybase.org/reports/FBrf0213601.html)

*Ellison, H, *Morgan, S, ***Schwartz, N**, *Sun, K (2012). Antifungal properties of plants in Costa Rica. *Vertices – Duke University Journal of Science and Technology***.** Vol 27. (*all authors contributed equally)

Schwartz NU, Zhong L, Bellemer A, Tracey WD. (2012). Egg laying decisions in Drosophila are consistent with foraging costs of larval progeny. *PLoS One*. 7:e37910. doi.org/10.1371/journal.pone.0037910

RESEARCH TALKS

Nov 2017 — Stony Brook Symposium in Neuroscience, Stony Brook, NY
Decreased Ceramide Underlies Mitochondrial Dysfunction in Charcot-Marie-Tooth 2F

Oct 2017 — Stony Brook MSTP Research Day, Setauket, NY
Decreased Ceramide Underlies Mitochondrial Dysfunction in Charcot-Marie-Tooth 2F

June 2017 — Program in Neuroscience Advanced Student Seminar, Stony Brook, NY
Altered ceramide generation in charcot marie tooth 2f

May 2017 — International Ceramide Conference, Port Jefferson, NY
Altered ceramide generation in charcot marie tooth 2f

Apr 2017 — American Academy of Neurology Annual Meeting, Boston, MA
Altered ceramide generation in charcot marie tooth 2f

Mar 2017 — 3MT Competition, Stony Brook University
Sphingolipids: A New Approach to Understanding Charcot Marie Tooth Disease

Mar 2017 — Department of Medicine Research Seminar, Stony Brook University
Decreased Ceramide in Charcot Marie Tooth 2F Mediates Mitochondrial Dysfunction

RESEARCH POSTER PRESENTATIONS

Apr 2017 — MSTP Research Day, Stony Brook University
Altered sphingolipid metabolism and mitochondrial dysfunction in Charcot Marie Tooth 2f

Apr 2017 — American Physician Scientist Association Meeting, Chicago, IL
Altered sphingolipid metabolism and mitochondrial dysfunction in Charcot Marie Tooth 2f

Nov 2016 — Society for Neuroscience, San Diego, CA
Altered ceramide generation in charcot marie tooth 2f

Oct 2016 — Stony Brook MSTP Retreat, Setauket, NY
The Role of Heat Shock Protein 27 and Lipid Metabolism in Charcot Marie Tooth 2F.

Jul 2016 — National MD/PhD Student Conference, Keystone, CO
The Role of Heat Shock Protein 27 and Lipid Metabolism in Charcot Marie Tooth 2F.

Apr 2016 — MSTP Research Day, Stony Brook University
The Role of Heat Shock Protein 27 and Lipid Metabolism in Charcot Marie Tooth 2F.

Nov 2015 — SBU Symposium in Neuroscience, Port Jefferson, NY
The Role of Heat Shock Protein 27 and Lipid Metabolism in Charcot Marie Tooth 2F.

Nov 2015 — Stony Brook MSTP Retreat, Setauket, NY
The Role of Heat Shock Protein 27 and Lipid Metabolism in Charcot Marie Tooth 2F.

Jul 2015 — RIKEN BSI Summer Program, Tokyo
The Role of Sphingolipid Metabolism in Charcot Marie Tooth Disease

Apr 2015 — MSTP Research Day, Stony Brook University
The Role of Heat Shock Protein 27 and Lipid Metabolism in Charcot Marie Tooth 2F.

Nov 2014 — Stony Brook MSTP Retreat, Setauket, NY
The Role of Heat Shock Protein 27 and Lipid Metabolism in Charcot Marie Tooth 2F.

Apr 2012 — Neuroscience Major Presentation Fair, Duke University
Egg laying decisions in Drosophila are consistent with foraging behaviors of larval progeny.

Mar 2012 — Drosophila Genetics Conference, Chicago, IL
Egg laying decisions in Drosophila are consistent with foraging behaviors of larval progeny.

Aug 2011 — Summer Undergraduate Research Fellowship, Rockefeller University
Characterizing oviposition behavior in the mosquito Aedes aegypti.

Apr 2011 — Trinity College Research Forum in Neuroscience, Duke University
Egg laying decisions in Drosophila are consistent with foraging behaviors of larval progeny.

Nov 2010 — Research Practicum Poster Presentation, Organization of Tropical Studies, Costa Rica
Anti-fungal Properties of Plants in Costa Rica.

Aug 2009 — Howard Hughes Undergraduate Research Fellowship Presentation, Duke University
Using Drosophila melanogaster egg-laying behavior as a model for decision making.

RESEARCH EXPERIENCE

Fall 2014-present Neuroscience Graduate Student, Lab of Dr. Lina Obeid

	Stony Brook University
	Role and Regulation of Sphingolipids in Neuropathy.
Summer 2014	Research Rotation, Lab of Dr. Bo Li
	Cold Spring Harbor Laboratory
	Using Optogenetics to Probe Circuitry of the Amygdala
Summer 2013	Research Rotation, Lab of Dr. Josh Dubnau
	Cold Spring Harbor Laboratory
	Effects of Ago2 in Sleep Deprivation in Flies
Summer 2012	Research Rotation, Lab of Dr. Alfredo Fontanini
	Stony Brook University
	Characterizing ethanol preferences in rats, learning basic electrophysiology techniques
Summer 2011	Summer Undergraduate Research Fellowship, Lab of Dr. Leslie Vosshall
	Rockefeller University
	Characterizing oviposition behavior in the mosquito Aedes aegypti.
Spring 2011	Research based course in Genomics, taught by Dr. Eric Spana
	Duke University
	Projects: Fosmid assembly, Array comparative genome hybridization, Analyzing next-gen reads for a mutation.
Fall 2010	Research Project, Organization of Tropical Studies, Costa Rica.
	Antifungal properties of plants in Costa Rica.
Summer 2009-12	Undergraduate Researcher, Work Study and Independent Study, Howard Hughes Undergraduate Research Fellowship, Lab of Dr. Dan Tracey
	Duke University

Egg laying decisions in Drosophila are consistent with foraging behaviors of larval progeny and *Functional Characterization of the Piezo gene in Drosophila melanogaster.*

TEACHING EXPERIENCE

Teacher's Assistant, Mind, Brain and Behavior
Stony Brook University School of Medicine, 2015

Teacher's Assistant, Molecular Foundations of Medicine
Stony Brook University School of Medicine, 2013

Teacher's Assistant, Foundations of Medicine
Stony Brook University School of Medicine, 2013-14

ACT Course Instructor
The Princeton Review, 2008

HONORS/AWARDS

Outstanding Manuscript of the Year Award, Stony Brook University Program in Neuroscience, 2017

Combining Clinical and Research Careers in Neuroscience – Selected Participant with Travel Award, Washington, DC, 2017

Travel Award to American Academy of Neurology Annual Meeting, Boston, MA— 2017

Stony Brook Three Minute Thesis Competition Finalist —2017

Stony Brook University Graduate Student Organization Distinguished Travel Award —2016

Travel Award to RIKEN Brain Science Institute Summer Program Lecture Course, Tokyo — 2015

Travel Award to NIGMS/UAB Metabolomics Workshop, Birmingham, AL — 2015

Travel Award to NIMH MD/PhD Meeting and Molecular Psychiatry Meeting, San Francisco — 2014

Phi Beta Kappa Society, Beta Chapter of North Carolina — 2013

Duke University Faculty Scholar Award Finalist — 2012

Duke University Dean's List With Distinction — Fall 2008, Fall 2010

Duke University Dean's List — Spring 2009, Fall 2009, Spring 2010, Spring 2011, Fall 2012

Graduation with Distinction in Neuroscience, Duke University — Spring 2012

Trinity College Research Forum in Neuroscience Fellow, Duke University — Spring 2011

AP Scholar with Distinction — 2008

National Merit Scholar Finalist — 2008

National Chemistry Olympiad Qualifier (1 of 10 students in region) — Spring 2007

CONFERENCES/MEETINGS

Oct 2017 — Meeting of the Minds, Stony Brook, NY

Apr 2017 — American Academy of Neurology Annual Meeting, Boston, MA

Apr 2016 — American Physician Scientist Association Meeting, Chicago, IL

Nov 2016 — Society for Neuroscience, San Diego, CA

Oct 2016 — Meeting of the Minds, Stony Brook, NY

Nov 2015 — Meeting of the Minds, Stony Brook, NY

Jul 2015 — RIKEN BSI Summer Program, Tokyo, Japan

Jun 2015 — NIGMS/UAB Metabolomics Workshop, Birmingham, AL

Nov 2014 — Molecular Psychiatry Meeting, San Francisco, CA

Nov 2014 — NIMH MD/PhD Student Conference, San Francisco, CA

Nov 2013 — American Medical Association, Medical Student Section, Interim Meeting, National Harbor, M

Mar 2012 — Drosophila Genetics Conference, Chicago, IL

Jan 2011 — Duke University Winter Forum: *Pandemic 2011*, Durham, NC

PROFESSIONAL MEMBERSHIP

Society for Neuroscience
American Academy of Neurology
American Medical Association
Medical State Society of New York
Suffolk County Medical Society
American Medical Student Association
Genetics Society of America

EXPERIENCE ABROAD

Duke in Greece — The Birth of Reason in Ancient Greece, 1 credit – 4 weeks

Duke in Oxford — Science, Ethics, and Society, 2 credits – 6 weeks

Organization of Tropical Studies, Costa Rica — Global Health, 4 credits – 15 weeks

RECENT EXTRACURRICULAR ACTIVITIES

Stony Brook SOM Student Interest Group in Neurology, Co-President (2013-14)

Stony Brook SOM Honor Code Committee (2012-16, full term)

Stony Brook Mobile Medical Education Committee (2015-present)

Stony Brook SOM AMA — Recruitment Chair (2013-14), First-Year Committee (2012-13)

Stony Brook SOM Curriculum Reform, Committee Member on Academic Resources – (2013-15)

Chapter 1

SPHINGOLIPID METABOLISM IN NEUROPATHY AND NEURODEGENERATION

Chapter 1: Sphingolipid Metabolism in Neuropathy and Neurodegeneration

Overview of Sphingolipid Metabolism in Neurodegeneration

The first isolation of sphingolipids was performed from brains. In fact, many of the first discovered classes of sphingolipids carry names that highlight their early origins, such as sphingomyelin (SM) and cerebrosides (1). J.L.W. Thudichum named these discovered lipid species with a sphingosine background after the Egyptian Sphinx because of their mysterious nature (2). Since 1884, we have still not completely answered the riddle of the role of sphingolipids in neuropathy, although studies from the past 100 years have yielded a tremendous wealth of knowledge.

Sphingolipids have been linked to almost every major cellular pathway and have been found to have increasing relevance in almost every major disease state (3). The family of sphingolipids contain a large diversity of individual species which have poor water solubility and are constantly in a state of rapid flux. These properties have made the study of sphingolipids traditionally difficult for groups not especially focusing on sphingolipid metabolism. However, foundational advances in identifying all the key metabolic enzymes, development of a variety of animal model systems, technical progression such as advancing liquid chromatography—mass spectrometry (LC/MS), and development of imaging modalities such as matrix-assisted laser desorption/ionization (MALDI) and positron emission tomography (PET) have made research involving sphingolipids accessible to more scientists. As such, we have rapidly increased our understanding of sphingolipid dysregulation in disease (3).

The sphingolipid pathway exhibits intricate regulation and interacts with a complex variety of biological pathways; thus, it is able to exert a multiplicity of effects (4). Moreover, increasing evidence has clarified that ceramide serves as a family of distinct molecules with closely related structures but oftentimes distinct functions. Multiple connected “hubs” of ceramides located in distinct compartments coordinate intracellular sphingolipid metabolism (5). These hubs organize the conversion of ceramide into many types of intermediates with structural and functional roles in the cell.

Ceramides are converted to other more complex sphingolipid species, such as glucosylceramide (GlcCer), sphingomyelin (SM), acylceramides, and ceramide-1-phosphate by modifications at the 1-hydroxyl position. Species-specific enzymes exist to hydrolyze these molecules back to ceramide, which can be deacylated to form sphingosine, which can then be phosphorylated to form sphingosine-1-phosphate (S1P). S1P can be either degraded by S1P lyase (SPL) into free aldehydes and ethanolamine phosphate or converted back to sphingosine (3). Ceramide accumulation has been demonstrated to induce both apoptotic cell death and promote differentiation in a variety of neuronal cells. These differential effects are dependent on cell type, developmental stage, ceramide concentration, and cellular location of action. S1P, while traditionally associated with proliferation, has also been shown to induce neurite retraction and apoptosis (6). There are six isoforms of ceramide synthase (CerS), a set of six enzymes each using specific fatty acyl CoAs to catalyze N-acylation of sphingoid bases in generation of ceramide. All CerS except CerS3 are expressed in the central nervous system (CNS), with CerS1 expression being the highest. CerS2, however, is

most highly expressed in the peripheral nervous system (PNS) and is necessary for proper myelin organization (7).

More complex sphingolipid species include GlcCers and other glycosphingolipids (GSLs or glycolipids), whose expression is tied to both cell type and developmental state and have shown to be highly important in the nervous system (8). Hundreds of distinct GSLs can be generated, causing a tremendously powerful array of different signaling molecules (9). All GSLs are dependent on GlcCer generation, which is catalyzed by glucosylceramide synthase (GCS), also known as Ugcg (UDP-glucose:ceramide glucosyltransferase). This is thought to occur from vesicular transport of ceramide to the *cis*-Golgi, whereas transport by CERT to the *trans*-Golgi is typically associated with SM production. Contrarily, subsequent addition of a galactose moiety to GlcCer generates lactosylceramide (LacCer), which can be further modified with additions of sialic acid or N-acetylgalactosamine (GalNAc) groups to a saccharide chain by a network of further enzymatic glycosyltransferase reactions that act in parallel pathways in ganglioside generation (8–10). The relative expression of SialT-1, SialT-2 and SialT-3 compared to GalNAc-T can affect the predominance of species made in each pathway (11). Notably, addition of sialic acid to lactosylceramide generates GM3. GSLs and SM are thought to be highly enriched in “lipid raft” domains in the plasma membrane (12). GSLs are essential for brain development, as mice deficient in GCS are non-viable (13), and neuronal specific deletions in mice result in neurons with decreased axon branching and dendritic complexity, and impairment of cerebellum and peripheral nerve function (14). Moreover, loss of the enzyme necessary for producing

GalCer and sulfatides, results in many severe neural defects, presumably due to abnormal myelin (15).

Gangliosides are defined as GSLs that contain at least one sialic acid residue and comprise approximately 1% of all lipids in the brain and typically exist in the plasma membrane. Over 95% of human brain gangliosides consist of four species: GM1, GD1a, GD1b, and GT1b. The ceramide backbone typically contains a sphingosine chain that is 18 or 20 carbons in length and a saturated acyl chain. These chains derived from ceramide extend within the outer leaflet of the plasma membrane, allowing species-specific glycan chains to extend into the extracellular space and interact with other membrane molecules in the same or adjacent cells (16, 17). Gangliosides have been shown to be particularly important for recognition of myelin, a membrane that wraps around and insulates nerves and serves to enhance speed of signal transmission and nurture axons**.** In human development, brain ganglioside expression increases in the third trimester through the second year of life, coincident with active myelination. Myelin-associated glycoprotein (MAG) is a lectin receptor with high binding affinity to sialic acids, specifically in GD1a and GT1b, but not with other gangliosides with a different saccharide terminus. Diseases in ganglioside enzymes are typically associated with defective catabolism, including many of the lysosomal diseases, although defects of enzymes involved in ganglioside synthesis, such as mutations in *GM3 synthase*, have also been reported to cause clinical syndromes (16–18). On the other hand, administration of GM1 ganglioside has shown to protect neurons from many different

stresses in laboratory settings, although clinical trials have largely failed to show strong benefits in treating neurodegenerative disease (19).

Overall, the sheer diversity in structure and functions of sphingolipid molecules in the nervous system underlies the complexity of sphingolipid signaling. It is an evolutionary marvel, that no doubt draws some of the most ambitious scientists to the field. Careful dissection of particular species' involvement in select cellular localizations in specific cell types at certain developmental stages in distinct conditions will be absolutely necessary to draw the most accurate conclusions and progress the field. Nevertheless, this complexity also provides optimism that precise alterations in sphingolipid homeostasis can be explicitly identified, and selective therapeutic strategies can be developed with great potential efficacy.

Amyotrophic Lateral Sclerosis

Research involving sphingolipid metabolism has not been as extensively studied in amyotrophic lateral sclerosis (ALS), perhaps due to conflicting results in early studies. One study did not find changes in the major ganglioside species in ALS patient spinal cords besides the presence of three additional gangliosides (20). Another study reported increases in ceramide species in patient spinal cords and Cu/Zn-SOD model mice but hypothesized that these changes were due to increased oxidative stress and directly increased neuronal vulnerability to cell death (21). However, other early studies examining muscle from ALS patients reported twice the normal amount of sialic acid content (22), varied levels of different gangliosides in diverse brain regions. Notably there was decreased sialic acid selectively in the motor cortex (23), and elevated CSF

antibodies to almost all major gangliosides (24, 25). Evidence concerning serum ganglioside antibodies in disease is mixed (25).

However, recent studies suggest that there are alterations in GSLs, which should prompt a reexamination for novel pharmacological targets. Sphingolipid involvement was identified by two concordant studies in 2015 using patient samples and mouse models that both generally demonstrated increases in ceramide, GlcCer, and many downstream GSL species as well as the corresponding enzymes regulating their production and degradation (26, 27). These studies suggested that GCS inhibitors could have potential deleterious effects. However, there were substantial differences in the results of both studies which leave many questions unresolved.

Dodge *et al*. used patient and G93A mutant SOD1 (superoxide dismutase 1) mouse spinal cord tissue and further demonstrated that GCS inhibition via a small molecule applied to the CNS in the mouse model shortened lifespan and exacerbated the disease course whereas GM3 administration alleviated the disease course (26). These results suggest that the accumulation of GlcCer observed in ALS may be a compensatory response that is not directly toxic. This group separately analyzed gray matter and white matter in patient samples and observed increased sphingolipid species in both, particularly in gray matter. The variation between spinal cord regions used for analysis and increased precision from using LC/MS instead of thin-layer chromatography (TLC) isolation and quantification may explain why the aforementioned study did not observe large significant differences (20, 26). Interestingly though, many sphingolipids were decreased in symptomatic and partially paralyzed mice, although as

paralysis progressed these lipids tended to increase more. GM3 was notably increased in symptomatic mice, but GM3 was one of the few species not substantially increased in human spinal cord tissue (26). These results further suggest that increases in GlcCer and gangliosides may be compensatory as primary pathogenesis progresses. Gene expression profiling has shown hexosaminidase induction near symptom onset in G93A SOD1 mice and in patient spinal cords, perhaps explaining the lack of increase of GM3 in mice (26, 28). The mouse model also exhibited decreases in some sphingolipid enzymes in contrast to human samples which were typically elevated in gray matter (26). The authors suggest that the disease course may result in an initial decrease in ceramide, with later increases in ceramide and further shunting of ceramide to GlcCers to prevent accumulation of other more toxic ceramides. However, many questions still remain, as this does not explain the directly beneficial effects of GM3 administration, why ceramides accumulate later in the disease in patients, and the origin of these ceramides.

Similar to Dodge *et al*., Henriquez *et al*. also demonstrated that GCS inhibition in the PNS rather than the CNS seems to worsen the ALS phenotype by delaying regeneration of motor units and motor recovery in mice (27). Furthermore, this group showed that GCS is upregulated in muscle in the ALS model G86R SOD mice and patient tissue, leading to increases in GlcCer and many GSL species. As mechanically-induced limb and sciatic nerve injury produced similar increases that were not observed with GCS inhibition, this group also hypothesized these species were likely protective and induced in a compensatory mechanism. However, they did not observe a difference

in spinal cord GlcCer or GCS expression, and while GM1a ganglioside levels were increased, many spinal cord sphingolipids were significantly decreased. While these groups employed different mouse models, the time points used were similar, so the disparity in spinal cord sphingolipids should warrant further investigation.

Both of these studies implicated potential pharmacological therapies targeting GSL metabolism as another potential treatment strategy for ALS, and Hernandez *et al*., have subsequently followed up with evidence that Conduritol B epoxide (CBE), a partial inhibitor of glucocerebrosidase, decreases many measures of degeneration in the ALS mouse model. CBE delayed onset of ALS and improved motor function, increased neuromuscular junction function, and helped restore expression of genes important in axonal function. An *in vitro* model of neuromuscular junctions also showed beneficial effects of treatment (29).

Hereditary Sensory and Autonomic Neuropathy I

Mutations in the initial enzyme of *de novo* sphingolipid synthesis directly cause a form of inherited neuropathy called hereditary and sensory autonomic neuropathy type I (HSAN1) (30, 31). HSANs are a group of clinically heterogeneous disorders that result in progressive loss of sensation in the distal limbs that often progresses with age. Loss of pain and temperature with shooting and burning pain in the distal limbs is an especially prominent symptom, and can result in the development of many lesions on the distal limbs. Despite the name of the disease, many patients also exhibit loss of motor function (32). HSANs are categorized from I-V based on clinical symptomatology; HSAN1 most often presents in young adulthood to adulthood initially with loss of

sensory symptoms, progressively worsens throughout life with weakness, neuropathic pain, and skin ulceration (32, 33). A wide array of other symptoms can rarely occur in HSAN1, such as juvenile cataracts, retinal detachment, mental retardation, and vocal cord paralysis (34, 35). Symptoms are often most severe in men (32, 33). In 2001, multiple groups simultaneously discovered three point mutations occurring at the C133 and V144 residues of *SPTLC1* that were responsible for causing HSAN1 and caused an increase in GlcCer synthesis (36, 37).

SPTLC1 is one of three genes encoding the subunits of the enzyme serine palmitoyltransferase (SPT). SPT is the preliminary enzyme in sphingolipid synthesis, located the outer member of the ER, responsible for condensing serine and palmitoyl CoA to form a 3-ketodehydrosphinganine intermediate. This species can then subsequently be converted by a series of enzymes to ceramide and other more complex sphingolipids. SPT consists of dimers of LCB1 and either LCB2 or LCB3 subunits, which in humans are coded for by the *SPTLC1*, *SPTLC2*, and *SPTLC3* genes, respectively (38–40).

Subsequent follow-up studies using yeast, Chinese hamster ovary (CHO) cells, and patient-derived lymphoblasts, on the contrary, suggested that these mutations decreased the activity of both of the LCB1 and LCB2 subunits of SPT as a dominant effect, although reports were mixed whether this actually caused a decreased production of many sphingolipid species. However, the mutants still bound wild-type (WT) LCB2 subunit, suggesting that the autosomal dominant pattern of inheritance was due to dominant-negative effects due to competitive inhibition of the otherwise

functional LCB2 subunits (41–43). The lack of change in sphingolipid levels in lymphocytes from patients and a mutant mouse model demonstrating neuropathy with a similar disease course to humans suggested that an abnormal species could accumulate (43, 44). Further clinical reports discovered other mutations and detailed great variability in penetrance, age of onset, and presence of motor symptoms (34, 45, 46), but the cause of pathology remained elusive.

This remained uncertain for many years, until another set of papers were released, suggesting that these mutations altered SPT's catalytic activity, causing it to incorporate other amino acids and produce abnormal 1-deoxysphingoid bases (35, 47–51). The mutations effectively altered SPT's substrate specificity, causing SPT to increasingly incorporate alanine and glycine with acyl-CoA chains; it is debatable whether the mutants cause SPT to have an explicitly increased affinity for alanine (K_m) or increase the enzymatic activity of this reaction (V_{max}) (49, 50). These amino acids were correspondingly used to produce 1-deoxysphinganine (deoxySA) and 1-deoxymethylsphinganine, both of which are formed because they lack the hydroxyl group of serine. Deoxysphingoid bases were elevated in the plasma of patients and sciatic nerve of mutant mice and decreased neurite formation and length in dorsal root ganglia cultures, suggesting that deoxysphingoid bases may play a pathological role in HSAN1. Deoxysphingoid bases can accumulate as the lack of hydroxyl group prevents addition of a phosphate group to the sphingoid base, which both inhibits the conversion of ceramide to more complex sphingolipid species and its degradation by SPL. Moreover, these studies showed that the mutations did not alter the total level of

sphingolipids. These deoxysphingoid bases were similarly discovered to accumulate in the inhibition of *de novo* ceramide synthesis and have toxic effects on many types of cells, potentially from increasing ER stress (50, 52–54).

Other groups have also confirmed that SPTLC2 mutants can cause HSAN1. Rotthier *et al*. demonstrated that mutations in *SPTLC2* can also cause HSAN and similarly reduce SPT activity and increase deoxySA (51). Other genetic screening studies have confirmed these findings, but failed to find mutations in SPTLC3 (55, 56). SPTLC3 may not be highly expressed in neurons, so its lack of involvement should not be surprising (39). Since this discovery, there are four other genes currently thought to cause HSAN-I, bringing the total to six: SPTLC1, SPTLC2, ATL1, ATL3, RAB7A, and DNMT1 (33, 57). A screening analysis of HSAN patients in 2012 concluded that SPTLC1 mutations were the most common cause of HSAN1 (58).

These results suggested that therapeutic strategies could focus on altering amino acid intake to prevent toxic deoxySL accumulation. HSAN1 mutant mice demonstrated decreased deoxysphingoid base accumulation and improvement in symptoms with a diet that contained as little as 10% additional serine. Decreases in deoxysphingoid bases were also observed in a small patient cohort using serine supplementation. Conversely, alanine supplementation increased deoxysphingoid base levels and worsened signs of neuropathy (59). Alanine supplementation also increased deoxysphingoid bases and worsened morphological defects in synapses in a mutant SPTLC1 *Drosophila* HSAN1 model, with serine co-administration partially rescuing many of these defects (60). Serine supplementation has also been shown to decrease

deoxysphingoid bases in HSAN1 patients with *SPTLC2* mutations (61), whereas contrarily, serine deprivation elevates deoxysphingolipids (deoxySLs) (62). Studies examining serine and alanine administration on cells transfected with a variety of mutations have shown consistent effects (63), suggesting that serine administration or alanine reduction in diet may be therapeutic for all patients. Finally, a Phase I clinical trial has proved safety and a potential improvement in signs of neuropathy in a small patient population, providing hope for potential treatment (64).

Other results have tried to further examine the biological consequences of increased deoxySLs. Building on the findings of increased ER stress by Gable *et al*., Oswald *et al*. also observed that ER function was disturbed by the mutant SPT causing dysfunction in ER–Golgi trafficking, and neuronal function could be rescued by increasing ER–Golgi trafficking by expressing Rab1 (41, 60). Decreased ER–Golgi trafficking has also been demonstrated with knockout of ORM proteins, which are known regulators of SPT (65). Altered expression of ER proteins have also been reported in patient lymphoblasts and cell models (66–68). DeoxySA is thought to be toxic and cause apoptosis and necrosis by altering intracellular signaling and disrupting the actin cytoskeleton via activation of Rac1 (49, 69). Lipid droplets, tiny organelles that facilitate the intracellular transport of lipids and some membrane proteins, have been shown to be increased in HSAN patient-derived lymphoblasts (70, 71). Additional work will need to further investigate the effects of downstream metabolites, deoxydihydroceramides (deoxydhCers) and deoxyceramides (deoxyCers), and determine how they exactly contribute to biological changes associated with

deoxysphingoid bases. DeoxySA can induce ceramide synthase 5 expression and deoxydihydroceramide is thought to exert toxic effects observed from deoxySA (69). Recently, CYP4F enzymes have been reported to hydroxylate deoxySLs, suggesting deoxySLs may be further metabolized and should not necessarily be considered as "dead end" metabolites. Induction of CYP4F enzymes may have therapeutic value for HSAN1 patients (72).

Deoxysphingoid bases and their subsequent metabolites have also been suggested to be toxic to mitochondria when elevated. HSAN1 patient lymphoblasts demonstrate swollen mitochondria with discontinuous outer membranes and abnormal cristae (71). Mitochondria further demonstrated an altered expression of various proteins (73). DeoxySA localizes to mitochondria and causes mitochondrial structural defects, including swelling, fragmentation, and loss of internal cristae, as well as functional defects in decreased respiratory capacity and reduced cellular ATP levels. Inhibition of ceramide synthase with fumonisin B1 rescues these defects, suggesting deoxydhCers or deoxyCers may mediate the observed mitochondrial toxicity (54).

Attempts to correlate the location of mutations of SPTLC1 and SPTLC2 with clinical and biological phenotypes have suggested that mutations in the active site are associated with a mild phenotype whereas mutations on the surface of the protein are associated with a severe phenotype (63). Mutations with worse clinical phenotypes were associated with increased utilization of C20 sphingoid bases instead of C18 bases in HEK293 cells. Contrary to earlier studies, Bode *et al*. did not observe a decrease in SPT activity in any of the 17 mutations they expressed in HEK293 cells, and in fact,

observed that 3 mutations actually increased SPT activity (63). Further, Bode *et al*. observed that some mutants did not demonstrate an increase in deoxySL generation in response to fumonisin B1. Taken together, these results suggest there is a great degree of heterogeneity in disease-causing mutations, and that these mutations may result in clusters biological and clinical phenotypes based on the structural location of the mutation. Going forward, further examination of the effects of different mutations and implicating the role of deoxydhCers and deoxyCers in HSAN1 will be critical to improve our understanding of this disease.

Charcot-Marie-Tooth Disease

Ironically, mutations in what could be considered the *last* enzyme in the sphingolipid pathway are also capable of causing a similar neuropathy. SPL is responsible for degrading sphingolipids by cleaving S1P into a long-chain aldehyde and phosphoethanolamine (74). Mutations in SPL were recently discovered in patients with Charcot-Marie-Tooth disease (75), the most commonly inherited neurological disorder representing a heterogeneous array of mutations that cause motor and sensory loss in patients, typically in young adulthood to older age (76). An I184T mutation that caused partial protein degradation and an S316* mutation that triggered nonsense-mediated mRNA decay of SPL were both observed in two related patients. These patients had a sphingosine:sphinganine ratio that was approximately increased by 4 times. However, the level of S1P was only very moderately elevated, suggesting that this deficiency may cause a backup of other sphingolipid intermediates. The authors also showed that decreased expression of SPL in *Drosophila* neurons alters synaptic architecture (75).

While S1P is traditionally viewed to behave antagonistically to ceramide, S1P has been shown to have both proliferative and apoptotic effects in different types of neural cells. Studies have shown a relatively high level of phosphorylation of sphingoid bases species in neurons, suggesting that S1P is functionally important in nervous tissue, and altered SPT activity in feedback mechanisms to regulate sphingolipid synthesis (77). Previously, deficiency of SPL has been shown to decrease degradation of APP in lysosomes, suggesting that its impairment may play a role in Alzheimer's (78). While sphingosine kinase (SK) 1 and SK2 deficient mice are embryonic lethal due to neurodevelopmental and vascular defects (79), SPL deficient mice can demonstrate tremendous relative increases in S1P and sphingolipids (80). The relatively moderate increase in S1P observed in the CMT mutant mice drastically differs from neuronal cultures derived from SPL KO mice that demonstrate up to 2000% increases in S1P (75, 80). However, SPL KO mice exhibited slightly larger relative increase in Sph (sphingosine) than dhSph (sphinganine), similar to increased Sph:dhSph ratio reported in the CMT mutant mice. Interestingly, despite impaired degradation, and backup of intermediates, levels of ceramide, SM, GlcCer and various gangliosides were largely unaffected in SPL KO mice, besides decreases in some dhCer and dhSM species, due to decreased *de novo* synthesis (80). A different study using mouse serum and liver tissue, in contrast, observed quite substantial elevation of many ceramides and SMs, and even greater elevations in sphingoid species (81). An earlier study by the same group determined that the increased S1P that is toxic to these mouse cerebellar cells is specifically derived from SK2 action rather than SK1 (82, 83). Moreover, due to the

results from their model, the authors argue that increases in ceramides are less responsible for the neuronal degeneration. SK2 is typically localized to the ER as opposed to the plasma membrane like SK1, and studies suggest SK2-derived S1P may also exhibit an ER localization (83–85). As SPL has been shown to be localized to the ER, this suggests that the minor increases in S1P observed in CMT could potentially be due to accumulation of S1P at the ER (86). The origin of S1P alters its biological effects, and backup of S1P in nerve cells could alter the relative cellular distribution of S1P produced. Compartment specific effects are a common theme for many species of sphingolipids (5). Since SPL KO mice had decreased *de novo* synthesis, similar hypotheses should be entertained for other sphingolipid species, even if their total levels do not appear altered.

As HSAN and CMT present very similarly, it should be expected that there will be more reports of defects in *de novo* synthesis in these and other related neuropathies. These studies may reveal common intracellular mechanisms from neuropathies resulting from distinct mutations. Focus will likely be directed at investigating potential alterations in and effects of deoxySLs, particularly in the mitochondria.

Friedreich's Ataxia

Two recent studies have suggested that there is an increase in sphingolipid synthesis in Friedreich's ataxia using two different animal models. In Friedreich's ataxia, mutations in *Frataxin (FXN)* cause a progressive degeneration of nerves in the spinal cord and PNS, causing problems with ambulation, heart disease, diabetes, and other chronic conditions. The authors showed that loss of the *FXN* gene through a mutation in

Drosophila is lethal before animals reach the adult fly stage, including when the mutation is only expressed in neurons, glia, and muscles. To study the effects of the mutation in the adult fly nervous system, the authors generated mosaic mutant clones of adult photoreceptors, in which they observed an increase in lipid droplets in glial cells. The authors observed that the mutation causes an accumulation of iron in the nervous system, which successively increased sphingolipid synthesis. Moreover, there were elevations in dhSph and sphingosine in larva; ceramide and dhCer were also elevated. According to the authors' model, increased synthesis of sphingolipids activates 3-phosphoinositide dependent protein kinase 1 (Pdk1) and myocyte enhancer factor-2 (Mef-2), altering Mef-2's role in regulating transcription. However, artificially decreasing sphingolipids by RNA inhibition or pharmacological inhibition, or similarly reducing iron ore Pdk1/Mef-2 activation, decreased symptoms (87), suggesting the increases in sphingolipid species are involved in the mechanism of pathogenesis. Similar results were soon after reported by the same group using a mouse model with decreased *Fxn* expression, which allowed for a more nuanced investigation of FXN's effects on the nervous system. These mice displayed many signs of motor dysfunction, neuronal damage in the brain, and signs of iron accumulation and increased expression of Pdk1 and Mef-2. However, relative changes in sphingolipids were reported for human heart tissue but not nervous system tissue in neither mice nor humans. Many ceramide and dhCer species, as well as dhSph and Sph were increased, although very long chain ceramides and dhCers did not seem to be affected (88).

These studies have suggested that increased sphingolipids are involved in the pathology of Friedreich's ataxia, although their exact role in causing neuronal and cardiac pathology remains unclear. Previous studies in yeast have also provided some evidence that high iron can increase sphingolipids and decreasing sphingolipid synthesis can alleviate this toxicity (89, 90). A recent study on cystic fibrosis also demonstrated that C4-ceramide is capable of autophosphorylating Pdf (91). However exactly which sphingolipid species are altered by iron, the mechanism of how this occurs, particularly in mammalian cells, and how these lipids cause changes in downstream signaling in Friedreich's ataxia, remain unknown. Another consideration that future studies will need to address will be to profile changes in different types of tissues and cells. Levels of different species can be highly tissue specific, so investigation of mouse model and clinical nervous system samples will be vital for understanding effects in dysregulation. Likewise, for the research community to better understand primary alterations in sphingolipids, absolute values of individual species, or at least totals, should be provided. While showing the full profile of relative changes in different ceramides and sphingoid bases in heart tissue gives insight into particular species that may be important in the disease, it does not convey overall trends as were shown in *Drosophila.* Neither of these studies measured sphingolipids in nervous system tissue, which will be important going forward. Finally, given the wide variation in results of potential iron accumulation from different studies on Friedreich's ataxia, it is worthwhile for other groups to replicate sphingolipid studies in other model systems to determine if the reported increases are robust.

Spinal Muscular Atrophy with Progressive Myoclonic Epilepsy

Spinal Muscular Atrophy associated with progressive myoclonic epilepsy (SMA-PME) has been reported as an autosomally dominant, adult-onset disorder as early as 1979 (92), and reports of patients even exist earlier in the decade (93). However, SMA-PME was only first clinically identified as a distinct etiology from SMN1-induced SMA in 2002, with a similar onset in childhood with severe symptoms (94). Investigation of the bovine form of spinal muscular atrophy (SMA), which was known to map to a distinct location from the *SMN* gene as typically seen in humans, uncovered a point mutation in the gene responsible for producing 3-ketodihydrosphingosine reductase in the *de novo* pathway of ceramide genesis and inhibited enzymatic activity (95).

Subsequently, SMA-PME was linked to a point mutation (with deletion potentially in occurring in the other allele) inherited in an autosomal recessive manner in *ASAH1* (N-acylsphingosine amidohydrolase 1), which reduced acid ceramidase activity to about a third of normal in patient fibroblasts (96). However, this T42M mutant did not affect splicing nor *ASAH1* expression. Furthermore, transfection of the mutant gene into human fibroblasts lacking acid ceramidase function caused similar reductions in ceramide levels compared to transfection wild-type acid ceramidase, although there was decreased expression of the alpha-subunit. Morpholino knockdown of *ASAH1* in zebrafish caused structural defects with curving of the body, increased cell death in the spinal cord and decreased motor neuron branching, with similar acid-ceramidase activity and unaffected ceramide content, similar to human fibroblast data, further suggesting *ASAH1* mutations as a causative factor of SMA-PME.

ASAH1 deficiency is also a known cause of the more severely presenting Farber's Disease, which typically initially presents with pathology in multiple organs by 4 months of age, including notably the triad of arthritic joint deformation, subcutaneous nodules (lipogranulomas), and laryngeal involvement causing hoarseness, and leads to death by 5 years. SMA-PME, on the other hand, typically presents after 3 years of age with pathology restricted to the CNS, and results in death after 12 years (96). It is suspected that a less robust deficiency of acid ceramidase with greater residual function may cause the reduced phenotype in SMA-PME, especially since Farber Disease often presents with hypotonia and signs of neuronal degeneration later in the disease course (96–98). Since total ceramide levels are not altered in SMA-PME, the cause of pathology is unknown, although it is possible that compensation from other enzymes in the sphingolipid network accommodate for the decreased acid ceramidase activity. This compensation, alternatively, could be responsible for the pathology.

These results have ushered in many other studies, in total identifying 11 individuals with SMA-PME as recently as 2016, as reviewed by Topaloglu and Melki (99). In all but one identified patient, lower motor degeneration is progressive and precedes epileptic incidents between 2.5 and 6 years, with patients notably having difficulties in gait, changing positions, and decreased deep tendon reflexes, progressing all the way to respiratory insufficiency. By 12 years of age, myoclonic, along with atonic and absence seizures present along with EEG patterns consist with epilepsy, however any cognitive impairment is relatively mild. Systemic symptoms in skin and joints that are typical in Farber disease are generally not observed (99).

However, one recent case report identified a patient with in-frame and missense *ASAH1* mutations inherited from parents presenting at 3 years of age initially with polyarticular arthritis and later at 5 years with progressive muscular weakness, but a lack of epileptic seizures or myoclonic jerks. Interestingly, patient leukocyte acid ceramidase levels were less than 5% of those in the parents, which is similar to results seen in Farber disease but represents a much greater reduction than observed by Zhou *et al*. in SMA-PME (96, 100). It is possible that reduced *ASAH1* expression resulted in accumulation of sphingolipids that imparted pro-inflammatory effects similar to Farber disease, although sphingolipid species were not analyzed in the patient. It is also conceivable that pro-inflammatory sequelae, such as lipogranulomas, are only observed with sphingolipids that are elevated over certain thresholds, whereas decreased ceramidase activity may bestow apoptotic effects. These results suggest that SMA-PME due to *ASAH1* mutations may exist more on a spectrum with Farber disease than previously thought (100).

Further supporting heterogeneity in clinical presentation caused by mutations of *ASAH1*, another patient initially presented with atonic and absence seizures—motor neuron degeneration was only investigated and confirmed as causing proximal muscle weakness once mutations in *ASAH1* were identified. Interestingly, similar to data from Teoh *et al*., patient fibroblasts also demonstrated a decrease to less than 5% of normal acid ceramidase activity. Furthermore, patient fibroblasts showed over twice as much total ceramide. It is notable that this patient presented with K152N and G284X mutations occurring in the beta-subunit of ceramidase, and only a minor level of this

subunit was expressed. It is unknown if either of these dual mutations cause the delayed motor involvement, or if the mutations impart an additive effect on pathophysiology. Given the recent discovery of *ASAH1* and lack of other similarly presenting patients, it is also unknown if there are any predisposing factors that may cause a similar initial presentation. However, increased awareness of *ASAH1* as a cause of PME-SMA should lead to further surveillance, especially in patients presenting with seizures or motor neuron disease and polyarticular arthritis (101).

Nervous system involvement in Farber disease has been traditionally difficult to study given the rare prevalence of the disease and difficulty in generating a viable mouse model. However, a recent study specifically examined CNS defects in a viable homozygous mutant *ASAH1* Farber mouse model, and determined elevations of many sphingolipid species, particularly with a 100-fold increase in hydroxyl-ceramides. These mice seemed to display many motor defects, such as decreased movement, strength, and coordination. They pathologically present with granuloma-like inclusions similar to those seen in other tissue types and incur abnormal accumulations of microglia and macrophages particularly in cerebellum (102, 103).

While *ASAH1* mutations involve an enzyme involved in degradation of ceramide, PME-SMA has also recently been discovered to be caused by mutations in Ceramide Synthase 1 (CerS1), one of the six isomers of CerS necessary for the *de novo* synthesis of ceramide species selectively using a variety of acyl chain lengths (104). Homozygous H183Q mutations result in decreased CerS1 activity, producing decreased levels of C18-ceramide, which is thought to increase endoplasmic reticulum stress (104–106).

These mutations are believed to underlie a form of PME with cognitive impairment (107), which is also thought to occur with heterozygous CerS2 deletion that predominantly decreases very long-chain acylated ceramides and sphingomyelins (C24:0 and C26:0) (108). CerS1 is generally thought to be the most highly expressed isoform in the nervous system (109). Naturally occurring CerS1 mutations can cause a loss of catalytic activity, and experimentally induced mutations can cause a loss of protein expression in mice and similarly produce a neuronal phenotype with accumulation of lifofuscin and ubiquitination, Purkinje cell degeneration and resulting ataxia, depletion of all major classes of gangliosides in the brain, and motor defects (110, 111). Similarly, CerS2 KO mice present also present with a neural phenotype similar to PME with brief periods myoclonic jerks followed by loss of posture that were associated with abnormal electroencephalogram (EEG) activity. This is thought to be due to observed encephalopathy characterized by progressive loss of myelination, degeneration, and formation of microcysts in the cerebellum, and vacuolization and gliosis occurring throughout, especially in motor cortex, cingulate gyrus, retrosplenial cortex, thalamus, and anterior and posterior colliculi (112, 113). Structural defects of myelination of peripheral nerves were also observed in the PNS (112).

These groups have postulated that the aforementioned defects are likely due to loss of GalCer and ceramide-derived gangliosides necessary for nervous system development and maintenance (111, 113), although other groups have more recently suggested that neurodegenerative defects, at least as observed in CerS1 KO mice, may result from accumulation of sphingosine. CerS2 overexpression suppressed pathology

in CerS1 KO mice, potentially by decreasing abnormally increased levels of free sphingoid bases without rescuing the deficiency in C18 ceramide levels (114). These long-chain sphingoid bases induce neurite fragmentation in cultured cells at levels similar to those observed with CerS1 KO (114). Given the complex cell and tissue specific effects and compensatory mechanisms induced by artificially altering the sphingolipid network, it is possible multiple specific species may be involved.

Providing additional evidence for the dysregulation of CerS in neurodegenerative disorders with epilepsy, another study involving patients with a variant of juvenile neuronal ceroid lipofuscinosis (NCL), a neurodegenerative disease presenting in children, were shown to harbor mutations in *CLN5*, causing a truncated CLN5 protein. CLN5 is thought to be an activator of CerSs, as experiments using mouse fibroblasts with this mutation demonstrated decreased CerS activity and ceramide species, in addition to increased apoptosis, which was corrected with increased CerS1 or CLN8 protein expression (115). Other NCLs have also been shown to have altered sphingolipids (116). An early onset epileptic syndrome has also been shown to occur with a mutation in *GM3 Synthase* resulting in accumulation of lactosylceramides (117). Further understanding of how these sphingolipid defects result in epileptic syndromes will aid in our ability to develop potential sphingolipid-based treatments for PME (116).

Spastic Paraplegia

Introduction

Hereditary spastic paraplegias (HSPs) are a large group of genetically heterogeneous inherited disorders that cause progressive spasticity and weakness. All

forms cause weakness in lower limbs that typically worsens with age and results in an abnormal gait and difficulty with ambulation. “Uncomplicated” disease is usually limited to spastic gait, lower limb hypertonicity, hyperreflexia, extensor-plantar response, and muscle weakness, while “Complicated” or “Complex” disease also includes neurological or other signs such as mental retardation, peripheral neuropathy, ataxia, epilepsy, and defects with vision and hearing (118). Three defects in sphingolipid metabolism have been identified in Hereditary Spastic Paraplegia. These mutations have been shown to occur in the enzymes *beta-1,4,N-acetyl-galactosaminyltransferase 1* (*B4GALNT1)*, *beta-glucosylceramidase 2* (*GBA2),* and *FA2H (fatty acid 2-hydroxylase)* (31).

B4GALNT1 mutations cause SPG26

HSP due to mutations in *B4GALNT1* (also known as GM2/GD2 synthase and *Galgt1, or GalNAc-T*) is known as SPG26. *B4GALNT1* encodes a transferase responsible for adding the third glucan subunit to complex glycosphingolipids to generate GM2 and GD2 gangliosides. Four different research groups have recently identified families across the world possessing a variety of different mutations in *B4GALNT1* causing SPG26 (119–122). Disease inheritance occurs in an autosomal recessive pattern, with no apparent effects in heterozygous carriers (122). Patient presentation ranges from a mild, uncomplicated spastic paraplegia to disease with severe spasticity and complicated with factors such as severe intellectual disability, peripheral neuropathy, and cerebellar ataxia. The degree of severity and specific symptoms vary, even within families. For example, two patients described in Dad *et al*.

show only mild spasticity with no muscle wasting in young adulthood, while another younger patient exhibits attacks of febrile ataxia (122).

Despite multiple clinical reports, relatively little is known about the pathophysiology of SPG26. Previously, only one other inherited disease, an infantile-onset epileptic syndrome, was known to be due to a defect in the ganglioside synthetic pathway. This disease, most common in the Amish community, is characterized by mutations in *SIAT3*, which is responsible for producing GM3 synthase deficiency (117). It is suspected that pathology may be due to GM3 accumulation or reduction of other species. Cultured skin fibroblasts from patients demonstrated an increase in GM3 and decrease in GM2, suggesting the mutations produce an enzymatic dysfunction. Moreover, these patients appear to generate a novel sialyated Gb3, perhaps due to ectopic STGALLII catalyzation due to lower concentrations of GM2 and more complex GSLs (120). However, it is unknown if this species is either directly toxic or compensates for deficiency in GSLs. Total GSLs were increased by about 25% in patient fibroblasts, although it is premature to conclude this is a real increase without reproduction of these results (120).

Many groups have studied *B4GALNT1* mouse models to understand pathology resulting from the mutation, which appears to be due to faulty myelination. These mice exhibit increased levels of simple gangliosides, such as GM3 and GD3, yet no increase is observed in total GSL levels, which contrasts with the minor increases in total GSLs observed in patients in Harlalka *et al*. (120, 123). While an early study by Takamiya *et al.* did not observe a substantial alteration in brain morphology in *B4GALNT1* KO mice,

more recent studies have shown these mice exhibit defects in myelination and axonal degeneration in both the CNS and PNS (123–125). As these mice have reduced MAG expression and phenotypically resemble mice with a disrupted MAG gene, they likely suffer from defective axon-myelin stability since MAG cannot bind to the simple GSLs that are produced due to the enzymatic deficiency (125).

GBA2 mutations cause SPG46

HSP due to mutations in *GBA2* is also known as SPG46. GBA2, also known as microsomal bile acid beta-glucosidase, catalyzes the hydrolysis of GlcCer into glucose and ceramide in membranes nonlysosomally. Thus, *GBA2* function is critical in the extra-lysosomal metabolism of GSLs. GBA2 is thought to be most highly expressed in the forebrain and cerebrum, although it is controversial if GBA2 is localized as a transmembrane protein, plasma membrane-bound enzyme, or at the ER or Golgi, adjacent to GlcCer synthesis. GBA2 has been linked in neuronal differentiation in many different contexts and may increasingly localize to the plasma membrane as cells become more differentiated. Glucocerebrodase, also known as GBA1 or simply as GBA, catalyzes a similar reaction in the lysosome. Mutations in GBA1 cause Gaucher disease (126).

A variety of different groups have reported cases of cerebellar ataxia and SPG resulting from *GBA2* mutations (127–131). Hammer *et al*. first reported the association of two nonsense and a missense mutation in *GBA2* with ataxia in Tunisian patients in 2013. Given that all patients presented with ataxia juvenile onset, the authors designated these *GBA2* mutations as an etiology of Autosomal-recessive cerebellar

ataxia (ARCA). Yet, they noted that patients afterwards developed spasticity in the lower and then upper limbs and other signs of pyramidal syndrome as well as sensory neuropathy. Some individuals developed signs of complicated syndromes such as structural deformities of the feet, abnormalities in ocular tracking, and mild intellectual disability. However, other groups have reported clinical syndromes due to other *GBA2* mutations that first present with lower limb spasticity (128, 129). Nevertheless, many of the same ataxic and cerebellar features as well as many of the same complicated signs predominate with disease progression. Overall, while there is great variety in signs and symptoms and their severity, both spastic paraplegia and ataxia are generally common in patients. A later study seemed to implicate an intermediate and mild form of these two entities, suggesting *GBA2* mutations may cause a syndrome that exists on a spectrum from HSP to ARCA (130). Increased utilization of unbiased screening approaches should aid in delineating the phenotypic spectra associated with *GBA2* mutations (132).

In contrast to using mice as a model organism for the disease, perhaps the best evidence of *GBA2* involvement in pathology was performed in a zebrafish model using morpholino knockdown of the *GBA2* orthologue. Zebrafish demonstrated abnormal locomotion and decreased axon outgrowth. Transfection of the human WT but not the mutant mRNA rescued the defects, suggesting *GBA2* mutations play a role in the pathology (128). Nonetheless, the *GBA2* KO mouse is largely void of neuronal symptoms, most prominently displaying morphological and functional defects in sperm and impaired fertility, despite demonstrating GlcCer accumulation in the brain, testes,

and liver (133). However, despite the KO of the protein, there was still residual enzymatic activity, suggesting the mouse model may not approximate human disease (133). Lymphoblasts isolated from an SPG46 patient and COS-7 and HeLA cells transfected with 10 different mutations causing SPG46 showed essentially no activity (128, 134). Some of these transfected mutants were more highly expressed than WT GBA2, suggesting that the mutations decrease enzymatic activity rather than defective expression (134). Furthermore, since affected male patients have fathered multiple children (127), it is possible that *GBA2* has different functions in humans. However, further mechanistic studies are lacking. It's not well known if GBA1 compensates for deficient GBA2 in HSP. *GBA2* deletion has been shown to reduce the Gaucher disease phenotype in a conditional GBA1 knockout mouse, potentially due to reducing toxic levels of sphingosine (135). These results suggest compensatory increases in the other GBA in the presence of a deletion may be deleterious.

FA2H mutations cause SPG35

HSP due to mutations in *FA2H* is also known as SPG35. FA2H is an ER integral protein that converts free fatty acids to 2-hydroxy fatty acids that can be transferred to dihydrosphingosine by CerS and incorporated into ceramide and GalCer. These hydroxy-GalCer species are thought to be an especially important constituent of myelin, as enzymes such as galactosyltransferase show a preference for using hydroxy-ceramides and more than half of myelin GalCer and sulfatide contain these hydroxy chains (136). Similar to disease associated *GBA2* mutations, *FA2H* mutations have also been initially associated with multiple diseases. The first report by Edvardson *et al*. tied

FA2H mutations to leukodystrophy with spastic paraparesis and dystonia, although the first clinical signs began in childhood with lower limb spasticity and gait disturbance (137). In some patients, cerebellar and cognitive dysfunction soon followed and the disease progressed to the point where patients lost ambulatory ability. White matter degeneration was apparent on MRI in these patients. Patients with the more severe clinical presentation carried an intronic point mutation that resulted in a splicing defect with the loss of two exons, while the milder mutation caused a substitution point mutation.

Two years later, distinct *FA2H* mutants were identified as a cause of SPG35 and Neurodegeneration with Brain Iron Accumulation (NBIA) (138, 139). The HSP case was associated with seizures, intellectual disability, loss of ambulation, and white matter abnormalities on MRI, suggesting that despite the different categorization, a similar pathology may be responsible (138). Kruer *et al*. report FA2H mutations as causing NBIA, but otherwise clinical presentation was generally similar with spasticity, loss of motor ability, and white matter degeneration (139). The authors suggest there is evidence of iron deposition on MRI images in the earlier two studies done by Edvardson *et al*. and Dick *et al*., however, this is controversial (140). A variety of other case reports have been documented, as compiled by Marelli *et al*. in 2015 and Cao *et al.* in 2013 (140, 141). Interestingly, multiple reports have recently suggested that SPG35 may be inherited through uniparental disomy, which is otherwise rarely observed for neurodegenerative diseases (142, 143).

FA2H KO mouse models have recapitulated many neurological defects observed in patients. Mice exhibit an age-related decline in myelination that induces axonal degeneration, suggesting that FA2H is necessary for myelin maintenance (144). CNS and PNS tissue from FA2H KO mice contained decreased GalCer, due to a large decrease in 2-hydroxylated GalCer and sulfatide, and a small, presumably compensatory, increase in non-hydroxylated GalCer. These results were largely reproduced by Potter *et al.*, who observed axonal demyelination and degeneration in 12 month old mice brains, but also noted regions of profound axon loss and some enlarged axons (145). These mice exhibited abnormal cerebellar organization and deficits in motor coordination at 7 months. Deficits in memory and learning were also present as early as 4 months, but were not observed in models with conditional FA2H KO in oligodendrocytes and Schwann cells, suggesting that dysfunction of FA2H outside of myelinating cells can still affect these behaviors. Transfection of COS7 cells with D35Y mutant caused a complete loss of FA2H enzymatic activity (137). Similarly, transfection of CHO-K1 cells with R235C and the observed 18 base pair deletion produced an 80% reduction and complete loss of enzymatic activity, respectively (138); this corresponds with a milder disease course observed due to the point mutation, which is thought to occur with other mutations as well (141).

With that being said, biological mechanisms are lacking. Macrophages isolated from bone marrow have stained PAS-positive, suggestive of a lysosomal storage defect (139). Large macrophages containing lipids have also been observed in multiple layers of the rectum (146). Further research will need to continue to explore the potential link

to lysosomal storage disorders, unorthodox models of inheritance, and effects of FA2H both within and outside of the nervous system.

Chapter 2

CHARCOT-MARIE-TOOTH 2F DISEASE

Chapter 2: Charcot-Marie-Tooth 2F Disease

Discovery

The other sesquipedalian name of Hereditary Motor and Sensory Neuropathy, Charcot-Marie-Tooth (CMT) Disease, owes substantially to its coincidentally concurrent discovery. While earlier descriptions had been reported by other clinicians, Professor Jean Martin Charcot, his student Pierre Marie, and medical student Howard Henry Tooth, are credited for simultaneously identifying the disease in 1886. Tooth, in fact, correctly surmised was CMT was a neuropathy (147–149). In 1957, Gilliatt and Thomas reported reduced nerve conduction velocity (NCV) occurred in peripheral nerve pathologies (150).

Then, in a pair of papers in *JAMA* in 1968, Peter James Dyck and Edward Lambert described two distinct clinical presentations of CMT. Each featured symptoms of neuropathy such as gait disturbance, weakness of muscles at the extremities, and physical abnormalities of the extremities such as *pes cavus*. However, upon careful inspection, a clear subset of cases featured marked decreases in nerve conduction velocities (NCVs) of peripheral nerves, while conduction velocities in the other subset were only at most mildly impaired. Symptoms were also reported to occur later in this second form of CMT (151). This division later became the basis for the categorization of CMT1 and CMT2, the former which was generally defined by a NCV below 38 m/s (152). Since then, an intermediate division of CMT with NCVs above and below 38 m/s and both demyelination and axonal pathology has been described (153). Many less

common subtypes of CMT have been also identified, raising the current total to nine (154).

As genetic sequencing technologies have developed, it became clear that even CMT1 and CMT2 were genetically heterogeneous disorders owing to a diverse cast of distinct mutations. The first genetic etiology of CMT was identified in 1991 as a DNA duplication causing CMT1A (155), leading the way to the discovery of many distinct types of CMT. Generally speaking, genes mutated in CMT1 have been shown to be involved in myelin function, and often contain “myelin” or “Schwann” in their names. Genes that are mutated in CMT2, on the other hand, tend to be expressed in neurons, although they often subserve fundamental cellular functions in a variety of intracellular locations and tissue types. Examples include amino-acyl tRNA synthases, heat shock proteins, and enzymes involved in lipid metabolism (154). Determining how the dysregulation of these proteins contributes to a purely peripheral nervous system (PNS) phenotype remains one of the greatest challenges in CMT research. As such, the biological consequences of CMT2 mutations resulting in pathology are not as well understood as CMT1. Many recent reviews have served to update research on CMT (76, 154, 156–160), however efforts have not specifically focused on CMT2F. This chapter will focus specifically on examining, comparing, and analyzing the accumulated knowledge we have developed on CMT2F.

CMT Clinical Overview

The prevalence of CMT is estimated at 1 in 2,500 (161, 162). CMT typically presents similarly to neuropathy, except that motor weakness is more common as an

early symptom of CMT (163). Decreases in sensation and balance can lead to ulcerations, amputations, and fractures due to falls (163). Cross-sectional studies have determined a significant relationship between age and severity of symptoms, suggesting a worsening of phenotype with age. However, despite great disability, lifespan is unaffected (161, 164). Most types and cases of CMT are inherited in an autosomal dominant manner, although some cases exhibit X-linked or autosomal recessive inheritance. The recessive cases are thought to often present with a more severe disease course and potential mild central nervous system involvement (161). The differential diagnosis includes the most common cause of distal symmetric polyneuropathy, diabetes mellitus, which often initially presents with loss of pain and temperature elicited upon testing. Further history and laboratory testing can rule out other etiologies of neuropathy such as alcohol, Vitamin B12 deficiency, Guillain-Barre syndrome, chronic inflammatory demyelinating polyneuropathy, and chemotherapy, although the differential is large (163, 165).

The first prospective clinical study of CMT2 in 2003 followed 43 previously identified Dutch CMT2 patients for 5 years. The results supported the traditional clinical picture of CMT. Patients most often incurred moderately increased motor degeneration, incidence of clawed toes, requirement of aids for ambulation, and disability in daily activities. Earlier disease onset correlated with specific physical deformities, while clawed toes increased in incidence over the course of the disease. Interestingly, these data suggested that pain and muscle cramps may present with onset but remit during the course of the disease (166).

Diagnosis of CMT is rapidly changing as genetic testing is continuously more prevalent and cost-effective. Traditionally, diagnosis was achieved with a thorough medical history and neurological exam. Electrodiagnostic measures could also be performed if suspicion of CMT was high. However, genetic testing is becoming more common as it becomes increasingly cost-effective (163). Advances in whole-genome sequencing (WGS) and whole-exome sequencing (WES) have exponentially augmented our understanding of the genetic underpinnings of CMT (167–169). While increased utilization of genetic testing modalities may lead to further discovery of novel genetic causes of CMT, its usage alone is not always diagnostic. Estimations made as late as 2011 show that only half of CMT patients possess a causative mutation in a known gene (170). Genetic abnormalities were identified in less than 20% of patients in a cohort of 17,880 individuals with peripheral neuropathy in 2014 (171). In another recent study, only around one half of families with a history consistent of CMT were found to possess a CMT-causing mutation using whole-exome sequencing (172).

Nevertheless, genetic testing may hold most promise in screening many of the more common types of CMT. Among a set of 14 common genes tested, copy number variations (CNVs) in *PMP22*, comprising CMT1A, accounted for approximately 75% of genetically identifiable caused CMT cases. When combined with data from the genes *GJB1*, *MFN2*, *MPZ*, and *PMP22*, that number jumped to approximately 95% of CMT, suggesting that physicians might be best served beginning clinical assessment by screening this panel of genes (171). Over 80 genes and 1000 specific mutations have been associated with CMT (169), and many clinical sequencing studies have failed to

identify genetic causes for many cases (173), necessitating more extensive genetic to identify patients with less common subtypes of CMT2.

CMT2F Clinical Presentation

Human genetics

CMT2F was initially discovered in 2001 through linkage analysis in a Russian family as a novel mutation mapping to a region in Chromosome 7 (174). In 2004, missense mutations in heat shock protein 27 (Hsp27) were identified as the cause of CMT2F (175). The vast majority of CMT2F cases are due to point mutations, although a premature stop codon in the C-terminus of Hsp27 has also been reported to present similarly (176). Clinical evidence points almost exclusively to an autosomal dominant mode of inheritance (162, 177, 178). However, very rarely in some families, CMT occurring from Hsp27 mutations (L99M) presents in a autosomal recessive manner (178, 179).

Hsp27 is a member of the class of small heat shock proteins, which are capable of binding with partially denatured proteins to prevent aggregation. Many recent reviews have extensively documented functional roles of small heat shock protein (sHsp) function (180–182). As chaperones, they sequester proteins until ATP-dependent chaperones are available to assist in refolding or targeting the misfolded protein for degradation (183–185). These proteins also subserve many other functions including modulation of cytoskeletal elements, promotion of cell growth and differentiation, and apoptosis (184).

Hsp27 itself performs many of these functions. In brief, Hsp27 is ubiquitously expressed and able to protect cells, including peripheral neurons, from various cellular stresses and apoptosis (186, 187). Hsp27 is thought to bind to targeted proteins and serve, at least temporarily, to prevent their degradation in an ATP-independent process (188–191). By preventing protein aggregation and regulating proteasomally mediated protein degradation, as well as regulating caspase activity, redox state, proliferation, and cytoskeletal integrity, Hsp27 and other sHsps are important regulators of cell death (192). Hsp27 has been implicated as a contributing and protective factor in disease states ranging from neurodegenerative disease to cancer to cardiovascular disease (193).

Hsp27 contains a similar structure to many sHsps with a conserved α-crystallin domain of approximately 90 amino acids with a beta-sheet facilitating dimer formation. N-terminal and C-terminal regions flank both sides of the α-crystallin domain (194). Both terminal regions are thought to have independently evolved, suggesting that they may be functionally differentiated from other sHsps (195). The α-crystallin domain is thought to be capable of dimer formation while the termini may facilitate the formation of larger oligomers (196, 197). Oligomerization seems to largely be regulated by phosphorylation, which occurs at three serine residues in the N-terminus (198). By dynamic control of the rate of oligomerization and disassembly, Hsp27 can control its function as a chaperone (194, 199).

Epidemiology

Clinical studies suggest the prevalence of CMT2F and dHMN II is worldwide. Table 1 lists all known mutations of CMT2F reported in the literature to date. CMT2F has been reported in China (177), Russia (174, 175), Belgium (175), England (178, 179), France (178), Finland (173, 200), Italy (201–206), Korea (207), Taiwan (208), and Armenia (178).

dHMN occurring due to Hsp27 mutations has been reported in England (175), Ireland (209), Japan (210–213), England (175, 179), France (178, 214), Finland (200), Germany (215), Belgium (175, 214), Croatia (175, 214), Austria (175, 214), Korea (216), and Italy (178, 201, 203–205, 217), Portugal (178), India (179), Pakistan (179), Algeria (178) and the Ivory Coast (178). CMT2F and dHMNII are thought to comprise about 4% to 0.3% and 8% of CMT and dHMN, respectively (171, 178, 203).

Clinical presentation

The clinical presentation of CMT2F generally mirrors the loss of axonal function seen in CMT2. The first presenting symptom is often foot drop, initially occurring unilaterally in most patients (178). Many patients often first complain of decreased ambulatory ability and often suffer from falling (177, 212). Sometimes the degree of limb involvement may be asymmetrical (218). Axonal biopsy typically reveals atrophy without acute degeneration nor substantial change in myelination (201). Nevertheless, even though CMT2 has been traditionally classified by axonal degeneration instead of demyelination, some patients exhibit decreased NCVs in the lower limbs (177, 202). In concordance with denervation, lower limb muscle with fatty replacement wasting occurs

most drastically distally (206). Serum creatine kinase levels are generally moderately elevated, presumably secondarily due to muscle degeneration resulting from neuropathy (178).

Other aspects of clinical presentation are also similar to other types of CMT2. Some evidence suggests males may be affected earlier and more severely than females, although no comprehensive clinical studies have specifically addressed differences in presentation due to gender (202). Age at onset appears to generally decrease over succeeding generations, often by as much as 30 years (177, 201, 213, 216)However, this could be due to CMT's relatively insidious onset and greater surveillance from both patients and physicians for individuals with a family history. There is still great variability of onset though – patients have exhibited symptoms in their feet as early as age 6 while as others do not develop symptoms until their late 30s (177, 215), mid-50s (179) or even their 60s (203). dHMN patients may not present with symptoms until much later in their mid-50s and fail to show changes in NCVs (215, 219).

While most identified mutations in CMT2F have been point mutations, a nonsense frameshift mutation at position S158 has been identified in an Italian family, presenting in a child at 3 months of age after a tetanus vaccination and worsening after a subsequent booster dose months later (205). The patient subsequently lost ambulatory ability and lacks motor or sensory NCVs. This suggests nonsense mutations may cause a more dramatic phenotype, however the unvaccinated father has had a rather typical course of disease with mildly impaired motor loss and no sensory loss. It

is unknown whether truncated forms of Hsp27 can cause a much earlier onset and more severe disease, and whether immunizations or other potential stressors in susceptible patients may exacerbate the disease course.

Other cases have also presented specific mutations that present as either CMT2F or dHMN II. It may be difficult to generalize rules for certain point mutations such as R136L presenting as CMT2F and dHMN II, even in a single study (203). One study determined that R136L patients present with greater loss of plantarflexion than dorsiflexion in the ankles (202), whereas a different mutation encoding a premature stop codon presented with equal loss of each type of flexion (176). Furthermore, it appears that certain mutations may present slightly differently between different families – for example, an R127W mutation in a Chinese family presents with an later age of onset but with sensory involvement in hands compared to an R136W mutation in an Italian family (177, 204), while onset of K141Q has differed in Japanese families (211, 213). Additionally, even cases inherited within a single family have presented with consistent motor but a wide spectrum of sensory symptoms, from no loss to severe failure, which also further suggests that CMT2F and dHMN exist as a continuum and other factors may affect symptom presentation (204, 206).

Considering that many of these same mutations occur in CMT2F and dHMN II, especially the commonly reported 404C>T (S135F), the categorical distinction of these two diseases is likely more based on symptomatology than differences in cellular pathology (175, 203, 207). Furthermore, many CMT2F patients show relatively minor deficits in sensory function (49). However, determining why almost all patients with

related Hsp27 mutations consistently develop motor systems, while only a subset develop sensory symptoms, remains a lingering question. It is still unclear whether genetic or environmental differences among individuals contribute to a varying clinical presentation. While some studies have suggested that mutations in the C-terminus of Hsp27 may cause a strictly motor phenotype (220), mutations in other regions of the gene can produce a pure loss of motor capabilities (203), while some cases of C-terminal mutations present with a mixed motor and sensory picture (176).

This level of variance suggests that if mutation location has an effect on symptomatology, it is not generalizable. Consequently, researchers should exercise caution when generalizing clinical findings that occur only in the presence of specific mutations as pathological mechanisms that explain symptomatology, such as observed alterations in mitochondrial transport in S135F but not P182L cells, as discussed more later (220). As keenly pointed out by Rossor *et al.*, 2012, the lack of patient-reported sensory symptoms does not preclude sensory involvement of the disease on examination (176). The later onset of dHMN II may also reflect a milder disease presentation.

Finally, clinical studies have also demonstrated heterogeneity in clinical presentation beyond motor and sensory loss in limbs. A recent case report identified a novel D129E Hsp27 mutation thought to cause both motor neuropathy and a distal myopathy, although there was substantial variation in presentation, as the second generation patient had only minor symptoms of cramping (209). Other reports have detailed patients that demonstrate hearing loss that precedes motor and sensory

symptoms (202), or ocular symptoms such as optic atrophy and ocular myopathy (161). Interestingly, some patients also present with positive pyramidal signs including a positive Hoffmann sign or Babinski sign, suggesting upper motor neuron deficits in the corticospinal tract may also be present and potentially masked by peripheral dysfunction (202, 203). However, signs of pathology have generally not been detected clinically in the brain and spinal cord (178).

Patient data in further clinical reports should augment our understanding of how certain mutations impart different likelihoods of developing distinct clinical phenotypes. Thus far, the low prevalence of CMT2F among patients presenting with distal symmetrical polyneuropathy has presented a challenge to producing sufficient data to assertively shape conclusions about prevalence. However, as diagnostic sequencing increases in ubiquity across the world, we should expect that our insight into the effects of specific point mutations, genetic environment, and environmental exposures will considerably increase our knowledge on CMT2F.

CMT2F Experimental Reports

Hsp27 knockout mice

Hsp27 is commonly referred to as Hsp β-1 or HspB1 in mice. As far as I know, HspB1 knockout (KO) mice have been created and described in publications by three different groups to date. Huang *et al*. 2007 ablated HspB1 and replaced it with a knock-in of the *lacZ* reporter gene under the HspB1 promoter, allowing visualization of HspB1 tissue expression at different developmental stages (221). Despite the ubiquity of *HspB1* in mouse tissue, particularly in musculature, these mice were viable, fertile, and

lacked any apparent musculoskeletal or visual abnormalities. HspB1 was notably expressed in the spinal cord but expression was limited in the brain, and no neural phenotypes were reported. The lack of phenotypes was thought to be due to synergistic action as the levels of other Hsps, such as Hsp70, remained constant. However, upon heat stress, isolated mouse skin ear fibroblasts (MSFs) showed reduced viability (221). A second Hsp27 KO mouse model generated by Crowe *et al*. with deletion of all three exons of HspB1 demonstrated decreased wound healing and increased inflammatory markers in isolated mouse embryonic fibroblasts (MEFs). This suggests that HspB1 may physiologically restrain the immune response and promote progression of the cell cycle (222). A third HspB1 KO generated by homologous recombination resulted in male mice that exhibited diminished weight, reduced plasma lipids, and myofibrillar abnormalities in muscle organization (223).

Hsp27 KO in fruit flies (224) and transient reduction through antisense phosphorodiamidate morpholino oligonucleotides (PMOs) in zebrafish (225) further suggest a lack of drastic developmental or neural phenotypes. Flies did have a reduced stress response to starvation and decreased mean lifespan. The lack of stark phenotypes in KO models may result from compensatory mechanisms from other sHsps that otherwise could not similarly compensate gain-of-function mutations observed in CMT2F (223).

Chaperone function

While Hsps operate as molecular chaperones under thermal and cellular stresses arising from ischemic, oxidative, and toxic etiologies, Hsps also can operate to

promote these functions in unstressed conditions (184). Given its intimate role as a chaperone, Hsp27 has been examined in many CMT2F studies in both stressed and unstressed states. Initially, the P182L Hsp27 mutation was found to irregularly cluster in the soma instead of spreading into neurites when overexpressed in primary cortical neurons (226). Minor levels of aggregation were also observed in the presence of WT Hsp27, but were drastically increased by co-transfection with P182L. This suggested that the P182L mutant could exert a dominant effect by drastically increasing the degree of a normal aggregative process. Moreover, unlike the majority of WT Hsp27, P182L mutant demonstrated predominantly insolubility in a Triton X-100 detergent solution, a property of other proteins mutated in neurodegenerative diseases, further suggesting that this mutation causes insoluble aggregates (226). However, this work did not clarify if this pathology resulted primarily from the formation of Hsp27 aggregates in the soma or the loss of WT Hsp27 in neurites.

The work by Ackerley *et al*. encouraged further exploration of aggregation of Hsp27 using other cellular models. Increased aggregation of Hsp27 was further observed in HeLa cells expressing the G84R, S135F, R136W, and P182L mutants compared to WT, as well as two mutants in Hsp22 (218), suggesting that many CMT2F mutations can disrupt Hsp27's chaperone function. The greatest levels of aggregation were measured with the P182L mutant, suggesting that mutations in the C-terminus may especially predispose Hsp27 to clumping in the cytoplasm (218). Recently, Echaniz-Laguna *et al*. have also shown that the S187L mutant, but not P7S, G53D, nor Q128R, displayed clumping, further suggesting that C-terminal mutations may

selectively cause this phenotype. This group also presented evidence that these aggregates are cleared via proteasomes and not autophagosomes (178). Increased aggregation was also observed with another similar mutation, P182S, and may be due to its increased propensity to form large oligomers, which have low thermal stability and easily form aggregates (227). While these large oligomers can contain WT Hsp27, this effect was not observed for T180I, another C-terminal mutation, suggesting aggregation may be a mutation-specific phenomenon and not generalizable to all C-terminal mutations (227). Furthermore, another study using patient-derived fibroblasts and stably transfected neuroblastoma cells failed to demonstrate aggregation occurring with the P182L mutant (228). Overall, while multiple studies have reported aggregation induced by different mutants, these effects are still unclear.

Further studies examining the effects of different mutations also present less clear results. Three CMT2F mutations in the α-crystallin domain—R127W, S135F, and R136W—were interestingly found to *increase* Hsp27's chaperone function, associated with an increased monomeric state of Hsp27. This increase in function theoretically might have been able to explain the biological gain-of-function thought to underlie the typical autosomal dominant inheritance of CMT2F (229). However, three other mutations—S156Y, T151I, and P182L—had no overall effect on chaperone activity, suggesting that increased chaperone activity is not necessary for CMT2F disease progression. Moreover, these mutants had varied effects on thermotolerance—increasing, decreasing, or not altering responses. This suggested that either specific mutants caused different pathologies that still resulted in a similar clinical phenotype, or

direct measures of Hsp27 chaperone function may not be especially relevant in disease pathogenesis. Almeida-Souza *et al*. observed that the R127W and S135F mutants were increasingly present in monomeric form. The authors proposed that the mutant residues blocked otherwise stabilizing internal hydrogen bonds that facilitated protein dimerization. These two mutants, along with R136W, bound more to client proteins, further suggesting the mutants are hyperactivated and may have increased chaperone function in the monomeric form (229).

Additional results from other studies have made interpreting the effects of Hsp27 mutants on chaperone activity difficult. Other mutations (P7S, G53D, Q128R, and S187L) studied by Echaniz-Laguna *et al*. did not have an altered monomeric:dimeric ratio nor altered chaperone activity (178). Given that Q128R occurs between R127 and S135F, these results suggest that it may be difficult to extrapolate effects on chaperone activity from the general location of mutations in the protein. Further complicating matters, the R127L and a truncating C-terminal mutation were shown to impair heat tolerance both immediately and 48 hours following heat stress in fibroblasts isolated from patients; the effect of the truncating mutation was much greater (200). As the WT and truncated Hsp27 showed similar nuclear translocation and induction of heat shock protein genes, this suggests that immediate decreases in viability following heat shock could be due to structural deficits in Hsp27 induced by the mutation, preventing Hsp27 from binding and protecting denatured proteins. Both mutant conditions demonstrated an increased sensitivity to protein misfolding, as measured by increased apoptotic round cells, and the effect appeared earlier in the C-terminal truncated cells than the

R127L (200). However, Ylikallio *et al*. did not observe aggregates in the C-terminal truncation mutant as Ackerley *et al*., observed in P182L (200, 226). Ylikallio *et al*. also did not observe an increased monomeric fraction of R127L as Almeida-Souza *et al*. did for R127W, suggesting that either the specific point mutation confers different phenotypic effects or overexpression in neuroblastoma lines may produce different results than patient-derived fibroblasts (200, 229). Each of these models possesses a strength of either a neuronal background or endogenous expression levels. Induced pluripotent stem cells (iPSCs) largely carry both of these advantages and should be highly considered for future studies given this discrepancy.

Substantial work has also been undertaken to descriptively analyze the biochemical effects of mutations located in each portion of the protein. G84R and L99M mutants produce larger and less stable homooligomers and possess reduced chaperone activity, potentially by decreasing accessibility of the N-terminus and affecting dimer stability, respectively (230). Additionally, three N-terminal mutations have also been shown to produce earlier heat-induced aggregation, increased susceptibility to chymotrypsin-induced lysis, and reduced chaperone activity. These mutants also decreased phosphorylation preventing Hsp27 oligomer dissociation and were observed to form larger homooligomers (231). The R140G and K141Q mutations in the α-crystallin domain both decrease thermal stability; however, these mutants have varying effects on protein interactions, trypsinolysis, homo- and heterooligomer size, and chaperone activity, the latter which was decreased in R140G but not altered in K141Q (232). The more drastic effects of R140G compared to K141Q is comparable to

those observed for S135F and R136W and may be due to the fact that R140G mutation more severely disrupts the dimer interface than a mutation at the adjacent residue (229, 232). Focusing on the C-terminus, Chalova *et al*., analyzed parameters of chaperone function in four mutations and concluded that each confers a distinct biochemical mechanism of disruption. R188W possessed a decreased chaperone function likely due to altering polarity of the C-terminal extension while not altering quaternary structure. Conversely, the T164A mutation decreased quaternary structure and thermal stability without affecting chaperone function. While T180I and P182S occurred in a similar location in the C-terminal domain, T180I increased thermal stability while P182S decreased thermal stability and dramatically decreased chaperone activity (227).

Neurofilaments

One potential mechanism for decreased axonal transport may be through neurofilament (NF) dysregulation. NFs in the peripheral nervous system are typically heteropolymers made up of NF light (NF-L), medium, heavy, and peripherin subunits (233). NF-L chain levels have been shown to be highly associated in blood and cerebrospinal fluid with progression of neurodegenerative diseases in animal models and are becoming promising biomarkers in clinical settings. It is thought that their accumulation directly contributes to neuronal cell death (233–236). Mutations in NF-L, which is abundant in neurons, are known to cause CMT2E, often with an early and severe phenotype (237–239). In their seminal paper, Evgrafov *et al*. co-expressed NF-L with either WT or S135F mutant Hsp27 in adrenal carcinoma cells, and observed that the S135F mutant induced NF-L aggregates instead of a filamentous staining pattern

(175). Ackerley *et al*. similarly showed that the P182L mutant disrupts the NF network in primary cortical neurons (226).

Further work has sought to build upon these initial findings. WT Hsp27 was found to directly bind to WT and CMT2E-mutant NF-L and reduce mutant NF-L-induced aggregation and mutant NF-L-mediated motor neuron death. This suggested that mutations of Hsp27 underlying CMT2F dysfunction may have a related mechanism to CMT2E (240). Similar to mutant NF-L expression, expression of S135F mutant disrupted the NF network, causing NF-L aggregation and reducing viability of motor neurons. To determine if these effects on NF-L are necessary for CMT2F pathogenesis, Zhai *et al*. microinjected S135F cDNA into NFL KO mice and observed that isolated motor neurons had decreased growth. However, when WT mice were microinjected with S135F cDNA, there was a substantially greater decrease in motor neuron growth. Thus, while eliminating NF-L did not completely rescue cells from S135F-mediated toxicity, it hints at the possibility for common mechanism for CMT2E and CMT2F.

Further studies have largely focused on investigating NF regulation in CMT2F. Using neuroblastoma cell lines stably expressing CMT2F mutations, Holmgren *et al*. found CMT2F mutants reduced NF anterograde transport. This was partially explained by increased Cdk5 activity, which increased NF phosphorylation and thereby increased binding among NFs in all mutants tested but R127W; this caused decreased NF binding with kinesin (241). Increased phosphorylation of NFs has also been observed in S135F mouse tissue and SH-SY5Y cells stably transfected with P7S, G53N, Q128R, but not S187L mutants (178, 242). While R136W mutant mice generated by Srivastava *et al*.

demonstrated an increased NF density in axons, other studies have not focused on using electron microscopy to study NF function (243).

These results raise many questions on the mechanism by which CMT2F mutations alter regulatory kinases and in which cell types this occurs. The results suggest that C-terminal mutations may lack this effect, and further experiments should be performed with other C-terminal mutants as have been done on chaperone function. Cdk5 knockdown provided a substantial but incomplete reduction of NF phosphorylation, suggesting mutants could induce other distinct regulatory kinases and pathways (241). However, contrary to earlier studies, Holmgren *et al*. did not observe NF aggregates nor changes in NF staining patterns in cells transfected with S135F or P182L mutants, Echaniz-Laguna *et al*. did not observe alterations in NF architecture in SH-SY5Y cells using the NF-H (NF heavy) as a marker, and Kalmar *et al*. did not observe changes in NF-L staining using transduced mouse primary motor neurons (178, 241, 244). It is still unclear whether this pathology occurs *in vivo*, and if different mutants affect NF structure and transport to different degrees, as in chaperone function.

Microtubules

Another interesting and especially promising target for treatment in CMT2F is microtubules (MTs) and their associated dysfunction. MTs serve many important functions in axons such as regulating axonal morphology, conserving neuronal polarity, transporting of cargo, and modulating intracellular signaling through organizing hubs of kinases and other regulatory enzymes. They often exist in relatively dynamic states of assembly and disassembly that can be regulated by a variety of mechanisms including

associating proteins or chemical modifications to tubulin, although MTs in neurons are generally considered to be relatively stable (245, 246).

Evaluation of WT and mutant Hsp27 binding properties as chaperones led to the discovery of tubulin as a potential binding partner with increased binding in mutants (229, 247). While primary motor neurons transduced with viral constructs of mutants (P39L, R140G, and S135F) did not demonstrate changes in MT staining as evidenced by TUBB3 (beta III tubulin) (244), work performed *in vitro* and using dorsal root ganglia (DRGs) isolated from mice demonstrated that three of five CMT2F mutants tested (R127W, S135F, and R136W, but not T151I nor P182L) increasingly bound to both α-tubulin and assembled MTs. This increased binding of Hsp27 to MTs increased the stability of MTs in destabilizing conditions by reducing MT dynamic events (247). Further exploration of this binding interaction demonstrated a significantly greater co-localization of mutant Hsp27 and the tubulin marker TUBB3. However, this difference was slight and there was still high co-localization of WT Hsp27 and no apparent difference in pattern of the MT network. Nevertheless, MTs in mutant cells showed marginally decreased migratory ability, suggesting a more stabilized state. In confirmation, thorough evaluation of kinetics of individual MTs revealed that MTs in mutant Hsp27 cells spent more time in the stationary phase; even though some MTs exhibited bouts of *faster* depolymerization, these occurred less often. It remains unclear whether the increased stability over time or more rapid depolymerization could potentially induce pathological effects.

These findings generated great interest in MTs in CMT2F. Many other neurodegenerative diseases are associated with MT dysfunction, however typically, but not always, with a less stable state (246, 248–251). In addition, peripheral neuropathy is widely known as a common dose-limiting side effect of many MT-targeting chemotherapeutic agents (252, 253). Patient biopsy data from a clinical study also reveals an increased density of MTs in atrophic axons, potentially due to decreased NFs (201). In a seminal study by d'Ydewalle *et al*., S135F and P182L mutant mice were found to have decreased acetylation of α-tubulin in sciatic and sural nerves, suggesting a contrarily less stabilized (and increased dynamic) state. Furthermore, the authors also observed decreased MT-mediated trafficking of mitochondria, which became a candidate to underlie the pathological features presenting exclusively in peripheral neurons, given their high requirements for mitochondria (220). The decreased acetylation of α-tubulin was confirmed in median/ulnar and sciatic nerves from S135F transgenic mice generated by a different group, generating great excitement as a potential biological mechanism of degeneration (242).

However, like the variable in results observed in chaperone function and NF structure, decreased acetylation of α-tubulin has not been observed in many cell lines and may be strictly limited to peripheral tissue. Importantly, no change in acetylation of α-tubulin was observed for R127W, S135F, R136W, and P182L mutants—if anything, the R136W and P182L mutants demonstrate increased acetylation (247). Even more perplexing, these results suggest a more dynamic MT state, which falls in line with alterations observed in most neurological diseases, but opposes the results of Almeida-

Souza *et al*. It is possible that an initially stabilizing environment is present, and the overrecruitment of histone deacetylase (HDAC) inhibitors could overcompensate, causing deacetylation in the PNS. However, this possibility would presumably result in an increase in acetylation of α-tubulin in the system of Almeida-Souza *et al*., which was not observed, making reconciling these results somewhat difficult. As Almeida-Souza *et al*. mention, the increased speed of polymerization they observed could signify that the increased stabilization observed may only be a transient effect and not reflective of the true overall MT behavior (247). It is also possible that these results are exclusive to the cellular environment of peripheral neurons.

Mitochondria

In addition to providing energy in the form of ATP, mitochondria have many important functions in neurons including responding to rapidly changing cellular conditions, buffering intracellular calcium, and triggering apoptosis (251, 254). Neurons require an especially high energy demand for synaptic functions including synaptic assembly, generation of action potentials, and regulation of synaptic transmission, all of which can occur far from the nucleus. As such, neurons face especially difficult challenges in transporting sufficient mitochondria to axon terminals for energy generation and removing them when they become damaged (254). Defects in mitochondrial functioning, including fusion and fission, respiratory chain function, and mitophagy have been associated with a wide variety of neurodegenerative disorders (255).

Many studies point to a role of mitochondria in the pathology of CMT2F, as well as other types of CMT2. Multiple groups have discovered patients with mutations of both *MFN2* and *GDAP1*. As both of these genes mitochondrial dynamics, mitochondrial function may be a common mechanistic of CMT2 (256, 257). Moreover, specific mutations that typically lead to mild disease alone present with severe symptomatology when inherited together, suggesting a synergistic or additive effect of mutation burden (257). Impaired mitochondrial trafficking has been implicated in CMT2A (258), CMT2E (258, 259), and CMT2F (220, 244, 260), while other mitochondrial defects and proteins involved in mitochondrial function are impaired in many other forms of CMT (250).

In relation to decreases in α-tubulin acetylation, d'Ydewalle *et al*. determined that mitochondrial transport decreased in S135F mouse DRGs (220). Since MTs serve to transport mitochondria along axons, the group tried to rescue mitochondrial transport deficits by increasing MT acetylation using HDAC inhibitors. HDACs hydrolyze acetyl modifications selectively added by histone acetyltransferases (HATs) to lysine residues on histones and other molecules. HDAC6 ironically does not act on histones but is known to regulate acetylation of α-tubulin and other heat shock proteins (261). Indeed, HDAC6 inhibition using trichostatin A (TSA) and tubastatin increased mitochondrial movement, neuromuscular junction number and innervation, and rescued altered behavioral performance and compound muscle and sensory nerve action potentials (CMAPs and SNAPs) (220). Yet, other studies have not been able to completely confirm these findings. Kalmar *et al*., observed no difference in percentage of moving mitochondria using three mutations (P39L, R140G, and S135F) in transduced mouse

motor neurons (244). This group did, however, observe a decreased velocity of retrograde transport of mitochondria with no alterations in anterograde transport velocity or retrograde transport of other cargo, and increased mitochondrial pausing in all mutant conditions tested. The relative proportion of mitochondrial movement in the anterograde direction was increased only in the S135F mutant. Similarly, the early results of Ackerley *et al*. also did not observe an effect on anterograde transport of mitochondria in primary cortical neurons transfected with P182L (226).

Nevertheless, given the stark findings of d'Ydewalle *et al*. on mitochondrial transport, HDAC6 inhibitors stand as a promising candidate treatment for CMT2F. Different groups have identified multiple small molecules with hydroxamic acid moieties with similar HDAC6 inhibition selectively as TSA. Inhibitors tested by one group were found to possess more potent increases in acetylation of α-tubulin at low concentrations in N2a cells than TSA, and at higher concentrations increased mitochondrial transport in CMT2F mutant mouse DRG neurons similar to the degree observed in mice treated with TSA or WT mice (261). Another recent screening study identified two molecules that also demonstrated potent and selective HDAC6 inhibition and increased mitochondrial axonal trafficking. They were verified as biologically relevant by increasing innervation at neuromuscular junctions and improving motor and sensory nerve conduction in mice (262). Mitochondrial movement most drastically increased in a retrograde fashion, but also appeared to increase in anterograde motion as well, raising questions as to directional deficits in disease pathology and how HDAC6 inhibitor treatment may affect mitochondrial movement. Moreover, while these inhibitors seemed to rescue some

motor and sensory function, compared to previously reported degree of deficits (and without a direct positive control from WT mice), they may not fully alleviate symptoms (262). Two HDAC inhibitors developed by a third group were also shown to rescue defects in α-tubulin acetylation and mitochondrial trafficking observed in S135F and P182L cultured motor neurons differentiated from iPSCs derived from patient fibroblasts (260). While not a major conclusion of the paper, interestingly, two clones of P182L cells presented with markedly different mitochondrial properties—one clone, unlike the other, did not demonstrate a decreased absolute velocity of mitochondrial movement, but interestingly seemed to have an even more drastically diminished percentage of moving mitochondria (although the authors did not make this statistical comparison) (260). If these iPSC models are taken to be strong models of cellular pathology, this suggests that variability in phenotype may even exist within the same individual, potentially allowing a role for environmental influence. For this reason, more studies should be performed using iPSC models.

Further study also needs to evaluate other potential therapeutics and determine if long-term dosage can effectively reduce pathology in model systems. In addition, due to nucleotide substitution, hydroxyamates as a class are well known mutagens and safety profiling must be carefully performed to evaluate the potential carcinogenicity of potential treatments, especially since CMT is not a terminal diagnosis (263). Studies on sensory nerve endings will also be useful, especially given the variable presentation of sensory symptoms in CMT2F. Further research may consider also utilizing HATs to directly induce acetylation.

The observed decreased trafficking of mitochondria has led other studies to focus on mitochondrial alterations beyond MT-mediated transport in axons. The fact that transport of other signaling proteins has not been altered by CMT2F mutations suggest that deficiencies of mitochondrial transport may be primarily due to mitochondrial defects rather than generalized defects of transport machinery (244). There is some evidence that mitochondrial content may be increased in mutant cells. R136W mice axons demonstrated an increased overall mitochondria content by electron microscopy (243), potentially due to increased individual mitochondrial size. However, these results stand in opposition to d'Ydewalle *et al.*, who observed decreased total mitochondria in DRGs from S135F mice at 10 months but not 2 months, and demonstrated increases in mitochondrial number by HDAC6 inhibition using kymographs and spatio-temporal maps (220). The same group later showed slight increases in mitochondrial content in neurites with HDAC6 inhibition based on kymograph quantification (262). It is possible that this discrepancy in results could result from the different imaging modalities used.

Other studies have focused on determining effects on mitochondrial function. Kalmar *et al*. observed mitochondria with decreased membrane potential in the neurites of S135F mouse motor neurons. Using S135F mouse motor neurons, they observed decreased mitochondrial Complex I (but not Complex II) activity, increased superoxide in response to antimycin A treatment, and increased glutathione release and nitrotyrosine expression, all of which suggest an increased susceptibility to oxidative stress (244). Many of these studies used other mutants which, in some cases, were significantly different from WT, and in other cases also showed similar trends to the

S135F mutant. However, some notable exceptions still existed: P39L appeared to have similar levels of glutathione (if anything, increased in whole cells) and R140G similar levels of nitrotyrosine to WT, again suggesting that these mechanisms implicated may only pertain to certain mutants (244). The lack of a decrease in membrane potential in the neuronal cell bodies suggests that the mitochondrial defects occur in more distal processes and may be related to transport. It is unknown whether these structural and functional abnormalities in mitochondrial size and content, oxidative state, and respiratory function are related to trafficking defects. It is also unknown why decreased potential seems to be related to defects specifically in Complex I. However, decreased mitochondrial functioning could potentially lead to an increased basal level of oxidative stress over time, which may cause greatest effects in post-mitotic cells after extensive time, as observed in CMT.

Other molecular effects

Since CMT2F mutations are typically point mutations that produce a translated protein, investigators have typically focused on studying the biochemical properties and biological effects of the mutated protein rather than investigating potential defects in the molecular biology of the disease. However, one group recently discovered that the P182L mutation, but not WT nor R127W mutants, interacts with RNA-binding protein poly(C)binding protein 1 (PCBP1), another ubiquitously expressed protein that exists in peripheral nervous system tissue, and reduces its function of repressing translation. PCBP1 targets, which included many genes that when mutated are known causes of peripheral neuropathy, were expressed more highly in P182L mutants (228). However,

other mutations have not been studied for translational repression and the potential consequences of altered translational profiles pertaining to other neurodegenerative disease have not been mechanistically connected to CMT2F.

Other mutations have also been shown to increase Hsp27 binding to other proteins. Mutant Hsp27 (S135F, R136W, and R127W) has also been suggested to increase Hsp27 binding to F-actin, leading to increased dissociation of Drebrin from F-actin (264).

Other biological responses have received limited study and warrant more attention. Motor neurons differentiated and cultured from patient-derived iPSCs and mouse motor neurons transduced with mutant lentiviral constructs do not appear to have a stark difference in morphology or length and express similar neuronal markers as control motor neurons (244, 260). However, SH-SY5Y cells transfected with mutants (P39L, R140G, and S135F) demonstrate increased LDH release, suggesting increased cytolysis (244). R136W mice sciatic nerves contain cytoplasmic invaginations similar to secondary lysosomes (243). As mentioned earlier, axonal transport has been shown to be affected in a wide array of neuropathies beyond simply mitochondrial trafficking (245, 251). P182L was shown to co-localize and alter the localization of p150, a protein important in regulating neuronal retrograde transport, potentially sequestering p150 and preventing efficient retrograde transport (226). However, a later study did not find altered transport of p75, suggesting that generalized retrograde transport may not be altered (244) and necessitating further study to thoroughly evaluate transport deficits. Alterations in autophagy, a mechanism of delivering cell aggregates and debris to

lysosomes for recycling, are another common mechanism thought to potentially underlie many types of CMT (265).

Biological models and pathophysiological effects

Different groups have attempted to study the pathophysiology of CMT2F using mouse models, many of which recapitulate the human disease to a strikingly similar degree. Physical deformities and abnormal behavior have been noted in multiple mouse models. S135F and P182L transgenic mice generated by d'Ydewalle *et al*. demonstrated noticeable phenotypes, although the latter presents more like dHMN II than CMT2F with a lack of sensory symptoms (220). At 8 months of age, these mice have clawed hindpaws similar to the *pes cavus* that presents clinically. These mice present with clasping of hindpaws and decreased rotarod performance at 6 months of age and decreased grip strength at 4 and 7 months, in the P182L and S135F mutants, respectively; forepaw strength decreases a few months later, similar to clinical presentation. The 8-month old mice tested demonstrate an abnormal gait with a decreased stride length and an abnormal hindpaw, but not forepaw, angle and foot print area, again mirroring the distal lower limb alterations typically seen initially in humans (220). Interestingly, grip strength appeared to be markedly worse in the P182L mice, suggesting that the P182L mutant might present with a stronger motor phenotype than S135F.

However, CMT2F mouse models generated by other groups have notable differences. Behavior deficits reported by Lee *et al*. occur slightly earlier at 5 versus 6 months of age, but appear to be much more severe than the mouse models of

d'Ydewalle *et al*., which show a more gradual decline in many motor phenotypes (220, 242). Further complicating these findings, Lee *et al*. report no sensory phenotype in S135F mice, suggesting their model presents with a strict motor loss, similar to the P182L, but not the S135F mice of d'Ydewalle *et al*. In further contrast, the R136W mouse model did not demonstrate any functional or behavioral deficits (243). A fourth transgenic model attempting to express physiological levels of R127W and P182L mutant proteins to alleviate concerns of artifacts due to overexpression revealed a lack of pathology and behavioral deficits. While the authors attributed this to insufficient expression of Hsp27 under the ROSA26 locus, it may also indicate heterogeneity in the presentation of CMT2F mutations in animal models as well (266). The authors postulate that the other mouse models with Hsp27 overexpression could potentially promote formation heter- and homooligomers that would likely carry distinct functional consequences, potential mislocalization of Hsp27, and may lead to artificial phenotypes.

Despite the stark differences in phenotype, these mouse models display expected trends in neural physiology based on behavioral data. CMAPs were reduced in the models of d'Ydewalle *et al*. and Lee *et al*., and paralleling behavioral results, sensory nerve action potentials were decreased in the S135F but not P182L mice of d'Ydewalle *et al*. (220, 242). In the R136W mouse, decreases in sciatic motor amplitude were present at 1 year (but not 6 months), and no change in conduction velocity was observed (243). Similar to previously mentioned clinical data (206), fatty infiltration of the gastrocnemius muscle was described by Lee *et al*., while d'Ydewalle *et al*. noted atrophic muscle fibers with abnormal organization (220, 242). While Lee *et al*. report

demyelination in sciatic nerve tissue of 10 month mice, d'Ydewalle *et al.*, 2011 show axonal loss but a lack of demyelination in sciatic nerve tissue from 10 month old mice. Interestingly, R136W mice have an increased myelin thickness, foldings, and increased number of Schmidt-Lanterman incisures observed at 6 months of age (243). d'Ydewalle also noted both the S135F and P182L mice have a reduced number of axons in the distal but not proximal sciatic nerve, decreased acetylcholine receptor clusters per axon terminal, and increased percentage of denervated neuromuscular junctions (220). Despite some clear trends, such a wide variety of phenotypes should prompt additional CMT2F mouse models, both using the same as well as different mutations, to better understand the variability of CMT2F.

sHsps in Neurodegenerative disease

sHsps have been suggested to play a large role in many instances of neuropathy. As motor neurons have a greater threshold for heat shock induction and Hsp expression generally decreases with increased age, a reduced Hsp stress response could play a pathological role in CMT disease with presentation later in life and exclusively in peripheral neurons. A mutation in the promotor of Hsp27 that causes decreased Hsp27 expression in neurons is associated with Amyotrophic Lateral Sclerosis (ALS) (267). Hsp27 has been shown to accumulate in brains of patients with Alzheimer's and frontotemporal lobe dementia (FTLD) (268). Hsp27 may also be distinctly linked to myopathy, although further work must focus to delineate this pathology from CMT (269).

Upregulation of Hsp27 has shown potential in alleviating many neurodegenerative diseases, although beneficial effects observed between different models are not always consistent. Hsp27 overexpression improved impaired long-term potentiation and spatial memory in a mouse model of Alzheimer's Disease (270). Similarly, Hsp27 overexpression protects again protein aggregation and apoptotic effects from WT and mutant α-synuclein in cell models of Dementia with Lewy bodies and Parkinson's Disease, respectively (271, 272). Hsp27 overexpression reduces reactive oxygen species (ROS) levels and protects neuronal cells from cell death in a cellular model of Huntington's Disease (273). However, while there are hints *in vivo* viral vector expression of Hsp27 may reduce huntingtin protein aggregation (274), overall brain ROS and phenotype in transgenic mice are not improved (275). Furthermore, overexpression of Hsp27 did not protect superoxide dismutase 1 (SOD1) KO mice, a common model of ALS, from motor neuron degeneration (276).

Mutations in Hsp22, another small heat shock protein also known as HspB8, can cause dHMN II (277) and CMT2L (278, 279). Mutant Hsp22 is known to display greater binding to Hsp27, while S135F mutant Hsp27 has demonstrated greater binding to Hsp22, suggesting that increased binding of these proteins can cause neuropathy (277, 280). Furthermore, motor neurons transfected with mutant Hsp22 displayed substantial neuronal degeneration and reduced neurite growth. However, these phenotypes were absent in transfected cortical neurons and glial cells and only occurred in a small proportion of sensory neurons (281). These results also suggest that dHMN may cause cellular defects predominantly in motor neurons because they are more susceptible to

damage, while impairment of sensory neurons may be below the threshold of producing clinical signs. If similar mechanisms occur in CMT2F, varying thresholds of impairment in different individuals may explain why some patients present with sensory loss with the same mutation while others do not.

Mutations in α-crystallin are known to cause cataracts and cardiomyopathy. Many of these mutations are known to cause protein aggregation similar to Hsp27 mutants, however, WT Hsp27 co-expression has been shown to reduce both levels of aggregation and levels of inclusion bodies caused by mutants, similar to Hsp27's effect on mutant NFs (240, 282, 283). Neuropathies associated with other small heat shock proteins are extensively reviewed by Boncoraglio *et al*., Datskevich *et al*., and Benndorf *et al*. (284–286).

Concluding Themes

One common trend observed across various studies of CMT2F appears to be that different mutations produce different effects, even when studied by a single group. For example, R127W mutations may not affect NF interactions as S135F and P182L do (241), and T151I and P182L mutants were not found to bind and hyperstabilize MTs as S135F and R127W did (247). Moreover, some phenotypes have shown opposing effects from different mutants, as cells transfected with R127W and S135F exhibit greater thermotolerance, those with P182L less thermotolerance, and those with T151I and S156Y not demonstrating significant change. In this same study, R136W was found to have greater chaperone activity while P182L was unchanged (229). In a comparable disease state, CMT2D and distal spinal muscular atrophy type V are both caused by

glycyl tRNA synthase mutations, further suggesting that variable sensory symptoms can exist in the same disease process (287). The slightly different phenotypes from clones isolated from iPSCs from a single individual discussed earlier provide even stronger evidence for variability in CMT2F (260).

As such, it will be of critical significance to focus efforts on generating models from iPSCs derived from patients as has been done recently (258, 260). Not only do such systems facilitate relatively easy study in human cells but they allow for the study and direct comparison of WT Hsp27 and mutant proteins at endogenous levels. iPSCs can also be propagated in cell culture indefinitely and are relatively easily expandable, especially in facilitating experiments that test potential therapeutics including HDAC6 inhibitors. This relative ease of expansion could further be applied to high-throughput testing of many different mutations to better understanding heterogeneity in presentation. As previously mentioned, isolating multiple clones from the same individual may uniquely allow for increased understanding of variability in phenotype and any potential environmental influences on pathology and presentation. More cost-effective sequencing and greater emphasis on analyzing sequencing data for a wide spectrum of diseases may also allow for a greater understanding of the prevalence of common CMT2F-inducing mutations in non-presenting individuals and better estimates of the penetrance of mutations. As the S135F mutation has consistently demonstrated some of the most striking pathologies in experimental reports, and is consistently reported as one of the most common mutations, it is possible that it has a higher penetrance than other mutations that may not always result in a phenotype.

Given the high variability of effects of different mutations and experimental systems, studies must be carefully designed and performed to ensure a complete understanding of CMT2F pathology. Research papers should carefully consider alternative conclusions and potential limitations of model systems used. This is especially critical in mouse models – while the first paper presenting a transgenic mouse model contained exciting findings that led to a search for therapeutic targets, a second mouse model did not replicate the same basic pathology, and later models suggested these findings may be spurious due to overexpression of Hsp27. Given the advent and relative ease of using CRISPR-Cas9 technology to generate mutants, generation of additional mouse models with physiological levels of mutant Hsp27 expression need to be assessed, and findings from mouse models with overexpressed protein must be carefully considered in appropriate context. Novel phenotypes should ideally be assayed using many different mutations, and negative data should be prominently displayed, given issues with reproducibility. Studies demonstrating differences in phenotypes for mutants should be especially careful to repeat experiments with sufficient power to show effects, especially in the face of high experimental variation.

Nevertheless, the great wealth of knowledge developed in the short time period since 2001, when CMT2F was discovered, and 2004, when Hsp27 was identified as a causative agent, provides confidence that research in CMT2F will continue to progress at a rapid pace. Investigators from increasingly diverse disciplines are becoming involved in studying CMT2F, and such a multiformity of perspectives can only aid in

considering novel mechanisms and developing unconventional potential therapeutic strategies. It is likely that different forms of CMT2 share similar pathology and potential common mechanisms. CMT2E has been shown to present similarly to CMT2F with formation of aggregates, abnormal mitochondria, and resulting axonal transport defects (226, 288), while Hsp27 has been shown to rescue defects in CMT2E, and removing NFL alleviated the CMT2F phenotype, suggesting these diseases may possess convergent mechanisms (240, 288). Multiple mitochondrial phenotypes including an increased average size have been observed in CMT2F, suggesting that mutations in mitofusin 2 that cause CMT2A may induce similar pathological mechanisms (289). As an increasingly nuanced biochemical and cellular understanding of other forms of CMT2 develop, we can hope to extend our understanding CMT2F, and come closer to developing effective treatments.

Aims of study

Based on the strong ties of sphingolipids to many neurodegenerative diseases and neuropathies, previously unestablished molecular link of sphingolipids to CMT, and lack of complete molecular mechanisms in types of CMT such as CMT2F, I was interested in determining if sphingolipids were altered in CMT. If so, I was interested in developing an understanding of how sphingolipid dysregulation contributed to the pathology of CMT. Furthermore, given the recent discovery of deoxySLs in mammalian cells and links of their accumulation in neural dysfunction, I was interested in developing an effective method for profiling these species and determining if they increased in nervous system tissue in normal aging.

Chapter 3

METHODOLOGIES

Chapter 3: Methodologies

Cell culture and viruses

HT-22 cells were used for biological studies, HCT-116 were used for co-immunoprecipitation, and HEK-293T cells were cultured for viral production. HT-22 and HCT-293T were cultured with DMEM (Invitrogen, Carlsbad, CA) with 10% FBS Fetal Bovine Serum (FBS). Cells were monitored with MycoAlert to detect potential *Mycoplasma* contaminations. Human Hsp27 was cloned into pcDNA3.1 with an N-terminal HA tag. A QuikChange site-directed mutagenesis kit (Agilent, Santa Clara, CA) was used to generate S135F, P136W, and P182L mutations. HT-22 cells were transiently transfected with pcDNA3.1 constructs for 48 hours with Xtremegene 9 with a ratio of 1 ug DNA:4 uL Xtremegene:100 uL OptiMEM media. Cells were exposed to Fumonisin B1 (Enzo, Farmingdale, NY) or myriocin (Sigma, St. Louis, MO) for the time period indicated.

DRG cells were collected and cultured from mice with modifications as described previously (290). DRGs were collected from seven month old C57BL/6 mice (The Jackson Laboratory, Bar Harbor, ME) for cellular imaging experiments. 22 mm siliconized circular cover slides (Hampton Research, Laguna Niguel, CA) placed in a well of a 6-well plate were pre-treated 16 hours prior to dissection with 0.1 mg/mL poly-l-lysine (PLL) (Sigma) in PBS (phosphate-buffered saline). Four hours prior to plating DRGs, the PLL solution was removed, washed for 5 minutes with PBS, and replaced with 20 ug/mL laminin (ThermoFisher, Waltham, MA) in PBS. DRGs were collected in ice-cold Neurobasal medium (Invitrogen) and digested in 20 U/mL papain (Worthington,

Lakewood, NY) and papain activation solution (0.4 mg/ml L-cysteine, 50 nM EDTA, 1.5 uM CaCl in HBSS, pH 7.4) for 20 min at 37 degrees and subquently digested in a mixture of 5 mg/mL displase (Sigma) and collagenase type IV (Worthington) for 20 minutes at 37 degrees. Cells were then washed with PBS, triturated with three subsequently smaller fire polished Pasteur pipettes in F:12 HAMS DRG Culture Media, consisting of F12 nutrient HAMS media (11330-032, Invitrogen), 10% FBS (GE Healthcare HyClone, Logan, UT), 1x MEM Vitamins (Invitrogen), 1:100 penicillin/streptomycin (Invitrogen). The cells were subsequently centrifuged at 2,000 rpm, and resuspended in F:12 HAMS DRG Culture Media before straining (ThermoFisher). Laminin was removed from the plates, washed with PBS, and the cells were resuspended and plated and allowed to adhere for 3 hours, before another 3 mL of media was gently added. Cells were cultured for 4 days before imaging. A Neon transfection machine was used for electroporation. Neuronal identify was confirmed by co-staining for TrpV1 or Tuj1.

Immunoprecipitation

Anti-FLAG Immunoprecipitation (co-IP) done using HT-22 and HCT-116 cells was performed using Anti-FLAG M2 Affinity Gel (Sigma) according to the manufacturer's guidelines. For co-IP performed in mouse tissue, tissue was dissected, flash frozen, and later measured for protein. 1000 ug of brain, 500 ug of spinal cord, and 100 ug of sciatic nerve homogenates were incubated with 0.8 ug of Hsp27 antibody overnight at 4 deg. while shaking. The next day, 50 uL of Protein AG beads were

incubated with the mixture for 1 hour at 4 deg. while shaking. The mixtures were eluted by heating at 100 deg for 5 minutes and immunoblotting was performed.

Immunoblotting and antibodies

Cells were collected from 60 mm dishes 72 hours after plating and washed in PBS and lysed in a Triton-X 100 lysis buffer as used in co-IP experiments. Lysates were sonicated and centrifuged at 14k rotations per minute (rpm) for 10 min to pellet debris. Protein was measured using SpectraMax M5 (Molecular Devices, Sunnyvale, CA), and samples were normalized and mixed with loading buffer (NuPage LDL Sample Buffer 4x) and 0.72M 2-mercaptoethanol (Sigma) and boiled for 5 minutes. Protein samples were resolved on 4-20% gels (Invitrogen) at 150 V using the Criterion system (Bio-Rad, Hercules, CA) and transferred to PVDF membrane in Tris buffer (100 V, 60 min, 4 degrees). Membranes were blocked with 5% milk/PBS containing 0.1% Tween (PBS-T) for one hour at room temperature probed with primary antibody in 5% bovine serum albumin (Sigma) overnight at 4 degrees. Then they were washed quickly and then twice for 15 minutes, and probed with HRP-conjugated species-specific secondary antibody (Santa Cruz Biotechnology, Dallas, TX) for 1 hour at room temperature, then washed transiently and twice for 15 minutes. Immunoblotts were quantified using ImageJ. The antibodies used were as follows: Anti-FLAG (F3165, Sigma), anti-actin (A5441, Sigma), anti-HA (rabbit polyclonal, 3724, Cell Signaling, Danvers, MA; goat polyclonal, Y-11, Santa Cruz), anti-α-tubulin (TU-02, Santa Cruz), anti-acetyl-α-tubulin (6-11B-1, Santa Cruz), anti-Hsp27 (C-20, Santa Cruz), anti-LASS1/CerS1 (H-170, Santa Cruz), anti-calnexin (H-70, Santa Cruz), anti-LC3B (2775S, Cell Signaling), anti-TOM20 (FL-145,

Santa Cruz), TrpV1 (rabbit, Millipore, Billerica, MA), Tuj1 (mouse, Biolegend, San Diego, CA) and HRP conjugated secondary antibodies (Santa Cruz).

Immunofluorescence

HT-22 cells were plated on poly-D-lysine-coated 35-mm confocal dishes (MatTek) for 72 hours. Cells were washed and fixed with 4% freshly prepared paraformaldehyde (Sigma) in PBS for 10 minutes, washed, permeabilized with 0.1% Triton X-100 (Sigma) in PBS for 5 minutes, washed, blocked in 2% human serum for 1 hour, incubated with primary antibody in 2% serum for 1 hour at 37 degrees, washed, and incubated with secondary antibodies conjugated with Alexa Fluor dyes (Life Technologies, Carlsbad, CA) for 1 hour, then washed once quickly and twice for 15 minutes each. Vectashield DAPI-mounting medium (H-1200, Vector Laboratories, Burlingame, CA) was applied for 15 minutes before imaging. All washes were performed with sterile, 0.22 um filtered PBS and all steps were done at room temperature unless otherwise indicated. Images were obtained using a Leica TSC SP8 laser scanning confocal microscope. Mitochondria were visualized using 500 nM MitoTracker Deep Red FM (ThermoFisher) for 30 minutes according to the manufacturers instructions. Live cell imaging was performed at 37 degrees and 5% CO_2.

Mitochondrial morphology was quantified using the macro “Mitochondrial Morphology” developed by Ruben K. Dagda (291). Images were imported to ImageJ image version 2.0.0. Cells of interest were selected by confirming that they were transfected with Hsp27 by visualizing a fluorophore conjugated antibody attached to an

Hsp27 antibody. Cells were then encircled using the polygon selection tool and processed by removing both the nuclear DAPI channel and Hsp27 channel, thereby only displaying the mitochondria channel. The “Process” function within the Mitochondria Morphology macro was run on the image by applying the Autothreshold tool. Additional manual threshold adjustments were then made to ensure appropriate signal was present without any impeding background signal. The image was then evaluated using the Mitochondrial Morphology “Analyze” function. This macro takes measurements of all present mitochondria in the region of interest and provides quantification of mitochondria size, area, perimeter, count, circularity, and solidity. The tool also provides an area/perimeter value as an index for mitochondrial interconnectivity. Data was transferred to Microsoft Excel for analysis.

Mitochondrial function

A Seahorse 96XF machine (Agilent, Santa Clara, CA) was used to measure oxygen consumption rates according to the manufacturers instructions. 10,000 HT-22 cells were used to seed XF96 plates and experiments were performed according to guidelines established by the manufacturer. Three temporal measurements were taken and averaged to compute each basal condition. Following experiment cell cartridge was frozen and data was normalized to total protein.

Lipid analysis

Cells were washed with ice-cold PBS before collection. Protein levels of tissue samples and subcellular fractions were measured and masses submitted were normalized to total. High performance LC/MS of ceramide species were performed by

the Lipidomics Core at Stony Brook University as previously described (292). Lipids from cell culture experiments were normalized to total phosphate levels following LC/MS readings.

Deoxysphingolipid Analysis

Protein levels of tissue samples and subcellular fractions were measured and the final results were normalized to total protein content. Samples were fortified with an internal standard mix and lipids were extracted twice with a mixture of Ethyl acetate: Isopropanol: Water – 60: 28: 12%, as previously described (292). Two extracts, 2 mL each, were added together and dried down under nitrogen. The samples were resuspended in 150 uL of Mobile phase B (Methanol: 1mM Ammonium formate: 0.2% Formic acid). High performance LC/MS of ceramide species were performed by the Lipidomics Core at Stony Brook University as previously described (292).

Mass spectroscopy analyses were conducted on TSQ Quantum Ultra triple quad mass spectrometer with Accela 1250 HPLC system in MRM mode. The lipids were separated on a C8CR chromatography column and injected into the mass spectrometer, where they were separated and characterized according to their mass-to-charge ratio.

The presence of many other lipids in biological material extracts makes it difficult to identify separated species. The compounds were optimized using the aforementioned standards purchased from Avanti (Alabaster, Alabama). The quantification was performed by using internal standards and calibration standards for each lipid.

The MRM transitions that were used are shown in Table 2A. The collision energy was optimized with standard species (see Table 2A). RT linear regression analysis was performed to find the species which do not have standards. All standards were purchased from Avanti Polar Lipids, Inc (Alabaster, Alabama). C16-deoxyCer, C16-deoxydhCer, C24:1-DeoxyCer and C24:1-deoxydhCer standards were used for optimization of the MS transitions and all other MS parameters. Representative calibration curves demonstrated high linearity. C16-deoxyCer, C16-deoxyCer, C24:1-deoxyCer and C24:1-deoxyCer standards were used to determine parameters for accurately measuring deoxydhCer and deoxyCer species. Using these standards, as well as all standards for regular ceramides, I was able to calculate retention times (RTs) for C12, C14, C18, C18:1, C20, C20:1, C22, C22:1, C26, and C26:1 deoxyCer and deoxydhCer. The deoxy species were quantified using the closest by RT and by structure standard.

Metabolic Analysis

High performance liquid chromatography and untargeted mass spectroscopy were performed by the Stony Brook Metabolomic facility as previously described (293).

Cell assays

Cell viability was measured using the oxidation of the aqueous solution 3-(4,5-dimethylthiazol-2-yl)-2,5-diphenyltetrazolium bromide (MTT) to the insoluble formazan (Sigma) was previously described (294). Urea content was measured using a QuantiChrom Urea Assay Kit (DIUR-100) as following manufacturer's guidelines.

Subcellular fractionation

Protein lysate was collected with a Mitochondrial Isolation Kit for Cultured Cells (ThermoFisher) according to instructions as provided by the manufacturer. Spin speeds of 1,000g and subsequently 3,000g were respectively used in order to obtain an enhanced purity mitochondrial fraction. Sample pelleting at 1,000g was deemed nuclear; the supertant subsequently pelleting at 3,000g and also following a subsequent wash and 3,000g spin was deemed mitochondrial. Following the first 3,000g spin, supernatants were spun at 13,000g, and the resulting fraction was deemed cytosolic/microsomal.

Mouse tissue

All animal procedures were approved by the Stony Brook University Institutional Animal Care and Use Committee (IACUC) and followed the guidelines of the American Veterinary Medical Association. Sciatic nerve and brain tissue were dissected from C57BL/6 and Hsp27 KO mice (222) and flash frozen in liquid nitrogen and later homogenized using a QIAGEN TissueRuptor. Results were normalized to protein.

Statistical analysis

Unpaired Student's t test for single comparisons with a $P < 0.05$ were considered statistically significant for comparison of 2 groups, unless otherwise noted. Figures were marked with *, **, and *** for calculations that revealed that $P < 0.05$, $P < 0.01$, and $P < 0.001$, unless otherwise noted. Unless noted, wild-type (WT) conditions were compared with mutant or pharmacologially altered conditions. For experiments in which no observable substantial difference between groups was present, error bars are shown.

DeoxyCer and deoxydhCer levels were not statistically analyzed as the purpose of these experiments was to demonstrate the efficacy of this method and note general trends that are worthy of more detailed study. Data are represented as means with standard errors, unless otherwise noted. N = number of independent experiments, unless otherwise noted.

Chapter 4

DECREASED CERAMIDE UNDERLIES MITOCHONDRIAL DYSFUNCTION IN CHARCOT-MARIE-TOOTH 2F

Chapter 4: Decreased Ceramide Underlies Mitochondrial Dysfunction in Charcot-Marie-Tooth 2F

Introduction

Charcot-Marie-Tooth (CMT) Disease is the most commonly inherited peripheral neuropathy with a prevalence of about 1 in 2,500 (169). CMT was initially defined clinically by its alternate name, Hereditary Motor and Sensory Neuropathy, describing the typical patient presentation of symmetric distal polyneuropathy, gait abnormalities, pes cavus ("hammer toes"), and diminished sensation and deep tendon reflexes (151, 164). Over 70 genes have been implicated in CMT, highlighting its genetic heterogeneity (295). CMT type 1 (CMT1) comprises 80% of cases and presents with reduced motor nerve conduction velocity (MNCV), whereas CMT type 2 (CMT2) presents with normal MNCV but decreased compound muscle action potential (295). Unsurprisingly, most genes implicated in CMT1 are involved in homeostasis of myelin. Interestingly, despite causing symptoms only in peripheral neurons, genes involved in CMT2 are implicated in basic cellular processes. Current treatments for CMT are still quite limited.

CMT2F is specifically caused by mutations in Heat shock protein 27 (Hsp27) (175). Hsp27 is a member of the class of small heat shock proteins (sHsps) that are vital in cellular homeostatic mechanisms such as inflammation, longevity, cell division, cell survival, and apoptosis (296). While lacking intrinsic folding capacity, sHsps act as ATP-independent molecular chaperones, maintaining client proteins in a folding-competent state before passing them on to ATP-dependent chaperones for refolding or denaturation (196, 296). There is an extensive literature on the protective effects of

Hsp27 in the nervous system. Overexpression of Hsp27 reduces neuronal cell death and the severity of drug-induced seizures (297), and Hsp27 injection reduces severity of sequelae of cerebral ischemia in mice (298). Hsp27 expression is upregulated in neuronal injury and thought to have a role protecting injury-induced motor neuron death (187). Hsps are vital in promoting proteostasis, the homeostatic and quality control mechanisms assuring protein integrity, in neurons by preventing the accumulation and aggregation of misfolded proteins that can cause neural diseases (299). Evidence suggests that Hsp27 restricts cell death by reducing protein aggregation or other pathological mechanisms seen in Alzheimer's, Huntington's, Parkinson's Diseases, and Amyotrophic Lateral Sclerosis (270, 300). However, the pathogenesis of Hsp27 in CMT2F remains unknown, but is thought to be due to defects in axonal transport of mitochondria (260).

Sphingolipid metabolism involves a myriad of enzymes responsible for generating sphingoid bases and converting them into an array of structurally distinct sphingolipid molecules with a complex diversity of functions (301). Ceramides are a key sphingolipid intermediate predominantly produced by ceramide synthases (CerSs), and they function as bioactive molecules regulating growth arrest, senescence, apoptosis, and autophagy (5, 301–303). CerSs generate ceramides predominantly through the *de novo* generation of dihydroceramide from acylation of dihydrosphingosine or through the salvage pathway by acylating sphingosine generated from breakdown of complex sphingolipids (302). Six CerS isoforms (CerS1-6) have been identified, each of which uses different length fatty acyl-CoA chains to produce distinct ceramide species (301,

304). CerSs are active at the endoplasmic reticulum (ER), with enzymatic activity thought to occur on the cytosolic face of the ER (305, 306). CerSs have also been detected in additional compartments including mitochondria and nuclear membranes. CerS1, which catalyzes the formation of C18- and C18:1 ceramides (105, 106), is highly expressed in the nervous system, skeletal muscles, and testes (Illustration 1) (109). Mice with nonsense or certain point mutations in CerS1 show a neurodegenerative phenotype with reduced C18-ceramide biosynthesis, accumulation of ubiquitylated proteins and lipofuscin in the nervous system, neuronal cell death, and an ataxic phenotype (110). A mutation in the intial enzyme of the *de novo* pathway, serine palmitoyltransferase (SPT), causes Hereditary Sensory Neuropathy type 1 (HSAN1), which has a similar phenotype to CMT2F (49), suggesting that alterations in the *de* novo pathway of ceramide genesis may produce CMT-like phenotypes.

Here, LC/MS was performed on Hsp27 KO mouse sciatic nerve tissue yielding the novel observation that Hsp27 KO sciatic nerve demonstrates decreased ceramides. This decrease in ceramide was determined to occur acutely in the mitochondria of CMT2F mutant cells which present with less mitochondrial CerS1. This is proposed to occur via a novel CerS:Hsp27 interaction draws CerS away from the mitochondria, reducing mitochondrial ceramide species. This results in mitochondrial morphological and functional/metabolic changes that parallel decreases in ceramide. This work provides a novel mechanism for CMT degeneration through dysregulation of the ceramide synthesis pathway, implicating sphingolipids in CMT pathobiology.

Results

Hsp27 KO results in alterations in sphingolipid metabolism

To investigate the effects of the chaperone protein Hsp27 on ceramide regulation, we measured ceramide species in brain and sciatic nerve samples from Hsp27 KO mice. Interestingly, sciatic nerve tissue showed decreased ceramide, particularly at 6 months of age. These changes were most notable in longer chain length ceramides with saturated acyl chains (Fig. 1A-J). While large decreases in total ceramides occurred in sciatic nerve from older mice, they were not unanimously seen in brain tissue (Fig. 1K-L, Fig. 2). These data demonstrating selective sphingolipid decreases in sciatic nerve tissue from adult animals suggested that sphingolipid metabolism may be altered when peripheral neuropathy presents in CMT2F.

To determine if there were acutely altered sphingolipid levels in CMT2F in a cellular model, I established conditions for transfection of wild-type (WT) or S135F mutant Hsp27 into HT-22 cells (Fig. 3A), an immortalized line derived from mouse HT4 hippocampal cells (307, 308), as a biological model. In addition to replicating neuronal intracellular environment, decreased endogenous Hsp27 make HT-22 cells a strong model for the study of biological functions of Hsp27 in CMT2F pathology by introducing WT or mutant genes. Using LC/MS, ceramides were measured in HT-22 cells transfected with vector (V), WT Hsp27, and S135F Hsp27. Surprisingly, the S135F mutation did not cause altered cellular ceramide levels compared to the WT condition (Fig. 4). Nevertheless, a lack of change did not rule out compensatory mechanisms in the sphingolipid network that could mask the primary effects. In order to determine if the

S135F mutant specifically inhibited CerSs, cells were labeled with the non-endogenous precursor C_{17}-sphingosine for 20 minutes to evaluate the synthesis of ceramide species. However, labeling revealed no differences between HT-22 cells either transiently or stably transfected with WT and S135F (Fig. 5A-B). Total ceramides were also not affected in cells transiently transfected with three mutations known to cause CMT2A (Fig. 6) (309–312). These results raised the possibility that changes in ceramides may be compartment or tissue dependent.

Hsp27 mutant decreases mitochondrial ceramides

Mitochondrial trafficking defects have been shown in CMT2F, and mitochondrial proteins are known to be mutated in CMT2A, suggesting that acute alterations in sphingolipid metabolism may be restricted to mitochondria (220, 309, 310). To test this hypothesis, conditions were established for fractionating cells to isolate crude mitochondrial, nuclear, and cytoplasmic (including microsomes) fractions from V, WT, or S135F Hsp27 expressing cells (Fig. 7), and then ceramide species were measured in these fractions. The S135F Hsp27 cells showed a significant decrease in total mitochondrial ceramide levels, whereas cytoplasmic ceramides were slightly increased, while nuclear ceramides were unchanged as compared to WT Hsp27 cells (Fig. 8A-C). Ceramides from V cells were used for normalization and levels were similar to WT. These data suggest that that ceramide metabolism is altered in CMT2F.

Hsp27 mutant displays interactions with CerSs

Next, I sought to evaluate how Hsp27 affected ceramide levels. As CerSs are the predominant regulators of *de novo* ceramide synthesis, I hypothesized that they may be

dysregulated in CMT2F, producing deficits in ceramide production. To address this hypothesis, CerS regulation by Hsp27 was examined in HT-22 cells. First, to determine if Hsp27 interacted with CerS, FLAG tags were subcloned onto CerS1, CerS2 and CerS5, and each CerS was co-expressed with Hsp27 in HT-22 cells. Having established conditions for transfection and immunocytochemistry in HT-22 cells (Fig. 9A), I determined that each of these CerSs displayed co-localization with Hsp27 (Fig. 10A-C).

To evaluate the relative importance of different CerS in mouse peripheral neurons, sphingolipid levels were measured in dorsal root ganglia (DRG) from 7 month old female mice (Illustration 2). C18-ceramide was one of the highest species, suggesting that CerS1, which predominantly generates C18-ceramide, is highly expressed in these cells (Fig. 10D). This falls in line with other evidence linking high CerS1 expression in the nervous system. This prompted me to use CerS1 as a target to investigate the effects of sphingolipid biology on CMT2F.

CerS1 function has been shown to be highly dependent on cellular localization, and CerS1 mutations can induce dysfunction by altering its cellular location (304, 313). Furthermore, overexpressed ectopic expression of CerS1 does not alter its cellular localization (304). Next, studies were conducted to evaluate the co-localization of Hsp27 and CerS1 microscopically and determine the cellular localization of this interaction. Super-resolution Structured Illumination Microscopy (SIM) was used to determine that overexpressed WT and S135F Hsp27 and CerS1 further co-localize as indicated by the yellow overlap of the green anti-FLAG staining transfected CerS1 and red anti-Hsp27

staining (Fig. 10E-F). As expected, transfected CerS1 showed strong co-localization to the ER, as evidenced by the white overlap of green anti-FLAG and purple anti-calnexin (Fig. 10G). These data demonstrate the proximity of Hsp27 and CerS1, especially in the ER.

I further sought to demonstrate this interaction in DRGs that were similarly isolated and cultured from mice, allowing introduction of genes through electroporation (Fig. 9B). Endogenous Hsp27 (red) and CerS1 (green) in DRGs were confirmed to co-localize by presence of yellow (Fig. 10H). Furthermore, electroporated WT and S135F Hsp27 also co-localized with CerS1, as shown by a representative image of S135F and CerS1 co-transfection (Fig. 10I). Hence, these results suggest that the co-localization occurs with endogenous proteins in primary neurons as it would in the disease.

Increased Binding of Hsp27 Mutants to CerS1

To further evaluate the interaction of CerSs and Hsp27, a hemagglutinin (HA) tag was subcloned onto Hsp27 to aide in its discrimination and facilitate co-immunoprecipitation (co-IP) experiments. An HCT-116 colon cancer cell line that stably overexpresses CerS1 upon tetracycline induction was transiently transfected with either empty vector or WT, S135F, R136W, and P182L mutants. Successful inducible overexpression of WT and S135F Hsp27 was achieved in HCT-116 and validated by immunoblotting (Fig. 3B). Overexpression of CerS1 was validated by measuring sphingolipid levels and observing a substantial increase in C18 and C18:1-ceramide. However, the presence of overexpressed CerS1 did not cause there to a difference in sphingolipid levels between V, WT, and the three mutant conditions (Fig. 11). Co-IP of

CerS1 and Hsp27 in HCT-116 via pull-down of FLAG-tagged CerS1 with anti-FLAG beads and immunoblotting of Hsp27 confirmed the proteomic finding of a novel binding interaction between these two proteins (Fig. 12A-B). Moreover, CerS1 pulled down approximately 10 times the amount of Hsp27 mutants (S135F, R136W, P182L) compared to WT Hsp27. To confirm in a neuronal model, HT-22 cells were transiently transfected with CerS1 along with either empty vector, wild-type (WT) Hsp27, or S135F mutant Hsp27s. Pulldown of CerS1 with anti-FLAG beads and immunoblotting for Hsp27 in HT-22 cells confirmed the interaction of Hsp27 and CerS1 and showed the increased interaction of the S135F mutant compared to WT Hsp27 (Fig. 12C-E). Furthermore, co-IP supernatants were immunoblotted to determine if the increased S135F interaction to CerS1 resulted in a substantially decreased proportion of free S135F in the cell; however, there was no significant change between WT and S135F. These results demonstrate a very close interaction between CerS1 and Hsp27 resulting in co-IP of the two proteins, and furthermore show altered interaction between CerS and mutant Hsp27 which may contribute to the dysregulated ceramide levels in CMT2F.

As a further confirmatory measure, binding was assessed in an animal model. WT (C57B6) and Hsp27 KO mouse brain, spinal cord, and sciatic nerve were dissected and homogenized and pull-down was performed with Hsp27 incubated with Protein AG agarose beads and then probed with CerS1, CerS2, and CerS6 antibodies. These results demonstrate a close interaction of CerS1 and Hsp27 in brain tissue that is absent in the Hsp27 KO mice (Fig. 13). While this interaction could not be confirmed in spinal cord nor sciatic nerve tissue, these tissues demonstrated very low levels of

endogenous expression of CerS1, potentially making this interaction below the sensitivity of this co-IP assay.

Next, I sought to determine the location in the CerS1 protein in which this interaction occurs. Preliminary data suggested that the C-terminus of CerS1 was responsible for its binding to Hsp27. C-terminal CerS1, thyrodoxin, and buffer were bound to a Ni^{2+} column. Hsp27 was then applied to the column, washed, and eluted. Flow-through and elution samples that were probed with anti-Hsp27 antibody determined that both WT and S135F mutant bound to the C-terminus of CerS1 (Fig 14).

Hsp27 modulates localization of CerS1

Mitochondria as well as mitochondrial associated membranes (MAMs) have been shown to possess distinct ceramide pools through endogenous ceramide synthases (314). Decreased mitochondrial ceramides suggested the alteration of ceramide homeostasis may be a result of change in the localization of CerSs. To determine if WT or S135F altered the cellular localization of CerS1, HT-22 cells were simultaneously stained for CerS1 and either mitochondria or ER markers. Analysis of images from SIM microscopy using Pearson's Correlation Coefficient (PCC) and Manders' Overlap Coefficient (MOC) as quantitative measures of co-localization showed that expression of the S135F Hsp27 mutant caused a decrease in the localization of CerS1 to mitochondria when compared to cells expressing WT Hsp27 (Fig. 15A). However, WT and S135F Hsp27 themselves both displayed similar localization to mitochondria, irrespective of the mutation (Fig. 15B). Using a similar approach by staining with an ER instead of mitochondrial marker, I determined that neither CerS1 nor Hsp27 had any

differential localization to ER with expression of S135F mutant compared to WT Hsp27 (Fig. 15C-D). As a proxy for MAMs, I also analyzed ER and mitochondrial overlap in the presence of WT or S135F Hsp27; however, the mutant did not alter this parameter (Fig. 15E). I did not observe a notable difference in cells untransfected with Hsp27. Taken all together, these data suggest that mitochondrial association of CerS1 is altered by mutant Hsp27, causing a diversion of ceramide production away from the mitochondria.

Hsp27 mutant alters mitochondrial morphology and involving sphingolipids

Next, it became imperative to determine whether the observed decreased mitochondrial ceramides and decreased mitochondrial localization of CerS1 by S135F mutants reflected substantial alterations in mitochondrial structure and function induced by mutant Hsp27 and whether sphingolipids play a role in these effects. It should be noted that Hsp27 mutants have been associated with decreased mitochondrial trafficking (220), but not mitochondrial morphological effects.

Therefore, mitochondrial morphology in cells transfected with either WT or S135F Hsp27 was evaluated. Compared to mitochondria in WT cells (Fig. 16A), mitochondria in S135F cells appeared larger (Fig. 16B) with increased area and greater interconnectivity as quantitated by increased ratio of area/perimeter (Fig. 16C-D). Thus, mutant Hsp27 exerts significant effects on mitochondrial morphology.

To determine if the reduced ceramide generation is involved in these changes, CerS was inhibited with Fumonisin B1 (FB1) in order to mimic the decrease in ceramides observed with mutant Hsp27. FB1 application at 50 uM for 24 hours

reproduced the increases in mitochondrial size and interconnectivity as seen in the presence of the S135F mutant (Fig. 16C-D). These results show that attenuation of ceramide specifically (with FB1) recapitulates the morphologic effects of the decrease in ceramides induced by mutant Hsp27.

These results suggested that mitochondria may demonstrate increased fusion. In order to measure dynamic events in mitochondria, live cells transfected with WT and S135F were rapidly imaged 100 times over 5 minutes – every other image was used for analysis, resulting in images approximately 6 seconds apart. The number of mitochondria were calculated and the standard deviation in the total count was measured for a 5-minute time window. Compared to WT cells, S135F mutant cells exhibited a trend with an increased standard deviation in count, although this was not significant, potentially due to the low number of trials (Fig. 17). This suggests that S135F mutant may cause mitochondria to be more dynamically active, although further work must verify these findings.

Hsp27 mutants decrease mitochondrial respiration and involving sphingolipids

Next, I sought to determine if the observed swollen mitochondria in mutant cells were associated with decreased respiratory functioning (Illustration 3). Indeed, mutant HT-22 cells (S135F, P182L) displayed decreased basal and maximal oxygen consumption rates (OCR) and substantial decreases in spare respiratory capacity (Fig. 18A-C). These studies reveal important functional effects of mutant Hsp27 on mitochondrial function.

To determine if this decrease in mitochondrial functioning is also a result of the decreased ceramides, FB1 was applied. The results showed that FB1 caused a significant decrease in the same respiratory parameters (Fig. 18A-C), suggesting that CerS inhibition underlies the defective respiration in CMT2F mutants.

Hsp27 mutant increases autophagic flux but not cellular proliferation

Decreased respiratory ability of cells may affect their ability to replicate and survive. S135F mutant transiently transfected into N2a cells was previously shown to decrease cellular survival by about 30% at 48 hours post-transfection (175). Since increased ceramide is linked to apoptosis, I set out to determine if observed altered ceramides could modulate cell viability in the HT-22 model. Analysis of vector, wild-type, and S135F transfected cells showed no difference in proliferation within 48 hours (Fig. 19A). To evaluate if the S135F mutant modulated growth responses to metabolic stress, I applied 2-deoxyglucose at concentrations of 2.5 uM and 25 uM as determined empirically (and glucose as osmotic controls) to decrease HT-22 cell viability (315). Cell counts were not altered even in the presence of the 2-DG (2-deoxyglucose) (Fig. 20A). This suggests that CMT2F pathology is not directly related to apoptosis or necrosis, which supports clinical and mouse model findings of substantial atrophy, aberrant myelination, and axon loss that is mild and often accompanied by regeneration (177, 217, 242).

An important biologic response involved in clearing compromised mitochondria is autophagy, a process in which autophagosomes sequester damaged cellular components including mitochondria and target them for degradation (316). While

autophagy has been shown to be involved in some forms of CMT and suggested as a common pathological mechanism (265), it has not been shown to be altered in CMT2F. However, activated Hsp27 has been shown to be a potent stimulator of autophagy in lipid clearance (317), and induces autophagy in response to cisplastin (318) and acute kidney injury to prevent cell death (319). Furthermore, ceramide has been shown to be an important regulator of cellular autophagy (106). Therefore, given these associations, I set out to determine if the S135F mutant regulates cellular autophagy in CMT2F. HT-22 cells were transfected with WT and S135F Hsp27 and immunoblotted for LC3B-II, a common marker of autophagy. S135F mutants display greater LC3B-II than WT transfected Hsp27 HT-22 cells (Fig. 19B-C), suggesting that autophagy is upregulated in CMT2F mutants. To validate this result, HT-22 cells, transfected with WT and S135F Hsp27, were stained for LC3B and Hsp27. Increased autophagic flux in mutant cells was also demonstrated by increased LC3B co-localization with S135F than WT Hsp27 and increased relative LC3B signal (Fig. 19D-E). Through three different methods, these results suggest autophagic flux and autophagy are increased in CMT2F. This suggests an entirely novel cellular view of CMT2F, with decreased ceramide production leading to impaired mitochondrial function, resulting in enhanced autophagy that leads to neuronal degeneration.

S135F has also been linked to tubulin function by increased co-localization of S135F Hsp27 with neuron-specific class III beta-tubulin (also known as Tuj1 or TUBB3) (247). To determine if CerS1 function alters this property, WT and S135F were alternatively co-transfected in HT-22 cells with either CerS1 or Vector. Similarly, a trend

of increased co-localization of Tuj1 with S135F compared to wild-type Hsp27 was observed (Fig. 21). However, in the presence of overexpressed WT Hsp27, there was also a relative increase in co-localization observed in the S135F mutant, suggesting that CerS1 overexpression does not alter this disease phenotype.

S135F mutant does not alter α-tubulin acetylation in tissue

I also sought to determine if other reported cellular phenotypes were altered in a neuronal model. S135F mouse sciatic nerve has been reported to reduce α-tubulin acetylation, resulting in diminished microtubule-mediated transport of mitochondria (220). Some studies using cellular models have confirmed a decrease in α-tubulin acetylation in S135F cells (242), while others have failed to observe a difference (247). In this model, I was not able to observe a change in α-tubulin acetylation. To investigate a potential effect of sphingolipid metabolism on acetylation of tubulin in CMT2F, HT-22 cells were transfected both stably and transiently with Vector, WT, and S135F, but showed no difference in the ratio α-tubulin acetylation (Fig. 20B-C). Transient Hsp27 overexpression was repeated with co-overexpression of CerS1 or vector, which also revealed no change in the ratio the ratio α-tubulin acetylation (Fig. 20B-C).

Metabolomic Screen of S135F and P182L Mutants.

These results prompted us to further examine biochemical consequences of the determined mitochondrial impairment in CMT2F. Metabolomic profiling has been used to find a disturbances in mitochondrial metabolism in Alzheimer's, Parkinson's, and ALS (320). Metabolomic studies on CMT have been very limited; recently, CMT2D mutant glycyl tRNA synthetase (GARS) mice spinal cord were profiled for metabolite changes

compared to WT mice (321), however, there are few other related studies as reference. This study reported that mutants had reduced carnitine, which facilitates fatty acid transport into mitochondria. To determine if metabolites involved in mitochondrial function were similarly dysregulated in CMT2F, a targeted mass spectrometry approach utilizing positive/negative ion-switching was undertaken to measure approximately 300 metabolites in transiently transfected Vector, WT, and S135F and P182L Hsp27 HT-22 cells. Principal component analysis revealed that the S135F and P182L mutants cluster similarly based on metabolic makeup in each experiment in both positive and negative ion mode (Fig. 22A-B). In each experiment, urea was significantly increased in both mutants (Fig. 22C). Creatinine was also increased in the S135F mutant and trended as higher levels in the P182L mutant (Fig. 22D). Glutamine strongly trended to decrease in each mutant (Fig. 22E). However, attempts to confirm increases in urea using a kit did not demonstrate a consistent change (Fig. 23). These results suggest that metabolic waste products may be increased in CMT2F, although further verification is needed before any conclusions can be definitively made.

CerS1 forms dimers with other CerS

It has been reported that distinct CerS enzymes are able to form dimers, which can modulate their action (322). It is possible that increased interaction of mutant Hsp27 with CerS1 may cause reduced binding of other CerS to CerS1, decreasing the enzymatic action of other CerS. To evaluate the possibility that other CerS bind to CerS1 in neuronal systems, I overexpressed FLAG-tagged CerS1 and pulled it down with anti-FLAG beads in order to immunoblot for endogenous CerS2 and CerS6, which

both have antibodies suitable for detection via immunoblotting. Indeed, CerS6 demonstrated strong binding to CerS1, and CerS2 also appeared to bind, as observed by a lack of band in the condition in which CerS1 was not overexpressed (Fig. 24A). Rat siRNA was used against CerS2 and CerS6, but did not have a strong effect on these endogenous enzymes in mouse cells. To evaluate if Hsp27 binding to CerS1 reduces the degree of binding from other CerS, I also co-expressed WT and S135F Hsp27 and quantified the amount of binding. There was a significance decrease in the amount of binding of CerS6 to CerS1 in the presence of S135F compared to WT Hsp27 (Fig. 24B). In order to evaluate if similar results occurred in mitochondria, a similar pull-down procedure was performed in mitochondrial fractions. However, potentially due to insufficient sample, no CerS were observed to be pulled down to Hsp27 in mitochondrial fractions (Fig. 25). Altogether, this data suggests that by binding CerS1, S135F mutant decreases the binding of other CerS, potentially decreasing their enzymatic function.

Decreased deoxySA in S135F mutant

Decreased ceramide production from CerS inhibition can result in a backup of sphingolipid intermediates in the *de novo* pathway, potentially causing altered SPT activity. In order to evaluate this, I analyzed deoxysphingoid bases in HT-22 cells. While deoxySO was below quantifiable levels, there is a relatively minor but significant decrease in deoxySA (Fig. 26). This suggests that deoxysphingolipid metabolism may be altered in CMT2F, although the mechanism of this remains unclear.

Fumonisin B1 decreases dhCers in HT-22 cells

Application of FB1 was used to pharmacologically decrease CerS activity. To further confirm this decrease in CerS in HT-22, I measured ceramide levels. Indeed, all species of ceramide were drastically decreased (data not shown). Interesting though, I observed an increased in dhCers. Further evaluation of the full spectrum of dhCers revealed many species of dhCers were substantially decreased (Fig. 27). This suggests that FB1 may have a more complex mechanism than simple inhibition of CerS. It is possible these effects are due to FB1 creating relatively very high levels of dhSph (data not shown), which are then shuttled to species of dhCers.

Chapter 5

QUANTIFYING 1-DEOXYSPHINGOLIPIDS IN MOUSE NERVOUS SYSTEM TISSUE

Chapter 5: Quantifying 1-deoxysphingolipids in Mouse Nervous System Tissue

Introduction

Out of these many incredibly important findings, one of the most impressive was the link of HSAN1 to SPT mutations and production of deoxysphingoid bases (33, 47, 49, 53). Deoxysphinganine (deoxySA) accumulates in both HSAN1 cellular models and patient plasma samples, and causes neurotoxicity by interfering with the formation and development of neurites (49). The loss of the C_1-hydroxyl group in these molecules is responsible for altering their structural and functional properties. Absence of this polar hydroxyl group near the end of the sphingoid chain further augments the nonpolar nature of their associated ceramides, which may have altered their biophysical properties in membranes. Furthermore, phosphate groups cannot be added due to the absence of the 1-hydroxyl, preventing the addition of different head groups and the formation of more complex sphingolipid species similar to sphingomyelin (SM), glucosylceramides, and gangliosides (323). However, while such deoxysphingolipid (deoxySL) species have long been known to exist in many plants and animal species (324), the physiological and pathological roles of deoxySLs in mammals, especially the nervous system, are still prime for exploration.

Most research on the toxicity of deoxySLs to date has focused on deoxysphingoid bases, although increasing evidence has linked deoxydhCers and deoxyCers to the nervous system, particularly their accumulation in pathological states. C24:1-deoxyCer along with C24-ceramide and many SM species were found to be reduced in the serum of ADHD patients (325). Furthermore, increases in deoxySLs

such as C24 and C22:1 deoxyCer and C22:1 and C18:1 deoxydhCers have been correlated with the progression of neuropathy in breast cancer patients treated with paclitaxel, a chemotherapeutic with dose-limiting peripheral neuropathy (326). DeoxySA demonstrates concentration dependent neurotoxic effects on primary neurons that are thought to be due to excessive N-methyl-d-aspartate (NMDA) activation. Based on responses from inhibiting ceramide synthase, this is thought to be due to increased deoxyCer levels (327).

While deoxySLs have been profiled in cells lines such as mouse embryonic fibroblasts (54), they have not been carefully characterized in nervous system tissue, despite many studies implicating their dysregulation in neural disease states. While some studies have used brain, spinal cords, and sciatic nerves to study deoxySLs in the nervous system, they have focused on measuring deoxysphingoid bases such as deoxySA and deoxySO, finding accumulation of these species in sciatic nerve (48, 59). It has been suggested that deoxySA and its associated deoxydhCers are more likely to result in neuronal toxicity than deoxySO and its associated deoxyCers, although extensive evidence to support this claim is lacking (59). Likewise, many studies have not yet analyzed the full spectrum of acyl chain lengths of deoxyCer and deoxydhCer species (325, 328), and have measured these species in plasma (325, 326, 328), cells (326), or only using brain tissue (62).

To this end, I sought to develop an efficient and accurate method of reliably measuring and determining the accumulation deoxySL species in neural tissues. To encompass a diverse range of tissue types in the central and peripheral nervous

systems that can be relatively easily isolated and probed, I chose to analyze mouse brain, spinal cord, and sciatic nerve tissue. Time points of 1 months, 3 months, and 6 months were used for sets of male and female mice in order to track the effect of age and potential sex differences. Using standards of C16 and C24:1 deoxydhCer and deoxyCer, I was able to reliably measure many specific deoxySL species in these tissue samples. There were no generally observable differences between male and female levels, so this data was grouped together to increase the power of comparisons**.** I was able to accurately measure C24-deoxyCer in brain as well as a variety of deoxydhCer species in brain, spinal cord, and sciatic nerve, most predominantly C22-deoxydhCer. An increase in total deoxydhCers, most noticeably in sciatic nerve in 6 month old mice, was observed, suggesting that these species may progressively accumulate in peripheral tissue. This method will facilitate straightforward profiling of deoxyCers and deoxydhCer in many neural model mouse systems.

Results

Parameters for deoxyCer measurements.

I set out to measure deoxysphingoid, deoxydhCer, and deoxyCer species produced from alanine and palmitoyl-CoA in *de novo* synthesis (Illustration 4). C16 and C24:1 deoxydhCer and deoxyCer standards were used to determine parameters for accurately measuring deoxydhCer and deoxyCer species. Using these standards, I was able to calculate the parameters for measuring C12, C14, C18, C18:1, C20, C20:1, C22, C22:1, C26, and C26:1 deoxydhCers and deoxyCers. Parent ion peak, product ion peak, collision energy, and retention time for all these species are listed (Table 2A). To

empirically determine these “target” values, I used specific “source” curves from standards and previously identified species (Table 2B).

To verify the identity of the aforementioned lipids, I manually inspected peaks produced at the correct mass and predicted retention time. Representative peaks for C24-DeoxydhCer and C22-DeoxydhCer demonstrate relatively high peaks with little background signal (Fig. 28A-B). Thus, these peaks can be designated as deoxydhCers and further quantified by calculating the area under the curve with high confidence. To further verify the identity designated to these detected entities, calibration curves were inspected to ensure linearity. Calibration curves for C16-deoxydhCer, C24:1-deoxydhCer, C16-deoxyCer, and C24:1-deoxyCer demonstrate high linearity further validating our use of these parameters to identify these molecules (Fig. 28C-F).

Deoxysphingoid bases are largely unaltered with age

Brain, spinal cord, and sciatic nerve dissected and flash frozen from mice were chosen as relevant models to represent a diversity of neuronal tissues. Results from analysis of brain, spinal cord, and sciatic nerve were analyzed at ages of 1, 3, and 6 months. Males and females did not show large changes in any lipid species analyzed (data not shown). To increase the power of comparisons, data from males and females was grouped together and stratified by age to identify alterations in deoxySL species during nervous system development as mice reached adulthood. I considered the general similarity of male and female mouse data as further validity of our method of quantification. Sphingolipid species that were below the limit of quantification in many samples or those that did not possess symmetrical peaks clearly distinct from

background signal on analysis of LC/MS data were not included in the presentation of the data. This ensures that displayed data represent true peaks identifying deoxySL species.

As such, sphingoid and deoxysphingoid bases were initially analyzed in all tissues (Fig 29A-C). Notably, deoxySO levels were below the limit of quantification in all three tissues. DeoxySA was below quantification in sciatic nerve but was observed in brain and spinal cord tissue; however, it was not drastically altered with increased age. Similarly, sphingosine levels were relatively stable with increased age. Sphinganine, however, demonstrated an age-related decline. Additionally, greater levels of sphingosine than sphinganine were observed in all tissues, in contrast to the presence of deoxySA and absence of accurately quantifiable deoxySO in brain and spinal cord. Taken together, this data suggests that deoxysphingoid bases may not be as readily desaturated as sphingoid bases.

These results suggested that ceramide would also be higher than dhCer. Indeed, mouse embryonic fibroblast cells show about 10-fold greater ceramide levels than dhCers (329). To validate these results in a neuronal model, I measured ceramide and dhCer species using HT-22 cells. HT-22 cells demonstrate approximately a 25-fold increase of ceramide compared to dhCer, and large increases in ceramide were consistent for every species in which dhCer was quantifiable (data not shown). As a confirmatory measure, I measured C16-ceramide and C16-dhCer levels in all nervous system tissues used, consistent with our use of C16 standards. Consistently, C16-ceramide was much more abundant than C16-dhCer. Ceramides demonstrated

approximately a 100-fold, 10-fold, and 15-fold increase in brain, spinal cord, and sciatic nerve tissue, respectively, and demonstrated similar trends (Fig. 30A-C). Consistent with the established overview view of *de novo* ceramide metabolism, I concluded that dhCers are predominantly converted to ceramides, which are typically associated with biological function and conversation to other more complex sphingolipids or sphingoids (3).

DeoxydhCers are abundant and increase with age in spinal cord and sciatic nerve

Since much less is known about deoxydhCer and deoxyCer species, it was necessary to accurately quantify levels of both. Only one species of deoxyCer was sufficiently present in tissue for accurate quantification—C24-deoxy ceramide in the brain (Fig. 31). Interestingly, while this species was much less abundant than C24-ceramide, it appeared to slightly rise with increased age, in contrast to C24-ceramide which sharply decreased. This suggests that C24-deoxyCer may serve an important role in aging in the brain.

I determined that there was a general decrease in ceramide levels between 1 and 6 month old mice in each tissue (Fig. 32). Similarly, brain tissue also demonstrated a decrease in deoxydhCers that appeared to be even slightly sharper than the decrease in ceramides in the brain. Interestingly, however, deoxydhCers appeared to increase in the spinal cord and sciatic nerve with increasing age. This was especially stark in the sciatic nerve, with almost a doubling in total deoxydhCer content between 1 and 6 month old mice, despite the overall decrease in ceramides between these two time points. This suggests that in peripheral nervous system tissue, deoxydhCers may

increase with nervous system development, despite decreases in total ceramide levels. Furthermore, total deoxydhCers were especially abundant in peripheral tissue. Sciatic nerve tissue displayed around a 100-fold increase in deoxydhCers compared to brain, despite sciatic nerve only containing about 5 times as much total ceramide as brain. These results suggest that deoxydhCer may increasingly accumulate in the peripheral nervous system.

C22 is the predominant deoxydhCer in mouse neural tissue

To further investigate these trends in deoxydhCers, I analyzed individual species (Fig. 33). In all three tissue types, C22-deoxydhCer was the most prevalent species. This was especially noticeable in spinal cord tissue, in which C22-deoxydhCer dwarfs the contribution of other deoxydhCer species. Generally, C18 and C24:1 species were next highest in abundance. Generally, species that were present above quantification were longer acyl chain deoxydhCers. C18, C22, C24, and C24:1 were common in all species, with C22:1 also being a minor component present in the brain. Generally, for each species there were similar trends in levels with age. These results suggest that common species of deoxydhCer are present in different types of nervous system tissue and that C22-deoxydhCer may play an important role.

Chapter 6

DISCUSSION

Chapter 6: Discussion

Altered Sphingolipids in CMT2F

Summary of results

Alterations in sphingolipids have been associated with a wide variety of neurodegenerative diseases. Several sphingolipids serve as bioactive signaling molecules in a plethora of pathways and have been implicated in Alzheimer's (180, 330), Parkinson's (331), and Amyotrophic Lateral Sclerosis (27). I sought to determine if changes in sphingolipid metabolism may mediate CMT phenotypes. The results here present the first evidence that directly and mechanistically links CMT to sphingolipid dysregulation. I identified a novel interaction of Hsp27 and CerSs and determine that decreased mitochondrial localization of CerS1 occurs in CMT2F mutation, reducing mitochondrial ceramide levels. The CMT2F mutation produces alterations in mitochondrial morphology that are accompanied by decreases in respiratory function. Importantly, these alterations are reproduced by decreasing ceramide synthesis pharmacologically.

The results specifically begin to connect mutant Hsp27 to mitochondrial ceramide levels and function (Illustration 5). WT and S135F mutant Hsp27 interact with CerS in neuronal cells, with evidence of increased interaction of the mutant. While most CerS localize to the ER, there is a population of CerS at the mitochondria in neuronal cells. The S135F mutant decreases this mitochondrial CerS population while increasing cytoplasmic CerS. While this shift does not alter total cellular ceramide production, it results in decreased mitochondrial ceramides, without affecting the intrinsic activity of

total cellular populations of CerS. Decreased ceramide production by pharmacological inhibition of CerS recapitulates all the major effects of mutant Hsp27 noted; thus, FB1 causes increases in size and connectivity of neuronal mitochondria that are also observed in the S135F mutant. Moreover, decreased ceramide production also reduced mitochondrial respiratory function, which again was observed in mutant mitochondria. These mitochondrial dysfunctions in the mutant underlie increased autophagic flux, suggesting that decreased mitochondrial ceramides are responsible for cellular pathology in CMT2F.

Mitochondrial ceramides

The function of endogenous ceramides generated in the mitochondria is still poorly understood, especially in the context of neuronal dysfunction. Ceramide has been innately connected to mitochondrial apoptosis (332), and has been implicated as an inhibitor of the mitochondrial permeability transition pore (333). In other cellular systems related to cancer pathology, ceramide has been shown to modulate the targeting of autophagosomes to mitochondria in promoting mitophagy (106). My results demonstrate an important role for steady state levels of mitochondrial ceramide in maintenance of mitochondrial functions. Such a role does not negate a role for increased mitochondrial ceramide in inducing pathophysiologic responses.

Further understanding of how these mitochondrial pools of ceramide species are dysregulated in nervous system diseases and their specific effects on mitochondria will further enhance our understanding of CMT pathology. It also remains unknown why particularly long-chain ceramides, such as C24 and C26-ceramide, demonstrate the

largest decreases in Hsp27 KO sciatic nerve tissue. In this context, CerSs have been shown to form heterodimers with the implication that different CerSs have complex regulatory effects upon each of their activity (322). Such interactions may explain the aforementioned noted complex changes in ceramides. Additionally, CerS1 lacks a homeobox-like (hox-like) domain region, unlike the other human and mouse CerS, which may make it more suited for mitochondrial functions than other CerS which may be more preferentially targeted to the nucleus (302, 334). Recent evidence suggests that hox-like domains found in CerS may not be necessary for CerS activity but serve to increase transcriptional activation independently from their direct effects catalyzing ceramide synthesis (335, 336).

Sphingolipid signaling in CMT

Understanding the regulatory environment of different types of neural tissue on the sphingolipid network will provide greater clarity on why sphingolipid changes in Hsp27 KO mice occurred predominantly in sciatic nerve tissue rather than brain. Since CMT symptomatology is thought to exclusively present in the peripheral nervous system, these results further suggest sphingolipid alterations are involved in CMT2F. Sphingolipid profiling from S135F mutant mice generated using Clustered Regulatory Interspaced Short Palindromic Repeats (CRISPR)—Cas9 should further explicate the role of the sphingolipids in the disease state (Fig. 34). Better mouse models without overexpression should strongly clarify results. In collaboration with another laboratory, I analyzed sciatic nerve and brain tissue for changes in α-tubulin acetylation in attempt to replicate results produced in the literature. However, I did not observe any alteration in

acetylation in α-tubulin in sciatic nerve, as reported by others (220). Furthermore, sciatic nerve and brain tissue from P182L mice were found to be lacking expression of the transgene (Fig. 35). These data suggest that this mouse model may not provide strong reproducible results. Nevertheless, in order to determine if there were alterations in sphingolipid content, sciatic nerve and brain tissue were analyzed for ceramides. Sciatic nerve tissue demonstrated a significant decrease in C18-ceramide content (representative of CerS1 function and in line with other species), and these changes were not observed in the brain (Fig. 36). However, given the questionable nature of this mouse model, these data must be considered with reservation.

Additional evidence is beginning to implicate sphingolipids in other forms of CMT. Deficiency of the gene responsible for clearing sphingolipids, sphingosine 1-phosphate lyase (SPL), was recently discovered to be a novel cause of CMT, with a greatly increased sphingosine:sphinganine (SO:SA) ratio in the disease state (75) yet a relatively much smaller increase in S1P levels. Such a drastic alteration of SO:SA content without a similar increase in S1P from SPL dysfunction is difficult to explain from simple, canonic mechanistic models of sphingolipid metabolism, and suggests that alterations to sphingolipid networks may produce dramatic and complex effects on sphingolipid content and metabolism in the cell. While I have identified a depletion in mitochondrial ceramides, it is unknown whether these decreases are due to a global change in CerS or compensations in the sphingolipid network. More complex alterations in ceramide production may involve modulation in the activity and formation of complexes of CerSs.

Mitochondrial dysfunction

The impairment of mitochondria is in line with other research on CMT. Electron micrography from CMT2F mutant mice demonstrates increased total mitochondrial content, although number and size were not precisely quantified (243). Additionally, other types of CMT2 have shown mitochondrial dysfunctions, such as CMT2A, which is directly caused by mutations in mitofusin (309, 310). The increased size of mitochondria in the S135F mutant suggests there may be an increase in fusion in CMT2F. This underlies the possibility that a common mechanism may exist between CMT2A and CMT2F. Is it currently unknown whether the genetic etiologies of CMT2 subtypes have distinct mechanisms or converge on a pathway that will offer common targets for treatment. Mitochondrial morphology also has been linked to other neurodegenerative diseases, including Parkinson's Disease and ALS (291, 337, 338). Enlarged, swollen mitochondria similarly produced dysfunctional changes in Ullrich congenital muscular dystrophy (339). In addition to our data demonstrating mutant mitochondria have reduced respiratory functioning, S135F mutants have been found to hyperstabilize the microtubule network and thus decrease anterograde mitochondrial trafficking (220). It is unclear if these processes are connected and how they contribute to overall mitochondrial function.

Autophagy

While CMT1C has been associated with increased autophagy (340), studies on CMT2 and autophagy are lacking. Interestingly, curcumin, which stimulates protein translocation to the plasma membrane and as such is thought to increase autophagy,

has been shown to be effective in mouse models (295, 341). Curcumin has also been shown to stimulate *de novo* ceramide synthesis (322), suggesting its therapeutic effects may potentially be mediated by ceramide. Using both immunoblotting and multiple imaging methods, our results suggest that CMT2F also presents with increased autophagy in cellular models. Whether this is a compensatory response to increased cellular stress by clearing misfolded Hsp27 proteins or functions as a primary pathological insult is unclear. While observed increases in autophagy are likely downstream of mitochondrial affliction, it is unknown whether these changes relate to increased mitophagy in cells. Further work should focus on studying autophagy in other types of CMT and proteasomal inhibitors as potential pharmacologically therapies.

Metabolomics

Many metabolites screened were found to be altered, interestingly including increases observed in all metabolites associated with the urea cycle. Urea has been proposed as a biomarker for a variety of diseases including Huntington's, as it has been found elevated in brain tissue in patients (342). As the urea cycle is partially localized to the mitochondria, urea cycle dysfunction can occur secondarily to mitochondrial impairments (343). Caveolin-1 deficiency has been shown to result in increased urea and mitochondrial dysfunction, and it has been suggested that altered mitochondrial ceramide may play a role in this process (344). While I observed an increase in urea in two sets of cells transfected with different CMT2F mutations, metabolites in the urea cycle were not unilaterally increased. Arginine was slightly decreased in both mutants and ornithine was not altered, suggesting that the entire urea cycle is not blocked, and

raising the possibility that CMT cells rapidly produce more urea than they can remove to keep urea at physiological levels intracellularly. Enhanced proteolysis resulting in increases urea formation that overwhelm urea export capacity has been proposed as a potential mechanism of Huntington's Disease. As the cells metabolite levels were measured 48 hours after transfection, the dramatic effects suggest that these mutations induce an acute effect on urea metabolism. Decreased glutamine could result from increased reductive carboxylation of glutamine derived alpha-ketoglutarate that is either used to directly produce pyruvate or citrate (345). Reductive carboxylation utilizing glutamine is often present due to defects in mitochondrial respiration that cause increased glutamine to be shunted to fatty acid production instead of acetyl CoA (346).

Future Directions

Verification of the Hsp27:CerS binding interaction will strengthen and further inform our knowledge. To build upon microscopy results, Proximity Ligation Assay can be performed to determine if there is a close interaction of Hsp27 and CerS1. Experiments demonstrating the binding of the C-terminus of CerS1 to Hsp27 using a Ni^{2+} column should be repeated ideally with less background signal. To build upon these results, a Biacore T2000 system can be utilized to confirm C-terminal binding findings and moreover determine binding kinetics, which may provide further insight into the apparently increased binding interaction of mutant Hsp27 with CerS. Finally, the binding of the C-terminus does not necessarily exclude the possibility that other parts of CerS1 bind and potentially may be necessary for binding Hsp27. Thus, experiments should be performed carefully evaluating the possibility of binding occurring from other subunits,

especially the N-terminus. If multiple subunits of CerS1 bind Hsp27, it is more likely that this binding may disrupt the binding of CerS1 to other proteins.

In this way, the binding results presented that suggest that the C-terminus of CerS1 is responsible for binding Hsp27 have important implications for the study of CerS dimerization. The decreased binding of CerS6 to CerS1 in the presence of S135F Hsp27, in line with the increased binding of S135F to CerS1, suggests that Hsp27 and CerS6 may share the same binding site on CerS1. CerS6 and CerS1 activity would then expected to be decreased when these proteins are less predisposed to form heterodimers (322). However, potential decreased activity must be determined empirically, through methods such as sphingoid labeling. Electrophoresis experiments using native gels can also be attempted to demonstrate the presence of these dimers and oligomers. Furthermore, the specific CerS1 binding site for CerS6 must be resolved. These results suggest that potentially increasing CerS6 expression may also decrease the binding of Hsp27 and CerS1 binding, and this can also be empirically determined. Potentially, this may mitigate pathological effects of mutations.

Additionally, other tools can be used to confirm alterations in mitochondrial ceramides in CMT2F. Mitochondrial analysis can be potentially improved to obtain less crude fractions of mitochondria. Furthermore, C_{17} labeling can be performed on these fractions immediately after isolation while CerS may be expected to still have physiological activity to determine if there is a decrease in CerS in the mutant. Given the discussed disparity in phenotypes of mutations that cause CMT2F in the literature, mutants other than S135F can be tested to determine if there is a decrease in

mitochondrial ceramides. Furthermore, mitochondrial ceramides can be decreased with other tools such as targeting ceramidase to the mitochondria, and assayed for changes in mitochondrial structure and function. Similarly, sphingomyelinase can be targeted to mitochondria in cells transfected with S135F mutations to determine if increasing mitochondrial ceramides is capable of rescuing defects in mitochondrial structure and function attributed to the S135F mutation.

Furthermore, the lack of alteration in total cellular ceramides in HT-22 cells with CMT2A mutations should not be taken as definitive evidence of a lack of involvement of perturbations in sphingolipid signaling in CMT2A. After all, HT-22 cells did not demonstrate a change in total ceramides, and only exhibited a decrease in ceramides when mitochondrial fractions were analyzed. Mitochondrial fractions similarly need to be analyzed for cells transfected with CMT2A mutations to determine if these mutations may induce similar changes in sphingolipid metabolism as observed in CMT2F. If so, these mutations can be evaluated in a similar manner for mitochondrial pathology, and protein interactions with enzymes involved in sphingolipid metabolism should be entertained.

DeoxySLs will also need to be more carefully examined in CMT2F. Given the aforementioned extensive literature on increases in deoxySLs in HSAN1, I hypothesized that deoxySA would be increased in CMT2F, due to inhibition of CerS and an expected backup of intermediates in the *de novo* synthesis pathway. However, the relatively minor decrease in deoxySA observed in HT-22 cells suggests a different mechanism may be involved. Given that deoxySA has recently been shown to localize strongly to

mitochondria (54), this could be reflective of an overall decrease in mitochondrial ceramides. Although it may be technically challenging, it will be important to attempt to measure deoxySA in mitochondria. DeoxydhCer and deoxyCer levels did not generally change in S135F transfected HT-22 cells and observed more variance than ceramide levels (data not shown), however, attempts should be made to measure these species in mitochondria going forward.

Additionally, identifying commonly altered metabolites may provide hints at common biochemical mechanisms of CMT. Future metabolomic studies should consider whether urea can be used as a tool to monitor severity of CMT2F or correlates to the degree of pathology in other CMT diseases. I believe the increase in urea is due to mitochondrial disorder, but the exact nature of the mechanism and spatial and temporal details of its accumulation are still unknown. Further study should also consider using a variety of tissue types, ideally from disease-bearing humans, including blood, to provide further utility in studying metabolites such as urea as potential biomarkers of CMT progression. Given CMT's strict clinical presentation and sphingolipid changes observed predominantly in the peripheral nervous system, peripheral nervous system models such as DRGs or sciatic nerve should ideally be used for future clinical or mouse studies.

Conclusions

In conclusion, the data presented here strongly suggest that sphingolipid alterations underlie CMT2F, and also provides evidence that mitochondrial dysfunction and autophagy play a role in the disease pathogenesis. I provide evidence of a novel

Hsp27:CerS interaction, and decreased CerS in the mitochondria along with decreased mitochondrial ceramides in the S135F mutant. Through these studies, I explore a topic—ceramide synthesis—that could lead to new targets for novel treatments to prevent or reduce the severity of CMT2F or other neuropathies with similar mechanisms. In particular, validating the implications presented here would create an imperative for developing small molecule inhibitors of the Hsp27:CerS interaction that could be therapeutic for this disease paradigm.

Measuring DeoxydhCers and DeoxyCers in the Nervous System

Summary of results

I developed a method to accurately determine deoxydhCer and deoxyCer levels in mouse nervous system tissue, given the increasingly suspected importance of these species in nervous system pathology. I used C57B6 mice as an experimental model to demonstrate the presence of deoxySLs in WT mice without any manipulation. The method that I developed makes use of recently available standards using a general mass spectrometry method that has been published for quite some time. Therefore, this demonstrates a feasible method for groups using mouse models of HSAN1, diabetic neuropathy, ADHD, chemotherapeutic treatments implicated in causing neuropathy, or other neural models to evaluate changes in deoxySLs.

A major observation was the much greater quantity and variety of deoxydhCer than deoxyCer in tissue. C24-deoxyCer was the only deoxyCer species detectable above quantification. This is similar to other studies that only detect deoxyCers with very long acyl chains (54). As mouse age increased, this species increased in abundance,

whereas C24-Cer notably decreased. This suggests that C24-deoxyCer may play an important role in aging in the nervous system, as its accumulation cannot be directly tied to an increase in non-selective C24 acylation of sphingoid bases.

Desaturation of deoxySLs

Similar to results published using MEF cells, deoxydhCers are present in greater quantity than deoxyCers (54), suggesting that contrary to most ceramide species, most deoxyCer species are desaturated. This suggests that desaturase activity may be differentially regulated in acting upon these deoxySL species, potentially by the action of a distinct desaturase enzyme. Supporting this hypothesis, deoxySO is further thought to differ in structure from sphingosine by having distinct placement of the double bond in its sphingoid backbone at the 14 position instead of the 4 position as observed in sphingosine (347). Similar to published distributions of deoxydhCers from cells grown in culture, a relative abundance of C24, C24:1, C18 (but not C16 species) were observed in all tissue types (54). This suggests that different CerS may similarly possess distinct affinity or specificity for deoxySL species in catalyzing acyl chain additions. The quantifiable levels of brain C24:1-deoxyCer observed in both mouse strains could simply be due to the greater total lipid content in brain – however, it could also suggest a tissue-type specific increase in desaturase activity acting on the deoxySL for the C24:1 species.

Structural properties of deoxySLs

Preliminary studies have begun to investigate the biophysical properties of the deoxydhCers and deoxyCers. Due to their high hydrophobicity, deoxydhCers and

deoxyCers have lower miscibility with SM in bilayers than their non-deoxy SL counterparts (323). Potential functional roles include serving as scaffolds for antigen presentation by selectively binding specific cluster of differentiation proteins due to their highly hydrophobic nature (348). Species derived from deoxySO with relatively low acyl chain length tend to demonstrate the greatest hydrophobicity (323). However, much is yet to be discovered about how these molecules can change membrane properties in different organelles such as endoplasmic reticulum and affect biological functioning of different cell types. DeoxySA localizes to Golgi and ER, and causes ER stress, similar to results seen in HSAN patients, as measured by GADD153 levels and XBP1 splicing (50, 54, 71). Furthermore, deoxySA has been shown to induce mitochondrial fragmentation and dysfunction that precedes axonal degeneration, although the effects of deoxyCer and deoxydhCer on mitochondria have not been carefully examined (54). Similar morphological findings have been found in HSAN patient lymphoblasts (71).

SPT

There is strong evidence that SPT is responsible for generating deoxySLs. Inhibition of SPT pharmacologically with myriocin inhibits deoxyCer generation and studies using ^{13}C-labeled alanine have shown preferential incorporation into 1-deoxySa instead of sphinganine (53). DeoxySA is increased in cells treated or animals fed diets with fumonisin B1, an inhibitor of ceramide synthesis that is thought to cause back up the products of the *de novo* pathway of ceramide genesis (53). This suggests that many biologies resulting from the block of the *de novo* pathway could be caused by altered deoxyCer levels.

Increases in deoxySLs due to paclitaxel treatment are due to increased SPT activity in paclitaxel-treated cells, producing increased sphingolipids and even greater relative increases in deoxySLs, although it is unclear whether this is due to an altered relative specificity of SPT or relatively decreased ability to clear deoxySLs (326). The cytochrome P450 4F enzymes were recently shown to be capable of hydroxylating and degrading deoxySL species (72). C24 and C22:1 1-deoxyCers and C22:1 and C18:1 1-deoxydhCers all increased with paclitaxel and correlated to progression of neuropathy, suggesting that these species may play a role in the pathogenesis of neuropathy (326).

HSAN1

Likely, the most immediate application of research on deoxySLs and specifically deoxyCer and deoxydhCer will lie in understanding the pathology and developing treatments for HSAN1. HSAN1 is typically inherited in an autosomal dominant fashion, suggesting it acts through a dominant-negative mechanism. Both oral supplementation of diets with serine in mice and overexpression of wild-type SPT1 in disease models reduce the severity of disease, suggesting therapies that reduce the utilization of alanine by SPT may be effective (48, 59). Only a 10% increase in serine was able to drastically reduce deoxySLs to physiological levels in mice in 4 days and prevent mice from developing neurological dysfunction due to the disease, while treatment in older mice improved peripheral phenotypes. Alanine supplementation, in contrast, acutely increased deoxySLs and worsened the disease status (59). These experiments have been extended to preliminary trials on humans with promising results of decreased deoxySLs in serine supplemented diets (59, 61, 64). Furthermore, increases in neurite

length and p-ERM expression from growth cones from DRGs isolated from HSAN mice were lost with administration of myriocin, serine, or removal of alanine (349). This could be due to cytoskeletal disruption (327).

Transgenic mice overexpressing both mutated and WT copies of SPT largely show a loss of alteration in SPT activity and neuropathy, supporting the hypothesis that the mutant SPT is not inherently toxic but instead that its altered products are harmful (48). This is in accordance with observed intermediate levels of deoxySLs in double transgenic mice for WT and mutant SPT. Expression of HSAN1 mutants in yeast cells demonstrate that while mutant HSAN enzyme complexes have the same relative preference for incorporating different acyl-CoA chain lengths, mutant SPT complexes have a greater effect on the V_{max} than K_m for amino acid incorporation. This suggests that mutations studied do not affect the binding site, but more efficiently allow bound alanine to react with acyl-CoA substrates (50).

DeoxySLs in diabetes

DeoxySLs have been suggested to play a role in the pathology of many other diseases; diabetes mellitus in particular has been examined multiple times. Diabetic neuropathy presents similarly to HSAN1 with late and insidious loss of peripheral nerve function, especially sensory modalities. While paclitaxel treatment produces increased SPT activity, diabetes increases relative utilization of alanine in *de novo* sphingolipid synthesis. Multiple studies have suggested that serum from patients with diabetes mellitus type 2 contains increased deoxySO and deoxySA (328, 350), potentially due to the increased alanine:serine ratio in plasma of these patients (328). Increased

deoxySLs have also been observed in patients with metabolic syndrome, although type 2 diabetics do not present with significantly different levels, potentially limiting the use of deoxySLs use as a biomarker of disease progression (351). Further evidence suggests many deoxyCer species are increased in diabetic patients, although more thorough studies focusing on deoxydhCers and deoxyCers in patients with metabolic syndrome and diabetes need to be performed (326). Interestingly, while deoxySL levels have not been associated with type 1 diabetes (350), type 1 diabetes patients exhibiting peripheral neuropathy demonstrated increased C24-deoxyCer, along with C24 and C26 ceramides (352). However, the relative decrease in C24-deoxyCer was relatively small, potentially limiting its power as a useful biomarker (352).

Future Directions

The results presented here make clear that WT mice produce deoxySLs without perturbation. It is still not well understood if these deoxySL species serve a structural and/or bioactive role, or if they are byproducts from promiscuous action of SPT due to proximal alanine. Future work must seek to delineate if there are physiological roles of deoxySLs in mammalian cells. Furthermore, deoxydhCers were observed to be especially abundant in sciatic nerve tissue compared to that of brain and even spinal cord. It is unknown why levels deoxydhCer levels are so much higher in peripheral nerves. Future study should seek to analyze these changes in more specific compartments of the peripheral nerves. Sciatic nerves contain distinct motor and sensory divisions, and these may be separately dissected and analyzed to potentially reveal differential roles of deoxySLs. Furthermore, there may be length dependent

changes in these peripheral nerves as well, as more distal components often demonstrate greatest pathology in degeneration. Similar analyses with more distinct dissection and analysis can similarly be performed in spinal cord and brain tissue.

Further study should seek to investigate deoxydhCers and deoxyCers in therapeutic application. DeoxySA has been carefully studied as a potential anti-cancer therapeutic, although it has failed to show significant promise in early clinical trials. Originally isolated from the clam, *Mactromeris polynyma*, deoxySA, also known as spisulosine or ES-285, decreased cell growth, prevented stress fiber formation, and increased apoptotic signaling by activation of caspases 3 and 12 and modifying p53 phosphorylation (52, 353). DeoxySA was further shown to be an activator of specific PKC isoforms, and induce *de novo* ceramide production in cell culture (353, 354). However, phase I clinical trials demonstrated that administration of deoxySA to patients with advanced solid tumors was linked to dose-limiting neuro- and hepatotoxicities and pyrexia with often mild to unobservable objective anti-cancer effects, resulting in discontinuation of clinical development for spisulosine in cancer patients (355–358). DeoxydhCers and deoxyCers, given their early link to toxic effects, may also demonstrate clinical side effects, but their effectiveness as chemotherapeutics is largely unknown.

Conclusions

In conclusion, through close collaboration with members of the Lipidomics Core Facility and many others, I have developed a novel method for accurately determining deoxydhCer and deoxyCer levels in brain, spinal cord, and sciatic nerve of mice. Data

suggests that deoxydhCers accumulate in peripheral nervous tissue with aging and that C22-deoxydhCer is highly produced throughout the nervous system. This method will facilitate efficient screening and determination of deoxyCer and deoxydhCer levels in many mouse models of neural disease and dysfunction, providing us with a better understanding of the pathophysiology of deoxySLs in the nervous system.

References

1. Merrill, A. H., Schmelz, E. M., Dillehay, D. L., Spiegel, S., Shayman, J. A., Schroeder, J. J., Riley, R. T., Voss, K. A., and Wang, E. (1997) Sphingolipids - The Enigmatic Lipid Class - Biochemistry, Physiology, and Pathophysiology. *Toxicol. Appl. Pharmacol.* **142**, 208–225

2. Thudichum, J. L. W. (1884) A treatise on the chemical constitution of the brain. Bailliere, Tindall, and Cox, London

3. Hannun, Y. A. and Obeid, L. M. (2017) Sphingolipids and their metabolism in physiology and disease. *Nat. Rev. Mol. Cell Biol.*

4. Hannun, Y. A. and Obeid, L. M. (2008) Principles of bioactive lipid signalling: lessons from sphingolipids. *Nat. Rev. Mol. Cell Biol.* **9**, 139–150

5. Hannun, Y. A. and Obeid, L. M. (2011) Many ceramides. *J. Biol. Chem.* **286**, 27855–27862

6. Luberto, C., Kraveka, J. M., and Hannun, Y. A. (2002) Ceramide Regulation of Apoptosis versus Differentiation: A Walk on a Fine Line. Lessons from Neurobiology. *Neurochem. Res.* **27**, 609–617

7. Ben-David, O. and Futerman, A. H. (2010) The Role of the Ceramide Acyl Chain Length in Neurodegeneration : Involvement of Ceramide Synthases. *Neuromol Med* **12**, 341–350

8. Yu, R. K., Bieberich, E., Xia, T., and Zeng, G. (2004) Regulation of ganglioside biosynthesis in the nervous system. *J. Lipid Res.* **45**, 783–793

9. D'Angelo, G., Capasso, S., Sticco, L., and Russo, D. (2013) Glycosphingolipids : synthesis and functions. *FEBS J.* **280**, 6338–6353

10. Pohlentz, G., Klein, D., Schwarzmann, G., Schmitz, D., and Sandhoff, K. (1988) Both GA2, GM2, and GD2 synthases and GM1b, GD1a, and GT1b synthases are single enzymes in Golgi vesicles from rat liver. *Proc. Natl. Acad. Sci. U. S. A.* **85**, 7044–7048

11. Maccioni, H. J. F., Giraudo, C. G., and Daniotti, J. L. (2002) Understanding the stepwise synthesis of glycolipids. *Neurochem. Res.* **27**, 629–636

12. Sonnino, S., Prinetti, A., Mauri, L., Chigorno, V., and Tettamanti, G. (2006)

Dynamic and Structural Properties of Sphingolipids as Driving Forces for the Formation of Membrane Domains. *Chem. Rev.* **106**, 2111–2125

13. Yamashita, T., Wada, R., Sasaki, T., Deng, C., Bierfreund, U., Sandhoff, K., and Proia, R. L. (1999) A vital role for glycosphingolipid synthesis during development. *Proc. Natl. Acad. Sci.* **96**, 9142–9147

14. Jennemann, R., Sandhoff, R., Wang, S., Kiss, E., Gretz, N., Zuliani, C., Schorle, H., Kenzelmann, M., Bonrouhi, M., Martin-villalba, A., Ja, R., Wiegandt, H., and Gro, H. (2005) Cell-specific deletion of glucosylceramide synthase in brain leads to severe neural defects after birth. *Proc. Natl. Acad. Sci.* **102**, 12459–12464

15. Coetzee, T., Fujita, N., Dupree, J., Shi, R., Blight, A., Suzuki, K., Suzuki, K., and Popko, B. (1996) Myelination in the Absence of Galactocerebroside and Sulfatide : Normal Structure with Abnormal Function and Regional Instability. *Cell* **86**, 209–219

16. Sandhoff, K. and Harzer, K. (2013) Gangliosides and Gangliosidoses : Principles of Molecular and Metabolic Pathogenesis. *J. Neurosci.* **33**, 10195–10208

17. Schnaar, R. L. (2010) Brain gangliosides in axon – myelin stability and axon regeneration. *FEBS Lett.* **584**, 1741–1747

18. Baumann, N. and Pham-Dinh, D. (2001) Biology of Oligodendrocyte and Myelin in the Mammalian Central Nervous System. *Physiol. Rev.* **81**, 871–927

19. Posse de Chaves, E. and Sipione, S. (2010) Sphingolipids and gangliosides of the nervous system in membrane function and dysfunction. *FEBS Lett.* **584**, 1748–1759

20. Dawson, G. and Stefansson, K. (1984) Gangliosides of human spinal cord: Aberrant composition of cords from patients with amyotrophic lateral sclerosis. *J. Neurosci. Res.* **12**, 213–220

21. Cutler, R. G., Pedersen, W. A., Camandola, S., Rothstein, J. D., and Mattson, M. P. (2002) Evidence That Accumulation of Ceramides and Cholesterol Esters Mediates Oxidative Stress – Induced Death of Motor Neurons in Amyotrophic Lateral Sclerosis. *Ann Neurol.* **52**, 448–457

22. Kundu, S., Harati, Y., and Misra, L. (1984) Sialosylglobotetraosylceramide: a marker for amyotropic lateral sclerosis. *Biochem. Biophys. Res. Commun.* **118**, 83–89

23. Rapport, M. M., Donnenfeld, I., Brunner, W., Hungund, B., and Bartfeld, H. (1985) Ganghoside Patterns in Amyotrophc Lateral Sclerosis Brain Regions. *Ann Neurol.* **18**, 60–67

24. Stevens, A., Weller, M., and Wietholter, H. (1993) A characteristic ganglioside antibody pattern in the CSF of patients with amyotrophic lateral sclerosis. *J. Neurol. Neurosurg. Psychiatry* **56**, 361–364

25. Kollewe, K., Wurster, U., Sinzenich, T., Körner, S., and Dengler, R. (2015) Anti-Ganglioside Antibodies in Amyotrophic Lateral Sclerosis Revisited. *PLoS One* **10**, 1–11

26. Dodge, J. C., Treleaven, C. M., Pacheco, J., Cooper, S., Bao, C., Abraham, M., Cromwell, M., Sardi, S. P., Chuang, W.-L., Sidman, R. L., Cheng, S. H., and Shihabuddin, L. S. (2015) Glycosphingolipids are modulators of disease pathogenesis in amyotrophic lateral sclerosis. *Proc. Natl. Acad. Sci.* **112**, 8100–8105

27. Henriques, A., Croixmarie, V., Priestman, D. A., Rosenbohm, A., Dirrig-Grosch, S., D'Ambra, E., Huebecker, M., Hussain, G., Boursier-Neyret, C., Echaniz-Laguna, A., Ludolph, A. C., Platt, F. M., Walther, B., Spedding, M., Loeffler, J.-P., and Gonzalez De Aguilar, J.-L. (2015) Amyotrophic lateral sclerosis and denervation alter sphingolipids and up-regulate glucosylceramide synthase. *Hum. Mol. Genet.* **24**, 7390–7405

28. Olsen, M. K., Roberds, S. L., Ellerbrock, B. R., Fleck, T. J., Mckinley, D. K., and Gurney, M. E. (2001) Disease Mechanisms Revealed by Transcription Profiling in SOD1-G93A Transgenic Mouse Spinal Cord. *Ann Neurol.* **50**, 730–740

29. Henriques, A., Huebecker, M., Blasco, H., Keime, C., Andres, C. R., Corcia, P., Priestman, D. A., Platt, F. M., Spedding, M., and Loeffler, J.-P. (2017) Inhibition of β-Glucocerebrosidase Activity Preserves Motor Unit Integrity in a Mouse Model of Amyotrophic Lateral Sclerosis. *Sci. Rep.* **7**, 5235

30. Fridman, V. and Reilly, M. M. (2015) Inherited Neuropathies.

31. Astudillo, L., Sabourdy, F., Therville, N., Bode, H., Ségui, B., Andrieu-Abadie, N., Hornemann, T., and Levade, T. (2015) Human genetic disorders of sphingolipid biosynthesis. *J. Inherit. Metab. Dis.* **38**, 65–76

32. Fridman, V., Oaklander, A. L., David, W. S., Johnson, E. A., Ran, J., Novak, P., Brown, R. H., and Eichler, F. S. (2015) Natural history and biomarkers in hereditary sensory neuropathy type 1. *Muscle and Nerve* **51**, 489–495

33. Rotthier, A., Baets, J., Timmerman, V., and Janssens, K. (2012) Mechanisms of disease in hereditary sensory and autonomic neuropathies. *Nat. Rev. Neurol.* **8**, 73–85

34. Rotthier, A., Baets, J., Vriendt, E. De, Jacobs, A., Bonello-palot, N., Kilic, S. S., Auer-grumbach, M., Le, N., Weis, J., Jordanova, A., Jonghe, P. De, and Timmerman, V. (2009) Genes for hereditary sensory and autonomic neuropathies: a genotype–phenotype correlation. *Brain* **132**, 2699–2711

35. Rotthier, A., Penno, A., Rautenstrauss, B., Auer-Grumbach, M., Stettner, G. M., Asselbergh, B., Van Hoof, K., Sticht, H., Levy, N., Timmerman, V., Hornemann, T., and Janssens, K. (2011) Characterization of Two Mutations in the SPTLC1 Subunit of Serine Palmitoyltransferase Associated with Hereditary Sensory and Autonomic Neuropathy. *Hum. Mutat.* **87**, 513–522

36. Dawkins, J. L., Hulme, D. J., Brahmbhatt, S. B., Auer-grumbach, M., and Nicholson, G. A. (2001) Mutations in SPTLC1, encoding serine palmitoyltransferase, long chain base subunit-1, cause hereditary sensory neuropathy type I. *Nat. Genet.* **27**, 309–312

37. Bejaoui, K., Wu, C., Scheffler, M. D., Haan, G., Ashby, P., Wu, L., de Jong, P., and Brown Jr., R. H. (2001) SPTLC1 is mutated in hereditary sensory neuropathy, type 1. *Nat. Genet.* **27**, 261–262

38. Hanada, K. (2003) Serine palmitoyltransferase, a key enzyme of sphingolipid metabolism. *Biochim. Biophys. Acta* **1632**, 16–30

39. Hornemann, T., Richard, S., Ru, M. F., Wei, Y., and Eckardstein, A. Von. (2006) Cloning and Initial Characterization of a New Subunit for Mammalian Serine-palmitoyltransferase. *J. Biol. Chem.* **281**, 37275–37281

40. Gault, C. R., Obeid, L. M., and Hannun, Y. A. (2010) An overview of sphingolipid metabolism: from synthesis to breakdown. *Adv Exp Med Biol.* **688**, 1–23

41. Gable, K., Han, G., Monaghan, E., Bacikova, D., Natarajan, M., Williams, R., and Dunn, T. M. (2002) Mutations in the Yeast LCB1 and LCB2 Genes , Including Those Corresponding to the Hereditary Sensory Neuropathy Type I Mutations , Dominantly Inactivate Serine Palmitoyltransferase. *J. Biol. Chem.* **277**, 10194–10200

42. Bejaoui, K., Uchida, Y., Yasuda, S., Ho, M., Nishijima, M., Brown, R. H., Holleran, W. M., and Hanada, K. (2002) Hereditary sensory neuropathy type 1 mutations confer dominant negative effects on serine palmitoyltransferase, critical for

sphingolipid synthesis. *J. Clin. Invest.* **110**, 1301–1308

43. Dedov, V. N., Dedova, I. V, Merrill, A. H., and Nicholson, G. A. (2004) Activity of partially inhibited serine palmitoyltransferase is sufficient for normal sphingolipid metabolism and viability of HSN1 patient cells. *Biochim. Biophys. Acta* **1688**, 168–175

44. McCampbell, A., Truong, D., Broom, D. C., Allchorne, A., Gable, K., Cutler, R. G., Mattson, M. P., Woolf, C. J., Frosch, M. P., Harmon, J. M., Dunn, T. M., and Brown, R. H. (2005) Mutant SPTLC1 dominantly inhibits serine palmitoyltransferase activity in vivo and confers an age-dependent neuropathy. *Hum. Mol. Genet.* **14**, 3507–3521

45. Klein, C., Wu, Y., Kruckeberg, K., Hebbring, S., Anderson, S., Cunningham, J., Dyck, P., Klein, D., Thibodeau, S., and Dyck, P. (2005) SPTLC1 and RAB7 mutation analysis in dominantly inherited and idiopathic sensory neuropathies. *J. Neurol. Neurosurg. Psychiatry* **76**, 1022–1025

46. Houlden, H., King, R., Blake, J., Groves, M., Love, S., Woodward, C., Hammans, S., Nicoll, J., Lennox, G., Donovan, D. G. O., Gabriel, C., Thomas, P. K., and Reilly, M. M. (2006) Clinical, pathological and genetic characterization of hereditary sensory and autonomic neuropathy type 1 (HSAN I). *Brain* **129**, 411–425

47. Hornemann, T., Penno, A., and von Eckardstein, A. (2008) The accumulation of two atypical sphingolipids cause hereditary sensory neuropathy type 1 (HSAN1). *Chem. Phys. Lipids* **154**, S62

48. Eichler, F. S., Hornemann, T., McCampbell, A., Kuljis, D., Penno, A., Vardeh, D., Tamrazian, E., Garofalo, K., Lee, H.-J., Kini, L., Selig, M., Frosch, M., Gable, K., von Eckardstein, A., Woolf, C. J., Guan, G., Harmon, J. M., Dunn, T. M., and Brown, R. H. (2009) Overexpression of the wild-type SPT1 subunit lowers desoxysphingolipid levels and rescues the phenotype of HSAN1. *J. Neurosci.* **29**, 14646–14651

49. Penno, A., Reilly, M. M., Houlden, H., Laurá, M., Rentsch, K., Niederkofler, V., Stoeckli, E. T., Nicholson, G., Eichler, F., Brown, R. H., von Eckardstein, A., and Hornemann, T. (2010) Hereditary sensory neuropathy type 1 is caused by the accumulation of two neurotoxic sphingolipids. *J. Biol. Chem.* **285**, 11178–11187

50. Gable, K., Gupta, S. D., Han, G., Niranjanakumari, S., Harmon, J. M., and Dunn, T. M. (2010) A disease-causing mutation in the active site of serine palmitoyltransferase causes catalytic promiscuity. *J. Biol. Chem.* **285**, 22846–22852

51. Rotthier, A., Auer-Grumbach, M., Janssens, K., Baets, J., Penno, A., Almeida-Souza, L., Van Hoof, K., Jacobs, A., De Vriendt, E., Vondra, P., Schlotter-Weigel, B., Lo, W., Seeman, P., Jonghe, P. De, Van Dijck, P., Jordanova, A., Hornemann, T., and Timmerman, V. (2010) Mutations in the SPTLC2 Subunit of Serine Palmitoyltransferase Cause Hereditary Sensory and Autonomic Neuropathy Type I. *Am. J. Hum. Genet.* **87**, 513–522

52. Cuadros, R., Montejo De Garcini, E., Wandosell, F., Faircloth, G., Fernández-Sousa, J. M., and Avila, J. (2000) The marine compound spisulosine, an inhibitor of cell proliferation, promotes the disassembly of actin stress fibers. *Cancer Lett.* **152**, 23–29

53. Zitomer, N. C., Mitchell, T., Voss, K. A., Bondy, G. S., Pruett, S. T., Garnier-Amblard, E. C., Liebeskind, L. S., Park, H., Wang, E., Sulllards, M. C., Merrill, A. H., and Riley, R. T. (2009) Ceramide synthase inhibition by fumonisin B1 causes accumulation of 1-deoxysphinganine. A novel category of bioactive 1-deoxysphingoid bases and 1-deoxydihydroceramides biosynthesized by mammalian cell lines and animals. *J. Biol. Chem.* **284**, 4786–4795

54. Alecu, I., Tedeschi, A., Behler, N., Wunderling, K., Lauterbach, M. A. R., Gaebler, A., Ernst, D., Veldhoven, P. P. Van, Al-amoudi, A., Latz, E., Othman, A., Kuerschner, L., and Hornemann, T. (2016) Localization of 1-deoxysphingolipids to mitochondria induces mitochondrial dysfunction. *J. Lipid Res.* **58**, 42–59

55. Murphy, S. M., Ernst, D., Wei, Y., Laura, M., Liu, Y., Polke, J., Blake, J., Winer, J., Houlden, H., Hornemann, T., and Reilly, M. M. (2013) Hereditary sensory and autonomic neuropathy type 1 (HSANI) cased by a novel mutation in SPTLC2. *Neurology* **80**, 2106–2111

56. Ernst, D., Murphy, S. M., Sathiyanadan, K., Wei, Y., Othman, A., Laura, M., Liu, Y.-T., Penno, A., Blake, J., Donaghy, M., Houlden, H., Reilly, M. M., and Hornemann, T. (2015) Novel HSAN1 Mutation in Serine Palmitoyltransferase Resides at a Putative Phosphorylation Site That Is Involved in Regulating Substrate Specificity. *Neuromol Med* **17**, 47–57

57. Kornak, U., Mademan, I., Schinke, M., Voigt, M., Krawitz, P., Hecht, J., Barvencik, F., Schinke, T., Gießelmann, S., Beil, F. T., Pou-Serradell, A., Vilchez, J. J., Beetz, C., Deconinck, T., Timmerman, V., Kaether, C., Jonghe, P. De, Hubner, C. A., Gal, A., Amling, M., Mundlos, S., Baets, J., and Kurth, I. (2014) Sensory neuropathy with bone destruction due to a mutation in the membrane-shaping atlastin. *Brain* **137**, 683–692

58. Davidson, G. L., Murphy, S. M., Polke, J. M., Laura, M., Salih, M. A. M., Muntoni, F., Blake, J., Brandner, S., Davies, N., Horvath, R., Price, S., Donaghy, M.,

Roberts, M., Foulds, N., Ramdharry, G., Soler, D., Lunn, M. P., Manji, H., Davis, M. B., Houlden, H., and Reilly, M. M. (2012) Frequency of mutations in the genes associated with hereditary sensory and autonomic neuropathy in a UK cohort. *J Neurol* **259**, 1673–1685

59. Garofalo, K., Penno, A., Schmidt, B. P., Lee, H. J., Frosch, M. P., Von Eckardstein, A., Brown, R. H., Hornemann, T., and Eichler, F. S. (2011) Oral L-serine supplementation reduces production of neurotoxic deoxysphingolipids in mice and humans with hereditary sensory autonomic neuropathy type 1. *J. Clin. Invest.* **121**, 4735–4745

60. Oswald, M. C. W., West, R. J. H., Lloyd-Evans, E., and Sweeney, S. T. (2015) Identification of dietary alanine toxicity and trafficking dysfunction in a Drosophila model of hereditary sensory and autonomic neuropathy type 1. *Hum. Mol. Genet.* **24**, 6899–6909

61. Auranen, M., Toppila, J., Suriyanarayanan, S., Lone, M. A., Paetau, A., Tyynismaa, H., Hornemann, T., and Ylikallio, E. (2017) Clinical and metabolic consequences of L-serine supplementation in hereditary sensory and autonomic neuropathy type 1C. *Cold Spring Harb Mol Case Stud* **3**, 1–8

62. Esaki, K., Sayano, T., Sonoda, C., Akagi, T., Suzuki, T., Ogawa, T., Okamoto, M., Yoshikawa, T., Hirabayashi, Y., and Furuya, S. (2015) L-serine deficiency elicits intracellular accumulation of cytotoxic deoxysphingolipids and lipid body formation. *J. Biol. Chem.* **290**, 14595–14609

63. Bode, H., Bourquin, F., Suriyanarayanan, S., Wei, Y., Alecu, I., Othman, A., and Eckardstein, A. Von. (2016) HSAN1 mutations in serine palmitoyltransferase reveal a close structure–function–phenotype relationship. *Hum. Mol. Genet.* **25**, 853–865

64. Fridman, V., Novak, P., David, W., Macklin, E., McKenna-Yasek, D., Walsh, K., Oaklander, A. L., Brown, R., Hornemann, T., and Eichler, F. (2017) A randomized, double-blind, placebo-controlled, delayed-start trial to evaluate the safety and efficacy of l-serine in subjects with hereditary sensory and autonomic neuropathy type 1 (HSAN1) (s45.001). *Neurology* **88**

65. Han, S., Lone, M. A., Schneiter, R., and Chang, A. (2010) Orm1 and Orm2 are conserved endoplasmic reticulum membrane proteins regulating lipid homeostasis and protein quality control. *Proc. Natl. Acad. Sci.* **107**, 5851–5856

66. Stimpson, S., Myers, S. J., Stimpson, S. E., Coorssen, J. R., and Myers, S. J. (2015) Proteome Alterations Associated With the V144D SPTLC1 Mutation That Causes Hereditary Sensory Neuropathy-I Proteome Alterations Associated With

the V144D SPTLC1 Mutation That Causes Hereditary Sensory Neuropathy-I. *Electron. J. Biol.* **11**, 176–186

67. Stimpson, S. E., Lauto, A., Coorssen, J. R., and Myers, S. J. (2016) Isolation and Identification of ER Associated Proteins with Unique Expression Changes Specific to the V144D SPTLC1 Mutations in HSN-I. *Biochem. Anal. Biochem.* **5**, No. 1000248

68. Stimpson, S. E., Shanu, A., Coorssen, J. R., and Myers, S. J. (2016) Identifying Unique Protein Alterations Caused by SPTLC1 Mutations in a Transfected Neuronal Cell Model. *World J. Neurosci.* **6**, 325–347

69. Zuellig, R. A., Hornemann, T., Othman, A., Hehl, A. B., Bode, H., Güntert, T., Ogunshola, O. O., Saponara, E., Grabliauskaite, K., Jang, J., Ungethuem, U., and Wei, Y. (2014) Deoxysphingolipids, Novel Biomarkers for Type 2 Diabetes, Are Cytotoxic for Insulin-Producing Cells. *Diabetes* **63**, 1326–1339

70. Marshall, L. L., Stimpson, S. E., Hyland, R., Coorssen, J. R., and Myers, S. J. (2014) Increased lipid droplet accumulation associated with a peripheral sensory neuropathy. *J. Chem. Biol.* **7**, 67–76

71. Myers, S. J., Malladi, C. S., Hyland, R. a, Bautista, T., Boadle, R., Robinson, P. J., and Nicholson, G. a. (2014) Mutations in the SPTLC1 Protein Cause Mitochondrial Structural Abnormalities and Endoplasmic Reticulum Stress in Lymphoblasts. *DNA Cell Biol.* **33**, 399–407

72. Alecu, I., Othman, A., Penno, A., Saied, E. M., Arenz, C., Eckardstein, A. Von, and Hornemann, T. (2017) Cytotoxic 1-deoxysphingolipids are metabolized by a cytochrome P450-dependent pathway. *J. Lipid Res.* **58**, 60–71

73. Stimpson, S. E., Coorssen, J. R., and Myers, S. J. (2015) Mitochondrial protein alterations in a familial peripheral neuropathy caused by the V144D amino acid mutation in the sphingolipid protein, SPTLC1. *J Chem Bio* **8**, 25–35

74. Fyrst, H. and Saba, J. D. (2008) Sphingosine-1-phosphate lyase in development and disease: Sphingolipid metabolism takes flight. *Biochim. Biophys. Acta* **1781**, 448–458

75. Atkinson, D., Nikodinovic Glumac, J., Asselbergh, B., Ermanoska, B., Blocquel, D., Steiner, R., Estrada-Cuzcano, A., Peeters, K., Ooms, T., De Vriendt, E., Yang, X.-L., Hornemann, T., Milic Rasic, V., and Jordanova, A. (2017) Sphingosine 1-phosphate lyase deficiency causes Charcot-Marie-Tooth neuropathy. *Neurology* **88**, 1–10

76. Gutmann, L. and Shy, M. (2015) Update on Charcot–Marie–Tooth disease. *Curr. Opin. Neurol.* **28**, 462–467

77. van Echten-Deckert, G. and Herget, T. (2006) Sphingolipid metabolism in neural cells. *Biochim. Biophys. Acta* **1758**, 1978–1994

78. Karaca, I., Tamboli, I. Y., Glebov, K., Richter, J., Fell, L. H., Grimm, M. O., Haupenthal, V. J., Hartmann, T., Gräler, M. H., Echten-deckert, G. Van, and Walter, J. (2014) Deficiency of Sphingosine-1-phosphate Lyase Impairs Lysosomal Metabolism of the Amyloid Precursor Protein. *J. Biol. Chem.* **289**, 16761–16772

79. Mizugishi, K., Yamashita, T., Olivera, A., Miller, G. F., Spiegel, S., and Proia, R. L. (2005) Essential Role for Sphingosine Kinases in Neural and Vascular Development. *Mol. Cell. Biol.* **25**, 11113–11121

80. Hagen-Euteneuer, N., Lütjohann, D., Park, H., Merrill, A. H., and Echten-Deckert, G. Van. (2012) Sphingosine 1-Phosphate (S1P) Lyase Deficiency Increases Sphingolipid Formation via Recycling at the Expense of de Novo Biosynthesis in Neurons. *J. Biol. Chem.* **287**, 9128–9136

81. Bektas, M., Allende, M. L., Lee, B. G., Chen, W., Amar, M. J., Remaley, A. T., Saba, J. D., and Proia, R. L. (2010) Sphingosine 1-Phosphate Lyase Deficiency Disrupts Lipid Homeostasis in Liver. *J. Biol. Chem.* **285**, 10880–10889

82. Hagen, N., Van Veldhoven, P. P., Proia, R. L., Park, H., Merrill, A. H., and Van Echten-Deckert, G. (2009) Subcellular Origin of Sphingosine 1-Phosphate Is Essential for Its Toxic Effect in Lyase-deficient Neurons. *J. Biol. Chem.* **284**, 11346–11353

83. Hagen, N., Hans, M., Hartmann, D., and Swandulla, D. (2011) Sphingosine-1-phosphate links glycosphingolipid metabolism to neurodegeneration via a calpain-mediated mechanism. *Cell Death Differ.* **18**, 1356–1365

84. Maceyka, M., Sankala, H., Hait, N. C., Stunff Le, S., Liu, H., Toman, R., Collier, C., Zhang, M., Satin, L. S., Merrill, A. H., Milstien, S., and Spiegel, S. (2005) SphK1 and SphK2 , Sphingosine Kinase Isoenzymes with Opposing Functions in Sphingolipid Metabolism. *J. Biol. Chem.* **280**, 37118–37129

85. Don, A. S., Martinez-Lamenca, C., Webb, W. R., Proia, R. L., Roberts, E., and Rosen, H. (2007) Essential Requirement for Sphingosine Kinase 2 in a Sphingolipid Apoptosis Pathway Activated by. *J. Biol. Chem.* **282**, 15833–15842

86. Ikeda, M., Kihara, A., and Igarashi, Y. (2004) Sphingosine-1-phosphate lyase SPL is an endoplasmic reticulum-resident, integral membrane protein with the pyridoxal 5'-phosphate binding domain exposed to the cytosol. *Biochem. Biophys. Res. Commun.* **325**, 338–343

87. Chen, K., Lin, G., Haelterman, N. A., Ho, T. S.-Y., Li, T., Li, Z., Duraine, L., Graham, B. H., Jaiswal, M., Yamamoto, S., Rasband, M. N., and Bellen, H. J. (2016) Loss of Frataxin induces iron toxicity , sphingolipid synthesis, and Pdk1/Mef2 activation, leading to neurodegeneration. *Elife* **5**, 1–24

88. Chen, K., Ho, T. S. Y., Lin, G., Tan, K. L., Rasband, M. N., and Bellen, H. J. (2016) Loss of Frataxin activates the iron/sphingolipid/PDK1/Mef2 pathway in mammals. *Elife* **5**, 1–14

89. Shakoury-Elizeh, M., Protchenko, O., Berger, A., Cox, J., Gable, K., Dunn, T. M., Prinz, W. A., Bard, M., and Philpott, C. C. (2010) Metabolic Response to Iron Deficiency in Saccharomyces. *J. Biol. Chem.* **285**, 14823–14833

90. Lee, Y., Huang, X., Kropat, J., Henras, A., Merchant, S. S., Dickson, R. C., and Chanfreau, G. F. (2012) Sphingolipid Signaling Mediates Iron Toxicity. *Cell Metab.* **16**, 90–96

91. Caohuy, H., Yang, Q., Eudy, Y., Ha, T., Xu, A. E., Glover, M., Frizzell, R. A., Jozwik, C., and Pollard, H. B. (2014) Activation of 3-Phosphoinositide-dependent Kinase 1 (PDK1) and Serum- and Glucocorticoid-induced Protein Kinase 1 (SGK1) by Short-chain Sphingolipid C4-ceramide Rescues the Trafficking Defect of ΔF508-Cystic Fibrosis Transmembrane Conductance Regulator (Δ. *J. Biol. Chem.* **289**, 35953–35968

92. Jankovic, J. and Rivera, V. M. (1979) Hereditary Myoclonus and Progressive Distal Muscular Atrophy. *Ann Neurol* **6**, 227–231

93. Koskiniemi, R. I., Donner, R., Majuhi, H., and Norio, R. (1974) Progressive Myoclonus Epilepsy - A Clinical and Histopathological Study. *Acta Neurol. Scandinav.* **50**, 307–332

94. Haliloglu, G., Chattopadhyay, A., Skorodis, L., Manzur, A., Mercuri, E., Talim, B., Akc, Z., Renda, Y., Muntoni, F., and Topalog, H. (2002) Spinal Muscular Atrophy with Progressive Myoclonic Epilepsy:Report of New Cases and Review of the Literature. *Neuropediatrics* **33**, 314–319

95. Krebs, S., Medugorac, I., Röther, S., Strässer, K., and Förster, M. (2007) A missense mutation in the 3-ketodihydrosphingosine reductase FVT1 as candidate

causal mutation for bovine spinal muscular atrophy. *Proc. Natl. Acad. Sci. U. S. A.* **104**, 6746–6751

96. Zhou, J., Tawk, M., Tiziano, F. D., Veillet, J., Bayes, M., Nolent, F., Garcia, V., Servidei, S., Bertini, E., Castro-giner, F., Renda, Y., Andrieu-abadie, N., Gut, I., Levade, T., and Topaloglu, H. (2012) Spinal Muscular Atrophy Associated with Progressive Myoclonic Epilepsy Is Caused by Mutations in ASAH1. *Am. J. Hum. Genet.* **91**, 5–14

97. Samuelsson, K. and Zetterström, R. (1971) Ceramides in a Patient with Lipogranulomatosis (Farber's Disease) with Chronic Course. *Scand. J. Clin. Lab. Invest.* **27**, 393–405

98. Sugita, M., Dulaney, J. T., and Moser, H. W. (1972) Ceramidase Deficiency in Farber's Disease (Lipogranulomatosis). *Science (80-.).* **178**, 1100–1102

99. Topaloglu, H. and Melki, J. (2016) Spinal muscular atrophy associated with progressive myoclonus epilepsy. *Epileptic Disord* **18**, S128–S134

100. Teoh, H. L., Solyom, A., Schuchman, E. H., and Mowat, D. (2016) Polyarticular Arthritis and Spinal Muscular Atrophy in Acid Ceramidase Deficiency. *Pediatrics* **138**, e1–e4

101. Dyment, D. A., Sell, E., Vanstone, M. R., Smith, A. C., Garandeau, D., Carpentier, S., E, L. T., Sabourdy, F., and Beaulieu, C. L. (2014) Evidence for clinical , genetic and biochemical variability in spinal muscular atrophy with progressive myoclonic epilepsy. *Clin Genet* **86**, 558–563

102. Alayoubi, A. M., Wang, J. C. M., Au, B. C. Y., Carpentier, S., Garcia, V., Dworski, S., El-Ghamrasni, S., Kirouac, K. N., Exertier, M. J., Xiong, Z. J., Prive, G. G., Simonaro, C. M., Casas, J., Fabrias, G., Schuchman, E. H., Turner, P. V, Hakem, R., Levade, T., and Medin, J. A. (2013) Systemic ceramide accumulation leads to severe and varied pathological consequences. *EMBO Mol. Med.* **5**, 827–842

103. Sikora, J., Dworski, S., Jones, E. E., Kamani, M. A., Micsenyi, M. C., Sawada, T., Faouder, P. Le, Bertrand-michel, J., Dupuy, A., Dunn, C. K., Yang, C., Fabrias, G., Hampson, D. R., Levade, T., Drake, R. R., Medin, J. A., and Walkley, S. U. (2017) Acid Ceramidase Deficiency in Mice Results in a Broad Range of Central Nervous System Abnormalities. *Am. J. Pathol.* **187**, 864–883

104. Vanni, N., Fruscione, F., Ferlazzo, E., Striano, P., Robbiano, A., Traverso, M., Sander, T., Falace, A., Gazzerro, E., Bramanti, P., Bielawski, J., Fassio, A., Minetti, C., Genton, P., and Zara, F. (2014) Impairment of ceramide synthesis

causes a novel progressive myoclonus epilepsy. *Ann. Neurol.* **76**, 206–212

105. Venkataraman, K., Riebeling, C., Bodennec, J., Riezman, H., Allegood, J. C., Sullards, M. C., Merrill, A. H., and Futerman, A. H. (2002) Upstream of growth and differentiation factor 1 (uog1), a mammalian homolog of the yeast longevity assurance gene 1 (LAG1), regulates N-stearoyl-sphinganine (C18-(dihydro)ceramide) synthesis in a fumonisin B1-independent manner in mammalian cells. *J. Biol. Chem.* **277**, 35642–35649

106. Sentelle, R. D., Senkal, C. E., Jiang, W., Ponnusamy, S., Gencer, S., Selvam, S. P., Ramshesh, V. K., Peterson, Y. K., Lemasters, J. J., Szulc, Z. M., Bielawski, J., and Ogretmen, B. (2012) Ceramide targets autophagosomes to mitochondria and induces lethal mitophagy. *Nat. Chem. Biol.* **8**, 831–838

107. Ferlazzo, E., Striano, P., Italiano, D., Calarese, T., Gasparini, S., Vanni, N., Fruscione, F., Genton, P., and Zara, F. (2016) Autosomal recessive progressive myoclonus epilepsy due to impaired ceramide synthesis. *Epileptic Disord* **18**, S120–S127

108. Mosbech, M. B., Olsen, A. S., Neess, D., Ben-David, O., Klitten, L. L., Larsen, J., Sabers, A., Vissing, J., Nielsen, J. E., Hasholt, L., Klein, A. D., Tsoory, M. M., Hjalgrim, H., Tommerup, N., Futerman, A. H., Moller, R. S., and Faergeman, N. J. (2014) Reduced ceramide synthase 2 activity causes progressive myoclonic epilepsy. *Ann Clin Transl Neurol* **1**, 88–98

109. Jiang, J. C., Kirchman, P. A., Zagulski, M., Hunt, J., and Jazwinski, S. M. (1998) Homologs of the Yeast Longevity Gene LAG1 in Caenorhabditis elegans and Human. *Genome Res.* **8**, 1259–1272

110. Zhao, L., Spassieva, S. D., Jucius, T. J., Shultz, L. D., Shick, H. E., Macklin, W. B., Hannun, Y. a, Obeid, L. M., and Ackerman, S. L. (2011) A deficiency of ceramide biosynthesis causes cerebellar purkinje cell neurodegeneration and lipofuscin accumulation. *PLoS Genet.* **7**, e1002063

111. Ginkel, C., Hartmann, D., vom Dorp, K., Zlomuzica, A., Farwanah, H., Eckhardt, M., Sandhoff, R., Degen, J., Rabionet, M., Dere, E., Dörmann, P., Sandhoff, K., and Willecke, K. (2012) Ablation of neuronal ceramide synthase 1 in mice decreases ganglioside levels and expression of myelin-associated glycoprotein in oligodendrocytes. *J. Biol. Chem.* **287**, 41888–41902

112. Imgrund, S., Hartmann, D., Farwanah, H., Eckhardt, M., Sandhoff, R., Degen, J., Gieselmann, V., Sandhoff, K., and Willecke, K. (2009) Adult Ceramide Synthase 2 (CERS2)-deficient Mice Exhibit Myelin Sheath Defects , Cerebellar Degeneration, and Hepatocarcinomas. **284**, 33549–33560

113. Ben-David, O., Pewzner-Jung, Y., Brenner, O., Laviad, E. L., Kogot-Levin, A., Weissberg, I., Biton, I. E., Pienik, R., Wang, E., Kelly, S., Alroy, J., Raas-Rothschild, A., Friedman, A., Bru, B., Merrill, A. H., and Futerman, A. H. (2011) Encephalopathy Caused by Ablation of Very Long Acyl Chain Ceramide Synthesis May Be Largely Due to Reduced Galactosylceramide Levels. *J. Biol. Chem.* **286**, 30022–30033

114. Spassieva, S. D., Ji, X., Liu, Y., Gable, K., Bielawski, J., Dunn, T. M., Bieberich, E., and Zhao, L. (2016) Ectopic expression of ceramide synthase 2 in neurons suppresses neurodegeneration induced by ceramide synthase 1 deficiency. *Proc. Natl. Acad. Sci.* 201522071

115. Haddad, S. El, Khoury, M., Daoud, M., Kantar, R., Harati, H., Mousallem, T., Alzate, O., Meyer, B., and Boustany, R.-M. (2012) CLN5 and CLN8 protein association with ceramide synthase: biochemical and proteomic approaches. *Electrophoresis* **33**, 3798–3809

116. Boustany, R.-M. (2014) Ceramide Center Stage in Progressive. *Ann Neurol.* **76**, 162–164

117. Simpson, M. A., Cross, H., Proukakis, C., Priestman, D. A., Neville, D. C. A., Reinkensmeier, G., Wang, H., Wiznitzer, M., Gurtz, K., Verganelaki, A., Pryde, A., Patton, M. A., Dwek, R. A., Butters, T. D., Platt, F. M., and Crosby, A. H. (2004) Infantile-onset symptomatic epilepsy syndrome caused by a homozygous loss-of-function mutation of GM3 synthase. *Nat. Genet.* **36**, 1225–1229

118. Stevanin, G., Ruberg, M., and Brice, A. (2008) Recent Advances in the Genetics of Spastic Paraplegias. *Curr Neurol Neurosci Rep.* **8**, 198–210

119. Boukhris, A., Schule, R., Loureiro, J. L., Lourenço, C. M., Mundwiller, E., Gonzalez, M. A., Charles, P., Gauthier, J., Rekik, I., Acosta Lebrigio, R. F., Gaussen, M., Speziani, F., Ferbert, A., Feki, I., Caballero-Oteyza, A., Dionne-Laporte, A., Amri, M., Noreau, A., Forlani, S., Cruz, V. T., Mochel, F., Coutinho, P., Dion, P., Mhiri, C., Schols, L., Pouget, J., Darios, F., Rouleau, G. A., Marques, W., Brice, A., Durr, A., Zuchner, S., and Stevanin, G. (2013) Alteration of ganglioside biosynthesis responsible for complex hereditary spastic paraplegia. *Am. J. Hum. Genet.* **93**, 118–123

120. Harlalka, G. V., Lehman, A., Chioza, B., Baple, E. L., Maroofian, R., Cross, H., Sreekantan-Nair, A., Priestman, D. A., Al-Turki, S., McEntagart, M. E., Proukakis, C., Royle, L., Kozak, R. P., Bastaki, L., Patton, M., Wagner, K., Coblentz, R., Price, J., Mezei, M., Schlade-Bartusiak, K., Platt, F. M., Hurles, M. E., and Crosby, A. H. (2013) Mutations in B4GALNT1 (GM2 synthase) underlie a new disorder of ganglioside biosynthesis. *Brain* **136**, 3618–3624

121. Wakil, S. M., Monies, D. M., Ramzan, K., Hagos, S., Bastaki, L., Meyer, B. F., and Bohlega, S. (2014) Novel B4GALNT1 mutations in a complicated form of hereditary spastic paraplegia. *Clin. Genet.* **86**, 500–501

122. Dad, R., Walker, S., Scherer, S. W., Hassan, M. J., Alghamdi, M. D., Minassian, B. A., and Alkhater, R. A. (2017) Febrile ataxia and myokymia broaden the SPG26 hereditary spastic paraplegia phenotype. *Neurol. Genet.* **3**, e156

123. Sun, J., Shaper, N. L., Itonori, S., Heffer-Lauc, M., Sheikh, K. A., and Schnaar, R. L. (2004) Myelin-associated glycoprotein (Siglec-4) expression is progressively and selectively decreased in the brains of mice lacking complex gangliosides. *Glycobiology* **14**, 851–857

124. Takamiya, K., Yamamoto, A., Furukawa, K., Zhao, J., Fukumoto, S., Yamashiro, S., Okada, M., Haraguchi, M., Shin, M., Kishikawa, M., Shiku, H., Aizawa, S., and Furukawa, K. (1998) Complex gangliosides are essential in spermatogenesis of mice : *Proc. Natl. Acad. Sci. U. S. A.* **95**, 12147–12152

125. Sheikh, K. A., Sun, J., Liu, Y., Kawai, H., Crawford, T. O., Proia, R. L., Griffin, J. W., and Schnaar, R. L. (1999) Mice lacking complex gangliosides develop Wallerian degeneration and myelination defects. *Proc. Natl. Acad. Sci. U. S. A.* **96**, 7532–7537

126. Massimo, A., Maura, S., Nicoletta, L., Giulia, M., Valentina, M., Elena, C., Alessandro, P., and Rosaria, B. (2016) Current and Novel Aspects on the Non-lysosomal β-Glucosylceramidase GBA2. *Neurochem. Res.* **41**, 210–220

127. Hammer, M. B., Eleuch-fayache, G., Schottlaender, L. V, Nehdi, H., Gibbs, J. R., Arepalli, S. K., Chong, S. B., Hernandez, D. G., Sailer, A., Liu, G., Mistry, P. K., Cai, H., Shrader, G., Sassi, C., Bouhlal, Y., Houlden, H., Amouri, R., and Singleton, A. B. (2013) Mutations in GBA2 Cause Autosomal-Recessive Cerebellar Ataxia with Spasticity. *Am. J. Hum. Genet.* **92**, 245–251

128. Martin, E., Schüle, R., Smets, K., Rastetter, A., Boukhris, A., Loureiro, J. L., Gonzalez, M. A., Mundwiller, E., Deconinck, T., Wessner, M., Jornea, L., Oteyza, A. C., Durr, A., Martin, J. J., Schöls, L., Mhiri, C., Lamari, F., Züchner, S., De Jonghe, P., Kabashi, E., Brice, A., and Stevanin, G. (2013) Loss of function of glucocerebrosidase GBA2 is responsible for motor neuron defects in hereditary spastic paraplegia. *Am. J. Hum. Genet.* **92**, 238–244

129. Votsi, C., Zamba-Papanicolaou, E., Middleton, L. T., Pantzaris, M., and Christodoulou, K. (2014) A Novel GBA2 Gene Missense Mutation in Spastic Ataxia. *Ann Hum Genet.* **78**, 13–22

130. Citterio, A., Arnoldi, A., Panzeri, E., Grazia, M., Filosto, M., Dilena, R., Arrigoni, F., Castelli, M., Maghini, C., Germiniasi, C., Menni, F., and Martinuzzi, A. (2014) Mutations in CYP2U1 , DDHD2 and GBA2 genes are rare causes of complicated forms of hereditary spastic paraparesis. *J Neurol* **261**, 373–381

131. Yang, Y.-J., Zhou, Z.-F., Liao, X.-X., Luo, Y.-Y., Zhan, Z.-X., Huang, M.-F., Zhou, L., Tang, B.-S., Shen, L., and Du, J. (2016) SPG46 and SPG56 are rare causes of hereditary spastic paraplegia in China. *J. Neurol.* **263**, 2136–2138

132. Synofzik, M. and Schüle, R. (2017) Overcoming the Divide Between Ataxias and Spastic Paraplegias:Shared Phenotypes, Genes, and Pathways Discovering the Phenotypic and Genetic Spectrum. *Mov. Disord.* **32**, 332–345

133. Yildiz, Y., Matern, H., Thompson, B., Allegood, J. C., Warren, R. L., Ramirez, D. M. O., Hammer, R. E., Hamra, F. K., Matern, S., and Russell, D. W. (2006) Mutation of β -glucosidase 2 causes glycolipid storage disease and impaired male fertility. *J. Clin. Invest.* **116**, 2985–2994

134. Sultana, S., Reichbauer, J., Schüle, R., and Mochel, F. (2015) Biochemical and Biophysical Research Communications Lack of enzyme activity in GBA2 mutants associated with hereditary spastic paraplegia / cerebellar ataxia (SPG46). *Biochem. Biophys. Res. Commun.* **465**, 35–40

135. Mistry, P. K., Liu, J., Sun, L., Chuang, W.-L., Yuen, T., Yang, R., Lu, P., Zhang, K., Li, J., Keutzer, J., Stachnik, A., Mennone, A., Boyer, J. L., Jain, D., Brady, R. O., New, M. I., and Zaidi, M. (2014) Glucocerebrosidase 2 gene deletion rescues type 1 Gaucher disease. *Proc. Natl. Acad. Sci. U. S. A.* **111**, 4934–4339

136. Hama, H. (2010) Fatty acid 2-Hydroxylation in mammalian sphingolipid biology. *Biochim. Biophys. Acta* **1801**, 405–414

137. Edvardson, S., Hama, H., Shaag, A., Gomori, J. M., Berger, I., Soffer, D., Korman, S. H., Taustein, I., Saada, A., and Elpeleg, O. (2008) Mutations in the Fatty Acid 2-Hydroxylase Gene Are Associated with Leukodystrophy with Spastic Paraparesis and Dystonia. *Am. J. Hum. Genet.* **83**, 643–648

138. Dick, K. J., Eckhardt, M., Paisan-Ruiz, C., Alshehhi, A. A., Proukakis, C., Sibtain, N. A., Maier, H., Sharifi, R., Patton, M. A., Bashir, W., Koul, R., Raeburn, S., Gieselmann, V., Houlden, H., and Crosby, A. H. (2010) Mutation of FA2H Underlies a Complicated Form of Hereditary Spastic Paraplegia (SPG35). *Hum. Mutat.* **31**, 1251–1260

139. Kruer, M. C., Paisa, C., Boddaert, N., Yoon, M. Y., Hama, H., Gregory, A.,

Malandrini, A., Woltjer, R. L., Munnich, A., Gobin, S., Polster, B. J., Palmeri, S., Edvardson, S., Hardy, J., Houlden, H., and Hayflick, S. J. (2010) Defective FA2H Leads to a Novel Form of Neurodegeneration with Brain Iron Accumulation (NBIA). *Ann Neurol* **68**, 611–618

140. Marelli, C., Salih, M. A., Nguyen, K., Mallaret, M., Leboucq, N., Hassan, H. H., Drouot, N., Labauge, P., and Koenig, M. (2015) Cerebral Iron Accumulation Is Not a Major Feature of FA2H/SPG35. *Mov. Disord. Clin. Pract.* **2**, 8–12

141. Cao, L., Huang, X.-J., Chen, C.-J., and Chen, S.-D. (2013) Journal of the Neurological Sciences A rare family with Hereditary Spastic Paraplegia Type 35 due to novel FA2H mutations: A case report with literature review. *J. Neurol. Sci.* **329**, 1–5

142. Soehn, A. S., Rattay, T. W., Beck-wödl, S., Schäferhoff, K., Monk, D., Döbler-, M., Schüle, R., and Bauer, P. (2016) Uniparental disomy of chromosome 16 unmasks recessive mutations of FA2H / SPG35 in 4 families. *Neurology* **87**, 186–191

143. Bis, D. M., Schule, R., Reichbauer, J., Synofzik, M., Rattay, T. W., Soehn, A., De Jonghe, P., Schols, L., and Zuchner, S. (2017) Uniparental disomy determined by whole-exome sequencing in a spectrum of rare motoneuron diseases and ataxias. *Mol. Genet. Genomic Med.* **5**, 280–286

144. Zoller, I., Meixner, M., Hartmann, D., Bussow, H., Meyer, R., Gieselmann, V., and Eckhardt, M. (2008) Absence of 2-Hydroxylated Sphingolipids Is Compatible with Normal Neural Development But Causes Late-Onset Axon and Myelin Sheath Degeneration. *J. Neurosci.* **28**, 9741–9754

145. Potter, K. A., Kern, M. J., Fullbright, G., Bielawski, J., Steven, S., Yum, S. W., Li, J. J., Cheng, H. U. A., Han, X., and Venkata, J. K. (2011) Central Nervous System Dysfunction in a Mouse Model of FA2H Deficiency. *Glia* **59**, 1009–1021

146. Axpe, I. R., Elisa, B. M., Ainhoa, G. R., Bermejo-Ramirez, R., and Arroyo Andújar, D. (2017) Sensory-motor neuropathy in a casewith SPG35: Expanding the phenotype. *J. Neurol. Sci.* **380**, 98–100

147. Pearce, J. M. (2000) Howard Henry Tooth (1856-1925). *J Neurol* **247**, 3–4

148. Charcot, J. M. and Marie, P. (1886) Sur une forme particulière d'atrophie musculaire progressive souvent familiale débutant par les pieds et les jambes et atteignant plus tard les. *Rev. médecine* **6**, 96–138

149. Tooth, H. H. (1886) The peroneal type of progressive muscular atrophy : Thesis

for the degree of M.D. in the University of Cambridge.

150. Gilliatt, R. W. and Thomas, P. K. (1957) Extreme slowing of nerve conduction in peroneal muscular atrophy. *Rheumatology* **4**, 104–106

151. Dyck, P. J. and Lambert, E. H. (1968) Lower Motor and Primary Sensory Neuron Diseases With Peroneal Muscular Atrophy (I). *Arch Neurol* **18**, 603–618

152. Harding, A. and Thomas, P. (1980) The clinical features of hereditary motor and sensory neuropathy types I and II. *Brain a J. Neurol.* **17**, 259–280

153. Nicholson, G. and Myers, S. (2006) Intermediate Forms of Charcot-Marie-Tooth Neuropathy. *Neuromolecular Med.* **8**, 123–130

154. Ekins, S., Litterman, N. K., Arnold, R. J. G., Burgess, R. W., Freundlich, J. S., Gray, S. J., Higgins, J. J., Langley, B., Willis, D. E., Notterpek, L., Pleasure, D., Sereda, M. W., and Moore, A. (2015) A brief review of recent Charcot-Marie-Tooth research and priorities. *F1000Research* **4**, 53

155. Lupski, J. R., Montes de Oca-luna, R., Slaugenhaupt, S., Pentao, L., Guzzetta, V., Trask, B. J., Saucedo-Carclenas, O., Barker, D. F., Killian, J. M., Garcia, C. A., Chakravarti, A., and Patel, P. I. (1991) DNA Duplication Associated with Charcot-Marie-Tooth Disease Type 1A. *Cell* **66**, 219–232

156. Rossor, A. M., Tomaselli, P. J., and Reilly, M. M. (2016) Recent advances in the genetic neuropathies. *Curr. Opin. Neurol.* **29**, 537–548

157. Saporta, M. A. (2014) Charcot-Marie-Tooth Disease and Other Inherited Neuropathies. *Continuum (N. Y).* **20**, 1208–1225

158. Baets, J., Jonghe, P. De, and Timmerman, V. (2014) Recent advances in Charcot – Marie – Tooth disease. *Curr. Opin. Neurol.* **27**, 532–540

159. Mathis, S., Goizet, C., Tazir, M., Magdelaine, C., Lia, A., Magy, L., and Vallat, J. (2015) Charcot – Marie – Tooth diseases : an update and some new proposals for the classi fi cation. *J. Med. Genet.* **52**, 681–690

160. Pareyson, D., Saveri, P., and Pisciotta, C. (2017) New developments in Charcot–Marie–Tooth neuropathy and related diseases. *Curr. Opin. Neurol.* **30**, 471–480

161. Skre, H. (1974) Genetic and clinical aspects of Carcat-Marie-Tooth's disease. *Clin. Genet.* **6**, 98–118

162. Szigeti, K. and Lupski, J. R. (2009) Charcot–Marie–Tooth disease. *Eur. J. Hum. Genet.* **17**, 703–710

163. Callaghan, B. C., Price, R. S., Feldman, E. L., and Arbor, A. (2015) Diagnostic and Therapeutic Advances: Distal Symmetric Polyneuropathy. *JAMA* **314**, 2172–2181

164. MacMillan, J. C. and Harper, P. S. (1994) The Charcot-Marie-Tooth syndrome: clinical aspects from a population study in South Wales, UK. *Clin Genet* **45**, 128–134

165. England, J. D., Gronseth, G. S., Franklin, G., Carter, G. T., Kinsella, L. J., Cohen, J. A., Asbury, A. K., Szigeti, K., Lupski, J. R., Latov, N., Lewis, R. A., Low, P. A., Fisher, M. A., Herrmann, D., Howard, J. F., Lauria, G., Miller, R. G., Polydefkis, M., and Sumner, A. J. (2009) Evaluation of distal symmetric polyneuropathy: The role of laboratory and genetic testing (an evidence-based review). *Muscle and Nerve* **39**, 116–125

166. Teunissen, Laurien, Notermans, N. (2003) Disease Course of Charcot-Marie-Tooth Disease Type 2. *Arch. Neurol.* **60**, 823–828

167. Lupski, J. R., Reid, J. G., Gonzaga-Jauregui, C., Rio Deiros, D., Chen, D. C., Nazareth, L., Bainbridge, M., Dinh, H., Jing, C., Wheeler, D. A., Mcguire, A. L., Zhang, F., Satnkiewicz, P., Halperin, J. L., Yang, C., Gehman, C., Guo, D., Irikat, R. K., Tom, W., Fantin, N. J., Muzny, D. M., Muzny, D. M., and Gibbs, R. A. (2010) Whole-Genome Sequencing in a Patient with Charcot–Marie–Tooth Neuropathy. *N. Engl. J. Med.* **362**, 1181–1191

168. Choi, B., Koo, S. K., Park, M., Rhee, H., Yang, S., Choi, K., Jung, S., Kim, H. S., Hyun, Y. S., Nakhro, K., Lee, H. J., Woo, H., and Chung, K. W. (2012) Exome Sequencing is an Efficient Tool for Genetic Screening of Charcot–Marie–Tooth Disease. *Hum. Mutat.* **33**, 1610–1615

169. Timmerman, V., Strickland, A. V., and Zuchner, S. (2014) Genetics of Charcot-Marie-Tooth (CMT) disease within the frame of the human genome project success. *Genes (Basel).* **5**, 13–32

170. Braathen, G. J., Sand, J. C., Lobato, A., Høyer, H., and Russell, M. B. (2011) Genetic epidemiology of Charcot-Marie-Tooth in the general population. *Eur. J. Neurol.* **18**, 39–48

171. DiVincenzo, C., Elzinga, C. D., Medeiros, A. C., Karbassi, I., Jones, J. R., Evans, M. C., Braastad, C. D., Bishop, C. M., Jaremko, M., Wang, Z., Liaquat, K.,

Hoffman, C. A., York, M. D., Batish, S. D., Lupski, J. R., and Higgins, J. J. (2014) The allelic spectrum of Charcot-Marie-Tooth disease in over 17,000 individuals with neuropathy. *Mol. Genet. genomic Med.* **2**, 522–529

172. Gonzaga-Jauregui, C., Harel, T., Gambin, T., Kousi, M., Griffin, L. B., Francescatto, L., Ozes, B., Karaca, E., Jhangiani, S. N., Bainbridge, M. N., Lawson, K. S., Pehlivan, D., Okamoto, Y., Withers, M., Mancias, P., Slavotinek, A., Reitnauer, P. J., Goksungur, M. T., Shy, M., Crawford, T. O., Koenig, M., Willer, J., Flores, B. N., Pediaditrakis, I., Us, O., Wiszniewski, W., Parman, Y., Antonellis, A., Muzny, D. M., Katsanis, N., Battaloglu, E., Boerwinkle, E., Gibbs, R. A., and Lupski, J. R. (2015) Exome Sequence Analysis Suggests that Genetic Burden Contributes to Phenotypic Variability and Complex Neuropathy. *Cell Rep.* **12**, 1169–1183

173. Ylikallio, E., Johari, M., Konovalova, S., Moilanen, J. S., Kiuru-enari, S., Auranen, M., Pajunen, L., and Tyynismaa, H. (2014) Targeted next-generation sequencing reveals further genetic heterogeneity in axonal Charcot–Marie–Tooth neuropathy and a mutation in HSPB1. *Eur. J. Hum. Genet.* **22**, 522–527

174. Ismailov, S. M., Fedotov, V. P., Dadali, E. L., Polyakov, A. V, Broeckhoven, C. Van, Ivanov, V. I., Jonghe, P. De, Timmerman, V., and Evgrafov, O. V. (2001) A new locus for autosomal dominant Charcot-Marie-Tooth disease type 2 (CMT2F) maps to chromosome 7q11-q21. *Eur. J. Hum. Genet.* **9**, 646–650

175. Evgrafov, O. V, Mersiyanova, I., Irobi, J., Van Den Bosch, L., Dierick, I., Leung, C. L., Schagina, O., Verpoorten, N., Van Impe, K., Fedotov, V., Dadali, E., Auer-Grumbach, M., Windpassinger, C., Wagner, K., Mitrovic, Z., Hilton-Jones, D., Talbot, K., Martin, J.-J., Vasserman, N., Tverskaya, S., Polyakov, A., Liem, R. K. H., Gettemans, J., Robberecht, W., De Jonghe, P., and Timmerman, V. (2004) Mutant small heat-shock protein 27 causes axonal Charcot-Marie-Tooth disease and distal hereditary motor neuropathy. *Nat. Genet.* **36**, 602–606

176. Rossor, A. M., Davidson, G. L., Blake, J., Polke, J. M., Murphy, S. M., Houlden, H., Innes, A., Kalmar, B., Greensmith, L., and Reilly, M. M. (2012) A novel p.Glu175X premature stop mutation in the C-terminal end of HSP27 is a cause of CMT2. *J. Peripher. Nerv. Syst.* **17**, 201–205

177. Tang, B., Liu, X., Zhao, G., Luo, W., Xia, K., Pan, Q., Cai, F., Hu, Z., Zhang, C., Chen, B., Zhang, F., Shen, L., Zhang, R., and Jiang, H. (2005) Mutation analysis of the small heat shock protein 27 gene in chinese patients with Charcot-Marie-Tooth disease. *Arch. Neurol.* **62**, 1201–1207

178. Echaniz-Laguna, A., Geuens, T., Petiot, P., Pereon, Y., Adriaenssens, E., Haidar, M., Capponi, S., Maisonobe, T., Fournier, E., Dubourg, O., Degos, B., Salachas,

F., Lenglet, T., Eymard, B., Delmont, E., Pouget, J., Morales, R. J., Goizet, C., Latour, P., Timmerman, V., and Stojkovic, T. (2017) Axonal Neuropathies due to Mutations in Small Heat Shock Proteins: Clinical, Genetic, and Functional Insights into Novel Mutations. *Hum. Genome Var.* **38**, 556–568

179. Houlden, H., Vrie, F. W. De, Blake, J., Wood, N., and Reilly, M. M. (2008) Mutations in the HSP27 (HSPB1) gene cause dominant, recessive, and sporadic distal HMN/CMT type 2. *Neurology* **71**, 1660–1668

180. Bakthisaran, R., Tangirala, R., and Rao, C. M. (2014) Small heat shock proteins: role in cellular functions and pathology. *Biochim. Biophys. Acta* **1854**, 291–319

181. Haslbeck, M. and Vierling, E. (2015) A First Line of Stress Defense : Small Heat Shock Proteins and Their Function in Protein Homeostasis. *J. Mol. Biol.* **427**, 1537–1548

182. Mogk, A. and Bukau, B. (2017) Role of sHsps in organizing cytosolic protein aggregation and disaggregation. *Cell Stress Chaperones* **22**, 493–502

183. Hickey, E., Brandon, S. E., Potter, R., Stein, G., Stein, J., and Weber, L. A. (1986) Sequence and organization of genes encoding the human 27 kDa heat shock protein. *Nucleic Acids Res.* **14**, 4127–4145

184. Dierick, I., Irobi, J., De Jonghe, P., and Timmerman, V. (2005) Small heat shock proteins in inherited peripheral neuropathies. *Ann. Med.* **37**, 413–422

185. Carra, S., Crippa, V., Rusmini, P., Boncoraglio, A., Minoia, M., Giorgetti, E., Kampinga, H. H., and Poletti, A. (2012) Alteration of protein folding and degradation in motor neuron diseases: Implications and protective functions of small heat shock proteins. *Prog. Neurobiol.* **97**, 83–100

186. Wagstaff, M. J. D., Collaco-Moraes, Y., Smith, J., de Belleroche, J. S., Coffin, R. S., and Latchman, D. S. (1999) Protection of Neuronal Cells from Apoptosis by Hsp27 Delivered with a Herpes Simplex Virus-based Vector. *J. Biol. Chem.* **274**, 5061–5069

187. Benn, S. C., Perrelet, D., Kato, A. C., Scholz, J., Decosterd, I., Mannion, R. J., Bakowska, J. C., and Woolf, C. J. (2002) Hsp27 Upregulation and Phosphorylation Is Required for Injured Sensory and Motor Neuron Survival. *Neuron* **36**, 45–56

188. Stromer, T., Ehrnsperger, M., Gaestel, M., and Buchner, J. (2003) Analysis of the Interaction of Small Heat Shock Proteins with Unfolding Proteins. *J. Biol. Chem.*

278, 18015–18021

189. Wilhelmus, M. M. M., Boelens, W. C., Otte-höller, I., Kamps, B., Waal, R. M. W. De, and Verbeek, M. M. (2006) Small heat shock proteins inhibit amyloid- β protein aggregation and cerebrovascular amyloid- β protein toxicity. *Brain Res.* **1089**, 67–78

190. Cox, D. and Ecroyd, H. (2017) The small heat shock proteins α B-crystallin (HSPB5) and Hsp27 (HSPB1) inhibit the intracellular aggregation of α-synuclein. *Cell Stress Chaperones* **22**, 589–600

191. Yerbury, J. J., Gower, D., Vanags, L., Roberts, K., Lee, J. A., and Ecroyd, H. (2013) The small heat shock proteins α B-crystallin and Hsp27 suppress SOD1 aggregation in vitro. *Cell Stress Chaperones* **18**, 251–257

192. Acunzo, J., Katsogiannou, M., and Rocchi, P. (2012) Small heat shock proteins HSP27 (HspB1), αB-crystallin (HspB5) and HSP22 (HspB8) as regulators of cell death. *Int. J. Biochem. Cell Biol.* **44**, 1622–1631

193. Vidyasagar, A., Wilson, N. a, and Djamali, A. (2012) Heat shock protein 27 (HSP27): biomarker of disease and therapeutic target. *Fibrogenesis Tissue Repair* **5**, 7

194. Sun, Y. and Macrae, T. H. (2005) Small heat shock proteins: molecular structure and chaperone function. *Cell. Mol. Life Sci.* **62**, 2460–2476

195. Kriehuber, T., Rattei, T., Weinmaier, T., Bepperling, A., Haslbeck, M., and Buchner, J. (2010) Independent evolution of the core domain and its flanking sequences in small heat shock proteins. *FASEB J.* **24**, 3633–3642

196. Bagnéris, C., Bateman, O., Naylor, C., Cronin, N., Boelens, W., Keep, N., and Slingsby, C. (2009) Crystal structures of alpha-crystallin domain dimers of alphaB-crystallin and Hsp20. *J. Mol. Biol.* **392**, 1242–1252

197. Delbecq, S. P., Jehle, S., and Klevit, R. (2012) Binding determinants of the small heat shock protein, αB-crystallin: recognition of the “IxI” motif. *EMBO J.* **31**, 4587–4594

198. Kostenko, S. and Moens, U. (2009) Heat shock protein 27 phosphorylation : kinases , phosphatases , functions and pathology. *Cell. Mol. Life Sci.* **66**, 3289–3307

199. Aquilina, J. A., Shrestha, S., Morris, A. M., and Ecroyd, H. (2013) Structural and

Functional Aspects of Hetero-oligomers Formed by the Small Heat Shock Proteins αB-Crystallin and Hsp27. *J. Biol. Chem.* **288**, 13602–13609

200. Ylikallio, E., Konovalova, S., Dhungana, Y., Hilander, T., Junna, N., and Partanen, J. V. (2015) Truncated HSPB1 causes axonal neuropathy and impairs tolerance to unfolded protein stress. *BBA Clin.* **3**, 233–242

201. Benedetti, S., Previtali, S. C., Coviello, S., Scarlato, M., Cerri, F., Di Pierri, E., Piantoni, L., Spiga, I., Fazio, R., Riva, N., Natali Sora, M. G., Dacci, P., Malaguti, M. C., Munerati, E., Edoardo Grimaldi, L. M., Marrosu Giovanna, M., De Pellegrin, M., Ferrari, M., Comi, G., Quattrini, A., and Bolino, A. (2010) Analyzing Histopathological Features of Rare Charcot-Marie-Tooth Neuropathies to Unravel Their Pathogenesis. **67**, 1498–1505

202. Stancanelli, C., Fabrizi, G. M., Ferrarini, M., Cavallaro, T., Taioli, F., Di Leo, R., Russo, M., Gentile, L., Toscano, A., Vita, G., and Mazzeo, A. (2015) Charcot-Marie-Tooth 2F: phenotypic presentation of the Arg136Leu HSP27 mutation in a multigenerational family. *Neurol Sci* **36**, 1003–1006

203. Capponi, S., Geroldi, A., Fossa, P., Grandis, M., Ciotti, P., Gulli, R., Schenone, A., Mandich, P., and Bellone, E. (2011) HSPB1 and HSPB8 in inherited neuropathies: Study of an Italian cohort of dHMN and CMT2 patients. *J. Peripher. Nerv. Syst.* **16**, 287–294

204. Solla, P., Vannelli, A., Bolino, A., Marrosu, G., Coviello, S., Murru, M. R., Tranquilli, S., Corongiu, D., Benedetti, S., and Marrosu, M. G. (2010) Heat shock protein 27 R127W mutation: evidence of a continuum between axonal Charcot-Marie-Tooth and distal hereditary motor neuropathy. *J. Neurol. Neurosurg. Psychiatry* **81**, 958–962

205. Mandich, P., Grandis, M., Varese, A., Geroldi, A., Acquaviva, M., Ciotti, P., Gulli, R., Doria-lamba, L., Fabrizi, G. M., Giribaldi, G., Pizzuti, A., and Schenone, A. (2010) Severe Neuropathy After Diphtheria- Tetanus-Pertussis Vaccination in a Child Carrying a Novel Frame-Shift Mutation in the Small Heat-Shock Protein 27 Gene. *J. Child Neurol.* **25**, 107–109

206. Gaeta, M., Mileto, A., Mazzeo, A., Donato, R., Ascenti, G., and Blandino, A. (2012) MRI findings, patterns of disease distribution, and muscle fat fraction calculation in five patients with Charcot-Marie-Tooth type 2 F disease. *Skelet. Radiol.* **41**, 515–524

207. Kim, H. J., Lee, J., Hong, Y. Bin, Kim, Y. J., Lee, J. H., Nam, S. H., Choi, B.-O., and Chung, K. W. (2014) Ser135Phe mutation in HSPB1 (HSP27) from Charcot–Marie–Tooth disease type 2F families. *Genes Genomics* **37**, 295–303

208. Lin, K.-P., Soong, B.-W., Yang, C.-C., Huang, L.-W., Chang, M.-H., Lee, I.-H., Antonellis, A., Antonellis, A., and Lee, Y.-C. (2011) The mutational spectrum in a cohort of Charcot-Marie-Tooth disease type 2 among the Han Chinese in Taiwan. *PLoS One* **6**, e29393

209. Lewis-Smith, D. J., Duff, J., Pyle, A., Griffin, H., Polvikoski, T., Birchall, D., Horvath, R., and Chinnery, P. F. (2016) Novel HSPB1 mutation causes both motor neuronopathy and distal myopathy. *Neurol. Genet.* **2**, e110

210. Nishibayashi, M., Kokubun, N., Nakamura, A., Hirata, K., Yamamoto, M., and Sobue, G. (2007) Distal hereditary motor neuropathy type II with mutation in heat shock protein 27 gene. A case report. *Clin Neurol.* **47**, 50–52

211. Ikeda, Y., Abe, A., Ishida, C., Takahashi, K., Hayasaka, K., and Yamada, M. (2009) A clinical phenotype of distal hereditary motor neuronopathy type II with a novel HSPB1 mutation. *J. Neurol. Sci.* **277**, 9–12

212. Kijima, K., Numakura, C., Goto, T., Takahashi, T., Otagiri, T., Umetsu, K., and Hayasaka, K. (2005) Small heat shock protein 27 mutation in a Japanese patient with distal hereditary motor neuropathy. *J Hum Genet* **50**, 473–476

213. Maeda, K., Idehara, R., Hashiguchi, A., and Takashima, H. (2014) A Family with Distal Hereditary Motor Neuropathy and a K141Q Mutation of Small Heat Shock Protein HSPB1. *Intern. Med.* **53**, 1655–1658

214. Dierick, I., Baets, J., Irobi, J., Jacobs, A., De Vriendt, E., Deconinck, T., Merlini, L., Van Den Bergh, P., Rasic, V. M., Robberecht, W., Fischer, D., Morales, R. J., Mitrovic, Z., Seeman, P., Mazanec, R., Kochanski, A., Jordanova, A., Auer-Grumbach, M., Helderman-Van Den Enden, A. T. J. M., Wokke, J. H. J., Nelis, E., De Jonghe, P., and Timmerman, V. (2008) Relative contribution of mutations in genes for autosomal dominant distal hereditary motor neuropathies: A genotype-phenotype correlation study. *Brain* **131**, 1217–1227

215. Oberstadt, M., Mitter, D., Classen, J., and Baum, P. (2016) Late onset dHMN II caused by c.404C>G mutation in HSPB1 gene. *J. Peripher. Nerv. Syst.* **21**, 111–113

216. Chung, K. W., Kim, S.-B., Cho, S. Y., Hwang, S. J., Park, S. W., Kang, S. H., Kim, J., Yoo, J. H., and Choi, B.-O. (2008) Distal hereditary motor neuropathy in Korean patients with a small heat shock protein 27 mutation. *Exp. Mol. Med.* **40**, 304–312

217. Luigetti, M., Fabrizi, G. M., Madia, F., Ferrarini, M., Conte, A., Del Grande, A.,

Tasca, G., Tonali, P. A., and Sabatelli, M. (2010) A novel HSPB1 mutation in an Italian patient with CMT2/dHMN phenotype. *J. Neurol. Sci.* **298**, 114–117

218. James, P. A., Rankin, J., and Talbot, K. (2008) Asymmetrical late onset motor neuropathy associated with a novel mutation in the small heat shock protein HSPB1 (HSP27). *J. Neurol. Neurosurg. Psychiatry* **79**, 461–463

219. Rossor, A. M., Kalmar, B., Greensmith, L., and Reilly, M. M. (2012) The distal hereditary motor neuropathies. *J. Neurol. Neurosurg. Psychiatry* **83**, 6–14

220. d'Ydewalle, C., Krishnan, J., Chiheb, D. M., Van Damme, P., Irobi, J., Kozikowski, A. P., Vanden Berghe, P., Timmerman, V., Robberecht, W., and Van Den Bosch, L. (2011) HDAC6 inhibitors reverse axonal loss in a mouse model of mutant HSPB1-induced Charcot-Marie-Tooth disease. *Nat. Med.* **17**, 968–974

221. Huang, L., Min, J., Masters, S., Mivechi, N. F., and Moskophidis, D. (2007) Insights Into Function and Regulation of Small Heat Shock Protein 25 (HSPB1) in a Mouse Model With Targeted Gene Disruption. *Genesis* **45**, 487–501

222. Crowe, J., Aubareda, A., McNamee, K., Przybycien, P. M., Lu, X., Williams, R. O., Bou-Gharios, G., Saklatvala, J., and Dean, J. L. E. (2013) Heat shock protein B1-deficient mice display impaired wound healing. *PLoS One* **8**, e77383

223. Kammoun, M., Picard, B., Astruc, T., Gagaoua, M., Aubert, D., Bonnet, M., Blanquet, V., and Cassar-Malek, I. (2016) The invalidation of HspB1 gene in mouse alters the ultrastructural phenotype of muscles. *PLoS One* **11**, 1–19

224. Hao, X., Zhang, S., Timakov, B., and Zhang, P. (2007) The Hsp27 gene is not required for Drosophila development but its activity is associated with starvation resistance. *Cell Stress Chaperones* **12**, 364–372

225. Tucker, N. R., Ustyugov, A., Bryantsev, A. L., Konkel, M. E., and Shelden. (2009) Hsp27 is persistently expressed in zebrafish skeletal and cardiac muscle tissues but dispensable for their morphogenesis. *Cell Stress Chaperones* **14**, 521–533

226. Ackerley, S., James, P. A., Kalli, A., French, S., Davies, K. E., and Talbot, K. (2006) A mutation in the small heat-shock protein HSPB1 leading to distal hereditary motor neuronopathy disrupts neurofilament assembly and the axonal transport of specific cellular cargoes. *Hum. Mol. Genet.* **15**, 347–354

227. Chalova, A. S., Sudnitsyna, M. V, Strelkov, S. V, and Gusev, N. B. (2014) Characterization of human small heat shock proten hspb1 that carries c-terminal domain mutations associated with hereditary motor neuron diseases. *Biochim.*

Biophys. Acta **1884**, 2116–2126

228. Geuens, T., De Winter, V., Rajan, N., Achsel, T., Mateiu, L., Almeida-Souza, L., Asselbergh, B., Bouhy, D., Auer-Grumbach, M., Bagni, C., and Timmerman, V. (2017) Mutant HSPB1 causes loss of translational repression by binding to PCBP1, an RNA binding protein with a possible role in neurodegenerative disease. *Acta Neuropathol. Commun.* **5**, 1–15

229. Almeida-Souza, L., Goethals, S., de Winter, V., Dierick, I., Gallardo, R., Van Durme, J., Irobi, J., Gettemans, J., Rousseau, F., Schymkowitz, J., Timmerman, V., and Janssens, S. (2010) Increased monomerization of mutant HSPB1 leads to protein hyperactivity in Charcot-Marie-Tooth neuropathy. *J. Biol. Chem.* **285**, 12778–12786

230. Nefedova, V. V., Sudnitsyna, M. V., Strelkov, S. V., and Gusev, N. B. (2013) Structure and properties of G84R and L99M mutants of human small heat shock protein HspB1 correlating with motor neuropathy. *Arch. Biochem. Biophys.* **538**, 16–24

231. Muranova, L. K., Weeks, S. D., Strelkov, S. V., and Gusev, N. B. (2015) Characterization of mutants of human small heat shock protein HspB1 carrying replacements in the N-terminal domain and associated with hereditary motor neuron diseases. *PLoS One* **10**, 1–24

232. Nefedova, V. V, Datskevich, P. N., Sudnitsyna, M. V, Strelkov, S. V, and Gusev, N. B. (2013) Biochimie Physico-chemical properties of R140G and K141Q mutants of human small heat shock protein HspB1 associated with hereditary peripheral neuropathies. *Biochimie* **95**, 1582–1592

233. Yuan, A., Rao, M. V., Veeranna, and Nixon, R. A. (2012) Neurofilaments at a glance. *J. Cell Sci.* **125**, 3257–3263

234. Bacioglu, M., Maia, L. F., Preische, O., Schelle, J., Apel, A., Kaeser, S. A., Schweighauser, M., Eninger, T., Lambert, M., Pilotto, A., Shimshek, D. R., Neumann, U., Kahle, P. J., Staufenbiel, M., Neumann, M., Maetzler, W., Kuhle, J., and Jucker, M. (2016) Neurofilament Light Chain in Blood and CSF as Marker of Disease Progression in Mouse Models and in Neurodegenerative Diseases. *Neuron* **91**, 56–66

235. Byrne, L. M., Rodrigues, F. B., Blennow, K., Durr, A., Leavitt, B. R., Roos, R. A. C., Scahill, R. I., Tabrizi, S. J., Zetterberg, H., Langbehn, D., and Wild, E. J. (2017) Neurofilament light protein in blood as a potential biomarker of neurodegeneration in Huntington's disease: a retrospective cohort analysis. *Lancet Neurol.* **16**, 601–609

236. Alves, G. and Bonanni, L. (2017) Neurofilament light: A heavyweight diagnostic biomarker in neurodegenerative parkinsonism? *Neurology* **88**, 922–923

237. Mersiyanova, I. V., Perepelov, A. V., Polyakov, A. V., Sitnikov, V. F., Dadali, E. L., Oparin, R. B., Petrin, A. N., and Evgrafov, O. V. (2000) A New Variant of Charcot-Marie-Tooth Disease Type 2 Is Probably the Result of a Mutation in the Neurofilament-Light Gene. *Am. J. Hum. Genet.* **67**, 37–46

238. Jordanova, A., De Jonghe, P., Boerkoel, C. F., Takashima, H., De Vriendt, E., Ceuterick, C., Martin, J. J., Butler, I. J., Mancias, P., Papasozomenos, S. C., Terespolsky, D., Potocki, L., Brown, C. W., Shy, M., Rita, D. A., Tournev, I., Kremensky, I., Lupski, J. R., and Timmerman, V. (2003) Mutations in the neurofilament light chain gene (NEFL) cause early onset severe Charcot-Marie-Tooth disease. *Brain* **126**, 590–597

239. Dequen, F., Filali, M., Larivière, R. C., Perrot, R., Hisanaga, S. I., and Julien, J. P. (2010) Reversal of neuropathy phenotypes in conditional mouse model of Charcot-Marie-Tooth disease type 2E. *Hum. Mol. Genet.* **19**, 2616–2629

240. Zhai, J., Lin, H., Julien, J.-P., and Schlaepfer, W. W. (2007) Disruption of neurofilament network with aggregation of light neurofilament protein: a common pathway leading to motor neuron degeneration due to Charcot-Marie-Tooth disease-linked mutations in NFL and HSPB1. *Hum. Mol. Genet.* **16**, 3103–3116

241. Holmgren, A., Bouhy, D., De Winter, V., Asselbergh, B., Timmermans, J.-P., Irobi, J., and Timmerman, V. (2013) Charcot-Marie-Tooth causing HSPB1 mutations increase Cdk5-mediated phosphorylation of neurofilaments. *Acta Neuropathol.* **126**, 93–108

242. Lee, J., Jung, S.-C., Joo, J., Choi, Y.-R., Moon, H. W., Kwak, G., Yeo, H. K., Lee, J.-S., Ahn, H.-J., Jung, N., Hwang, S., Rheey, J., Woo, S.-Y., Kim, J. Y., Hong, Y. Bin, and Choi, B.-O. (2015) Overexpression of mutant HSP27 causes axonal neuropathy in mice. *J. Biomed. Sci.* **22**

243. Srivastava, A. K., Renusch, S. R., Naiman, N. E., Gu, S., Sneh, A., Arnold, W. D., Sahenk, Z., and Kolb, S. J. (2012) Mutant HSPB1 overexpression in neurons is sufficient to cause age-related motor neuronopathy in mice. *Neurobiol. Dis.* **47**, 163–173

244. Kalmar, B., Innes, A., Wanisch, K., Kolaszynska, A. K., Pandraud, A., Kelly, G., Abramov, A. Y., Reilly, M. M., Schiavo, G., and Greensmith, L. (2017) Mitochondrial deficits and abnormal mitochondrial retrograde axonal transport play a role in the pathogenesis of mutant Hsp27-induced Charcot Marie Tooth Disease. *Hum. Mol. Genet.* **26**, 3313–3326

245. Gentil, B. J. and Cooper, L. (2012) Molecular basis of axonal dysfunction and traffic impairments in CMT. *Brain Res. Bull.* **88**, 444–453

246. Dubey, J., Ratnakaran, N., and Koushika, S. P. (2015) Neurodegeneration and microtubule dynamics: death by a thousand cuts. *Front. Cell. Neurosci.* **9**, 1–15

247. Almeida-Souza, L., Asselbergh, B., d'Ydewalle, C., Moonens, K., Goethals, S., de Winter, V., Azmi, A., Irobi, J., Timmermans, J.-P., Gevaert, K., Remaut, H., Van Den Bosch, L., Timmerman, V., and Janssens, S. (2011) Small heat-shock protein HSPB1 mutants stabilize microtubules in Charcot-Marie-Tooth neuropathy. *J. Neurosci.* **31**, 15320–15328

248. Brunden, K. R., Trojanowski, J. Q., Smith, A. B., Lee, V. M. Y., and Ballatore, C. (2014) Microtubule-stabilizing agents as potential therapeutics for neurodegenerative disease. *Bioorganic Med. Chem.* **22**, 5040–5049

249. Brunden, K. R., Lee, V. M. Y., Smith, A. B., Trojanowski, J. Q., and Ballatore, C. (2017) Altered microtubule dynamics in neurodegenerative disease: Therapeutic potential of microtubule-stabilizing drugs. *Neurobiol. Dis.* **105**, 328–335

250. Pareyson, D., Saveri, P., Sagnelli, A., and Piscosquito, G. (2015) Mitochondrial dynamics and inherited peripheral nerve diseases. *Neurosci. Lett.* **596**, 66–77

251. Prior, R., Van Helleputte, L., Benoy, V., and Van Den Bosch, L. (2017) Defective axonal transport: A common pathological mechanism in inherited and acquired peripheral neuropathies. *Neurobiol. Dis.* **105**, 300–320

252. Lee, J. J. and Swain, S. M. (2006) Peripheral neuropathy induced by microtubule-stabilizing agents. *J. Clin. Oncol.* **24**, 1633–1642

253. Carlson, K. and Ocean, A. J. (2011) Peripheral neuropathy with microtubule-targeting agents: Occurrence and management approach. *Clin. Breast Cancer* **11**, 73–81

254. Sheng, Z. H. (2014) Mitochondrial trafficking and anchoring in neurons: New insight and implications. *J. Cell Biol.* **204**, 1087–1098

255. Burté, F., Carelli, V., Chinnery, P. F., and Yu-Wai-Man, P. (2015) Disturbed mitochondrial dynamics and neurodegenerative disorders. *Nat Rev Neurol.* **11**, 11–24

256. Cassereau, J., Casasnovas, C., Guegeun, N., Malinge, M. C., Guillet, V., Reynier, P., Bonneau, D., Amati-Bonneau, P., Banchs, I., Volpini, V., Procaccio, V., and

Chevrollier, A. (2011) Simultaneous MFN2 and GDAP1 mutations cause major mitochondrial defects in a patient with CMT. *Neurology* **76**, 1524–1526

257. Vital, A., Latour, P., Sole, G., Ferrer, X., Rouanet, M., Tison, F., Vital, C., and Goizet, C. (2012) A French family with Charcot-Marie-Tooth disease related to simultaneous heterozygous MFN2 and GDAP1 mutations. *Neuromuscul. Disord.* **22**, 735–741

258. Saporta, M. A., Dang, V., Volfson, D., Zou, B., Xie, X. S., Adebola, A., Liem, R. K., Shy, M., and Dimos, J. T. (2015) Axonal Charcot-Marie-Tooth disease patient-derived motor neurons demonstrate disease-specific phenotypes including abnormal electrophysiological properties. *Exp. Neurol.* **263**, 190–199

259. Brownlees, J., Ackerley, S., Grierson, A. J., Jacobsen, N. J. O., Shea, K., Anderton, B. H., Leigh, P. N., Shaw, C. E., and Miller, C. C. J. (2002) Charcot-Marie-Tooth disease neurofilament mutations disrupt neurofilament assembly and axonal transport. *Hum. Mol. Genet.* **11**, 2837–2844

260. Kim, J.-Y., Woo, S.-Y., Hong, Y. Bin, Choi, H., Kim, J., Choi, H., Mook-Jung, I., Ha, N., Kyung, J., Koo, S. K., Jung, S.-C., and Choi, B.-O. (2016) HDAC6 Inhibitors Rescued the Defective Axonal Mitochondrial Movement in Motor Neurons Derived from the Induced Pluripotent Stem Cells of Peripheral Neuropathy Patients with HSPB1 Mutation. *Stem Cells Int.* **2016**, 1–14

261. Shen, S., Benoy, V., Bergman, J. A., Kalin, J. H., Frojuello, M., Vistoli, G., Haeck, W., Van Den Bosch, L., and Kozikowski, A. P. (2016) Bicyclic-Capped Histone Deacetylase 6 Inhibitors with Improved Activity in a Model of Axonal Charcot-Marie-Tooth Disease. *ACS Chem. Neurosci.* **7**, 240–258

262. Benoy, V., Vanden Berghe, P., Jarpe, M., Van Damme, P., Robberecht, W., and Van Den Bosch, L. (2017) Development of Improved HDAC6 Inhibitors as Pharmacological Therapy for Axonal Charcot–Marie–Tooth Disease. *Neurotherapeutics* **14**, 417–428

263. Shen, S. and Kozikowski, A. P. (2016) Why Hydroxamates May Not Be the Best Histone Deacetylase Inhibitors - What Some May Have Forgotten or Would Rather Forget? *ChemMedChem* **11**, 15–21

264. Mata, M., Sun, X., and Fink, D. (2015) Regulation of Actin Interacting Protein Drebrin by Mutations in HSPB1. *FASEB J.* **29**

265. Haidar, M. and Timmerman, V. (2017) Autophagy as an Emerging Common Pathomechanism in Inherited Peripheral Neuropathies. *Front. Mol. Neurosci.* **10**,

1–17

266. Bouhy, D., Geuens, T., De Winter, V., Almeida-Souza, L., Katona, I., Weis, J., Hochepied, T., Goossens, S., Haigh, J. J., Janssens, S., and Timmerman, V. (2016) Characterization of New Transgenic Mouse Models for Two Charcot-Marie-Tooth-Causing HspB1 Mutations using the Rosa26 Locus. *J. Neuromuscul. Dis.* **3**, 183–200

267. Dierick, I., Irobi, J., Janssens, S., Theuns, J., Lemmens, R., Jacobs, A., Corsmit, E., Hersmus, N., Van Den Bosch, L., Robberecht, W., De Jonghe, P., Van Broeckhoven, C., and Timmerman, V. (2007) Genetic variant in theHSPB1 promoter region impairs the HSP27 stress response. *Hum. Mutat.* **28**, 830–830

268. Zhang, X., Shi, J., Tian, J., Robinson, A. C., Davidson, Y. S., and Mann, D. M. (2014) Expression of one important chaperone protein, heat shock protein 27, in neurodegenerative diseases. *Alzheimers. Res. Ther.* **6**, 78

269. Adriaenssens, E., Geuens, T., Baets, J., Echaniz-Laguna, A., and Timmerman, V. (2017) Novel insights in the disease biology of mutant small heat shock proteins in neuromuscular diseases. *Brain* 1–9

270. Tóth, M. E., Szegedi, V., Varga, E., Juhász, G., Horváth, J., Borbély, E., Csibrány, B., Alföldi, R., Lénárt, N., Penke, B., and Sántha, M. (2013) Overexpression of Hsp27 ameliorates symptoms of Alzheimer's disease in APP/PS1 mice. *Cell Stress Chaperones* **18**, 759–771

271. Zourlidou, A., Payne Smith, M. D., and Latchman, D. S. (2004) HSP27 but not HSP70 has a potent protective effect against α-synuclein-induced cell death in mammalian neuronal cells. *J. Neurochem.* **88**, 1439–1448

272. Outeiro, T. F., Klucken, J., Strathearn, K. E., Liu, F., Nguyen, P., Rochet, J.-C., Hyman, B. T., and McLean, P. J. (2006) Small heat shock proteins protect against alpha-synuclein-induced toxicity and aggregation. *Biochem. Biophys. Res. Commun.* **351**, 631–638

273. Wyttenbach, A., Sauvageot, O., Carmichael, J., Diaz-latoud, C., Arrigo, A., and Rubinsztein, D. C. (2002) Heat shock protein 27 prevents cellular polyglutamine toxicity and suppresses the increase of reactive oxygen species caused by huntingtin. **11**, 1137–1151

274. Perrin, V., Régulier, E., Abbas-Terki, T., Hassig, R., Brouillet, E., Aebischer, P., Luthi-Carter, R., and Déglon, N. (2007) Neuroprotection by Hsp104 and Hsp27 in Lentiviral-based Rat Models of Huntington's Disease. *Mol. Ther. J. Am. Soc.*

Gene Ther. **15**, 677–686

275. Zourlidou, A., Gidalevitz, T., Kristiansen, M., Landles, C., Woodman, B., Wells, D. J., Latchman, D. S., de Belleroche, J., Tabrizi, S. J., Morimoto, R. I., and Bates, G. P. (2007) Hsp27 overexpression in the R6/2 mouse model of Huntington's disease: Chronic neurodegeneration does not induce Hsp27 activation. *Hum. Mol. Genet.* **16**, 1078–1090

276. Krishnan, J., Vannuvel, K., Andries, M., Waelkens, E., Robberecht, W., and Van Den Bosch, L. (2008) Over-expression of Hsp27 does not influence disease in the mutant SOD1(G93A) mouse model of amyotrophic lateral sclerosis. *J. Neurochem.* **106**, 2170–2183

277. Irobi, J., Impe, K. Van, Seeman, P., Jordanova, A., Dierick, I., Verpoorten, N., Michalik, A., Vriendt, E. De, Jacobs, A., Gerwen, V. Van, Vennekens, K., Mazanec, R., Tournev, I., Hilton-Jones, D., Talbot, K., Kremensky, I., Bosch, L. Van Den, Robberecht, W., Vandekerckhove, J., Broeckhoven, C. Van, Gettemans, J., Jonghe, P. De, and Timmerman, V. (2004) Hot-spot residue in small heat-shock protein 22 causes distal motor neuropathy. *Nat. Genet.* **36**, 597–601

278. Tang, B.-S., Luo, W., Xia, K., Xiao, J.-F., Jiang, H., Shen, L., Tang, J.-G., Zhao, G.-H., Cai, F., Pan, Q., Dai, H.-P., Yang, Q.-D., Xia, J.-H., and Evgrafov, O. V. (2004) A new locus for autosomal dominant Charcot-Marie-Tooth disease type 2 (CMT2L) maps to chromosome 12q24. *Hum. Genet.* **114**, 527–533

279. Tang, B. S., Zhao, G. hua, Luo, W., Xia, K., Cai, F., Pan, Q., Zhang, R. xu, Zhang, F. feng, Liu, X. min, Chen, B., Zhang, C., Shen, L., Jiang, H., Long, Z. gao, and Dai, H. ping. (2005) Small heat-shock protein 22 mutated in autosomal dominant Charcot-Marie-Tooth disease type 2L. *Hum. Genet.* **116**, 222–224

280. Fontaine, J. M., Sun, X., Hoppe, A. D., Simon, S., Vicart, P., Welsh, M. J., and Benndorf, R. (2006) Abnormal small heat shock protein interactions involving neuropathy-associated HSP22 (HSPB8) mutants. *FASEB J.* **20**, 2168–2170

281. Irobi, J., Almeida-Souza, L., Asselbergh, B., de Winter, V., Goethals, S., Dierick, I., Krishnan, J., Timmermans, J. P., Robberecht, W., de Jonghe, P., van den Bosch, L., Janssens, S., and Timmerman, V. (2010) Mutant HSPB8 causes motor neuron-specific neurite degeneration. *Hum. Mol. Genet.* **19**, 3254–3265

282. Ito, H., Kamei, K., Iwamoto, I., Inaguma, Y., Tsuzuki, M., Kishikawa, M., Shimada, A., Hosokawa, M., and Kato, K. (2003) Hsp27 suppresses the formation of inclusion bodies induced by expression of R120G a B-crystallin , a cause of desmin- related myopathy. *Cell Mol. Life Sci.* **60**, 1217–1223

283. Raju, I. and Abraham, E. C. (2013) Biochemical and Biophysical Research Communications Mutants of human a B-crystallin cause enhanced protein aggregation and apoptosis in mammalian cells : Influence of co-expression of HspB1. *Biochem. Biophys. Res. Commun.* **430**, 107–112

284. Boncoraglio, A., Minoia, M., and Carra, S. (2012) The family of mammalian small heat shock proteins (HSPBs): Implications in protein deposit diseases and motor neuropathies. *Int. J. Biochem. Cell Biol.* **44**, 1657–1669

285. Datskevich, P. N., Nefedova, V. V, Sudnitsyna, M. V, and Gusev, N. B. (2012) Mutations of small heat shock proteins and human congenital diseases. *Biochemistry* **77**, 1500–5014

286. Benndorf, R., Martin, J. L., Kosakovsky Pond, S. L., and Wertheim, J. O. (2014) Neuropathy- and myopathy-associated mutations in human small heat shock proteins: Characteristics and evolutionary history of the mutation sites. *Mutat. Res. - Rev. Mutat. Res.* **761**, 15–30

287. Antonellis, A., Ellsworth, R. E., Sambuughin, N., Puls, I., Abel, A., Lee-Lin, S.-Q., Jordanova, A., Kremensky, I., Christodoulou, K., Middleton, L. T., Sivakumar, K., Ionasescu, V., Funalot, B., Vance, J. M., Goldfarb, L. G., Fischbeck, K. H., and Green, E. D. (2003) Glycyl tRNA Synthetase Mutations in Charcot-Marie-Tooth Disease Type 2D and Distal Spinal Muscular Atrophy Type V. *Am. J. Hum. Genet.* **72**, 1293–1299

288. Tradewell, M. L., Durham, H. D., Mushynski, W. E., and Gentil, B. J. (2009) Mitochondrial and Axonal Abnormalities Precede Disruption of the Neurofilament Network in a Model of Charcot-Marie-Tooth Disease Type 2E and Are Prevented by Heat Shock Proteins in a Mutant-Specific Fashion. *J Neuropathol Exp Neurol* **68**, 642–652

289. Cartoni, R. and Martinou, J.-C. (2009) Role of mitofusin 2 mutations in the physiopathology of Charcot-Marie-Tooth disease type 2A. *Exp. Neurol.* **218**, 268–273

290. Fleming, M. S., Vysochan, A., Paixão, S., Niu, J., Klein, R., Savitt, J. M., and Luo, W. (2015) Cis and trans RET signaling control the survival and central projection growth of rapidly adapting mechanoreceptors. *Elife* **2015**, 1–26

291. Dagda, R. K., Cherra, S. J., Kulich, S. M., Tandon, A., Park, D., and Chu, C. T. (2009) Loss of PINK1 function promotes mitophagy through effects on oxidative stress and mitochondrial fission. *J. Biol. Chem.* **284**, 13843–13855

292. Bielawski, J., Szulc, Z. M., Hannun, Y. A., and Bielawska, A. (2006) Simultaneous quantitative analysis of bioactive sphingolipids by high-performance liquid chromatography-tandem mass spectrometry. *Methods* **39**, 82–91

293. Yuan, M., Breitkopf, S. B., Yang, X., and Asara, J. M. (2012) A positive/negative ion-switching, targeted mass spectrometry-based metabolomics platform for bodily fluids, cells, and fresh and fixed tissue. *Nat. Protoc.* **7**, 872–881

294. Hernández-Corbacho, M. J., Canals, D., Adada, M. M., Liu, M., Senkal, C. E., Yi, J. K., Mao, C., Luberto, C., Hannun, Y. A., and Obeid, L. M. (2015) Tumor necrosis factor-α (TNFα)-induced ceramide generation via ceramide synthases regulates loss of focal adhesion kinase (FAK) and programmed cell death. *J. Biol. Chem.* **290**, 25356–25373

295. Harel, T. and Lupski, J. R. (2014) Charcot-Marie-Tooth disease and pathways to molecular based therapies. *Clin. Genet.* **86**, 422–431

296. Haslbeck, M., Franzmann, T., Weinfurtner, D., and Buchner, J. (2005) Some like it hot: the structure and function of small heat-shock proteins. *Nat. Struct. Mol. Biol.* **12**, 842–846

297. Akbar, M. T., Lundberg, A. M. C., Liu, K., Vidyadaran, S., Wells, K. E., Dolatshad, H., Wynn, S., Wells, D. J., Latchman, D. S., and de Belleroche, J. (2003) The neuroprotective effects of heat shock protein 27 overexpression in transgenic animals against kainate-induced seizures and hippocampal cell death. *J. Biol. Chem.* **278**, 19956–19965

298. Teramoto, S., Shimura, H., Tanaka, R., Shimada, Y., Miyamoto, N., Arai, H., Urabe, T., and Hattori, N. (2013) Human-derived physiological heat shock protein 27 complex protects brain after focal cerebral ischemia in mice. *PLoS One* **8**, e66001

299. Smith, H. L., Li, W., and Cheetham, M. E. (2015) Molecular chaperones and neuronal proteostasis. *Semin. Cell Dev. Biol.* **40**, 142–152

300. Sharp, P. S., Akbar, M. T., Bouri, S., Senda, A., Joshi, K., Chen, H.-J., Latchman, D. S., Wells, D. J., and de Belleroche, J. (2008) Protective effects of heat shock protein 27 in a model of ALS occur in the early stages of disease progression. *Neurobiol. Dis.* **30**, 42–55

301. Mullen, T. D., Hannun, Y. a, and Obeid, L. M. (2012) Ceramide synthases at the centre of sphingolipid metabolism and biology. *Biochem. J.* **441**, 789–802

302. Pewzner-Jung, Y., Ben-Dor, S., and Futerman, A. H. (2006) When do Lasses (longevity assurance genes) become CerS (ceramide synthases)?: Insights into the regulation of ceramide synthesis. *J. Biol. Chem.* **281**, 25001–25005

303. Lee, H., Rotolo, J. a, Mesicek, J., Penate-Medina, T., Rimner, A., Liao, W.-C., Yin, X., Ragupathi, G., Ehleiter, D., Gulbins, E., Zhai, D., Reed, J. C., Haimovitz-Friedman, A., Fuks, Z., and Kolesnick, R. (2011) Mitochondrial ceramide-rich macrodomains functionalize Bax upon irradiation. *PLoS One* **6**, e19783

304. Sridevi, P., Alexander, H., Laviad, E. L., Min, J., Mesika, A., Hannink, M., Futerman, A. H., and Alexander, S. (2010) Stress-induced ER to Golgi translocation of ceramide synthase 1 is dependent on proteasomal processing. *Exp. Cell Res.* **316**, 78–91

305. Morell, P. and Radin, N. S. (1970) Specificity in Ceramide Biosynthesis from Long Chain Bases and Various Fatty Acyl Coenzyme A's by Brain Microsomes. *J. Biol. Chem.* **245**, 342–350

306. Hirschberg, K., Rodger, J., and Futerman, A. H. (1993) The long-chain sphingoid base of sphingolipids is acylated at the cytosolic surface of the endoplasmic reticulum in rat liver. *Biochem. J.* **290**, 751–757

307. Sanderson, T. H., Raghunayakula, S., and Kumar, R. (2015) Release of Mitochondrial Opa1 following Oxidative Stress in HT22 cells. *Mol. Cell. Neurosci.* **64**, 116–122

308. Liu, J., Li, L., and Suo, W. Z. (2009) HT22 hippocampal neuronal cell line possesses functional cholinergic properties. *Life Sci.* **84**, 267–271

309. Neusch, C., Senderek, J., Eggermann, T., Elolff, E., Bähr, M., and Schneider-Gold, C. (2007) Mitofusin 2 gene mutation (R94Q) causing severe early-onset axonal polyneuropathy (CMT2A). *Eur. J. Neurol.* **14**, 575–577

310. Züchner, S., Mersiyanova, I. V, Muglia, M., Bissar-Tadmouri, N., Rochelle, J., Dadali, E. L., Zappia, M., Nelis, E., Patitucci, A., Senderek, J., Parman, Y., Evgrafov, O., Jonghe, P. De, Takahashi, Y., Tsuji, S., Pericak-Vance, M. a, Quattrone, A., Battaloglu, E., Polyakov, A. V, Timmerman, V., Schröder, J. M., and Vance, J. M. (2004) Mutations in the mitochondrial GTPase mitofusin 2 cause Charcot-Marie-Tooth neuropathy type 2A. *Nat. Genet.* **36**, 449–451

311. Detmer, S. A., Velde, C. Vande, Cleveland, D. W., and Chan, D. C. (2008) Hindlimb gait defects due to motor axon loss and reduced distal muscles in a transgenic mouse model of Charcot - Marie - Tooth type 2A. *Hum. Mol. Genet.*

17, 367–375

312. Strickland, A. V., Rebelo, A. P., Zhang, F., Price, J., Bolon, B., Silva, J. P., Wen, R., and Z??chner, S. (2014) Characterization of the mitofusin 2 R94W mutation in a knock-in mouse model. *J. Peripher. Nerv. Syst.* **19**, 152–164

313. Min, J., Mesika, A., Sivaguru, M., Van Veldhoven, P. P., Alexander, H., Futerman, A. H., and Alexander, S. (2007) (Dihydro)ceramide synthase 1 regulated sensitivity to cisplatin is associated with the activation of p38 mitogen-activated protein kinase and is abrogated by sphingosine kinase 1. *Mol. Cancer Res.* **5**, 801–812

314. Bionda, C., Portoukalian, J., Schmitt, D., Rodriguez-Lafrasse, C., and Ardail, D. (2004) Subcellular compartmentalization of ceramide metabolism: MAM (mitochondria-associated membrane) and/or mitochondria? *Biochem. J.* **382**, 527–533

315. Sundaram, K., Mather, A. R., Marimuthu, S., Shah, P. P., Snider, A. J., Obeid, L. M., Hannun, Y. A., Beverly, L. J., and Siskind, L. J. (2016) Loss of neutral ceramidase protects cells from nutrient and energy deprivation-induced cell death. *Biochem. J.* **473**, 743–755

316. Lee, J., Giordano, S., and Zhang, J. (2012) Autophagy, mitochondria and oxidative stress: cross-talk and redox signalling. *Harv. Bus. Rev.* **441**, 523–540

317. Shen, L., Qi, Z., Zhu, Y., Song, X., Xuan, C., Ben, P., Lan, L., Luo, L., and Yin, Z. (2016) Phosphorylated heat shock protein 27 promotes lipid clearance in hepatic cells through interacting with STAT3 and activating autophagy. *Cell. Signal.* **28**, 1086–1098

318. Chen, R., Dai, R., Duan, C., Liu, Y., Chen, S., Yan, D., Chen, C., Wei, M., and Li, H. (2011) Unfolded protein response suppresses cisplatin-induced apoptosis via autophagy regulation in human hepatocellular carcinoma cells. *Folia Biol. (Praha).* **57**, 87–95

319. Matsumoto, T., Urushido, M., Ide, H., Ishihara, M., Hamada-Ode, K., Shimamura, Y., Ogata, K., Inoue, K., Taniguchi, Y., Taguchi, T., Horino, T., Fujimoto, S., and Terada, Y. (2015) Small heat shock protein beta-1 (HSPB1) is upregulated and regulates autophagy and apoptosis of renal tubular cells in acute kidney injury. *PLoS One* **10**, 1–22

320. Jove, M., Portero-Otin, M., Naudi, A., Ferrer, I., and Pamplona, R. (2014) Metabolomics of human brain aging and age-related neurodegenerative diseases.

J. Neuropathol. Exp. Neurol. **73**, 640–657

321. Bais, P., Beebe, K., Morelli, K. H., Currie, M. E., Norberg, S. N., Evsikov, A. V., Miers, K. E., Seburn, K. L., Guergueltcheva, V., Kremensky, I., Jordanova, A., Bult, C. J., and Burgess, R. W. (2016) Metabolite profile of a mouse model of Charcot–Marie–Tooth type 2D neuropathy: implications for disease mechanisms and interventions. *Biol. Open* **5**, 908–920

322. Laviad, E. L., Kellys, S., Merrill, A. H., and Futerman, A. H. (2012) Modulation of ceramide synthase activity via dimerization. *J. Biol. Chem.* **287**, 21025–21033

323. Jimenez-Rojo, N., Sot, J., Busto, J. V., Shaw, W. A., Duan, J., Merrill, A. H., Alonso, A., and Goni, F. M. (2014) Biophysical Properties of Novel 1-Deoxy-(Dihydro)ceramides Occurring in Mammalian Cells. *Biophys. J.* **107**, 2850–2859

324. Pruett, S. T., Bushnev, A., Hagedorn, K., Adiga, M., Haynes, C. a, Sullards, M. C., Liotta, D. C., and Merrill, A. H. (2008) Biodiversity of sphingoid bases ("sphingosines") and related amino alcohols. *J. Lipid Res.* **49**, 1621–1639

325. Henriquez-Henriquez, M. P., Solari, S., Quiroga, T., Kim, B. I., Deckelbaum, R. J., and Worgall, T. S. (2015) Low serum sphingolipids in children with attention deficit-hyperactivity disorder. *Front. Neurosci.* **9**, 1–9

326. Kramer, R., Bielawski, J., Kistner-Griffin, E., Othman, A., Alecu, I., Ernst, D., Kornhauser, D., Hornemann, T., and Spassieva, S. (2015) Neurotoxic 1-deoxysphingolipids and paclitaxel-induced peripheral neuropathy. *FASEB J.* **29**, 4461–4472

327. Güntert, T., Hänggi, P., Othman, A., Suriyanarayanan, S., Sonda, S., Zuellig, R. A., Hornemann, T., and Ogunshola, O. O. (2016) 1-Deoxysphingolipid-induced neurotoxicity involves N-methyl-D-aspartate receptor signaling. *Neuropharmacology* **110**, 211–222

328. Bertea, M., Rütti, M. F., Othman, A., Marti-Jaun, J., Hersberger, M., von Eckardstein, A., and Hornemann, T. (2010) Deoxysphingoid bases as plasma markers in diabetes mellitus. *Lipids Health Dis.* **9**, 84

329. Siddique, M. M., Li, Y., Wang, L., Ching, J., Mal, M., Ilkayeva, O., Wu, Y. J., Bay, B. H., and Summers, S. A. (2013) Ablation of Dihydroceramide Desaturase 1, a Therapeutic Target for the Treatment of Metabolic Diseases, Simultaneously Stimulates Anabolic and Catabolic Signaling. *Mol. Cell. Biol.* **33**, 2353–2369

330. Mielke, M. M., Bandaru, V. V. R., Haughey, N. J., Xia, J., Fried, L. P., Yasar, S.,

Albert, M., Varma, V., Harris, G., Schneider, E. B., Rabins, P. V, Bandeen-Roche, K., Lyketsos, C. G., and Carlson, M. C. (2012) Serum ceramides increase the risk of Alzheimer disease: The Women's Health and Aging Study II. *Neurology* **79**, 633–641

331. Piccinini, M., Scandroglio, F., Prioni, S., Buccinnà, B., Loberto, N., Aureli, M., Chigorno, V., Lupino, E., DeMarco, G., Lomartire, A., Rinaudo, M. T., Sonnino, S., and Prinetti, A. (2010) Deregulated sphingolipid metabolism and membrane organization in neurodegenerative disorders. *Mol. Neurobiol.* **41**, 314–340

332. Patwardhan, G. A., Beverly, L. J., and Siskind, L. J. (2016) Sphingolipids and mitochondrial apoptosis. *J. Bioenerg. Biomembr.* **48**, 153–168

333. Novgorodov, S. a, Gudz, T. I., and Obeid, L. M. (2008) Long-chain ceramide is a potent inhibitor of the mitochondrial permeability transition pore. *J. Biol. Chem.* **283**, 24707–24717

334. Venkataraman, K. and Futerman, A. H. (2002) Do longevity assurance genes containing Hox domains regulate cell development via ceramide synthesis? *FEBS Lett.* **528**, 3–4

335. Mesika, A., Ben-Dor, S., Laviad, E. L., and Futerman, A. H. (2007) A new functional motif in hox domain-containing ceramide synthases: Identification of a novel region flanking the hox and TLC domains essential for activity. *J. Biol. Chem.* **282**, 27366–27373

336. Tirodkar, T. S., Lu, P., Bai, A., Scheffel, M. J., Gencer, S., Garrett-Mayer, E., Bielawska, A., Ogretmen, B., and Voelkel-Johnson, C. (2015) Expression of ceramide synthase 6 transcriptionally activates acid ceramidase in a c-Jun N-terminal Kinase (JNK)-dependent manner. *J. Biol. Chem.* **290**, 13157–13167

337. Xie, W. and Chung, K. K. K. (2012) Alpha-synuclein impairs normal dynamics of mitochondria in cell and animal models of Parkinson's disease. *J. Neurochem.* **122**, 404–414

338. Rodríguez, G. E., González, D. M. C., Monachelli, G. M. G., López, J. J., Nicola, A. F. De, and Sica, R. E. P. (2011) Morphological abnormalities in mitochondria of the skin of patients with sporadic amyotrophic lateral sclerosis. *Arq Neuropsiquiatr* **70**, 45–51

339. Angelin, A., Tiepolo, T., Sabatelli, P., Grumati, P., Bergamin, N., Golfieri, C., Mattioli, E., Gualandi, F., Ferlini, A., Merlini, L., Maraldi, N. M., Bonaldo, P., and Bernardi, P. (2007) Mitochondrial dysfunction in the pathogenesis of Ullrich

congenital muscular dystrophy and prospective therapy with cyclosporins. *Proc. Natl. Acad. Sci. U. S. A.* **104**, 991–996

340. Lee, S. M., Olzmann, J. A., Chin, L.-S., and Li, L. (2011) Mutations associated with Charcot-Marie-Tooth disease cause SIMPLE protein mislocalization and degradation by the proteasome and aggresome-autophagy pathways. *J. Cell Sci.* **124**, 3319–3331

341. Bouhy, D. and Timmerman, V. (2013) Animal models and therapeutic prospects for Charcot-Marie-Tooth disease. *Ann. Neurol.* **74**, 391–396

342. Patassini, S., Begley, P., Reid, S. J., Xu, J., Church, S. J., Curtis, M., Dragunow, M., Waldvogel, H. J., Unwin, R. D., Snell, R. G., Faull, R. L. M., and Cooper, G. J. S. (2015) Identification of elevated urea as a severe, ubiquitous metabolic defect in the brain of patients with Huntington's disease. *Biochem. Biophys. Res. Commun.* **468**, 161–166

343. Rossignol, D. A. and Frye, R. E. (2012) Mitochondrial dysfunction in autism spectrum disorders: a systematic review and meta-analysis. *Mol. Psychiatry* **17**, 290–314

344. Wernstedt Asterholm, I., Mundy, D. I., Weng, J., Anderson, R. G. W., and Scherer, P. E. (2012) Altered mitochondrial function and metabolic inflexibility associated with loss of caveolin-1. *Cell Metab.* **15**, 171–185

345. Metallo, C. M., Gameiro, P. A., Bell, E. L., Mattaini, K. R., Yang, J., Hiller, K., Jewell, C. M., Johnson, Z. R., Irvine, D. J., Guarente, L., Kelleher, J. K., Heiden, M. G. Vander, Iliopoulos, O., and Stephanopoulos, G. (2011) Reductive glutamine metabolism by IDH1 mediates lipogenesis under hypoxia. *Nature* **481**, 380–384

346. Mullen, A. R., Wheaton, W. W., Jin, E. S., Chen, P.-H., Sullivan, L. B., Cheng, T., Yang, Y., Linehan, W. M., Chandel, N. S., and DeBerardinis, R. J. (2012) Reductive carboxylation supports growth in tumour cells with defective mitochondria. *Nature* **481**, 385–388

347. Steiner, R., Saied, E. M., Othman, A., Arenz, C., Maccarone, A. T., Poad, B. L. J., Blanksby, S. J., von Eckardstein, A., and Hornemann, T. (2016) Elucidating the chemical structure of native 1-deoxysphingosine. *J. Lipid Res.* **57**, 1194–1203

348. Huang, S., Cheng, T.-Y., Young, D. C., Layre, E., Madigan, C. A., Shires, J., Cerundolo, V., Altman, J. D., and Moody, D. B. (2011) Discovery of deoxyceramides and diacylglycerols as CD1b scaffold lipids among diverse groove-blocking lipids of the human CD1 system. *Proc. Natl. Acad. Sci. U. S. A.*

108, 19335–19340

349. Jun, B. K., Chandra, A., Kuljis, D., Schmidt, B. P., and Eichler, F. S. (2015) Substrate Availability of Mutant SPT Alters Neuronal Branching and Growth Cone Dynamics in Dorsal Root Ganglia. *J. Neurosci.* **35**, 13713–13719

350. Wei, N., Pan, J., Pop-Busui, R., Othman, A., Alecu, I., Hornemann, T., and Eichler, F. S. (2014) Altered sphingoid base profiles in type 1 compared to type 2 diabetes. *Lipids Health Dis.* **13**, 161

351. Othman, A., Rütti, M. F., Ernst, D., Saely, C. H., Rein, P., Drexel, H., Porretta-Serapiglia, C., Lauria, G., Bianchi, R., von Eckardstein, A., and Hornemann, T. (2012) Plasma deoxysphingolipids: a novel class of biomarkers for the metabolic syndrome? *Diabetologia* **55**, 421–431

352. Hammad, S. M., Baker, N. L., El Abiad, J. M., Spassieva, S. D., Pierce, J. S., Rembiesa, B., Bielawski, J., Lopes-Virella, M. F., and Klein, R. L. (2016) Increased Plasma Levels of Select Deoxy-ceramide and Ceramide Species are Associated with Increased Odds of Diabetic Neuropathy in Type 1 Diabetes: A Pilot Study. *NeuroMolecular Med.*

353. Salcedo, M., Cuevas, C., Alonso, J. L., Otero, G., Faircloth, G., Fernandez-Sousa, J. M., Avila, J., and Wandosell, F. (2007) The marine sphingolipid-derived compound ES 285 triggers an atypical cell death pathway. *Apoptosis* **12**, 395–409

354. Sánchez, A. M., Malagarie-Cazenave, S., Olea, N., Vara, D., Cuevas, C., and Díaz-Laviada, I. (2008) Spisulosine (ES-285) induces prostate tumor PC-3 and LNCaP cell death by de novo synthesis of ceramide and PKCζ activation. *Eur. J. Pharmacol.* **584**, 237–245

355. Baird, R. D., Kitzen, J., Clarke, P. A., Planting, A., Reade, S., Reid, A., Welsh, L., Lopez Lazaro, L., de las Heras, B., Judson, I. R., Kaye, S. B., Eskens, F., Workman, P., deBono, J. S., and Verweij, J. (2009) Phase I safety, pharmacokinetic, and pharmacogenomic trial of ES-285, a novel marine cytotoxic agent, administered to adult patients with advanced solid tumors. *Mol. Cancer Ther.* **8**, 1430–1437

356. Massard, C., Salazar, R., Armand, J. P., Majem, M., Deutsch, E., García, M., Oaknin, A., Fernndez-García, E. M., Soto, A., and Soria, J. C. (2012) Phase i dose-escalating study of ES-285 given as a three-hour intravenous infusion every three weeks in patients with advanced malignant solid tumors. *Invest. New Drugs* **30**, 2318–2326

357. Schöffski, P., Dumez, H., Ruijter, R., Miguel-Lillo, B., Soto-Matos, A., Alfaro, V., and Giaccone, G. (2011) Spisulosine (ES-285) given as a weekly three-hour intravenous infusion: Results of a phase i dose-escalating study in patients with advanced solid malignancies. *Cancer Chemother. Pharmacol.* **68**, 1397–1403

358. Vilar, E., Grünwald, V., Schöffski, P., Singer, H., Salazar, R., Iglesias, J. L., Casado, E., Cullell-Young, M., Baselga, J., and Tabernero, J. (2012) A phase I dose-escalating study of ES-285, a marine sphingolipid-derived compound, with repeat dose administration in patients with advanced solid tumors. *Invest. New Drugs* **30**, 299–305

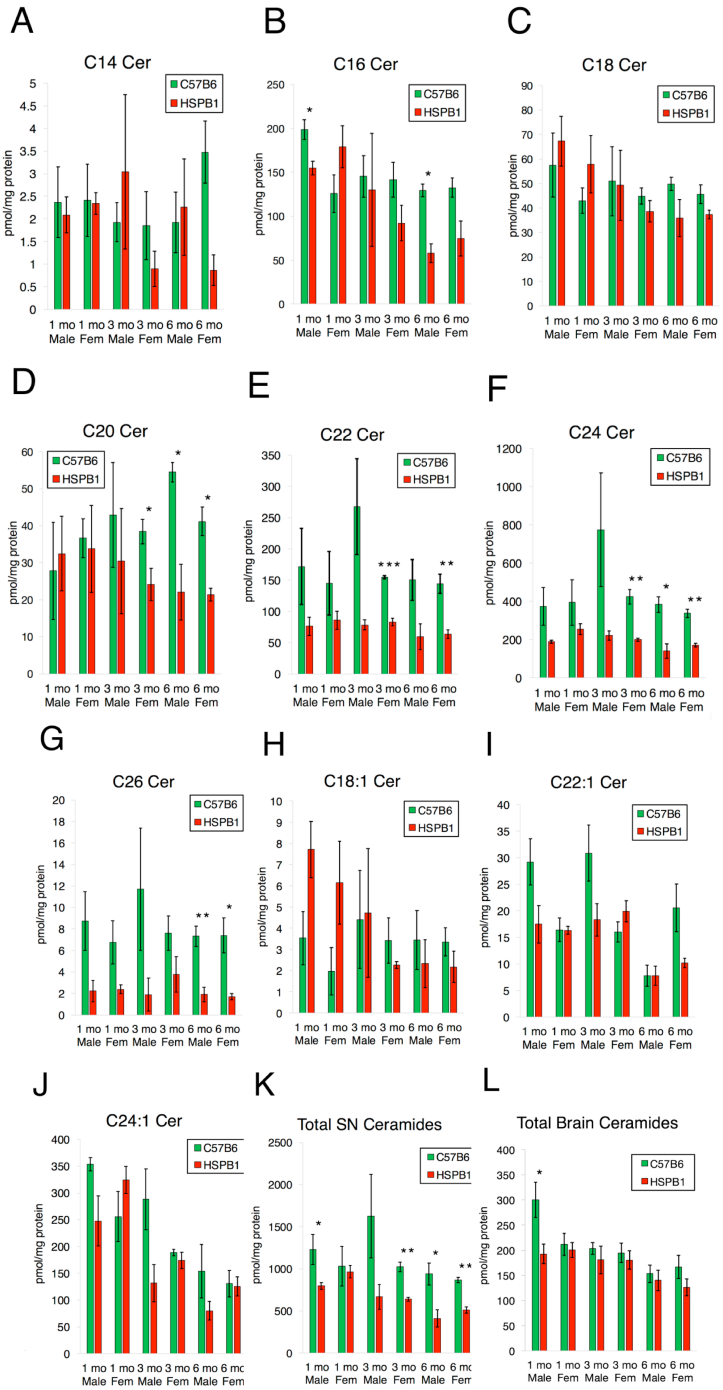

Figure 1. Decreased ceramides in Hsp27 KO sciatic nerve tissue.

(A-J) Sciatic nerve tissue from mice was homogenized and used for lipid measurements with LC/MS. C14, C16, C18, C20, C22, C24, C26, C18:1, C22:1, and C24:1 ceramides are shown, respectively (n=3). *(K-L)* Total ceramide levels from sciatic nerve and brain tissue (n=3) (*$P < 0.05$; ** $P < 0.01$; *** $P < 0.001$).

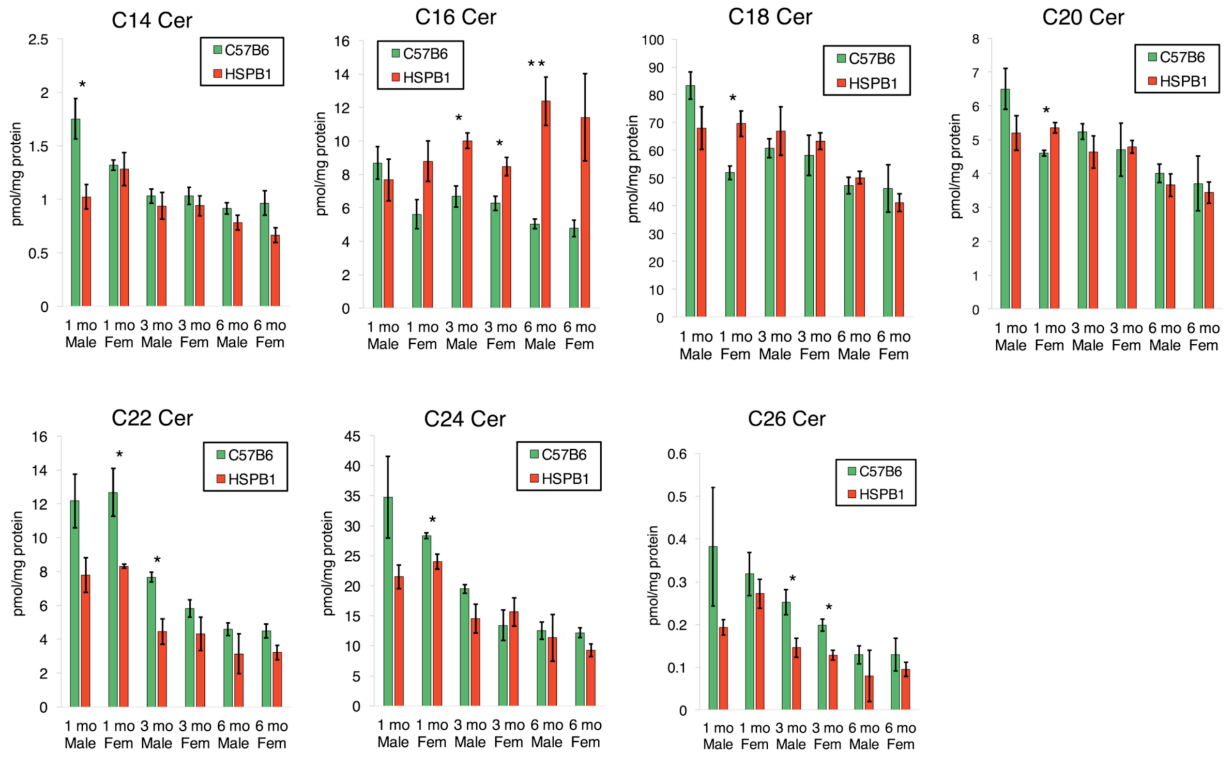

Figure 2. Ceramides are largely not altered in Hsp27 KO mouse brain.

Unlike sciatic nerve tissue, decreased species at old age are not observed.

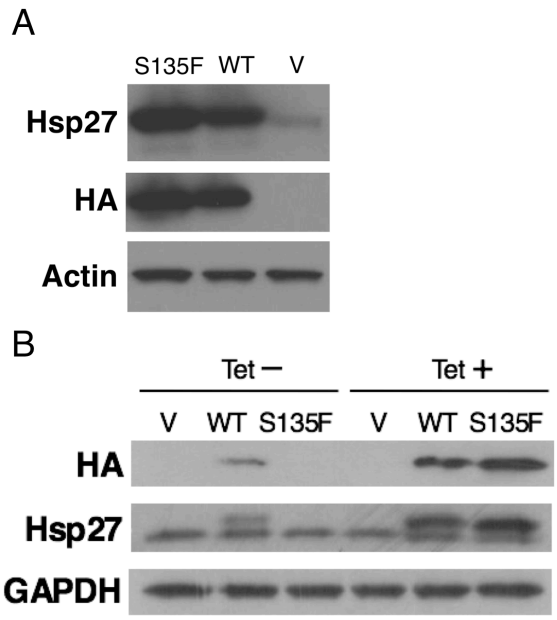

Figure 3. Wild-type and Mutant Hsp27 Expression in Cell Lines

(A) HT-22 transient transfection demonstrates high levels of expression in cells transfected with WT and S135F Hsp27 by Hsp27 and HA-tag antibodies. Relatively low levels of endogenous Hsp27 can be seen in the Vector condition using Hsp27 antibody. *(B)* HCT-116 cells transfected with pcDNA4/TO/myc-HisA vectors expressing wild-type (WT) Hsp27, the S135F, R136W, and P182L mutant Hsp27s, or control vector. The HA tag and linker add 2 kDa to the size of the endogenous protein.

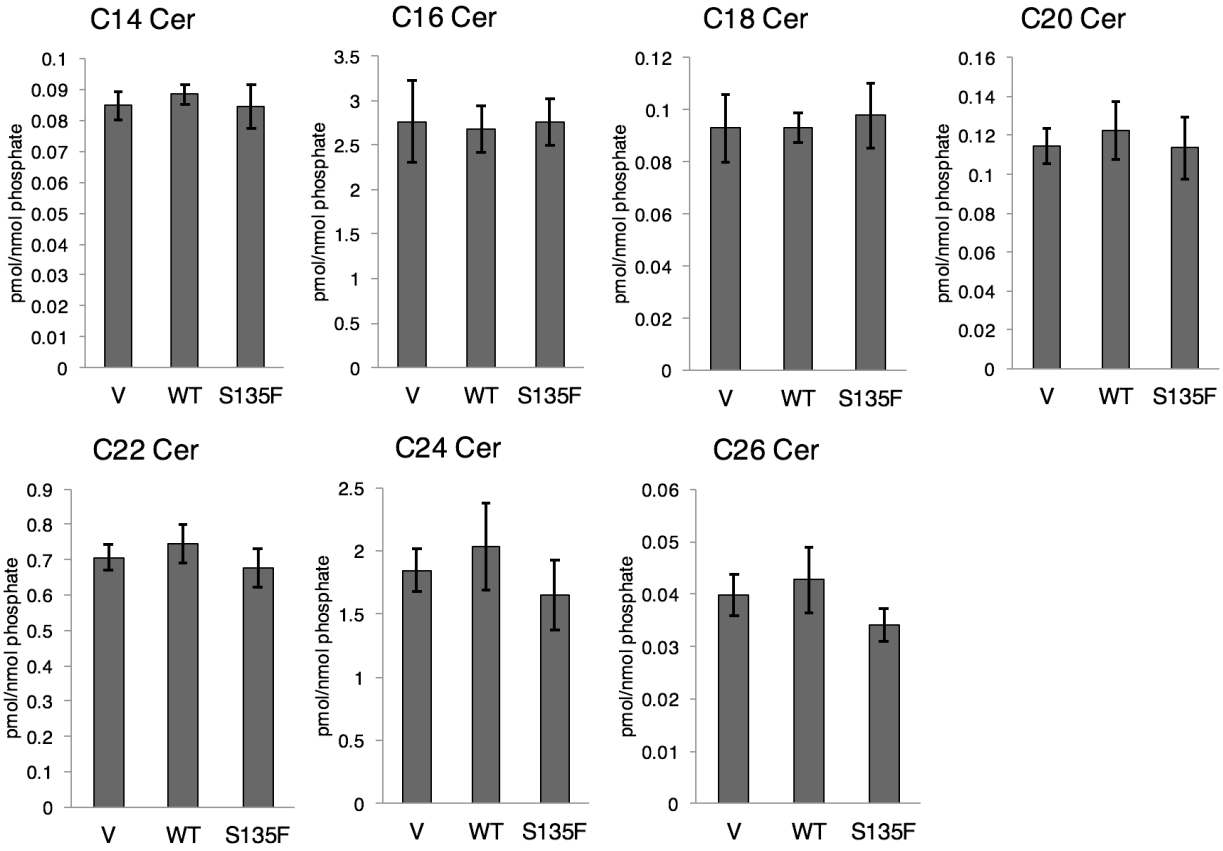

Figure 4. S135F mutation does not cause altered ceramide levels in HT-22 cells (n=3).

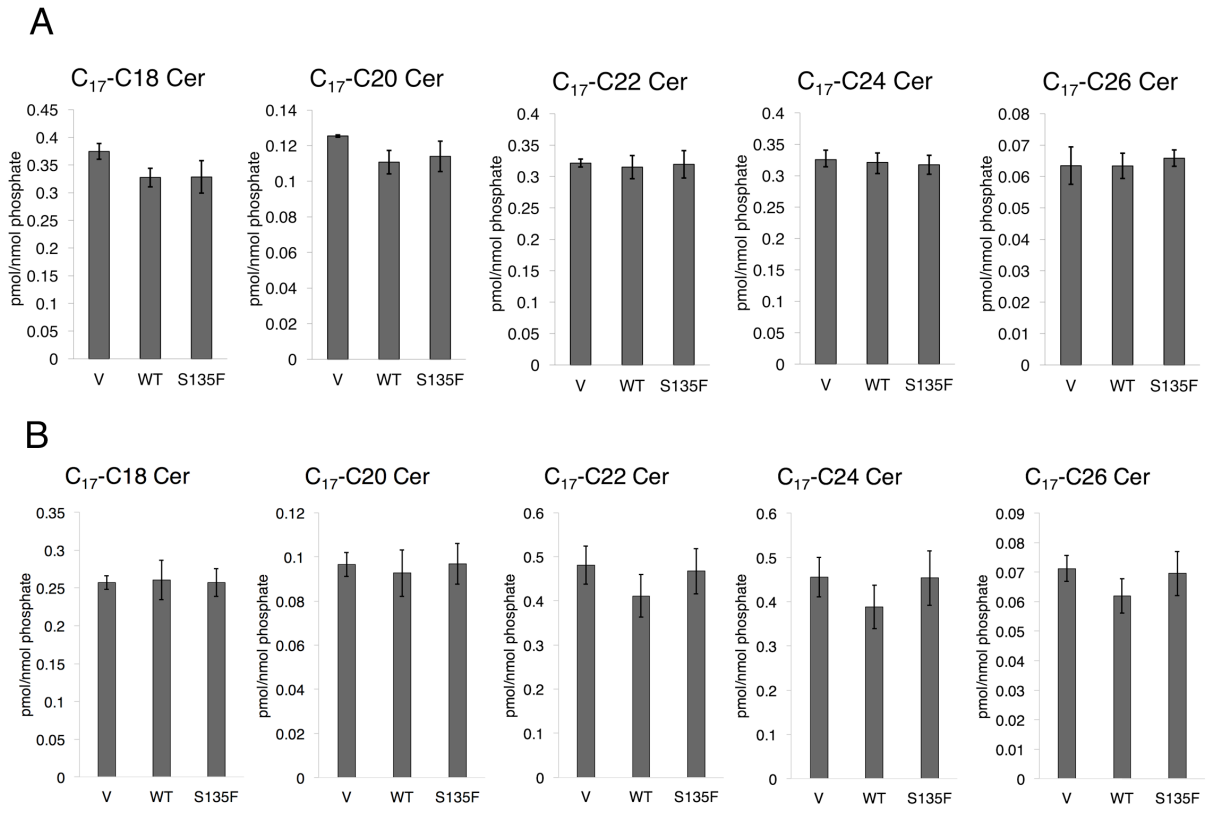

Figure 5. Ceramide synthase activity is not transiently altered via C_{17}-sphingosine labeling assay.

(A) Transient transfection of vector, WT Hsp27, and S135F Hsp27 does not alter ceramide synthase activity (n=3). *(B)* Stable transfections vector, WT Hsp27, and S135F Hsp27 does not alter ceramide synthase activity in S135F compared to WT (n=7).

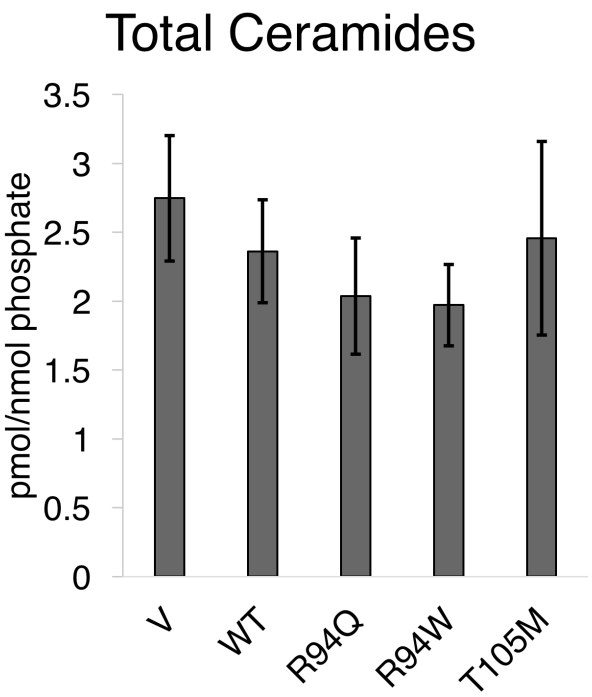

Figure 6. Total ceramide levels are not altered by CMT2A mutations.

Three mutations known to cause CMT2A were transiently transfected in HT-22 cells and sphingolipids were measured. No detection in total ceramides was observed (n=3).

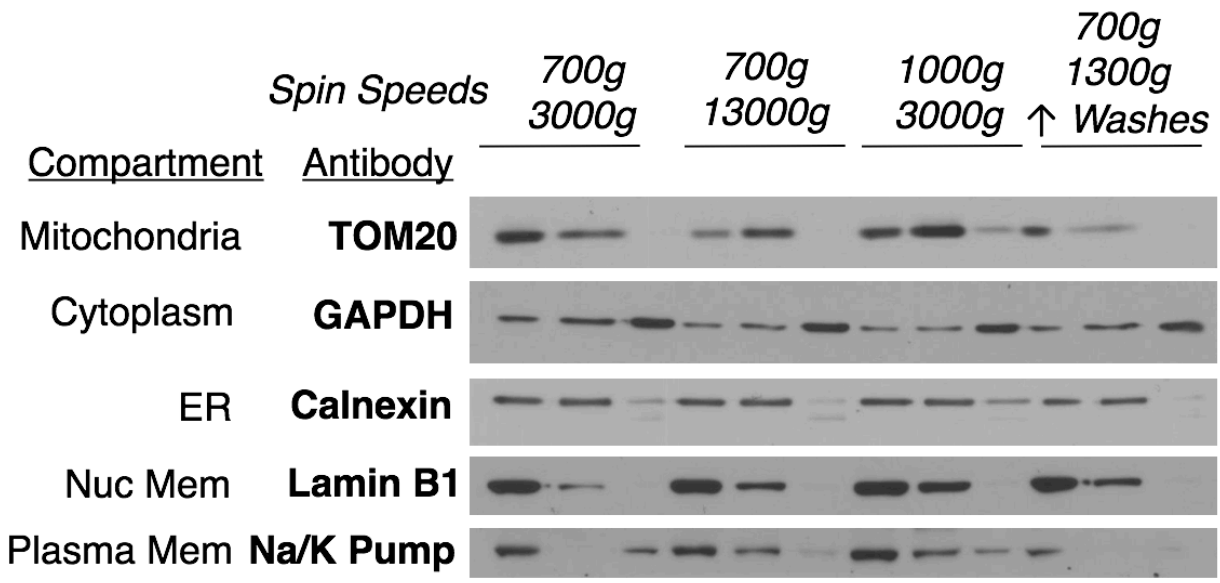

Figure 7. Subcellular Fractionation Optimization for Mitochondria.

Crude mitochondrial purification preparations analyzed by Western blot to evaluate purification quality. Preparations were performed with subsequent 1000g and 3000g spins to increase purity.

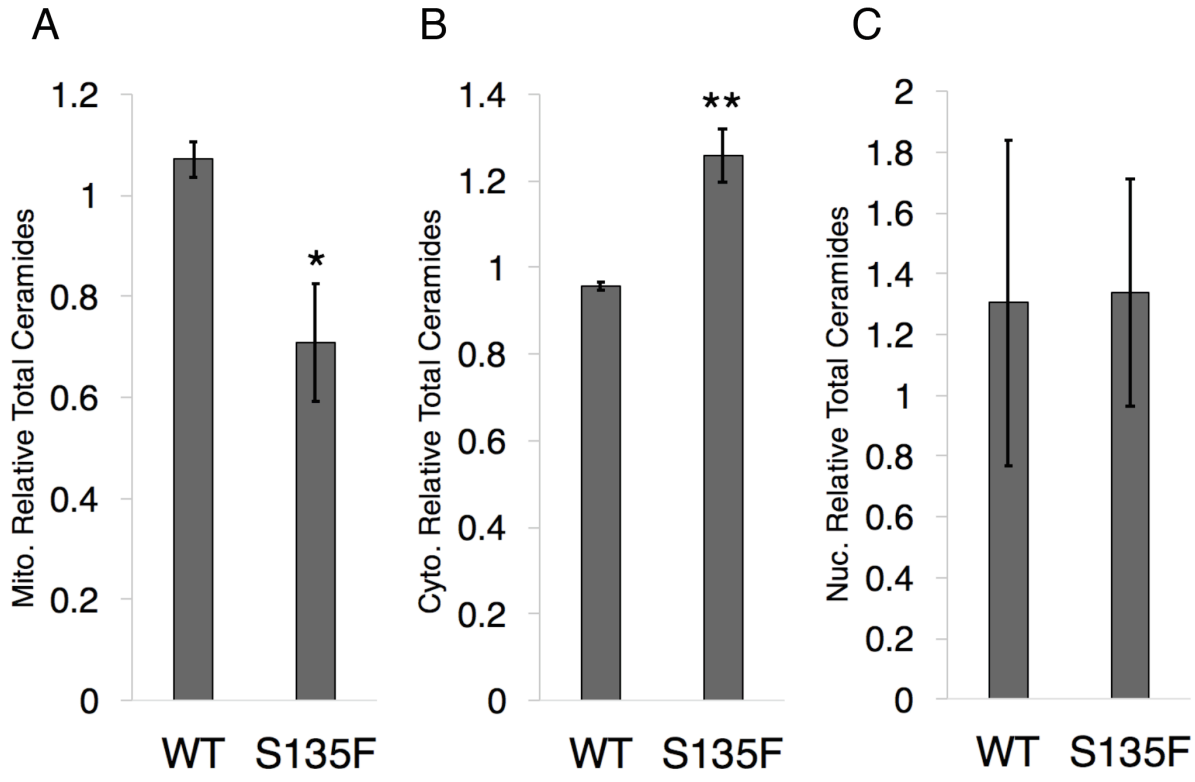

Figure 8. Decreased mitochondrial ceramides in S135F mutant HT-22 cells.

(A-C) Mitochondrial, cytoplasmic, and nuclear fractions of HT-22 cells were isolated and used for lipid measurements with LC/MS. Mitochondrial fractions demonstrate reduced total ceramide (*$P < 0.05$, n=4), cytoplasmic fractions with increased total ceramide, (**$P < 0.01$, n=4) and there is no change in nuclear ceramides ($P = 0.95$, n=4).

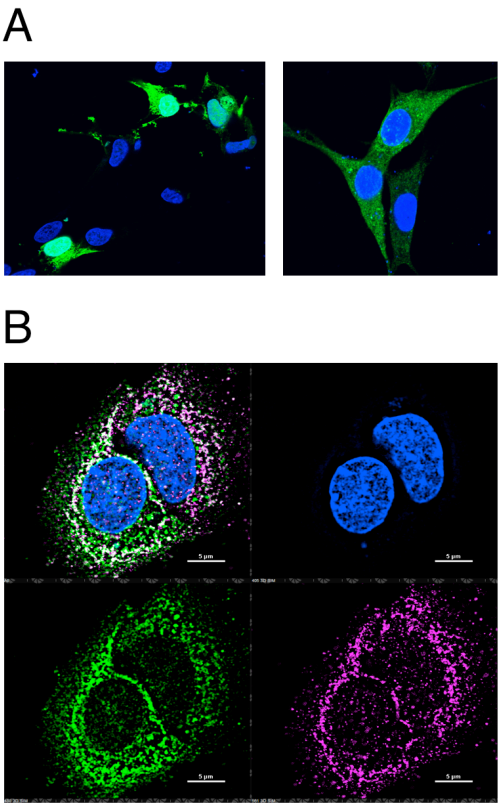

Figure 9. Successful transfection of HT-22 cells and dorsal root ganglia.

(A) Representative images of HT-22 transfection with eGFP. *(B)* Representative image of DRG transfection with eGFP (green) with TrpV1 (purple).

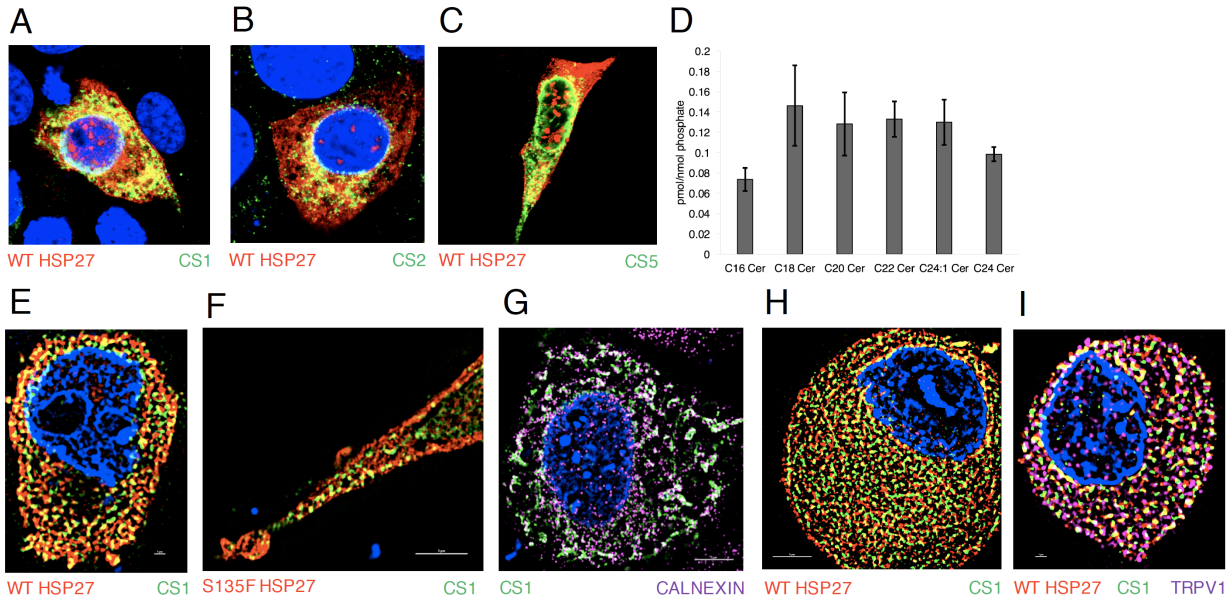

Figure 10. Hsp27:CerS1 interaction localizes to the endoplasmic reticulum.

(A-C) WT Hsp27 (red) co-localizes with FLAG-tagged CerS1, CerS2, and CerS5, respectively, (green) in HT-22 cells by confocal microscopy. (*D)* Ceramide profile from DRGs cultured for 4 days from 7 month female mice (n=3). (*E-F)* WT and S135F Hsp27 (red), respectively, co-localize with FLAG-tagged CerS1(green) in HT-22 cells by SIM microscopy. (*G)* FLAG-tagged CerS1 (green) and calnexin (pink) strongly co-localize. *(H)* Endogenous WT-Hsp27 (red) and anti-CerS1 (green) co-localize in mouse dorsal root ganglia (DRG). *(I)* Electroporated S135F Hsp27 (red) and FLAG-tagged CerS1 (green) co-localize in mouse DRG cells. Confirmation of neuronal identity with TrpV1 (pink).

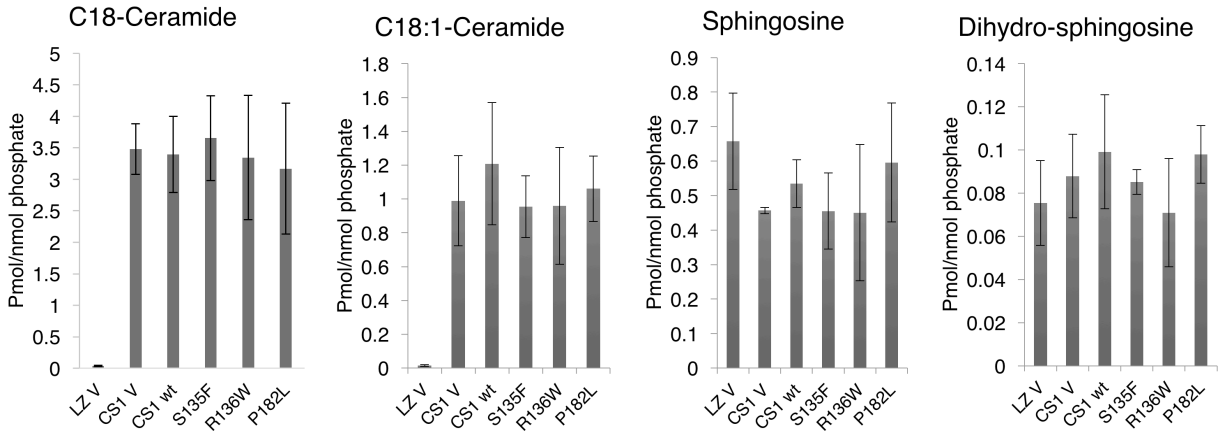

Figure 11. CerS1 overexpression increases C18 and C18:1 ceramides.

Tetracycline-induced overexpression of CerS1 causes a dramatic increase in C18-ceramide and C18:1-ceramide in HCT-116 cells. C18 and C18:1 sphingomyelins are also increased (data not shown), while other ceramide species are generally decreased (data not shown). S135F, R136W, and P182L mutations do not induce a change in ceramide or sphingomyelin levels.

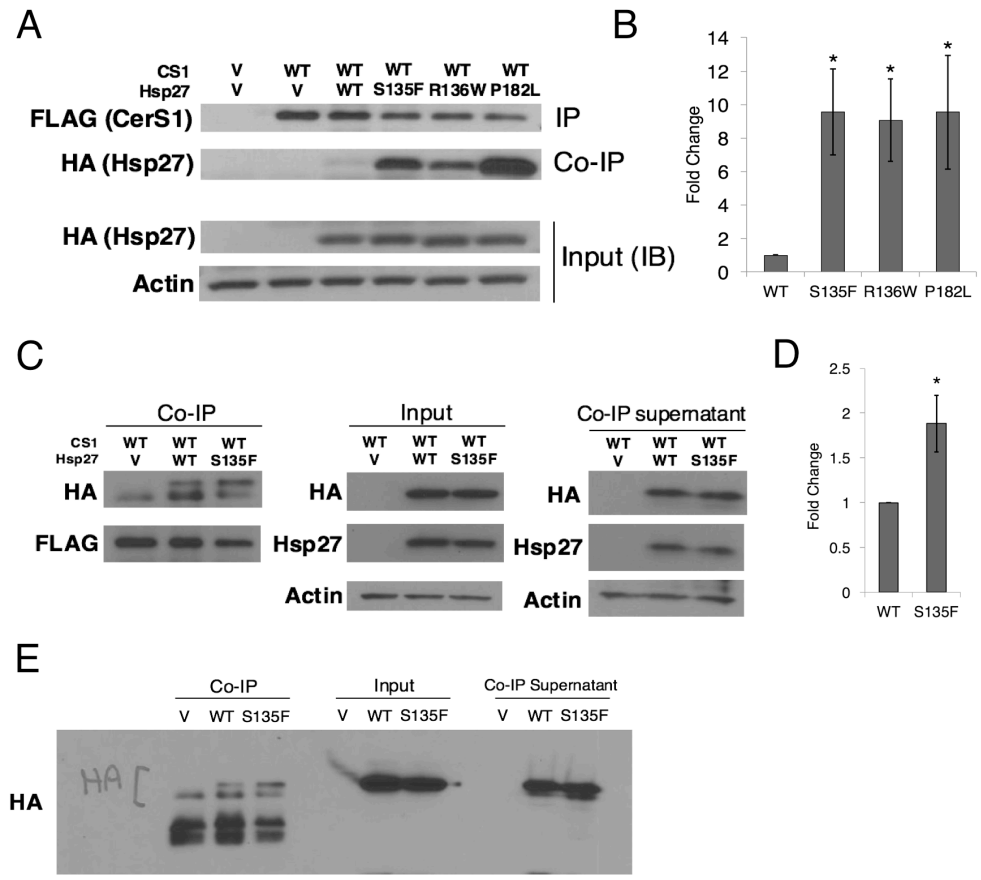

Figure 12. CerS1 binds to WT Hsp27 and Hsp27 mutant demonstrates increased binding.

(*A)* Interaction of WT and mutant forms of Hsp27 with CerS1 in HCT-116 cells. *(B)* Quantification of co-IP experiments (*$P < 0.05$, n=3). (*C)* Interaction of WT and mutant forms of Hsp27 with CerS1 in HT-22 cells. *(D)* Quantification of co-IP experiments (*$P < 0.05$, n=3). *(E)* Confirmation of HA band in co-IP in HT-22 cells. Scanned immunoblot from HT-22 co-IP showing uppermost band in leftmost three columns of co-IP corresponds to HA stained in total cell lysate and IP supernatant of WT and S135F transfected cells.

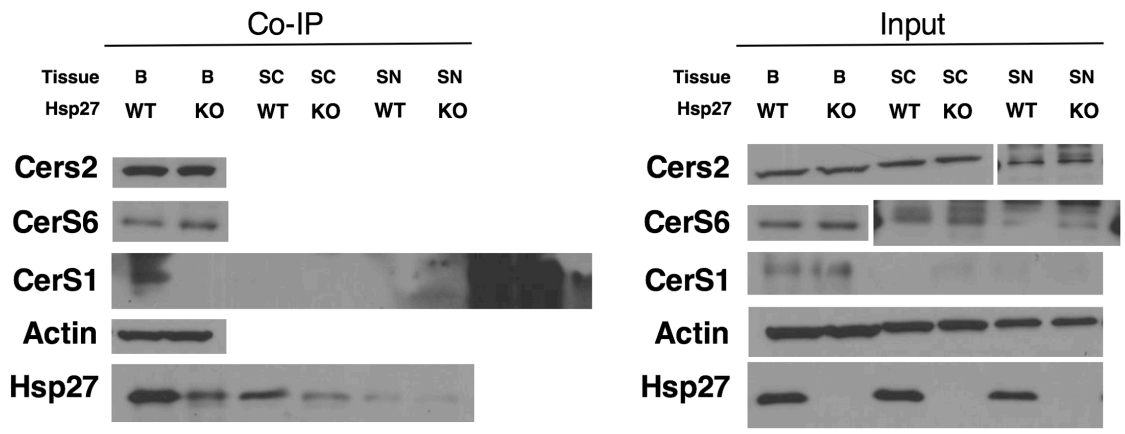

Figure 13. CerS1 Hsp27 demonstrate binding in mouse brain.

Pull-down of Hsp27 demonstrates co-IP of CerS1 in brain (B) from WT mice but not Hsp27 KO mice. Input lane on the left shows knockout of Hsp27 in brain, spinal cord (SC), and sciatic nerve (SN). Note that CerS1 expression is very low in spinal cord and sciatic nerve, potentially prohibiting the detection of Hsp27:CerS1 binding in these tissues.

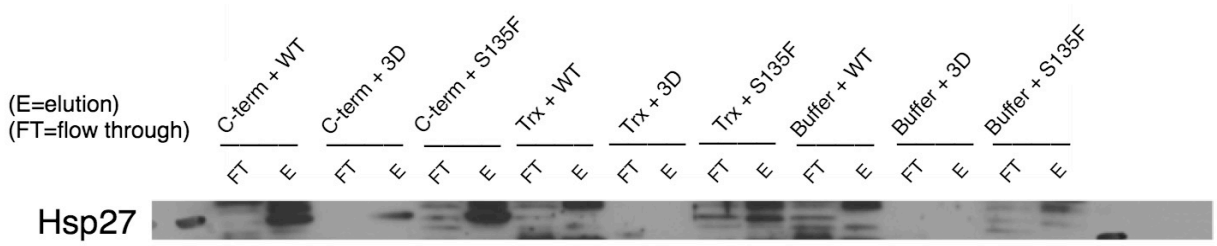

Figure 14. C-terminus of CerS1 interacts with WT and S135F Hsp27.

The positive signal in the Hsp27 elution column for WT, 3D (phosphomimetic) and S135F indicates C-terminal CerS1 binding to Hsp27.

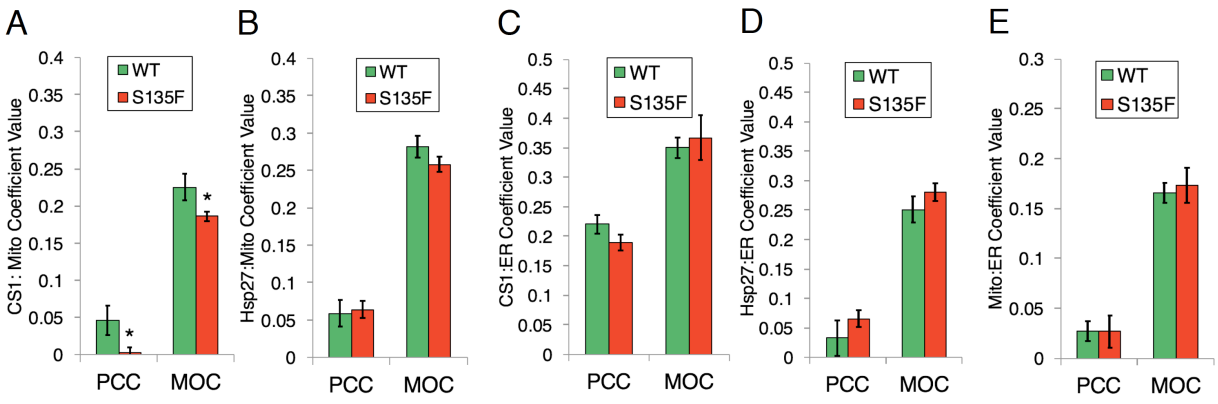

Figure 15. S135F mutant decreases CerS1 localization to mitochondria.

(A) CerS1 localizes to mitochondria in the presence of WT Hsp27 more than S135F in HT-22 cells. Quantification of Super-resolution Structured Illumination Microscopy (SIM) co-localization of FLAG (CerS1) and MitoTracker Deep Red (mitochondrial marker) was using Pearson's Correlation Coefficient (PCC) and Mander's Overlap Coefficient (MOC) (**P* < 0.05 for PCC, **P* < 0.05 for MOC; n=31 and n=35). *(B)* SIM quantification of FLAG and calnexin (ER marker) co-localization (*P* = 0.797 for PCC, *P* = 0.188 for MOC; n=24 and n=27). *(C)* CerS1 localizes to the Endoplasmic Reticulum (ER) in the presence of WT and S135F Hsp27 in HT-22 cells. SIM quantification FLAG and calnexin co-localization using PCC and MOC (*P* = 0.131 for PCC, *P* = 0.70 for MOC; n=15 and n=18). *(D)* SIM quantification of FLAG and calnexin co-localization was quantified using PCC and MOC (*P* = 0.324 for Pearson's, *P* = 0.287 for MOC; n=9 and n=10). *(E)* SIM quantification of calnexin and MitoTracker Deep Red (*P* = 0.324 for PCC, *P* = 0.287 for MOC; n=9 and n=10).

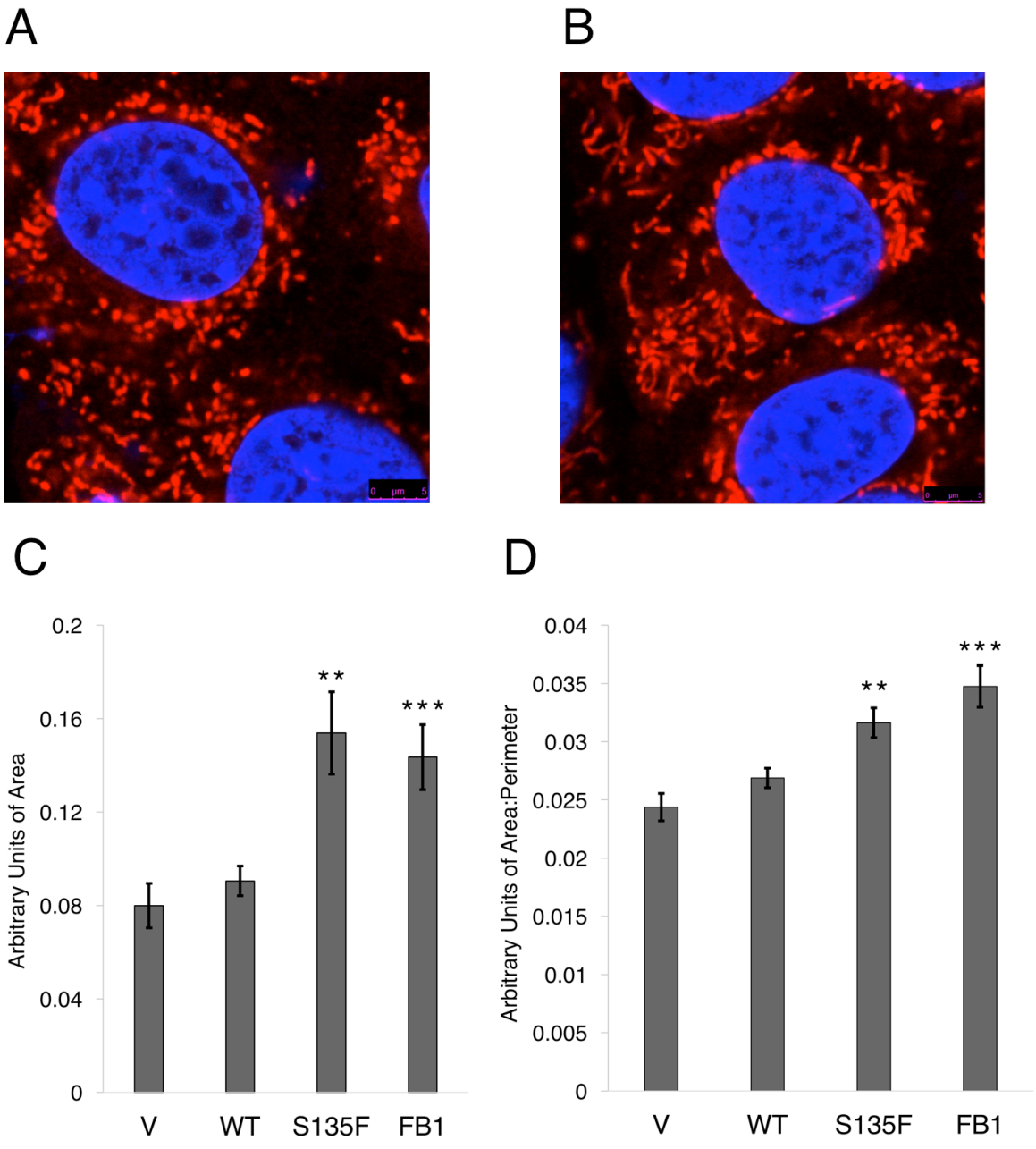

Figure 16. S135F mutant produces enlarged mitochondria consistent with decreased CerS function.

(*A-B)* Representative images of mitochondria in HT-22 cells transfected with WT and S135F Hsp27, respectively. (*C)* Increased area is observed in S135F mutant transfected HT-22 cells ($p<0.01$; n=41, 44) and cells treated with FB1 (***$P < 0.001$; n=15,13). *(D)* Increased area/perimeter ratio is observed in S135F mutant transfected HT-22 cells (**$P < 0.01$; n=41, 44) and cells treated with FB1 (***$P < 0.001$; n=15,13).

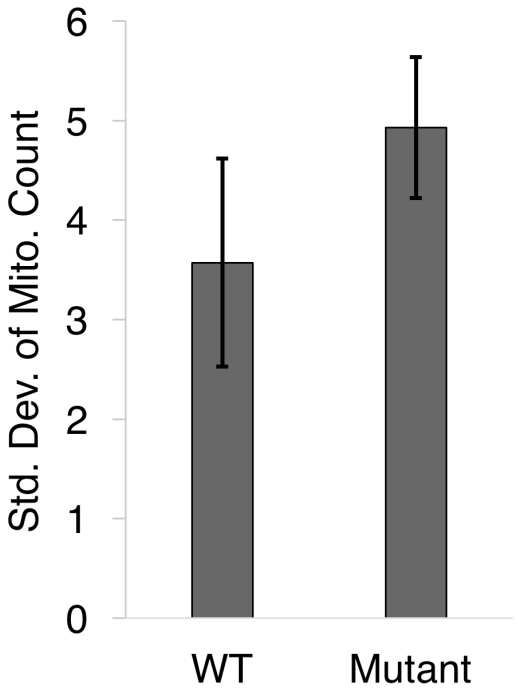

Figure 17. S135F may cause more dynamic mitochondria.

Mitochondria in WT and S135F transfected cells were imaged approximately 50 times in the span of 5 minutes. Total mitochondria were quantified and standard deviations in total mitochondrial number were used as a measure of mitochondrial activity (n=3).

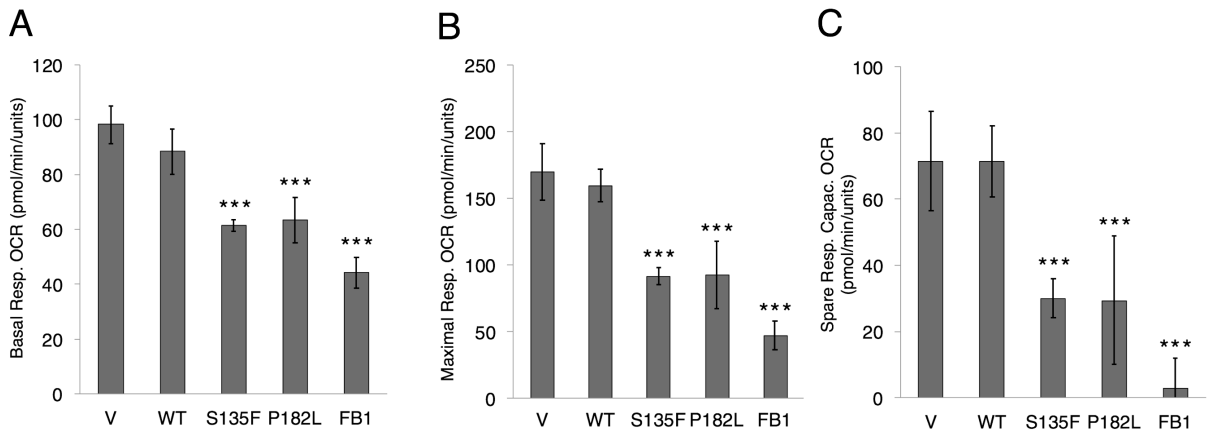

Figure 18. S135F and P182L mutants display decreased mitochondrial function consistent with decreased CerS function.

(A) Mutants (S135F and P182L) and FB1 display decreased basal respiration compared to WT and V, respectively (***$P < 0.001$). *(B)* Mutants and FB1 display decreased maximal respiration compared to WT and V, respectively (***$P < 0.001$). *(C)* Mutants and FB1 display decreased spare respiratory capacity compared to WT and V, respectively (***$P < 0.001$). All experiments were repeated at least twice with similar results; error bars represent standard deviations of a single experiment.

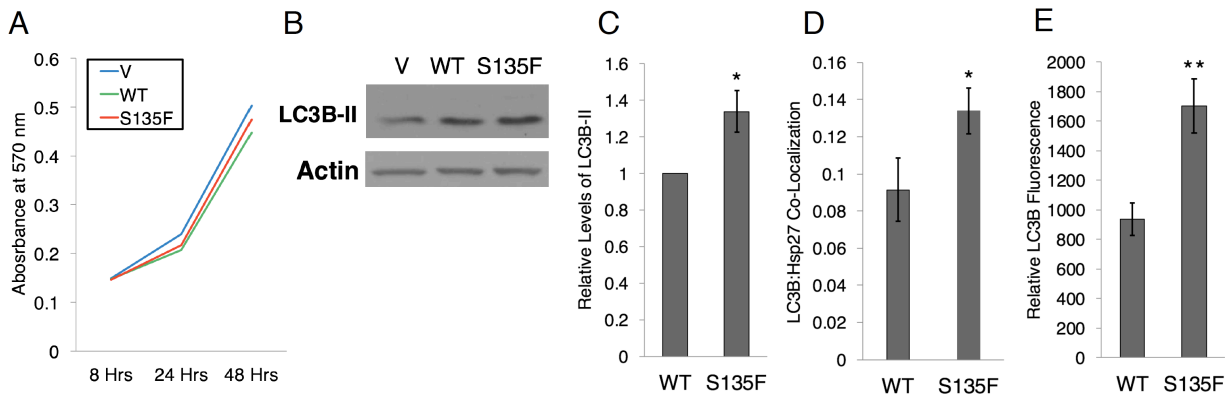

Figure 19. Increased autophagy but no change in growth of S135F mutant cells.

(A) S135F mutation does not affect cell proliferation. *(B)* Representative Western blot showing mildly increased LC3B signal in S135F compared to WT transfected HT-22 cells. *(C)* There is an approximate 1.3-fold increase in autophagy in S135F Hsp27 as indicated by LC3B-II signal by immunoblotting (*$P < 0.05$, n=6). *(D)* Quantification of confocal images reveals an increase in autophagy as indicated by LC3B:Hsp27 co-localization (*$P < 0.05$, n=22,23). *(E)* Quantification of intensity of LC3B staining as a measure of autophagy reveals increased autophagy in S135F (**$P < 0.01$, n=12,19).

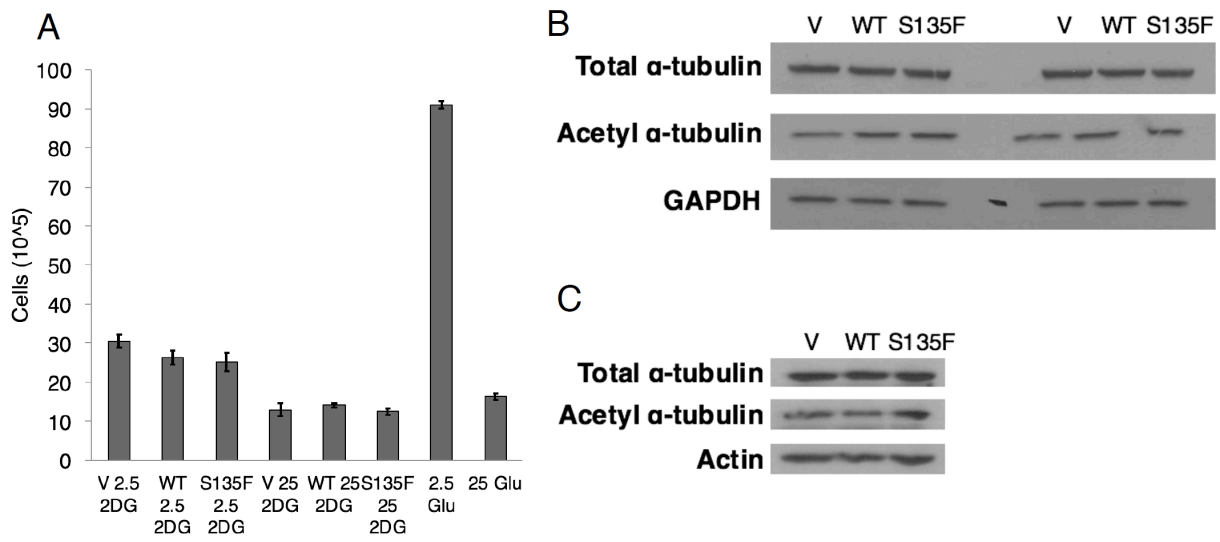

Figure 20. Cellular viability and tubulin acetylation not changed by mutant Hsp27.

(A) Trypan blue cell exclusion staining was used to count cells transiently transfected with Vector, WT Hsp27, or S135F for 48 hours and treated with either 2.5 uM or 25 uM 2-deoxyglucose (2-DG) or 2.5 uM or 25 uM glucose as a control. *(B)* S135F and P182L mutant Hsp27 do not alter α-tubulin acetylation in stably transfected HT-22 cells. *(C)* S135F and P182L mutant Hsp27 do not alter α-tubulin acetylation in transiently transfected HT-22 cells.

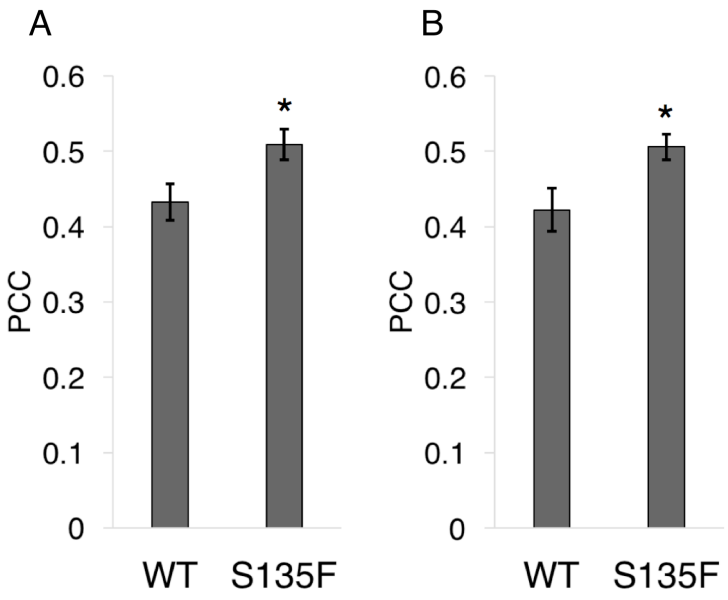

Figure 21. CerS1 overexpression does not alter propensity of S135F mutant to increasingly localize with Tuj1.

WT Hsp27 and S135F were alternatively co-transfected with either Vector *(A)* or CerS1 *(B)*. There is greater co-localization of S135F than WT Hsp27 with Tuj in co-transfection with vector ($p<0.05$, $n=15$) and CerS1 ($P<0.05$, $n=16$). The presence of CerS1 does not alter this co-localization.

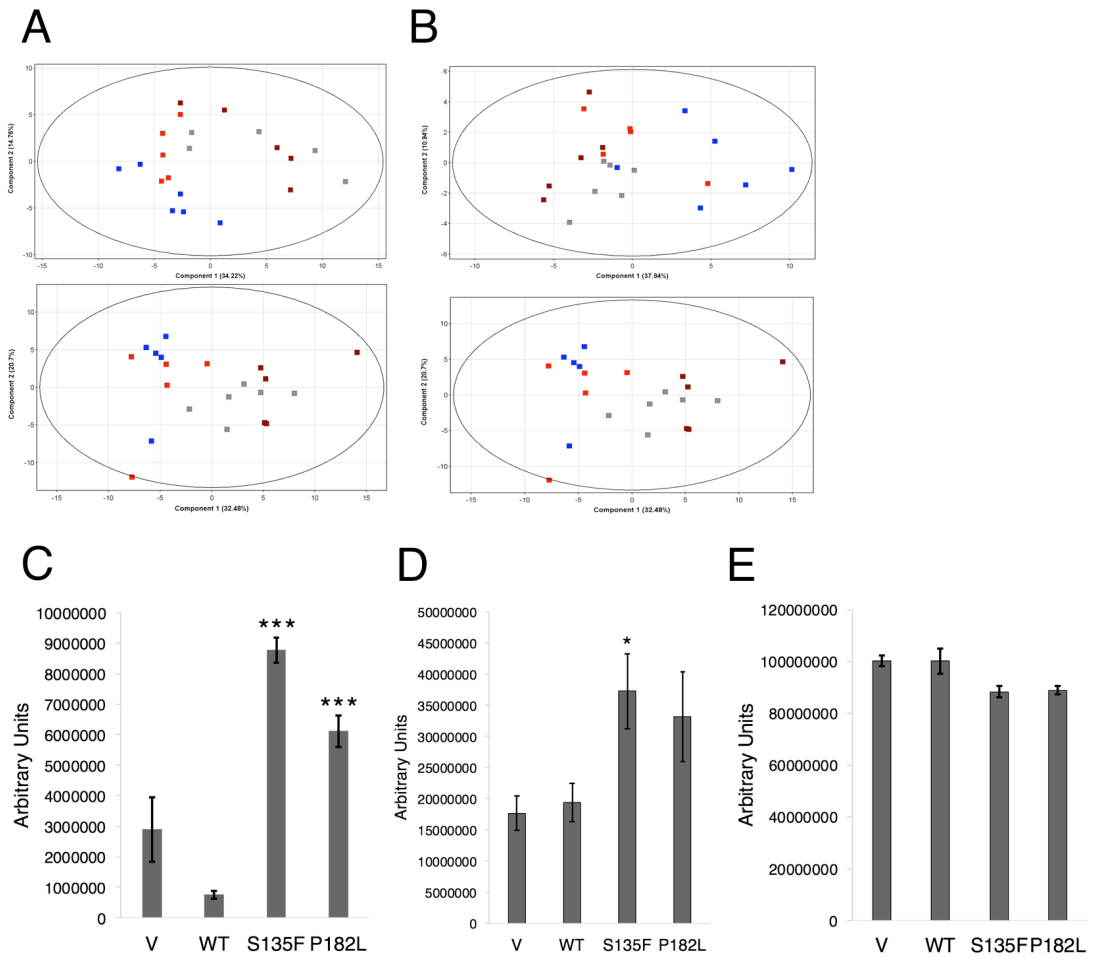

Figure 22. S135F and P182L mutants display similar metabolic characteristics.

(A) Principle Component Analysis (PCA) of metabolites from HT-22 cells transfected with Vector (maroon), WT (grey), S135F (blue), and P182L (red) Hsp27 was performed twice in positive ion mode revealing clustering of mutant analytes. *(B)* Principle Component Analysis (PCA) of the same conditions performed twice in negative ion mode revealing clustering of mutant analytes. *(C)* S135F and P182L mutants display greater urea than wild-type Hsp27 HT-22 cells (n=6; ***$P < 0.001$ for each mutant). *(D)* S135F mutant displays greater creatinine than wild-type Hsp27 HT-22 cells (n=5; $p<0.05$). *(E)* S135F and P182L mutants strongly trend with decreased glutamine compared to wild-type Hsp27 HT-22 cells (n=6, $P = 0.0504$; n=6, $P = 0.0504$).

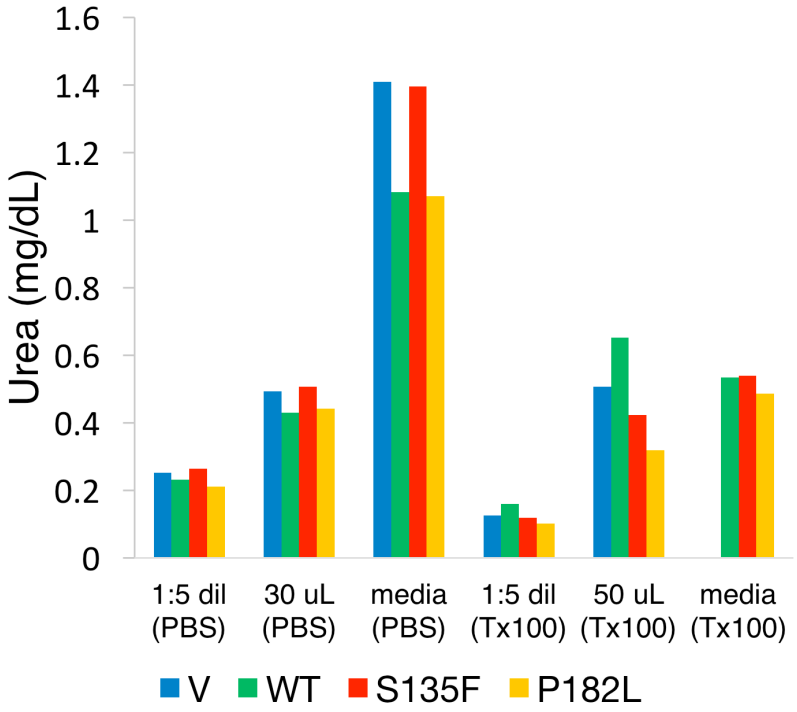

Figure 23. Urea Concentration is Unaltered in Mutants Using Urea Assay

Urea content was measured from media and cells, suspended in PBS or Triton-X 100 (Tx100). No substantial changes were observed in urea in this assay.

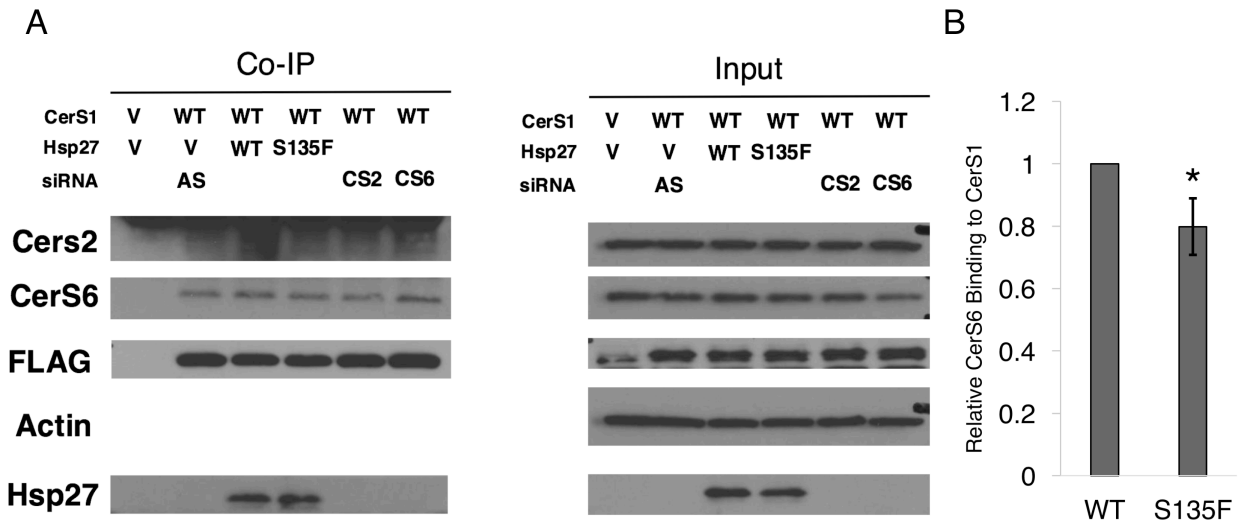

Figure 24. CerS1 binds CerS2 and CerS6.

(A) FLAG pulldown of overexpressed CerS1 was used to assess binding of endogenous CerS2 and CerS6. The presence of the CerS6 and potentially CerS2 in every Co-IP lane in which CerS1 was overexpressed suggests that CerS1 is able to bind these other CerS. *(B)* Quantification of the intensity of CerS6 co-IP bands with transfection of WT and S135F (n=3, $*P < 0.05$).

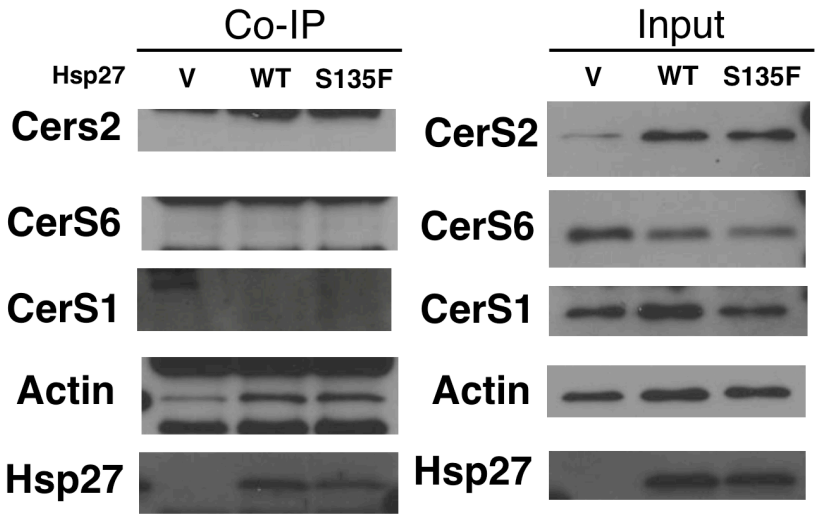

Figure 25. Failure to Demonstrate CerS pulldown to Hsp27 in Mitochondria.

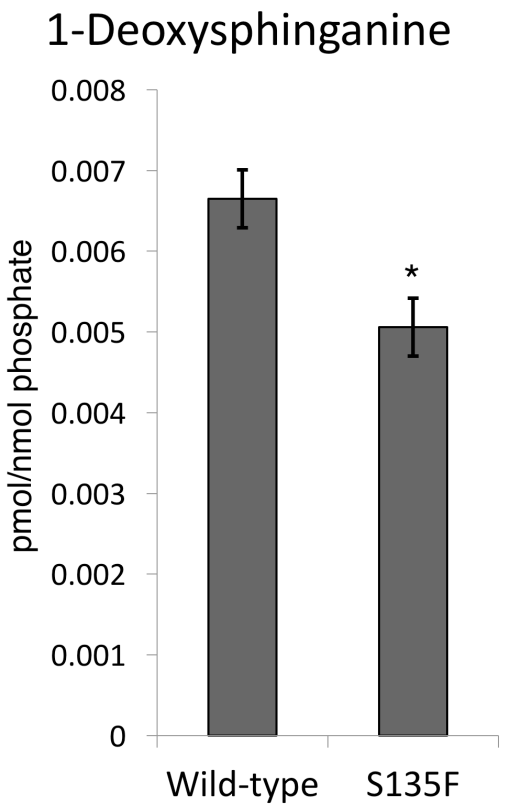

Figure 26. S135F mutant has reduced deoxysphingoid bases.

1–deoxysphinganine measured in HT-22 cells is significantly decreased in S135F mutants as well (*$P < 0.05$, n=6). 1-deoxysphingosine was measured but below reliable levels for quantification.

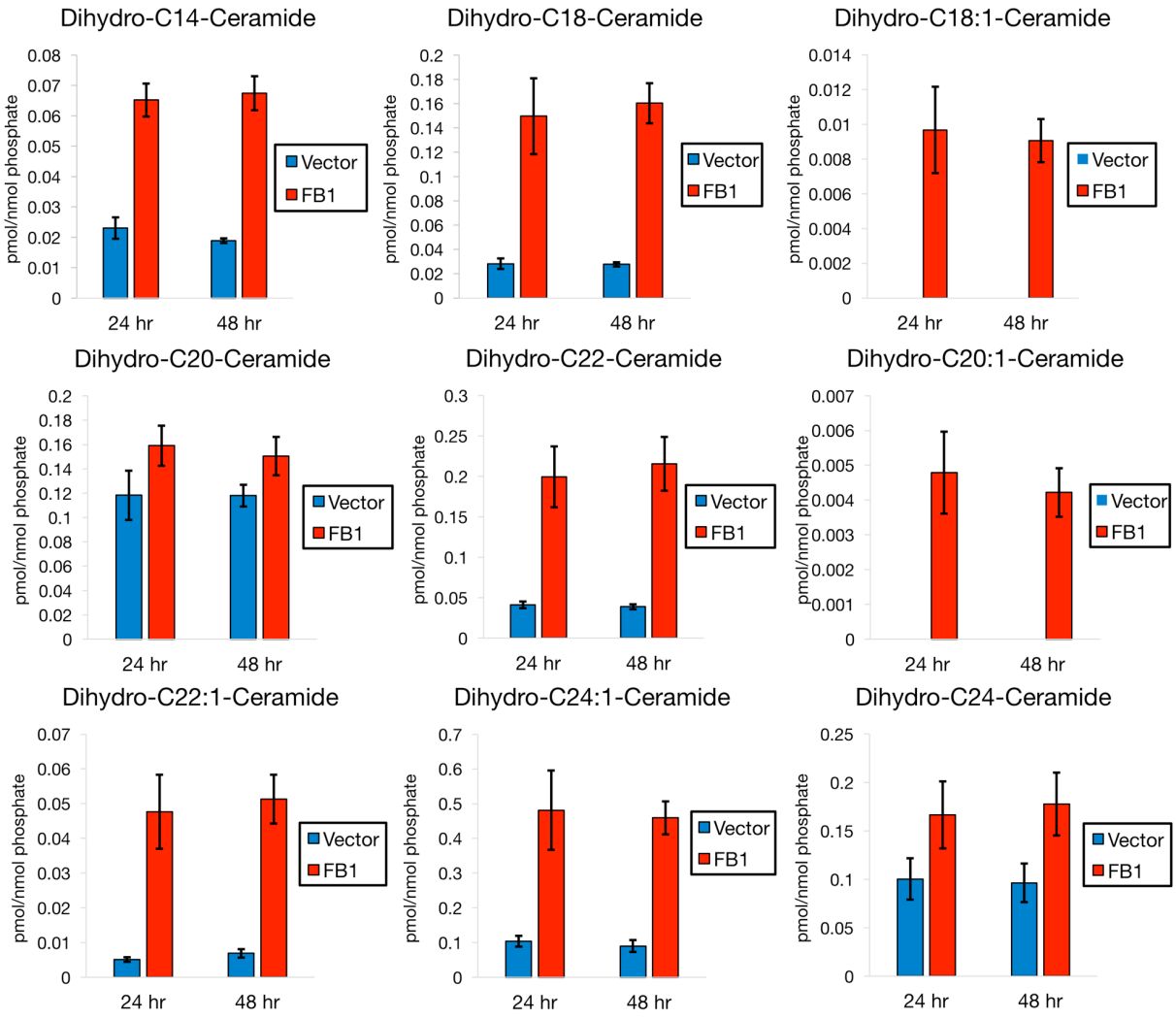

Figure 27. Fumonisin B1 increases dhCer in HT-22 cells.

Many species of dhCer are noticeably increased with FB1 treatment compared to controls that received no FB1 (“vector”). Note that C18:1 and C20:1 dhCers were below quantification in the condition without FB1 (statistical tests were not performed due to observable trends of large increases in many species).

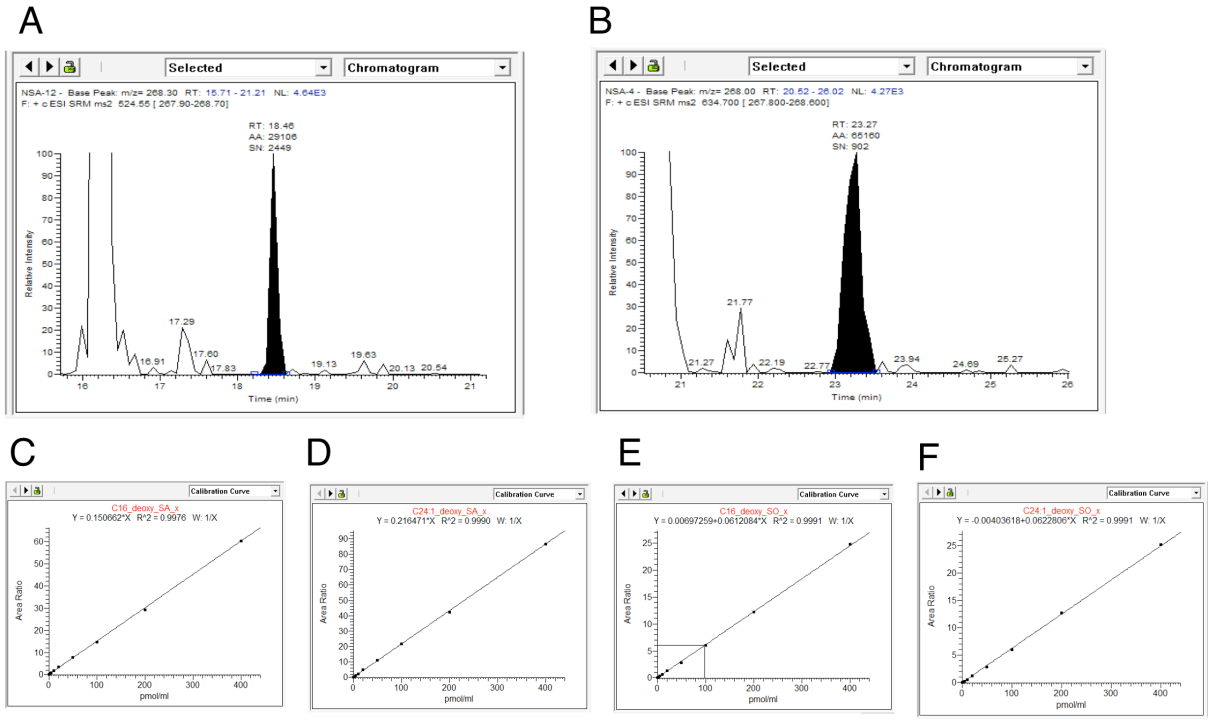

Figure 28. Verification of identified deoxySLs.

A-B) Sample peaks provided for C24-deoxydhCer and C22-deoxydhCer, respectively, demonstrating a reliable signal to noise ratio. *C-F)* Calibration curves for C16-deoxydhCer, C24:1-deoxydhCer, C16-deoxyCer, and C24:1-deoxyCer demonstrating high linearity validating the identified the method.

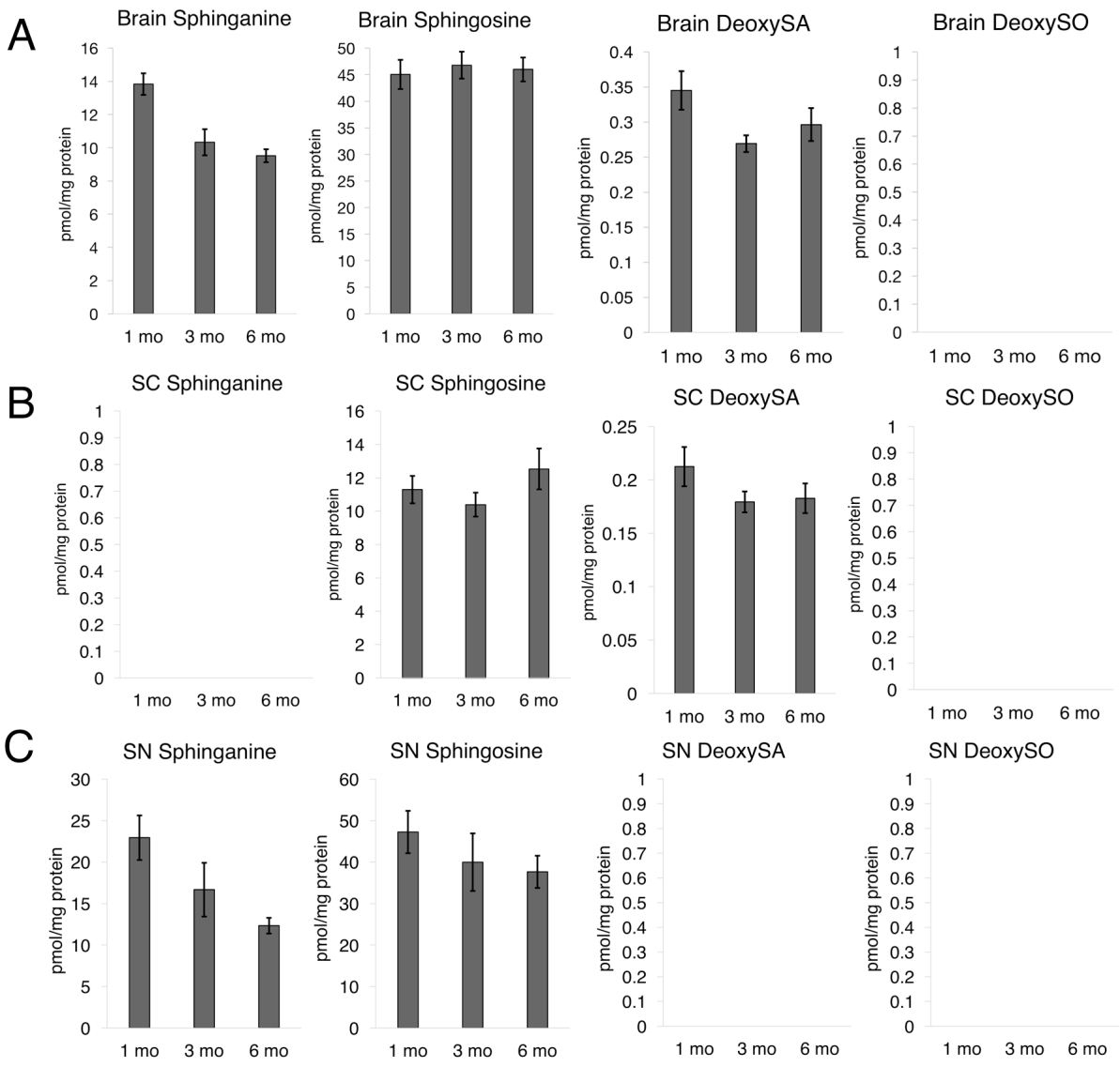

Figure 29. Sphingoid and deoxysphingoid base profile in mouse neural tissue.

A) Brain tissue from 1 mo, 3 mo, and 6 mo mice analyzed for sphinganine, sphingosine, deoxySA, and deoxySO (n=5, 6, 6). Note that empty graphs indicate a species was below the level of confident quantification. *B)* Spinal cord tissue analyzed as in 4A (n=6, 6, 6). *C)* Sciatic nerve analyzed as in 4A (n=6, 6, 6).

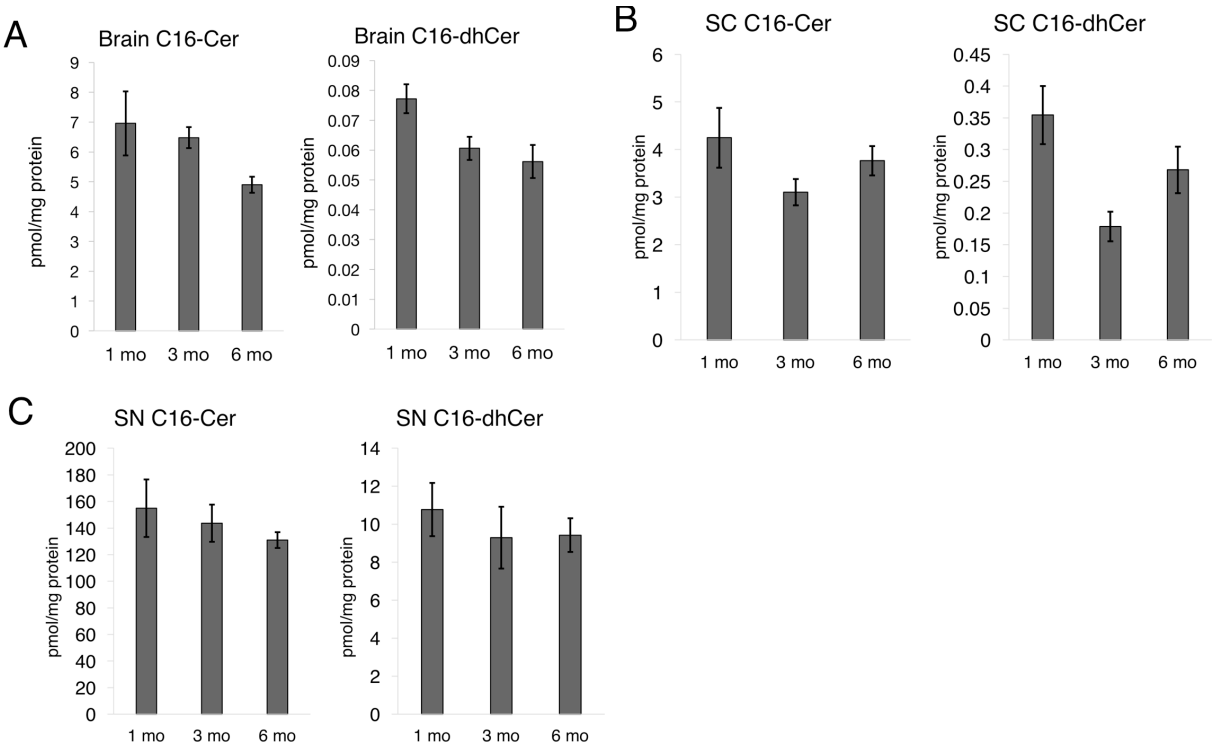

Figure 30. C16-ceramide predominates over C16-dhCer in mouse neural tissue.

A) Brain tissue from 1 mo, 3 mo, and 6 mo mice analyzed for C16-ceramide and C16-dhCer (n=5, 6, 6). *B)* Spinal cord tissue analyzed as in S1A (n=6, 6, 6). *C)* Sciatic nerve analyzed as in S1A (n=6, 6, 6).

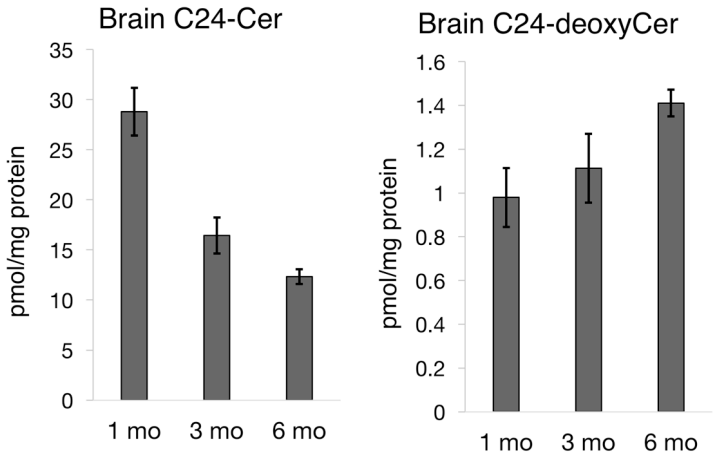

Figure 31. Brain C24-deoxyCer is the only deoxyCer above quantifiable limits.

Brain C24-ceramide and C24-deoxyCer for 1, 3, and 6 months. C24-deoxyCer in the brain was the only species of deoxyCer that was consistently measured above quantifiable limits (n=5, 6, 6).

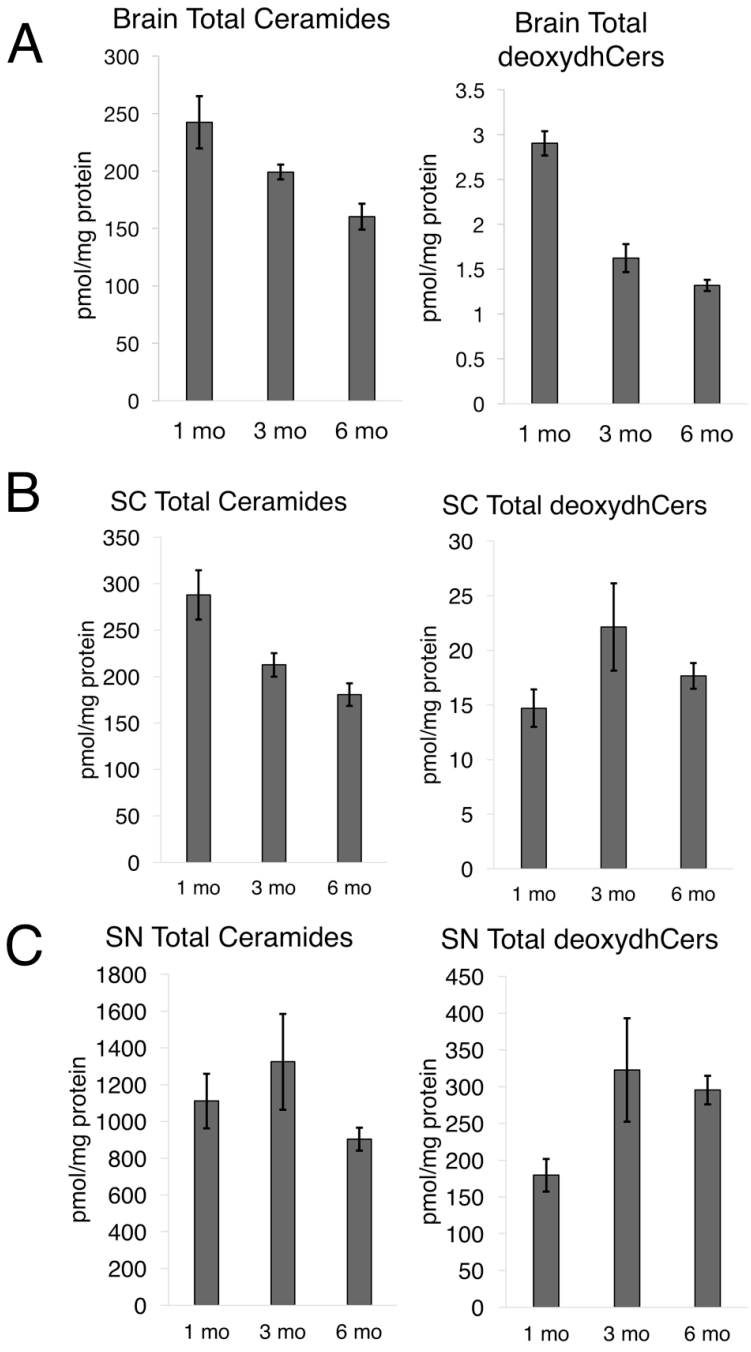

Figure 32. Ceramides and deoxydhCers in mouse neural tissue.

A) Brain tissue from 1 mo, 3 mo, and 6 mo mice analyzed for total ceramide and total deoxydhCer (n=5, 6, 6). *B)* Spinal cord tissue analyzed as in Fig. 30A (n=6, 6, 6). *C)* Sciatic nerve analyzed as in Fig. 30A (n=6, 6, 6).

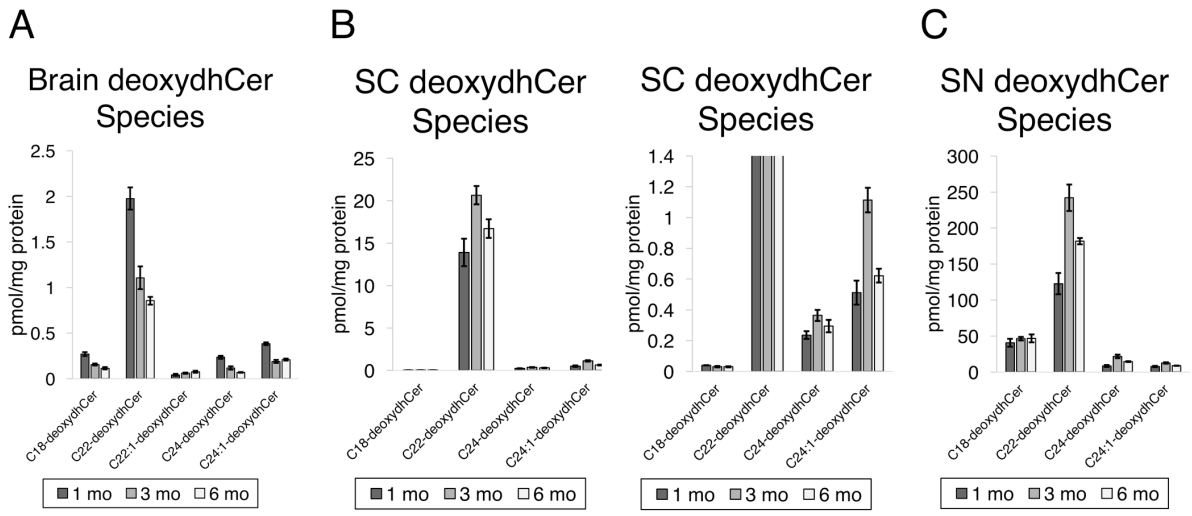

Figure 33. DeoxydhCer profile in mouse neural tissue.

A) DeoxydhCer species that were confidently measured from brain tissue from 1 mo, 3 mo, and 6 mo old mice (n=5, 6, 6). *B)* Spinal cord tissue analyzed as in Fig. 31A (n=6, 6, 6). Note multiple panels are presented to show relative levels of other species much less prevalent than C22-deoxydhCer. *C)* Sciatic nerve analyzed as in Fig. 31A (n=6, 6, 6).

Mus musculus strain C57BL/6J chromosome 5 genomic contig, GRCm38.p3 C57BL/6J MMCHR5_CTG21

NCBI Reference Sequence: NT_039314.8

Chr5: 135886919 - 135890563

```
ACATTATATATATATATATATATATATATATATATATATATATATATATAATAAAAAAAAAAAGCGGCCG
GGTGTGGTGGGGCACGCCTTTAATCCCAGCACTCCGGAGGCACGGGCAGGTGGATTTCTGAGTTCGAGGC
CAGCCTGGTCTACAAAGTGAATTCCAGGACAGCCAGGGCTATACAGAGAAACCCTGTCTCGAAAAACCAA
AAAAAAAAAAAAAAAAAAAAGCATCAAATAGCCCAGCGGTGGTGATGCACACCTTTAATCCCAGCACTTG
GGAGGCAGAGGCAGGCGGGTTTCTGAATTCGAGGCCAGCCTGGTCTACAAAGTGAGTTCCAGGACAACCA
GGGCTATGCAGAGAAACATTGTCTTCAGAAAAAAAAAAAAAAAAAAAAAAAAAAAAAGCAAAGCAAAACAA
AACAAAAAAAAAAGCATCAAAATAAAAAAAGAAAAATCCTACTTCAGAGAGAGAGAGAGAGAGAGAGAGAG
AGAGAGAGAGAGGAGAGAGGAGAGAGAAAGAGAGAAAGAAGAAAGAAAGTCAGTTTCTGGGTCAGAAA
GATACTCAGTGAACACTAAGGCGCCTGCCACGAAGCCTTTGCTCCCCAGGAGATACACTATAGAAGACAG
CTATCTTGCCGGTGTCATGAGACCTCCACAGGTGTGCCATGACATGTGTGTTCCCACGGGCCTCCTTCTG
GTTCAGACCAGGTTCAGTTGCTTCCCAGTTGCGACACAAAAGACCTAACCTCTCCTGGTTATTCTCAATA
AAAAATGGGGCTGGCCCCAGGCCACCGCCCTTCAGCCAGCAGTGTCCTAAACCCGACAGTGGGAATCGCT
CCAGCTACCGGTATTACGCCGTCATTTGTTTTCTTCAACAAGAGAAGTTTCCAGATGGGGGCAGAACCTT
CCTGGCCCCGCCTGCCCGCCCCCTTTGCAAGCTTAGGGGGAGGAATGCAGAGGGGAGGGGCGGCGAGGGG
CGGCCCCTGAGACGGTCATTGCCATTAATAGAGACCTGAAGCACCGCCTGCTAAAAATACCCGGCTGGGC
ACACATAAAAGCACGCTGGGGCTCCAGTCCGGCACTTCTCGGATCCTCAGCCCAGTGCTTCTAGATCCTC
AGCCTTGACCAGCCAAGAACATGACCGAGCGCCGCGTGCCCTTCTCGCTGCTGCGGAGCCCGAGCTGGGA
ACCATTCCGGGACTGGTACCCTGCACACAGCCGCCTCTTCGATCAAGCTTTCGGGGTGCCCCGGTTGCCC
GATGAGTGGTCGCAGTGGTTCAGCGCCGCTGGGTGGCCCGGATACGTGCGCCCGCTGCCCGCCGCGACCG
CCGAGGGCCCCGCGGCGGTGACCCTGGCCGCACCAGCCTTCAGCCGAGCGCTCAACCGACAGCTCAGCAG
CGGGGTCTCGGAGATCCGACAGACGGCTGATCGCTGGCGCGTGTCCCTGGACGTCAACCACTTCGCTCCG
GAGGAGCTCACAGTGAAGACCAAGGAAGGCGTGGTGGAGATCACTGGTGAGTTTCCCTTGTGCCCAGAGG
GGACGAAGCTGCCGAGGCGAGAGTGGTGGCTGGGGGGCTGAGGGTGGGGGCTGAAACCCTGAGGAATAGA
ACCCTGAGAAGTTAGAAATGAACCTAGGGACCCGGAGCCCGCATCATTCTCCTTTGCCTGCTTCTCTTGC
CCCGGAACGCGGGGTGCAGGTTGCTCTTAAAAGCTCTGTCATCTTCGATGATATGGACCAACAGCTGGGG
ATGTAGCTCAGGGTAGAGCTTCGCCTGGCCTGCCGGGAGGCCTTGAGGCTTTGCGTTCCACCCGCAGCAC
AGAAACAAAATGAAGGAAGACCCAACACACCTTCTGGAAGACCTCATTCCCAAATAAGCAAGCGGCAGGA
TCAGGGTCCCTAGACCCAGCCGCAGAGGCTTTGAGTATACCTACCCTGGTATCCAAGTCTGGGTCAGAGC
CAAGCCCTTCGCATCCCAAATCTCAGAAGGGAAGTTTCTGGAAAGTTTTAAGATTCCAGACAGTCAGGCA
CCCCGCCGCACTCGGGTTTGTTTGCCTCCCTGGGGGGTCCCAGCCACTCCTTAGCTAGGACAGCAGAGGG
CTGCTTCTGACCTTCTGTCCCCACCCACAGGCAAGCACGAAGAAAGGCAGGACGAACATGGCTACATCTT
TCGGTGCTTCACCCGGAAATACACGTGAGTTCTGATTCCTTGCATGGAGGGCGGGGAGGTGGGGGGGAGG
GGGAGCGGACCCAGGGCGGAGGGCGAAGAGCCCCGGGTCAGGAGGGATGTGTAACCCTTGCCCTGATTTT
CTGTGTGTCCAGGCTCCCTCCAGGTGTGGACCCCACCCTAGTGTCCTCTTCCCTATCCCCTGAGGGCACA
CTTACCGTGGAGGCTCCGTTGCCCAAAGCAGTCACGCAGTCAGCGGAGATCACCATTCCGGTTACTTTCG
AGGCCCGCGCCCAAATTGGGGGCCCAGAAGCTGGGAAGTCTGAACAGTCTGGAGCCAAGTAGAAGCCATC
AGCCTGCTGCCTATCTCCCATAGCCATTGCTGGCCACCCCTCTCTGTCAATCTGTGCGCTCTTTTGATAC
ATACATTTACCTGCTGTTTTTCTCAAATAAAAGTTGCAAGCTACTGCTCACCACCGTCTGACTCCAGAGT
TATTATGGTGGGCTAGGGATGGGTGTGCTAAATTGGAACACCCTTTGGGGTCTTTGCTAAGTGCTCACTA
TGGGCTCAGGCCCTTCCTGTGGGAAAAGAGATAACCTGGAGATTAAAAGTTTACCAGGGGGGCTGGAAAG
GTGGCTCAGCGGGTAAGAGCACTGACTGCTCTTCCGAAGGTCCTGAGTTCAAATCCCAGCAACCACATGG
TGGCTCACAACCACCCGTGATGAGGTCTGACACCCTCTTCTGGTGCATCTGAAGGCAGTTACGGTATACG
TACATATAATAATAAATAAATAAATCTTAAAAAAAAAAAAAAAGTTTACCAGGCTGGGTATAATGATGGTA
TAATTACATCTCCTGTAATTCCAGTATCCAAAAACGGATGCAAAAGCAGTGTGAATTTGAAGCCAGCCTG
```

Figure 34. Generation of S135F Mutant Mouse

Mouse Chromosome 5 (135886919 – 135890563) demonstrating a mutation analogous to S135F in human CMT2F. This mutation was generated using Clustered Regularly Interspaced Short Palindromic Repeat (CRISPR) – Cas9 technology.

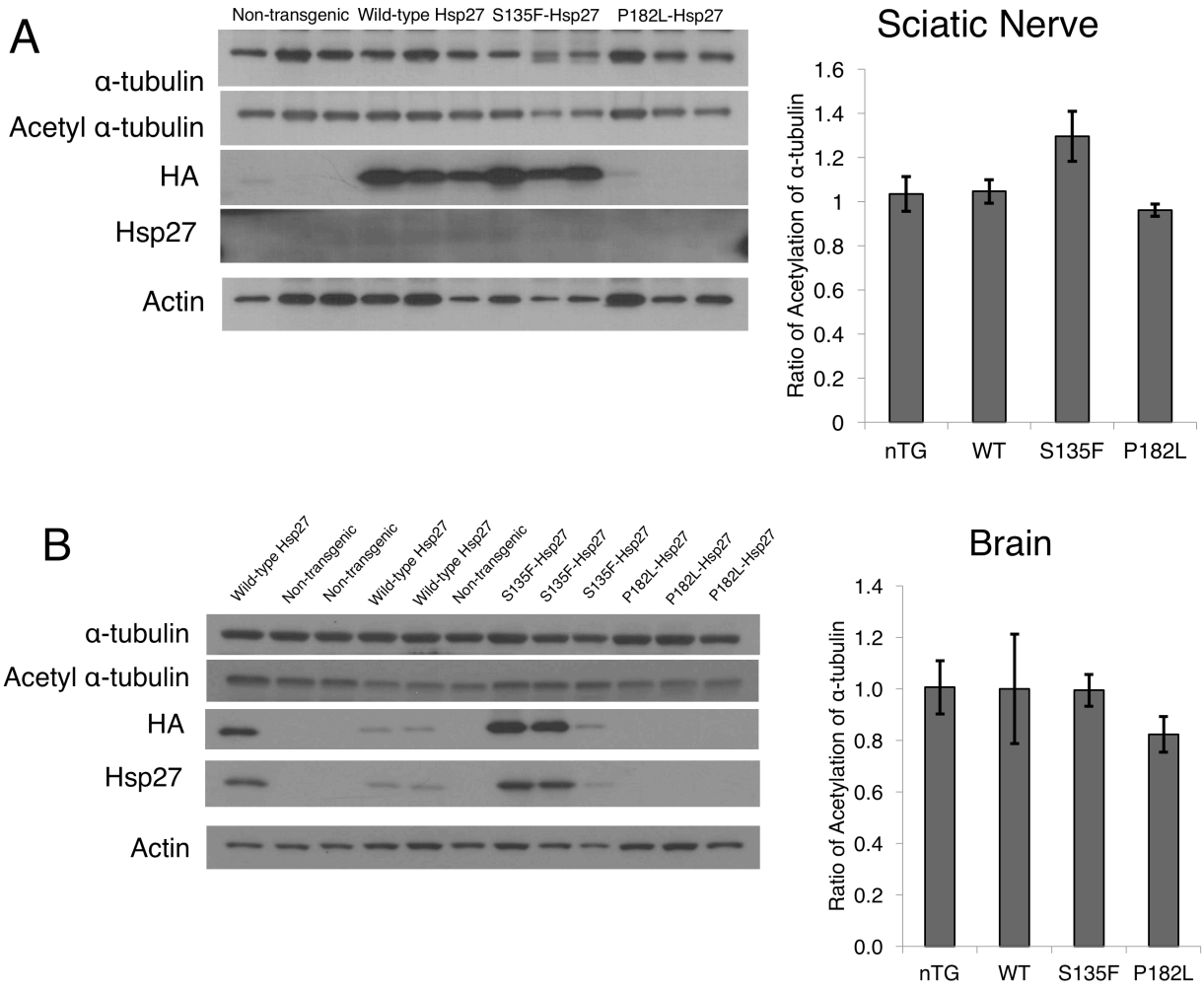

Figure 35. No Alterations in α-tubulin Acetylation in Mutant Mice

A) Sciatic nerve and *B)* brain tissue from non-transgenic (nTG), WT, S135F, and P182L mice analyzed for Hsp27 expression (with Hsp27 and HA antibodies) as well as acetylation of α-tubulin. No notable decrease in acetylation of α-tubulin is observed in sciatic nerve. Furthermore, there is a lack of expression of the P182L mutant.

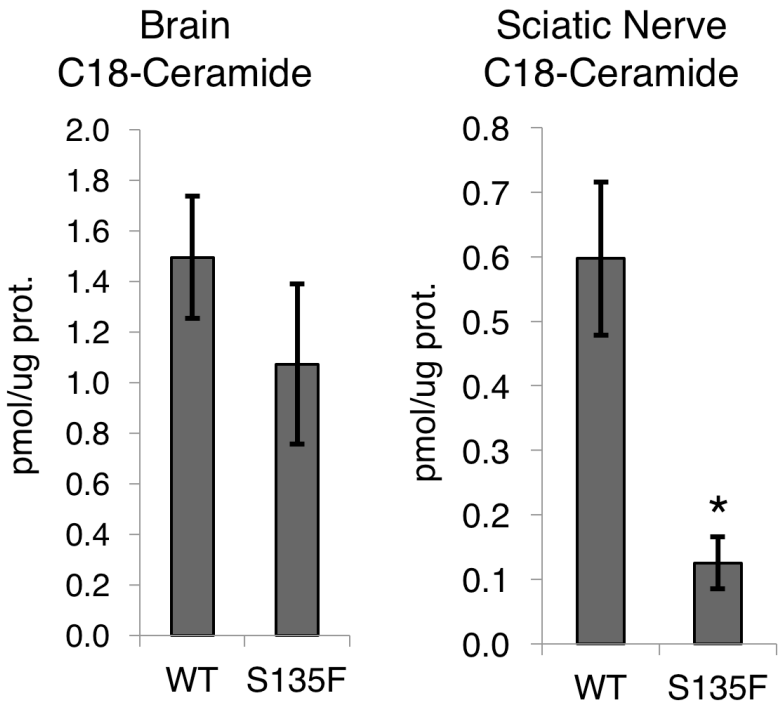

Figure 36. Decreased C18-ceramide in S135F sciatic nerve.

C18-ceramide measurements which are in line with other ceramides species and serve to represent CerS1 function. There is a significant decrease in C18-ceramide in sciatic nerve tissue that is not observed in brain (*$*P < 0.05$,* n=6).

CMT2F Mutation	DNA alteration	Country	Special Symptoms	Citation
P39L	116C>T	Italy		(203)
G84R	250G>C	England		(179)
R127L	380G>T	Finland		(200)
R127W	379C>T	China, Italy, France	Late onset, mild sensory, feet paresthesia, cramps.	(177), (204), (178)
S135F	404C>T	Russia, Korea, Armenia,	Relatively early onset, feet paresthesia	(174), (175), (207), (178)
S135Y	404C>A	Finland	Very mild sensory phenotype	(173)
S135C	404C>G	Italy		(201)
R136L	407G>T	Italy	Pyramidal signs, deafness	(203), (206), (202)
S158fs*200	476_477delCT	Italy	Potentially trigged in infancy from tetanus vaccination	(205)
T164A	490A>G	Taiwan		(208)
M169C*fs2	505delA	Finland		(200)
Q175*	523C>T	France, England	Feet paresthesia, early onset in some cases	(176), (178)
R188W	562C>T	Italy		(203)

dHMN mutations	DNA Alteration	Country	Special Symptoms	Citation
P7S	19C>T	Algeria		(178)
G34R	100G>A	Italy		(203)
P39L	116C>T	England, France		(179), (178)
E41K	121G>A	Italy		(203)
G53D	158G>A	Ivory Coast	Cerebellar ataxia	(178)
L58Afs*105	165_171dup	France		(178)
A61Rfs*100	180dup	France	Lower limb spasticity	(178)
G84R	349G>C		Asymmetrical weakness	(218)
L99M	295C>A	Pakistan	Reported autosomal recessive inheritance	(179)
R127L	380G>T	Finland		(200)
R127W	379C>T	Belgium, Italy, France	Lower limb spasticity, cramps	(175), (214), (201), (204), (178)
Q128R	383A>G	France	Lower limb spasticity	(178)
D129E	387C>G	Ireland	Decreased sensory conduction after progression in one patient, cramping	(209)

S135F	404C>T	England, France, Korea, Italy, Algeria	Rare early onset	(175), (216), (179), (178)
S135C	404C>G	Germany		(215)
R136L	407G>T	Italy		(203)
R136W	406C>T	Belgium		(175)
R140G	404C>T(?)	India	Fasciculations	(179)
K141Q	421A>C	Japan		(211), (213)
T151I	452C>T	Croatia, Japan, France		(175), (210), (214), (178)
S158fs*200	476_477delCT	Italy		(205), (203)
Q175*	523C>T	France		(176), (178)
T180I	539C>T	Italy, Portugal	Early onset, fasciculations	(217), (203), (178)
P182L	545C>T	Austria		(175), (214)
P182S	544C>T	Japan	Early onset	(212)
S187L	560C>T	France		(178)

Table 1. List of reported mutations in CMT2F.

A

Properties of Measured Deoxysphingolipid Species

Name	*Parent ion*	*Product ion*	*Collision Energy*	*Retention Time*
C12-deoxyCer	466.5	266.2	22	14.50
C12-deoxydhCer	468.6	268.2	22	15.00
C14-deoxyCer	494.5	266.2	22	16.30
C14-deoxydhCer	496.5	268.2	22	17.00
C16-deoxyCer	522.4	266.2	22	17.85
C16-deoxydhCer	524.5	268.2	25	18.50
C18-deoxyCer	550.6	266.2	25	19.30
C18-deoxydhCer	552.6	268.2	22	20.00
C20-deoxyCer	578.6	266.2	22	21.00
C29-deoxydhCer	580.6	268.2	22	21.60
C22-deoxyCer	606.6	266.2	22	22.70
C22-deoxydhCer	608.6	268.2	22	23.30
C24-deoxyCer	634.6	266.2	22	24.40
C24-deoxydhCer	636.6	268.2	22	25.20
C26-deoxyCer	662.6	266.2	22	26.50
C26-deoxydhCer	664.6	268.2	22	27.10
C18:1-deoxyCer	548.6	266.2	25	18.40
C18:1-deoxydhCer	550.5	268.2	25	18.90
C20:1-deoxyCer	576.6	266.2	25	19.90
C20:1-deoxydhCer	578.6	268.2	25	20.50
C22:1-deoxyCer	604.6	266.2	25	21.20
C22:1-deoxydhCer	606.5	268.2	25	21.80
C24:1-deoxyCer	632.6	266.2	25	23.00
C24:1-deoxydhCer	634.7	268.2	25	23.50
C26:1-deoxyCer	660.6	266.2	25	24.80
C26:1-deoxydhCer	662.5	268.2	25	25.50
DeoxySO	284.2	266.2	10	6.20
DeoxySA	286.3	268.2	12	6.40

B

Deoxysphingolipid Species Used for Calculations

Source	*Target*
C14-Cer	C12-Cer
C18:1-Cer	C20:1-Cer
C24:1-Cer	C22:1-Cer
C24:1-Cer	C26:1-Cer
C24-Cer	C26-Cer
C14-Cer	C12-deoxyCer
C14-Cer	C12-deoxydhCer
C14-Cer	C14-deoxyCer
C14-Cer	C14-deoxydhCer
C16-deoxyCer	C18:1-deoxyCer
C16-deoxydhCer	C18:1-deoxydhCer
C16-deoxyCer	C18-deoxyCer
C16-deoxydhCer	C18-deoxydhCer
C20-Cer	C20:1-deoxyCer
C20-Cer	C20:1-deoxydhCer
C20-Cer	C20-deoxyCer
C20-Cer	C20-deoxydhCer
C24:1-deoxyCer	C22:1-deoxyCer
C24:1-deoxydhCer	C22:1-deoxydhCer
C22-Cer	C22-deoxyCer
C22-Cer	C22-deoxydhCer
C24:1-deoxyCer	C24-deoxyCer
C24:1-deoxydhCer	C24-deoxydhCer
C24:1-deoxyCer	C26:1-deoxyCer
C24:1-deoxydhCer	C26:1-deoxydhCer
C24-Cer	C26-deoxyCer
C24-Cer	C26-deoxydhCer

Table 2. Parameters of deoxySL calculations.

A) Each species of SL measured is listed along with its parent ion, product ion, collision energy, and retention time. *B)* The source species were directly used for measurements of deoxySL targets.

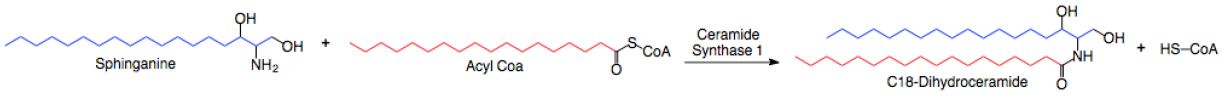

Illustration 1. Ceramide Synthase 1 (CerS1) is necessary for the *de novo* production of C18-Ceramide

C18-sphinganine (blue backbone above) is coupled to a C18-fatty acyl CoA group (red backbone) to produce C18-dihydroceramide. Dihydroceramide desaturase introduces a double bond to carbon 4 of the sphingoid base to produce ceramide.

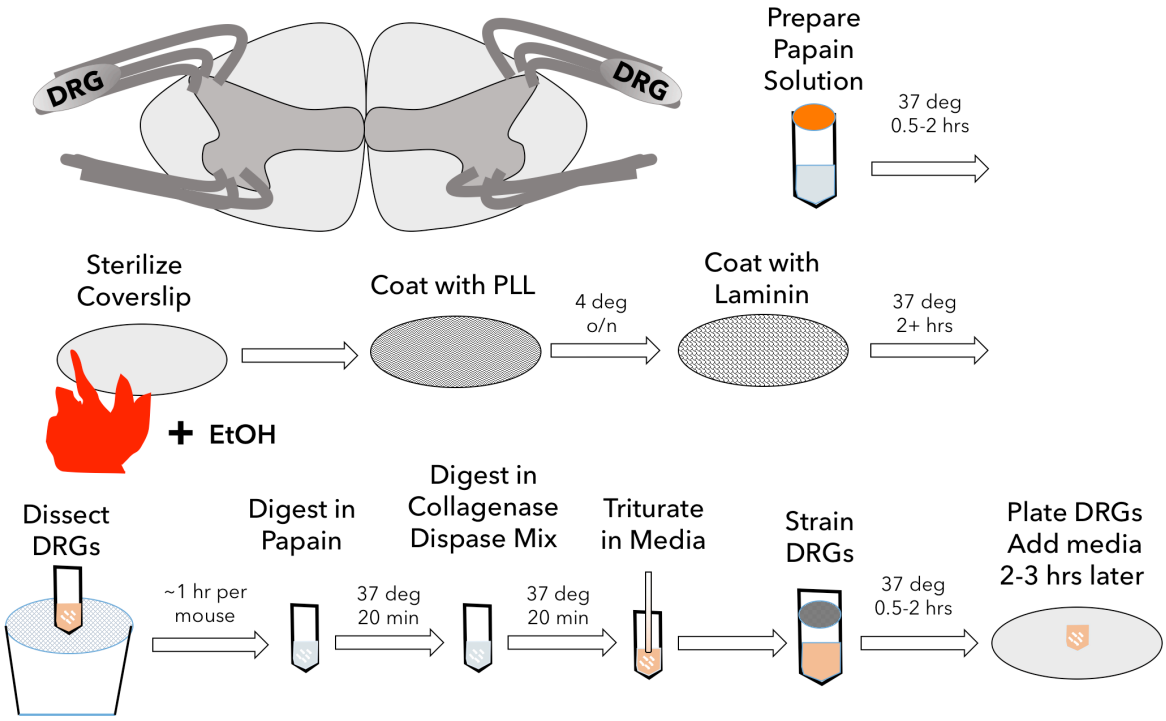

Illustration 2. Schematic of Dorsal Root Ganglia Isolation

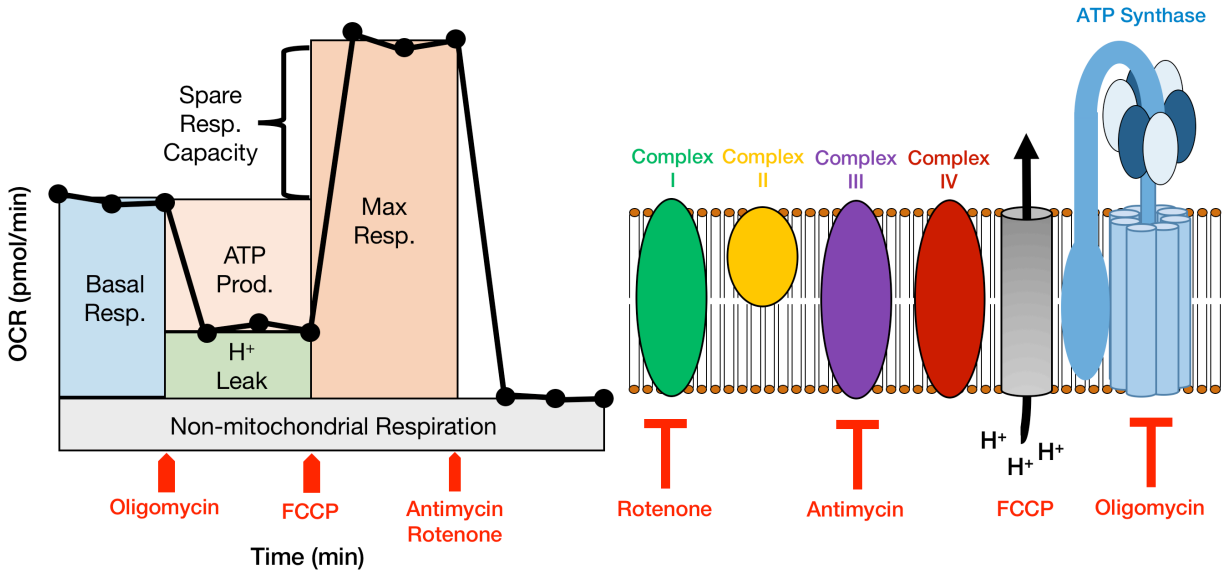

Illustration 3. Overview of measuring mitochondrial respiration using Seahorse.

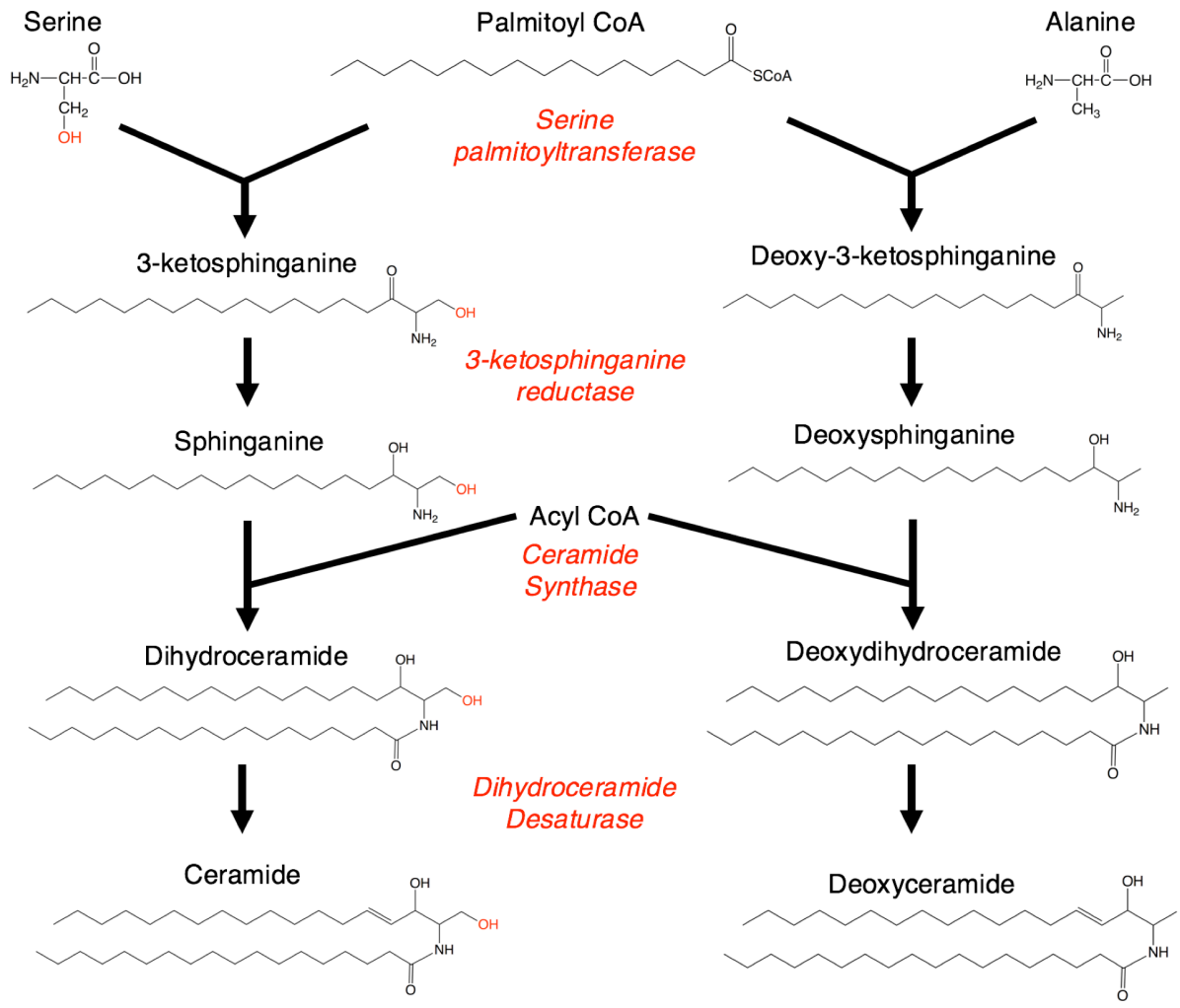

Illustration 4. Schematic of ceramide synthesis.

Serine palmitoyltransferase (SPT) is responsible for condensing palmitoyl CoA and serine to generate 3-ketosphinganine, which undergoes further modification by a series of enzymes in the generation of *de novo* ceramide. Incorporation of alanine, which resembles serine besides lacking a hydroxyl group, results in the formation of a 1-deoxy-3-ketosphinganine. Despite lacking the 1-hydroxyl at the end of the sphingoid chain, this species is presumably able to undergo modification by other enzymes in the *de novo* pathway of ceramide genesis to create 1-deoxyceramide.

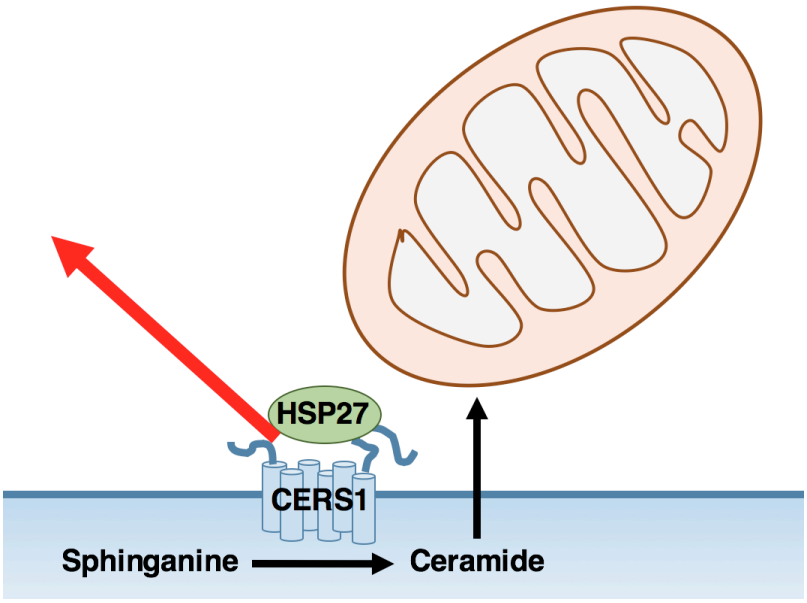

Illustration 5. Schematic of Sphingolipid Involvement in CMT2F

Hsp27 interacts with CerS1 and this interaction is increased in mutant Hsp27. Mutant Hsp27 causes decreased CerS1 localized to the mitochondria, decreasing mitochondrial ceramides. This produces changes in mitochondrial structure and function.